



THE UNIVERSITY OF QUEENSLAND
AUSTRALIA

3D food printing: Assessing the printability of dark chocolate

Sylvester Bin Mantihal
Master of Foodservice Management
Bachelor (Hons) Foodservice Management

*A thesis submitted for the degree of Doctor of Philosophy at
The University of Queensland in 2019
School of Agriculture and Food Sciences*

Abstract

3D food printing (3DFP) is an emerging novel technology in food fabrication, capable of creating food constructs with a layer-by-layer technique based on the desired design. The flexibility of this new technology offers the freedom to customise any preferred design. Among various type of 3D printing techniques, extrusion method is favourable to print the majority of fresh and edible foods. This method allows fresh foods in a paste, or liquid form to be extruded through the nozzle. Understanding the food material characteristic is the major factor that needs to be considered in choosing substrates for 3DFP. Dark chocolate was used as the main material in this work. It composed of cocoa butter (fat), cocoa solids, sugar, and lecithin. The important constituent in chocolate is cocoa butter (fat) containing the stable β -crystals in the chocolate matrix. These crystal fats help the chocolate to retain its quality such as glossy appearance, smooth texture and will set even after its being partially melted maintaining the β -crystal nuclei during printing. Extrusion method (auger) was applied in this work as the primary method to print the chocolate in powder form. Also, the addition of additive in auger extrusion is required to act as a flow enhancer, minimising the occurrence of slip-effect. Various physical properties, including analysing the effect of food additives, modification of internal structure, sensorial and potential consumers' perception and acceptance of 3D printed chocolates, were evaluated during this research work.

At the beginning of this work, several modifications to a commercial 3D printer were required. The modification included developing a new 3D printer bed, water re-circulating system and the attachment of an air blower. A custom stainless steel printer bed (200 mm x 200 mm x 10 mm) was designed with an in-built water recirculation system (flow rate of 6.3 mL/s and maintain the temperature at ~ 16 °C). Also, the printer bed was supported by a custom stabiliser printed by 3D filament printer using a plastic filament (Acrylonitrile Butadiene Styrene ABS). Additionally, an air blower was attached to avoid condensation that may occur on the printer bed due to cooling below room temperature. These modifications were done to ensure that the extruded chocolate solidifies efficiently upon extrusion. The optimisation of printing parameters was executed to determine the nozzle height and printing temperature. A series of comprehensive analysis including thermal properties, flow properties and tribological properties of printed chocolate was conducted. The original chocolate and the printed chocolate had a similar thermal melting profile (average melting peak of 32.9 ± 0.3 °C) as analysed by DSC suggesting that the printed chocolate had similar crystal forms. Food grade additives, magnesium stearate (Mg-ST) and native plant sterol (PS) were investigated for their suitability as a flow enhancer to reduce the slip-effect of the powdered chocolate

movement in the auger extrusion. The findings suggested that Mg-ST and PS did not influence the thermal and flow properties of the printed chocolate. However, tribology analysis indicated that chocolate samples with additives showing a higher coefficient of friction, possibly due to the effect of particle size.

The 3D printer has the capability of modifying the internal structure of a food construct. In this study, 3D food printer was utilised to alter the internal construct structure (5%, 30%, 60% and 100%) infill percentage-IP (star, Hilbert curve and honeycomb infill patterns) to modify the textural properties of 3D printed chocolate. The void fraction of the printed constructs become lesser as IP increased from 5% to 100%. A higher force (N) was required to break the constructs with high IPs. Chocolate printed with Hilbert curve pattern required less force to break the samples (regardless of infill percentages, from 5% to 60% IP) ranging from 1.9 ± 0.1 N to 11.7 ± 0.7 N. For the same variation of infill percentages, the force required to break the samples printed with star pattern and honeycomb pattern ranged from 6.1 ± 0.2 N to 45.3 ± 1.4 N and 9.0 ± 0.3 N to 47.4 ± 0.5 N, respectively. Honeycomb and star infill pattern exhibited more interlayer bonding zones than that of Hilbert curve infill pattern producing a tougher 3D printed chocolates. The mechanical strength of the cast sample was higher (required >110 N) as compared to printed chocolate (100% IP). The results demonstrate that IPs influence the mechanical strength of 3D printed chocolate, indicating a textural change of the chocolate. In the sensorial perspective, texture modified chocolate (printed in a honeycomb pattern with various infill percentage 25%, 50% and 100%) was given to panellist (age between 28 and 55 years) to assess their preferences based on appearance and texture of the printed chocolate. The panellist suggested that the appearance of 3D printed chocolate (100% IP) was favourable and indicated their preferences for chocolate printed in 25% IP. A similar preference of cast chocolate and 3D printed chocolate samples in 100% infill percentage was obtained. Consumer perception was obtained by the 3D printer and printed chocolate samples' display and using a survey questionnaire to assess their knowledge, perceived benefit and their attitudes towards 3DFP. The finding prominently indicated that most of the consumers in the investigated community (University of Queensland premises) were aware of 3D food printing technology. The display of 3D food printing contributed positive feedback from consumers as 3D printed dark chocolate samples were visible to the participants of the survey. These results demonstrated the positive attitudes of consumers toward 3D food printing technology.

Declaration by author

This thesis is composed of my original work, and contains no material previously published or written by another person except where due reference has been made in the text. I have clearly stated the contribution by others to jointly-authored works that I have included in my thesis.

I have clearly stated the contribution of others to my thesis as a whole, including statistical assistance, survey design, data analysis, significant technical procedures, professional editorial advice, financial support and any other original research work used or reported in my thesis. The content of my thesis is the result of work I have carried out since the commencement of my higher degree by research candidature and does not include a substantial part of work that has been submitted to qualify for the award of any other degree or diploma in any university or other tertiary institution. I have clearly stated which parts of my thesis, if any, have been submitted to qualify for another award.

I acknowledge that an electronic copy of my thesis must be lodged with the University Library and, subject to the policy and procedures of The University of Queensland, the thesis be made available for research and study in accordance with the Copyright Act 1968 unless a period of embargo has been approved by the Dean of the Graduate School.

I acknowledge that copyright of all material contained in my thesis resides with the copyright holder(s) of that material. Where appropriate I have obtained copyright permission from the copyright holder to reproduce material in this thesis and have sought permission from co-authors for any jointly authored works included in the thesis.

Publications included in this thesis

Mantihal, S., Prakash, S., Godoi, F. C., & Bhandari, B. (2017). Optimization of chocolate 3D printing by correlating thermal and flow properties with 3D structure modeling. *Innovative Food Science & Emerging Technologies*, 44(Supplement C), 21-29. The core content of this publication was incorporated as Chapter 4.

Contributors	Statement of contribution
Sylvester Mantihal (Candidate)	Designed experiments (70%) Carried out experiments (100%) Analysed experimental data (80%) Wrote the paper (70%)
Bhesh Bhandari (thesis principal advisor)	Designed experiments (20%) Analysed experimental data (10%) Edited the paper (20%)
Sangeeta Prakash (thesis co-advisor)	Designed experiments (10%) Analysed experimental data (10%) Edited the paper (5%)
Fernanda Condi de Godoi	Edited the paper (5%)

Mantihal, S., Prakash, S., Godoi, F. C., & Bhandari, B. (2019). Effect of additives on thermal, rheological and tribological properties of 3D printed dark chocolate. *Food Research International*, 119, 161-169. The core content of this publication was incorporated as Chapter 5.

Contributors	Statement of contribution
Sylvester Mantihal (Candidate)	Designed experiments (75%) Carried out experiments (100%) Analysed experimental data (70%) Wrote the paper (70%)
Bhesh Bhandari (thesis principal advisor)	Designed experiments (20%) Analysed experimental data (15%) Edited the paper (15%)
Sangeeta Prakash (thesis co-advisor)	Designed experiments (5%)

	Analysed experimental data (10%) Edited the paper (10%)
Fernanda Condi de Godoi	Analysed experimental data (5%) Edited the paper (5%)

Mantihal, S., Prakash, S., & Bhandari, B. (2019). Textural modification of 3D printed dark chocolate by varying internal infill structure. *Food Research International*, 121, 684-657. The core content of this publication was incorporated as Chapter 6.

Contributors	Statement of contribution
Sylvester Mantihal (Candidate)	Designed experiments (75%) Carried out experiments (100%) Analysed experimental data (80%) Wrote the paper (70%)
Bhesh Bhandari (thesis principal advisor)	Designed experiments (25%) Analysed experimental data (15 %) Edited the paper (20%)
Sangeeta Prakash (thesis co-advisor)	Analysed experimental data (5%) Edited the paper (10%)

Mantihal, S., Prakash, S., & Bhandari, B. (2019). Texture modified 3D printed dark chocolate: sensory evaluation and consumer study. *Journal of Texture Studies*, 50(5), 386-399. The core content of this publication was incorporated as Chapter 7.

Contributors	Statement of contribution
Sylvester Mantihal (Candidate)	Designed experiments (75%) Carried out experiments (100%) Analysed experimental data (80%) Wrote the paper (75%)
Bhesh Bhandari (thesis principal advisor)	Designed experiments (25%) Analysed experimental data (15 %) Edited the paper (20%)
Sangeeta Prakash (thesis co-advisor)	Analysed experimental data (5%) Edited the paper (5%)

Submitted manuscripts included in this thesis

No submitted manuscripts included in this thesis.

Other publications during candidature

a. Peer-reviewed papers:

Mantihal, S., Prakash, S., Godoi, F. C., & Bhandari, B. (2017). Optimization of chocolate 3D printing by correlating thermal and flow properties with 3D structure modeling. *Innovative Food Science & Emerging Technologies*, 44(Supplement C), 21-29.

Mantihal, S., Prakash, S., Godoi, F. C., & Bhandari, B. (2019). Effect of additives on thermal, rheological and tribological properties of 3D printed dark chocolate. *Food Research International*, 119, 161-169.

Mantihal, S., Prakash, S., & Bhandari, B. (2019). Textural modification of 3D printed dark chocolate by varying internal infill structure. *Food Research International*, 121, 684-657.

Mantihal, S., Prakash, S., & Bhandari, B. (2019). Texture modified 3D printed dark chocolate: sensory evaluation and consumer study. *Journal of Texture Studies*, 50(5), 386-399.

b. Conference abstract and presentation:

Mantihal, S., Prakash, S., & Bhandari, B. (2018). Textural modification of 3D printed dark chocolate by varying internal infill structure. *In 19th World Congress of Food Science and Technology (IUFoST 2018)*; Mumbai, India, 23 – 28 October, 2018 (poster presentation).

Contributions by others to the thesis

Prof Bhesh Bhandari and Dr. Sangeeta Prakash, contributed to the conception and design of the project as a whole, provided advice, critically reviewed the thesis content and conclusion.

The experimental works for sensorial analysis was conducted in sensory analysis laboratory, The University of Queensland with the assistance from Dian Widya Ningtyas. The distribution of

questionnaire (during 3D printer display) was assisted by Zhenbin Liu, Bhaskar Adhikari, Arianna Zambrano, Naomi Vinden and Dr. Su Hung Ching.

Statement of parts of the thesis submitted to qualify for the award of another degree

No works submitted towards another degree have been included in this thesis

Research Involving Human or Animal Subjects

No animal subjects were involved in this research. Human subjects, as trained panellist, were involved in this study and has been approved by Human Research Ethics Committees (2019001010) at the University of Queensland.

Acknowledgements

I received a tremendous helps, support and guidance from different persons in the course of my HDR study in the University of Queensland, Australia. First of all I would like to express my sincere gratitude to my HDR advisors:

- (i) Professor Bhesh Bhandari, who is my principal advisor, for his excellent mentorship, support and kind guidance. I gained new knowledge and improved my communication and writing skills.
- (ii) Dr Sangeeta Prakash, who is my co-advisor, for her kindness and support during my candidature. Their unfailing interest in my research throughout my Ph.D. has always inspired me to work to reach the pinnacle of success.

I thank Dr Fernanda Condi de Godoi, for her ideas, suggestions and feedback and her help to review my research chapters.

I also thank my thesis review committee members, Associate Professor Tony Howes and Dr Van Ho for their suggestions and feedback during milestone reviews. I express my sincere gratitude and appreciation to the Ministry of Education, Malaysia and the Universiti Malaysia Sabah for providing a 'Skim Latihan Akademik IPTA (SLAI)' scholarship for my HDR study. Also appreciation to the Dean of Faculty of Food Science and Nutrition (FSMP), Universiti Malaysia Sabah, Prof. Shariffudin for his constants support. I would also like to thank The University of Queensland for providing a Research Higher Degree Scholarship during my extension for a period of 3 months.

I would like to thank Kaye Hunt for her ongoing help and advice during my candidature.

I would like to thank Dr Polly Burey and Dr Phoung Thi Mac Nguyen for their technical supports with training on instruments and procedures. I also express my sincere thanks to all the members of Food Research Group and my friends in School of Agriculture and Food Sciences (Boon-Beng, Chun Hoong, Nguyen Nhiep, Crystal Concepcion, Dian Widya Ningtyas, Su Hung Ching) for their constant encouragement, advice, fun time and help in every possible way. My heartfelt thanks to my late father, thank you very much "Pak". And to my mother and sisters for their support that gives me the strength to accomplish my study.

Lastly, to my supportive partner Mark Shewan and his family, I express my sincere gratitude and appreciation for all the help, support and family time during my stay in Australia.

Financial support

This research was supported by a ‘Skim Latihan Akademik IPTA (SLAI)’ Scholarship by the Ministry of Education, Malaysia and the Universiti Malaysia Sabah, Malaysia.

This research was also supported by The University of Queensland through UQ Research Training Scholarship - Tuition fee offset and living stipend for 3 months.

Keywords

3D food printing technology, 3D printed chocolate, printing parameters, additives, thermal properties, rheology, tribology, sensory analysis, texture modification, infill pattern, infill percentage, consumer perception, consumer attitudes.

Australian and New Zealand Standard Research Classifications (ANZSRC)

ANZSRC code: 090899, Food Sciences 50%

ANZSRC code: 090805, Food Processing 50%

Fields of Research (FoR) Classification

FoR code: 0908, Food Sciences, 100%

Table of content

3D food printing: Assessing the printability of dark chocolate	i
Sylvester Bin Mantihal.....	i
Master of Foodservice Management	i
Bachelor (Hons) Foodservice Management	i
Abstract	i
Declaration by author	iii
Publications included in this thesis.....	iv
Submitted manuscripts included in this thesis.....	vi
Other publications during candidature.....	vi
Contributions by others to the thesis.....	vi
Statement of parts of the thesis submitted to qualify for the award of another degree	vii
Research Involving Human or Animal Subjects.....	vii
Financial support	ix
Keywords.....	ix
Australian and New Zealand Standard Research Classifications (ANZSRC).....	x
Fields of Research (FoR) Classification.....	x
Table of content.....	xi
List of Figures	xvii
List of Tables	xxi
List of Abbreviation	xxiii
Chapter 1 - Introduction.....	1
1.1 Background	1
1.2 Research aims and objectives	4
1.3 Objectives	4
1.4 Hypotheses.....	4
1.5 Expected outcomes and further application.....	5
1.5.1 Outline of the Dissertation	5

1.5.2 Chapter 1: Introduction	5
1.5.3 Chapter 2: Literature review	5
1.5.4 Chapter 3: 3D Printer modification and development of printing method for powdered chocolate	5
1.5.5 Chapter 4: Optimization of chocolate 3D printing by correlating thermal and flow properties with 3D structure modelling	6
1.5.6 Chapter 5: Effect of additives on thermal, rheological and tribological properties of 3D printed dark chocolate	6
1.5.7 Chapter 6: Textural modification of 3D printed dark chocolate by varying internal infill structure	6
1.5.8 Chapter 7: Sensory evaluation and consumer perception of 3D printed dark chocolate	6
1.5.9 Chapter 8: Conclusions and future recommendations	7
1.6 References.....	7
Chapter 2 - Literature review.....	10
2.1 Introduction.....	10
2.2 3D food printing techniques.....	11
2.2.1 Liquid binding	13
2.2.2 Selective laser sintering / hot air sintering	14
2.2.3 Extrusion method.....	15
2.3 The application of food additives in 3D food printing	16
2.4 Printable food materials	17
2.4.1 Sugar	17
2.4.2 Gelatine	18
2.4.3 Dough.....	19
2.4.4 Chocolate	20
2.5 3D printing as the tool to fabricate food texture	23
2.6 Consumer perceptions about 3D food printing	24
2.6.1 Sensory perceptions of 3D printed food products	25
2.6.2 Knowledge about 3D food printing	25

2.6.3 Perceived benefits	26
2.7 3D printing technology for food: Current status and future prospects	26
2.7.1 Application of 3DP for the individual user	27
2.7.2 Application of 3DP in small scale food production – restaurants, cafés, bakeries	28
2.7.3 Application of 3DP in industrial scale food production	28
2.7.4 Potential application of 3D food printing in hospitality industry	28
2.8 Conclusion	29
2.9 References	31
Chapter 3 - 3D Printer modification and development of printing method for powdered chocolate	37
3.1 Introduction	38
3.2 Materials and methods	39
3.2.1 Chocolate powder	39
3.2.2 3D printer	39
3.2.3 3D Printing design and software	40
3.2.4 Temperature profile of extruded chocolate	41
3.2.5 Statistical analysis	41
3.3 Results and discussion	41
3.3.1 Modification of printer bed and development of cold water circulation system	41
3.3.2 Printer bed stabiliser (support)	43
3.3.3 Addition of air blowing fan	44
3.3.4 3D model design	44
3.3.5 Optimization of nozzle height	45
3.3.6 Temperature profile of extruded chocolate	46
3.3.7 Chocolate printing	48
3.4 Conclusion	49
3.5 References	50
Chapter 4 - Optimization of dark chocolate 3D printing by correlating thermal and flow properties with 3D structure modelling	52

4.1 Introduction.....	53
4.2 Material and Methods.....	55
4.2.1 Supply material (ink) preparation.....	55
4.2.2 Melting point of chocolate before and after printing.....	55
4.2.3 Rheological measurement.....	56
4.2.4 Design and 3D printing of chocolate.....	56
4.2.5 Weight and dimension of 3D printed chocolate.....	58
4.2.6 Printing rate.....	58
4.2.7 Snap force of printed chocolate.....	58
4.2.8 Statistical analysis.....	59
4.3 Results and discussion.....	59
4.3.1 Flow behaviour of the chocolate.....	59
4.3.2 Thermal properties of chocolate.....	61
4.3.3 Evaluation of 3D printed geometry.....	64
4.3.4 Measurement of 3D printed constructs diameter and weight.....	64
4.3.5 Measurement of wall thickness and height.....	66
4.3.6 Printing rate.....	67
4.3.7 Mechanical strength of 3D constructs as a function of support structure.....	68
4.4 Conclusion.....	70
4.5 References.....	71

Chapter 5 - Effect of additives on thermal, rheological and tribological properties of 3D printed dark chocolate 73

5.1 Introduction.....	74
5.2 Material and Methods.....	76
5.2.1 3D design.....	76
5.2.2 3D printing of chocolate.....	77
5.2.3 Differential Scanning Calorimetry (DSC) analysis.....	77
5.2.4 Rheological Measurement.....	78
5.2.5 Measurement of tribology property of 3D printed chocolate.....	78

5.2.6 Statistical analysis.....	78
5.3 Results and discussion.....	78
5.3.1 Characterisation of thermal properties of 3D printed chocolate samples	79
5.3.2 Flow behaviour measurement	81
5.3.3 Tribological behaviour of chocolate.....	88
5.4 Conclusion.....	90
5.5 References.....	91
Chapter 6 - Textural modification of 3D printed dark chocolate by varying internal infill structure	95
6.1 Introduction.....	96
6.2 Materials and methods.....	98
6.2.1 Materials.....	98
6.2.2 Chocolate casting procedure	98
6.2.3 3D-chocolate printing	99
6.2.4 Shape fidelity and weight measurements of 3D printed chocolate	100
6.2.5 Textural characterisation of 3D printed chocolate	100
6.2.6 Statistical analysis.....	101
6.3 Results and discussion.....	101
6.3.1 Visual appearance of 3D printed chocolate	101
6.3.2 Dimensional evaluation of 3D printed chocolate	102
6.3.3 Voids of 3D printed chocolate	106
6.3.4 Mechanical strength of the 3D printed dark chocolate	109
6.4 Conclusion.....	113
6.5 References.....	114
Chapter 7 - Texture-modified 3D printed dark chocolate: Sensory evaluation and consumer perception study.....	117
7.1 Introduction.....	118
7.2 Materials and Method.....	120
7.2.1 Materials.....	120

7.2.2 Commercial dark chocolate casting process	121
7.2.3 Printing process	121
7.2.4 Dimensional and weight measurement of 3D printed chocolates	123
7.2.5 Texture properties of 3D printed chocolate	123
7.2.6 Sensory evaluation.....	123
7.2.7 Consumer survey	124
7.2.8 Statistical analysis.....	126
7.3 Results and Discussion	127
7.3.1 Evaluation of dimensional properties and weight of 3D printed chocolate.....	128
7.3.2 Textural evaluation of 3D printed and cast chocolate	130
7.3.3 Sensory evaluation of 3D printed dark chocolate.....	132
7.3.4 Consumer survey	134
7.4 Conclusion	141
7.5 References.....	142
Chapter 8 - General conclusions and recommendations	146
8.1 General conclusions	146
8.2 Recommendations for future research.....	150
Appendices	151
Appendix A. Supplementary figures for chapter 6	152
Appendix B. Supplementary tables for chapter 7	154
Appendix C. Institutional Human Research Ethics Approval.....	158

List of Figures

Figure 2.1: Schematic representation of steps from CAD design to final 3D printed construct.	11
Figure 2.2: 3DP application based on the state of materials (powder, semi-solid or paste)	13
Figure 2.3: Schematic diagram of SLS and LB process adapted from (Godoi et al., 2016).	14
Figure 2.4: Schematic diagram of 3D fused deposition process.....	16
Figure 2.5: 3D construct made by selective hot air sintering and melting (SHASAM) (a) SHASAM process (b) toroidal coil sculpture made of granulated sugar (Oskay & Edman, 2006). These images were reproduced from the data available at http://candyfab.org/ (c) Complex sugar geometry with fine colour detail (d) colourful sugar candies. These images were reproduced from the data available at http://www.3dsystems.com/culinary/gallery	18
Figure 2.6: 3D printed lemon juice gel printed at 24 mm ³ /s extruder rate, 1.0 mm nozzle size (a) anchor (b) gecko (c) snowflake (d) ring (e) pyramid. Adapted from Yang et al. (2018).	19
Figure 2.7: Representative images of dough printed using the Porimy 3D printer with various sucrose compositions (a) 3.3/100 g of formulation; (b) 5.0/100 g of formulation; (c) 6.6/100 g of formulation; (d) 8.2/100 g of formulation. Adapted from Yang et al. (2018).	20
Figure 2.8: Temperature regimes in different phases of tempering process: Phases I – IV.....	22
Figure 2.9: 2D printed chocolate with an intricate design produced by ChocEdge (a) Heart-in-heart shape (b) Hearts in Christmas tree (c) Heart in chicken. These images were reproduced from the data available at http://chocedge.com/gallery.html	23
Figure 2.10: Application of 3D food printing technology at three scales.	27
Figure 3.1: Schematic diagram of Porimy 3D chocolate printer printing mechanism (1. Information and control display screen, 2. Navigation knob, 3. SD card slot, 4. Printer bed, 5. Printer hopper, 6. Nozzle, 7. Heating component).	40
Figure 3.2: Flow diagram of the chocolate 3D printing process, starts with 3D design and proceeds to 3D printing process.	41
Figure 3.3: Cooling printer bed made in this study. The recirculation tubes (diameter 0.8 cm total 80 cm length) are enclosed as heat exchanger inside the plate.	42
Figure 3.4: Schematic diagram of water circulation system with a 12W submerged pump.	42
Figure 3.5: 3D chocolate printing system with additional feature (a) water circulation system (b) custom printer bed.....	43
Figure 3.6: Printer bed support printed using 3D filament printer (XYZ printing) with ABS filament.	43
Figure 3.7: Attachment of USB fan (2.25 W) on the 3D Porimy printer.	44
Figure 3.8: TinkerCad 3D online software. Available at https://www.tinkercad.com	45

Figure 3.9: Schematic illustration of effect of distance between nozzle tip and printer bed [nozzle size 0.78 mm, printing speed 70 mm/s, printer bed temperature ~ 16 °C and nozzle height (a) 0.5 mm (b) 1.0 mm (c) 0.78 mm].	46
Figure 3.10: Heart-in-heart 3D printed chocolate. (a) Three points (P1, P2 and P3) to determine extruded layer temperature (b) Recorded temperature (°C) on four point of extruded layer of heart-in-heart 3D shape after printing complete. (nozzle internal diameter: 0.78 mm, printing speed: 70 mm/s, printing time: 24 minutes, layer count: 12, temperature probe diameter; 0.26 mm, printer bed temperature: ~ 16 °C , ambient temperature: ~ 25 °C).	46
Figure 3.11: 3D chocolate printed using Porimy 3D printer (a) mickey mouse shape (b) heart shape (c) box with hollow square hole (d) cylinder shape. (Printing condition: Speed 70mm/s, Nozzle size 0.78mm and extrusion temperature 32 °C).	48
Figure 3.12: The effect of improper temperature setting on dark chocolate after extrusion (a) extruded chocolate at high temperature (>36 °C) (b) chocolate was not solidified and collapsed during extrusion.	49
Figure 4.1: 3D model design of hexagonal model with (a) cross support (b) parallel support (c) no support.	56
Figure 4.2: Schematic diagram of Porimy 3D chocolate printer and its printing mechanism.	57
Figure 4.3: Illustration of positioning of three different designs of printed chocolates for snap properties analysis by the texture analyser.	58
Figure 4.4: Apparent viscosity of (a) chocolate without Mg-ST (b) chocolate with Mg-ST measured at temperature ramp from 25 °C to 32 °C for 10 minutes at shear rate 100s ⁻¹ .	59
Figure 4.5: Apparent viscosity versus time of chocolate measured at 32 °C for 10 minutes at (a) 50s ⁻¹ and (b) 100s ⁻¹ for chocolate with Mg-ST.	60
Figure 4.6: DSC melting curves (at a heat scanning rate of 2 °C/min) of chocolate without magnesium stearate and added with magnesium stearate (5% w/w of total mixture).	62
Figure 4.7: Three model designs of printed 3D chocolates (a) hexagonal shape with cross-support (b) hexagonal shape with parallel support (c) hexagonal shape with no support.	64
Figure 4.8: Three model designs of printed 3D chocolates dimensions (diameter, height and wall thickness).	66
Figure 4.9: Force-distance curves measured by texture analyser of 3D printed chocolate with (a) cross support (b) parallel support (c) no support using break probe with a test speed 2.0 mm/s.	70
Figure 5.1: Graphic illustration of (a) 3D design from 3D software (b) 3D sliced design using Sli3er software and (c) Actual 3D printed chocolate.	76
Figure 5.2: Representative graphs of apparent viscosity as a function of temperature ranging from 25 °C to 40 °C of chocolate from (a) printer hopper (b) 3D printed chocolate. [Mg-ST: Magnesium Stearate and PS: Plant Sterol].	82
Figure 5.3: Representative graphs of apparent viscosity at 32°C as a function of shear rate from 0.1 to 100 (1/s) of chocolate from (a) printer hopper (b) 3D printed chocolate [Mg-ST: Magnesium Stearate and PS: Plant Sterol].	83

Figure 5.4: Shear stress as a function of shear rate ranging from 0.1 to 150 (1/s) at a constant temperature of 32°C of the chocolate sample from (a) printer hopper (b) 3D printed chocolate. [Mg-ST: Magnesium Stearate and PS: Plant Sterol]. Small screen in Figure represent the shear stress as a function of shear rate at 0 to 10 (1/s).	86
Figure 5.5: The coefficient of friction curve as a function of sliding speed of 3D printed chocolate with a constant temperature of 35 °C.	88
Figure 6.1: The self-made 3D chocolate mould generated from TinkerCad software and printed using Da Vinci 2.0 dual nozzle model XYZ printer with ABS filament.	99
Figure 6.2: 3D design of round shape (40 mm diameter) with (a) Star infill (b) Honeycomb infill (c) Hilbert curve infill patterns with a variation of infill density of 5%, 30%, 60% and 100%.	100
Figure 6.3: Illustration of positioning the 3D printed chocolate samples for snap properties analysis by the texture analyser (a) lateral view and (b) Anterior view.	101
Figure 6.4: Representative pictures of 3D printed chocolate samples. The letter signify chocolate formulation (a) Choc-1_control (b) Choc-2_Control (c) Choc-2+MgST and (d) Choc-2+PS. Numerical (in a row) represent the infill patterns (1) Hilbert curve (2) honeycomb (3) star. IP means Infill percentage.	102
Figure 6.5: Representative graph of 3D printed chocolate as increase infill percentage (5%, 30%, 60% and 100%) as a function of the mean value of weight (g).	104
Figure 6.6: Representative graph of the relationship between void fraction (%) and weight of 3D printed chocolate samples with infill percentage of 5%, 30% and 60% and infill patterns of Star, Hilbert curve and Honeycomb, of all chocolate samples; Cadbury dark chocolate (Choc-1), Callebaut dark chocolate (Choc-2), Callebaut dark chocolate incorporated with Magnesium stearate (Choc-2 + MgST) and Callebaut dark chocolate incorporated with Plant sterol (Choc-2 + PS).	109
Figure 6.7: Representative graph of force (N) as a function of distance (mm) of 3DP chocolate printed in various infill pattern with various infill percentage (a) 5 % (b) 30 % and (c) 60 % (d) 100 % and (e) cast sample with a pre-test speed of 1.0 mm/s and test speed 2.0 mm/s with 5.0g of trigger load of all chocolate sample (i) Choc-1 (ii) Choc-2 (iii) Choc-2+Mg-ST and (iv) Choc-2+PS. Red lines mean the maximum force (N) recorded for 3D printed samples.	110
Figure 6.8: Representative image infill pattern of (a) Hilbert curve-HC (b) honeycomb -HNY (c) Star that applied in printing chocolate.	112
Figure 7.1: The 3D cast printed using Da Vinci 2.0 dual nozzle model XYZ printer with ABS filament.	121
Figure 7.2: 3D model designs of rectangular shape (a) Model -1(20 mm x 50 mm and 5 mm thickness) with Honeycomb pattern in variation of infill density of 25%_IP, 50%_IP and 100%_IP (b) Model-2 (43.5 mm x 35.5 mm and 5 mm thickness) in rectilinear pattern with 100%_IP. IP refers to infill percentage.	122
Figure 7.3: Schematic illustration of Shinnove dual nozzle 3D printer and its components.	123
Figure 7.4: Various shapes, designs and internal structures (infill patterns and percentages) of 3D printed chocolates used in display session.	126

Figure 7.5: Representative images of 3D printed and cast chocolate samples – target geometry as reference. (a) Choc-1 is Cadbury dark chocolate – one sample was printed in 100% infill with rectilinear infill pattern, and the other is a cast sample. (b) Choc-2 is the Callebaut dark chocolate printed in various infill percentages, 25%, 50% and 100%, with a honeycomb infill pattern. IP means infill percentage. 128

Figure 7.6: Representative graphs of force (N) as a function of distance (mm) of 3DP chocolate printed and cast for samples (a) Choc-1 with 100% infill for 3DP (rectilinear pattern) and (b) Choc-2 samples various infill percentages of 25%, 60%, and 100% (honeycomb pattern) with a pre-test speed of 1.0 mm/s and test speed 2.0 mm/s with 5.0g of trigger load of all chocolate. 130

Figure 7.7: Distribution of the consumer preferences for texture for 3D printed Choc-1 in 100% infill and cast chocolate block. 134

Figure 7.8: Willingness of respondents (n=244) to have a 3D food printer at home. 139

List of Tables

Table 2.1: Additive manufacturing process categories classified by (ASTM, 2015).	12
Table 2.2: Crystal forms in cocoa butter.	21
Table 3.1: Recorded temperature (°C) of extruded layer of Heart-in-heart 3D shape during printing process denote as point 1 (P1), point 2 (P2) and point 3 (P3) based from the point indicated in Figure 3.10 (a).	47
Table 4.1: Sample dimensions for each chocolate design (model a, b and c) wall thickness was 2.0 mm for all samples.	57
Table 4.2: DSC data onset (T_o), peak (T_p), endset (T_c) and enthalpy ΔH	63
Table 4.3: Comparison between the designed and printed chocolate constructs.	65
Table 4.4: Mean value of wall thickness (mm) of 3D constructs according to sample diameter.	66
Table 4.5: Mean value of height (mm) of 3D constructs according to sample diameter.	67
Table 4.6: Mean value of printing rate (g/min) as a function of diameter of 3D chocolate constructs.	68
Table 4.7: Mean value of Force (N) required to break chocolate sample according to the type of support.	69
Table 5.1: DSC data of the melting peak (T_p), and enthalpy ΔH of chocolate samples from printer hopper and 3D printed sample.	79
Table 5.2: Apparent viscosity of dark chocolates at 32 °C (1) printer hopper and (2) 3D printed chocolate (measured at a constant shear rate of 100 s ⁻¹).	84
Table 5.3: Summary of rheological properties of chocolate samples (at 32°C) from printer hopper and 3D printed chocolate determined by Herschel-Bulkley model.	86
Table 6.1: The weight of 3D printed chocolate with infill density of 5 %, 30 %, 60 %, 100 % with various infill patterns and cast. Cadbury dark chocolate (Choc-1) was without any additive while Callebaut dark chocolate (Choc-2), Callebaut dark chocolate was incorporated with Magnesium stearate (Choc-2 + Mg-ST) and Plant sterol (Choc-2 + PS).	103
Table 6.2: The height of 3D printed chocolate with infill density of 5 %, 30 %, 60 %, 100 % with various infill patterns and cast. Cadbury dark chocolate (Choc-1) was without any additive while Callebaut dark chocolate (Choc-2), Callebaut dark chocolate was incorporated with Magnesium stearate (Choc-2 + Mg-ST) and Plant sterol (Choc-2 + PS).	105
Table 6.3: The diameter of 3D printed chocolate with infill density of 5 %, 30 %, 60 %, 100 % with various infill patterns and cast. Cadbury dark chocolate (Choc-1) was without any additive while Callebaut dark chocolate (Choc-2), Callebaut dark chocolate was incorporated with Magnesium stearate (Choc-2 + Mg-ST) and Plant sterol (Choc-2 + PS).	105
Table 6.4: Void fractions of 3D printed chocolate with infill density of 5 %, 30 %, 60 %, 100 % with various infill patterns and cast. Cadbury dark chocolate (Choc-1) was without any additive while	

Callebaut dark chocolate (Choc-2), Callebaut dark chocolate was incorporated with Magnesium stearate (Choc-2 + Mg-ST) and Plant sterol (Choc-2 + PS).....	107
Table 6.5: Recorded force (N) to break 3D printed chocolate with different patterns and various infill percentage (5%, 30%, 60% and 100%), and cast samples.	111
Table 7.1: Recorded dimensional properties (thickness, width, length) and weight of 3D printed Choc-1 with 100% infill (rectilinear pattern) and cast samples, and Choc-2 samples with infill of 25%, 50%, and 100% (honeycomb pattern).....	129
Table 7.2: Recorded force (N) to break the chocolate samples with various infill percentages (25%, 50%, and 100%), and cast samples.	131
Table 7.3: Recorded median and p-value of ranking of preferences (appearance, hardness and overall preferences) based on Friedman test for 3DP chocolate printed in various infill percentages (25%, 50%, and 100%).....	132
Table 7.4: Descriptive analysis of knowledge about 3D printing ($\alpha = 0.61$).....	135
Table 7.5: Recorded frequency of understanding of 3DFP. Pearson Chi-Square (X^2) derived from cross-tabulation of “I have heard/read and understand about 3D printing” and each question in Section 1b.....	136
Table 7.6: Descriptive analysis of perception of 3DFP benefits. Pearson Chi-Square (X^2) derived from cross-tabulation of “I have heard/read and understand about 3D printing” and seven questions in Section 3. ($\alpha = 0.784$).....	138
Table 7.7: Measure of perception of 3D printed chocolate including means and standard deviations (M=Mean, SE=Standard Error and SD=standard deviation).	139
Table 7.8: Measure of attitude toward 3D printed food, including means and standard deviations.	140

List of Abbreviation

ASTM	American Society of Testing and Materials
3DFP	3-dimension food printing
AM	Additive manufacturing
HME	Hot melt extrusion
HAS	Hot air sintering
SLS	Selective laser sintering
FDM	Fused deposition modelling
LB	Liquid binding
STL	stereolithographic file
CAD	Computer-aided design
ABS	Acrylonitrile Butadiene Styrene
PLA	Polylactic Acid
HNY	Honeycomb pattern
HC	Hilbert curve pattern
PS	Plant sterol
Mg-ST	Magnesium stearate
Choc-1	Cadbury dark chocolate
Choc-2	Callebaut dark chocolate
IP	Infill percentage
MPa	Mega Pascal
Pa.s	Pascal per second
SD	Standard deviation
Min	minutes
N	Newton
COF	Coefficient of friction

Chapter 1 - Introduction

1.1 Background

3D printing is a layer-by-layer three dimensional building process (Wegrzyn, Golding, & Archer, 2012). The process operates in a similar way to printing on a paper from a word processor program on a personal computer, except that it is in 3D. That is to say, in 2D printing, the image or text is printed row by row until it is complete across a length and width in a single layer (or a few layers in bold font function). However, the process of 3D food printing involves food grade products such as sugar, starches, or protein to create an edible printed food (van der Linden, 2015; Zimmerman, Walczyk, Crump, & Batchelder, 2012). In essence, printing food is done through the careful layering of tiny or thin semi-liquid food particles on top of each other to create a 3-dimensional novel processed food (Lam, Mo, Teoh, & Hutmacher, 2002).

There are four methods of AM (1) selective laser sintering, (2) hot air sintering, (3) liquid binding and (4) the extrusion method (Godoi, Prakash, & Bhandari, 2016). In selective laser sintering, a laser beam is directed into a powder bed via a scanner to fuse powder material (Liu, Zhang, Bhandari, & Wang, 2017). Similarly, in hot air sintering, hot air is used to fuse the powder bed. In liquid binding, a drop-on-demand method is used where liquid (a colour or flavour) acts as a binder to a powdered food material (Godoi et al., 2016). However, these methods can only be applied to powdered material such as sugar (Liu et al., 2017; Mumtaz & Hopkinson, 2010). In the extrusion method, material such as a paste, gel or powdered food substrates are useable (Lanaro et al., 2017; Le Tohic et al., 2018; Lee & Yeong, 2015; Z. Liu, Zhang, Bhandari, & Yang, 2018; Siqueira et al., 2017; Fanli Yang, Zhang, Bhandari, & Liu, 2018). Therefore, this makes the extrusion method more favourable for food printing.

3D printing of edible food materials such as chocolate, sugar and confectionery items has become a point of great interest to 3D technology producing companies such as ChocEdge (ChocEdge, 2013; Molitch-Hou, 2015), XYZ Printing (Alec, 2015) and Porimy (Porimy, 2014). These 3D printing manufacturers have all developed extrusion methods for 3D food printing. An extrusion method based on fused deposition modelling (FDM) is commonly used to extrude either hot or cold food through a nozzle (Lanaro et al., 2017). For these, two extrusion techniques that are widely applied are (1) rotary screw rotation and (2) syringe-base extrusion (Liu et al., 2017). In syringe-based extrusion, the piston is driven down gradually by a motor mimicking the injection process and this is more suitable for printing a high viscosity food material (Sun, Zhou, Yan, Huang, & Lin, 2018) than rotary screw

rotation extrusion. Thus a more extensive variety of food could be manipulated in 3D using the injection technique. In rotary screw extrusion, a rotational auger is utilized to dispense food material from the printer hopper (Porimy, 2014).

The rotational auger technique is more suitable for powdered material such as powdered chocolate. In this method, food substrates are more able to be filled as the food reservoirs are larger and attached externally. As the auger moves rotationally, additives can be used to improve the 3D printing performance. Cohen et al. (2009) suggested that hydrocolloids (carbohydrates and protein), starches and sugar could be used to enhance food material printability. For instance, Yang et al. (2018) demonstrated that 15 g potato starch added into 100g of lemon juice was the appropriate composition to produce a 3D printed gel construct. In tablet pharmaceutical production, additives (e.g., magnesium stearate) are added as a lubricant enhancer to reduce a slip effect in the channel and increase surface smoothness (Sugisawa, Kaneko, Sago, & Sato, 2009). Hence, the incorporation of additives is considered necessary in the auger extrusion technique. To incorporate a 3D extrusion technique into food printing, understanding the material characteristics of the ingredients is crucial (Godoi et al., 2016; Dankar et al., 2018). Material properties such as the thermal characteristics and rheology aid to determine essential parameters such as the extrusion temperature and viscosity.

Chocolate is a food with one of the highest potentials for 3D printability due to its relatively lower melting and solidifying temperatures. These characteristics are due to the unique crystalline composition in the chocolate that allows it to solidify after extrusion (Beckett, 2011). Beta (β) crystal, is the most stable crystal nucleated in the chocolate matrix and this form of crystal determines the quality attributes of the chocolate, notably its appearance, texture and snap ability (Afoakawa, 2011). Pre-crystallized chocolate was used in 3D printing as there are more of the stable β -crystals existing in that form of chocolate. Afoakwa (2010) reported that the onset melting point of a stable β -crystal ranges from 33.8 °C to 35 °C. As the 3D printing process does not undergo the same processing steps to produce chocolate (in manufacturing), the extrusion temperature, which is slightly higher than the onset melting temperature (32 °C), needs to be used in the 3D printing process. This way, during the chocolate deposition most of the partially melted β crystals are assumed to be still present in the chocolate and can act as nuclei in the matrix for further stable crystal growth. Faster crystallization of chocolate is essential as it helps the chocolate to solidify and hold its structure post-deposition.

Chocolate is solid and stable at room temperature (20 °C – 25 °C) and melts during consumption at oral temperature, 37 °C (Afoakawa et al., 2008). This condition is due to the milk fat and cocoa butter in chocolate that give its characteristic of smooth suspension (Duizer, 2013). However, other particles

present in the chocolate such as sugar, cocoa solids, milk powder and lecithin also influence the sensory properties of chocolate (Lee et al., 2002). The particle sizes of such added components would affect plastic viscosity, product spread and texture, all of which will influence the mouthfeel (Afoakawa et al., 2008). The rheology and lubrication properties of chocolate are influenced by the texture and composition of the chocolate mixture (Lee et al., 2004). Therefore, rheological and tribological analyses are crucial to determine the quality attributes of 3D printed chocolate.

In order to introduce new types of chocolate products into the market, it is necessary to develop a new internal structure and texture to the chocolate itself before 3D printing. However, there is no study on chocolate printing that has produced a 3D printed construct with a varying internal structure, as most previous research has concentrated on chocolate printing parameters. For instance, Hao et al. (2010) focused on printing parameters for chocolate extrusion using a ChocALM 3D printer. They reported that a 1.25 mm diameter of nozzle size and a nozzle height of approximately 2.9 mm were the optimal parameters to provide good bonding between interlayers to sustain an accurate square geometry. Also, they determined an axis-movement rate of 253 and an extrusion rate of 215 set in the ChocALM 3D software would provide a better printed chocolate. Lanaro et al. (2017) demonstrated that printer movement speeds ranging from 300 to 700 mm/min and an extrusion rate of 10-20% were the optimum parameters to improve the extruded chocolate spanning distance. Also, they found the spanning distance improved by directing air (lowering the air temperature by approximately 3.5 °C) during printing.

To date, there is still a limited body of work on food texture modification for use with 3D printing. Severini, Derossi, and Azzollini (2016) demonstrated that a support structure aids in building intricate 3D items. Textural modification of the product is possible by 3D printing as it allows the manipulation of the internal structure by controlling the infill percentage and also the order of the layers (infill pattern). As infill percentages influence the mechanical strength of a printed product (Le Tohic et al., 2018; Tang Dan, Khodos, Khairallah, Ramlal, & Budhoo, 2018), it will affect the texture of the 3D printed items and the consumers' sensory perception of them. It is worth noting that 3D printing technology is a promising technique that can produce chocolate with an advanced textural property. From the consumers' perspective, this technology is considered a new one in food production. Brunner, Delley, and Denkel (2018) reported that due to the lack of knowledge and misunderstandings about the 3D food printing (3DFP) concept, negative attitudes were found to hinder the consumers' acceptance of this novel food production technology. Therefore, a credible source of information and the perceived benefit of this new technology should be presented to influence consumers' acceptance (Bruhn, 2007).

As described above, in the past, the research on chocolate printability has been focused on the optimization of printing parameters and design construction (Godoi et al., 2016; Hao et al., 2010). However, this study emphasizes material characterization and controlling the mechanical strength of the 3D printed chocolate by altering the infill structure, sensorial evaluation and determining consumer awareness and perceptions about 3DFP.

1.2 Research aims and objectives

The goals of this study are to investigate the chocolate printability and the applicability of 3-dimensional food printing technology for manipulating the textural properties of dark chocolate.

1.3 Objectives

This research work comprises the following research objectives:

1. Modification of a 3D printer to optimize printing conditions.
2. Optimization of chocolate printing parameters by assessing thermal and rheological properties of chocolate.
3. Study of the effect of additives on the thermal properties, rheology and tribology of 3D printed chocolate.
4. Assessment of the textural modification of 3D printed dark chocolate by varying the infill structure.
5. Assessment of the overall acceptance of 3D printed chocolate by consumers through sensory analysis and an appraisal of consumer awareness of 3DFP.

1.4 Hypotheses

1. Modification of the 3D printer and optimization of parameters in chocolate printing are essential to produce an excellent 3D printed construct.
2. Inclusion of food additives may enhance the printability of powdered chocolate to achieve a better flowability during the auger-extrusion type of printing.
3. Modification of the textural properties of 3D printed chocolate is achievable by manipulating infill percentages and patterns.
4. Consumers may prefer texture-modified dark chocolate and may demonstrate a positive perception of 3D food printing technology.

1.5 Expected outcomes and further application

From this study, a better printable 3D chocolate will be achieved by combining its results with a modification and optimization of applicable printing parameters of the 3D printer. Obtaining a well-defined 3D printed chocolate with modification in infills will create a distinctive textural property. The sensory analysis conducted will ensure the success of textural modification. Hence, the 3D printing of chocolate will be a potentially appealing technology to be applied in the food production sector as an alternative to the conventional current practice of chocolate moulding.

1.5.1 Outline of the Dissertation

There are eight chapters in this thesis. The first chapter (Chapter 1) is a general introduction to the research. The second chapter (Chapter 2) includes the literature review. The research conducted for the project is presented in five consecutive chapters from Chapters 3 to 7 and are presented in a format of journal manuscripts. The final chapter (Chapter 8) is a general conclusion. It also provides recommendations for future works related to this research.

1.5.2 Chapter 1: Introduction

This chapter provides the background of the research. It explains the concept and the application of 3D printing into edible ink in general and how this thesis will explore the capability to produce 3D printed dark chocolate, the effect of additives in chocolate extrusion, textural modification and consumer perception towards 3D food printing technology.

1.5.3 Chapter 2: Literature review

Chapter 2 covers the review of literatures related to 3D printing technology and the emerging of this technology into food. It includes the description of several printing techniques that apply to edible ink and understanding of 3D technology principle. This chapter also provides an insight of producing a printable food object with modified textural properties and consumer acceptance of 3D printed food.

1.5.4 Chapter 3: 3D Printer modification and development of printing method for powdered chocolate

This chapter aimed to ensure that the extruded chocolate layer solidified within the appropriate time after extrusion. Therefore, a stainless steel printer bed was developed (replacing the acrylic printer bed). A water channel inside the printer bed allowed cold water to flow and enable it to cool the deposited layer to solidify on top of the bed. Addition of air blower aided in circulating air around the printer bed to avoid condensation. Also, a standard printing procedure was developed with proper printing parameters (printing temperature, printing speed, nozzle height).

1.5.5 Chapter 4: Optimization of chocolate 3D printing by correlating thermal and flow properties with 3D structure modelling

In Chapter 4, the optimisation of 3D printing chocolate in relation to thermal and flow properties were conducted. The determination of thermal as well as rheological properties aid in setting up the operational parameters of the 3D printer based on the melting point of chocolate. In this study, the use of flow enhancers was introduced to aid in the extrusion process of chocolate. Also, the work showed that printed samples with an additional support structure was important as self-support mechanism of 3D printed chocolate with large voids.

1.5.6 Chapter 5: Effect of additives on thermal, rheological and tribological properties of 3D printed dark chocolate

In this chapter, the effect of addition of flow enhancers, magnesium stearate (Mg-ST) and plant sterol (PS) into powdered chocolate feed was determined. Thermal, rheology and tribology profile of chocolate samples were analysed. This study also gives a useful insight on the mouthfeel perception for 3D printed chocolate.

1.5.7 Chapter 6: Textural modification of 3D printed dark chocolate by varying internal infill structure

In chapter 4, the texture of chocolate was accessed by varying infill structures of the constructs by 3D printing. Three different infill patterns star, Hilbert curve, and honeycomb were printed in 5%, 30%, and 60% infill densities. Infill density was correlated with the void fraction. Also, a complex infill patterns such as honeycomb and star required a higher force to break the chocolate sample. This study highlighted the influence of different infill configuration on the strength of chocolate structure, which is an essential element in evaluating the texture of the product.

1.5.8 Chapter 7: Sensory evaluation and consumer perception of 3D printed dark chocolate

This chapter included the sensory evaluation of 3D printed dark chocolate and consumer perspective on 3D food printing technology. During the sensory evaluation, panellists were given two sets of printed samples (1) samples with variable infill percentages (2) samples printed in 100% infill percentage and commercial chocolate. An open survey was conducted with a display of a 3D food printer and printed chocolates. A survey questionnaire was distributed to students, staffs and visitors at the University of Queensland premise to obtain consumers' perceptions towards this technology. This study provided a useful information on consumer preferences and their attitude toward 3D food printing.

1.5.9 Chapter 8: Conclusions and future recommendations

The final chapter includes a general conclusion and recommendations for future studies in the subject related to 3D printing of chocolate and other food materials.

1.6 References

- Afoakwa, E. O. (2010). *Chocolate science and technology*(Vol. 687). Oxford: Wiley-Blackwell.
- Afoakwa, E. O., Paterson, A., Fowler, M., & Vieira, J. (2008). Characterization of melting properties in dark chocolates from varying particle size distribution and composition using differential scanning calorimetry. *Food Research International*, 41(7), 751-757.
- Alec. (2015). XYZPrinting shows off their \$500 3D Food Printer at CES 2015 in Las Vegas. Retrieved from <http://www.3ders.org/articles/20150106-xyzprinting-shows-off-their-3d-food-printer-at-ces-2015-in-las-vegas.html>
- Beckett, S. T. (2011). *Industrial chocolate manufacture and use*: John Wiley & Sons.
- Bruhn, C. M. (2007). Enhancing consumer acceptance of new processing technologies. *Innovative Food Science & Emerging Technologies*, 8(4), 555-558.
- Brunner, T. A., Delley, M., & Denkel, C. (2018). Consumers' attitudes and change of attitude toward 3D-printed food. *Food Quality and Preference*, 68, 389-396.
- ChocEdge. (2013). Creation: a Selection of our Chocolate Creations. Retrieved from <http://www.chocedge.com/creations.php>
- Cohen, D. L., Lipton, J. I., Cutler, M., Coulter, D., Vesco, A., & Lipson, H. (2009). *Hydrocolloid printing: a novel platform for customized food production*. Paper presented at the Proceedings of solid freeform fabrication symposium (SFF'09).
- Dankar, I., Haddarah, A., Omar, F. E. L., Sepulcre, F., & Pujolà, M. (2018). 3D printing technology: The new era for food customization and elaboration. *Trends in Food Science & Technology*, 75, 231-242.
- Duizer, L. (2013). Food Oral Processing: Fundamentals of Eating and Sensory Perception. *Trends in Food Science & Technology*, 29(1), 81-82.
- Godoi, F. C., Prakash, S., & Bhandari, B. R. (2016). 3d printing technologies applied for food design: Status and prospects. *Journal of Food Engineering*, 179, 44-54.
- Hao, L., Mellor, S., Seaman, O., Henderson, J., Sewell, N., & Sloan, M. (2010). Material characterisation and process development for chocolate additive layer manufacturing. *Virtual and Physical Prototyping*, 5(2), 57-64.

- Lam, C. X. F., Mo, X., Teoh, S.-H., & Hutmacher, D. (2002). Scaffold development using 3D printing with a starch-based polymer. *Materials Science and Engineering: C*, 20(1), 49-56.
- Lanaro, M., Forrestal, D. P., Scheurer, S., Slinger, D. J., Liao, S., Powell, S. K., & Woodruff, M. A. (2017). 3D printing complex chocolate objects: Platform design, optimization and evaluation. *Journal of Food Engineering*, 215, 13-22.
- Le Tohic, C., O'Sullivan, J. J., Drapala, K. P., Chartrin, V., Chan, T., Morrison, A. P., . . . Kelly, A. L. (2018). Effect of 3D printing on the structure and textural properties of processed cheese. *Journal of Food Engineering*, 220, 56-64.
- Lee, J. M., & Yeong, W. Y. (2015). A preliminary model of time-pressure dispensing system for bioprinting based on printing and material parameters: This paper reports a method to predict and control the width of hydrogel filament for bioprinting applications. *Virtual and Physical Prototyping*, 10(1), 3-8.
- Liu, Zhang, M., Bhandari, B., & Wang, Y. (2017). 3D printing: Printing precision and application in food sector. *Trends in Food Science & Technology*, 69, 83-94.
- Liu, Z., Zhang, M., Bhandari, B., & Yang, C. (2018). Impact of rheological properties of mashed potatoes on 3D printing. *Journal of Food Engineering*, 220, 76-82.
- Molitch-Hou, M. (2015, 30 July 2015). Choc Creator 2.0 Plus Kicks Off 2nd Generation Chocolate 3D Printing. Retrieved from <http://3dprintingindustry.com/2015/07/30/choc-creator-2-0-plus-kicks-off-2nd-generation-chocolate-3d-printing/>
- Mumtaz, K., & Hopkinson, N. (2010). Selective laser melting of thin wall parts using pulse shaping. *Journal of Materials Processing Technology*, 210(2), 279-287.
- Porimy. (2014). Porimy Kunshan Bo Mai Three Dimensional Printing Technology Co., Ltd. Retrieved from <https://translate.google.com.au/translate?hl=en&sl=zh-CN&u=http://www.porimy.com/&prev=sea>
- Severini, C., Derossi, A., & Azzollini, D. (2016). Variables affecting the printability of foods: Preliminary tests on cereal-based products. *Innovative Food Science & Emerging Technologies*.
- Siqueira, G., Kokkinis, D., Libanori, R., Hausmann, M. K., Gladman, A. S., Neels, A., Studart, A. R. (2017). Cellulose Nanocrystal Inks for 3D Printing of Textured Cellular Architectures. *Advanced Functional Materials*, 27(12), 1604619
- Sugisawa, K., Kaneko, T., Sago, T., & Sato, T. (2009). Rapid quantitative analysis of magnesium stearate in pharmaceutical powders and solid dosage forms by atomic absorption: method development and application in product manufacturing. *J Pharm Biomed Anal*, 49(3), 858-861.
- Sun, J., Zhou, W., Yan, L., Huang, D., & Lin, L.-y. (2018). Extrusion-based food printing for digitalized food design and nutrition control. *Journal of Food Engineering*, 220, 1-11.
- Tang Dan, B., Khodos, D. R., Khairallah, O., Ramlal, R., & Budhoo, Y. (2018). *The Effect of the 3-D Printing Process on the Mechanical Properties of Materials*. Paper presented at the Mechanics of Additive and Advanced Manufacturing, Volume 9.

- van der Linden, D. (2015). 3D Food Printing. Retrieved from https://www.tno.nl/media/5517/3d_food_printivanng_march_2015.pdf.
- Wegrzyn, T. F., Golding, M., & Archer, R. H. (2012). Food Layered Manufacture: A new process for constructing solid foods. *Trends in Food Science & Technology*, 27(2), 66-72.
- Yang, F., Zhang, M., Bhandari, B., & Liu, Y. (2018). Investigation on lemon juice gel as food material for 3D printing and optimization of printing parameters. *LWT - Food Science and Technology*, 87, 67-76.
- Yang, F., Zhang, M., Prakash, S., & Liu, Y. (2018). Physical properties of 3D printed baking dough as affected by different compositions. *Innovative Food Science & Emerging Technologies*, 49, 202-210.
- Zimmerman, A., Walczyk, D. F., Crump, S. S., & Batchelder, J. S. (2012). Additive manufacturing system and method for printing customized chocolate confections. In: Google Patents.

Chapter 2 - Literature review

2.1 Introduction

The early concept of 3D printing (3DP) was rapid prototyping (RP), the process of modelling, assembling and fabrication via computer aided design (CAD) which was developed by Kodama from Japan in the late 1980s (3D Printing Industry, 2014). RP technology evolved into AM which is a more advanced form that can construct intricate 3D objects layer-by-layer, either by using plastic polymer filaments, metal and, more recently, edible materials such as sugar and chocolate (Sher & Tutó, 2015). 3D printing has begun to emerge in food production, and 3D food printers have been designed specifically for food fabrication. According to Gibson, Rosen and Stucker (2010) apart from RP, there are some broadly used technologies in AM which are stereolithography (SL), FDM and selective laser sintering (SLS). According to Sun, Peng, et al. (2015) there are a number of research studies and projects in 3D food printing in many areas which range from the development of conceptual ideas to an in-depth understanding of material properties.

The extrusion method is the most favourable technique in 3D food printing (Liu et al., 2017; Yang et al., 2017; Yang et al., 2015; Zoran & Coelho, 2011) as it allows fresh food (in pastes or liquid form) to be shaped. Understanding material properties such as the thermal properties, rheology and tribology of food material is vital in 3DFP (Godoi, Prakash, & Bhandari, 2016; Hao et al., 2010) due to food composition's complexity and its physical properties. Producing a better quality of 3D printed food product relies on how the 3DP process reacts with the specific food materials. For instance, powder based materials such as sugar are compatible with SLS, hot air sintering and liquid binding because powdered particles will bind in the presence of heat or liquid as a binding agent (Diaz, Bommel, Noort, Henket, & Brier, 2014; Godoi et al., 2016). In the extrusion method, food materials need to be in a semi-solid or viscous (Newtonian flow) condition to be easily dispensed through printer nozzles (Chen & Mackley, 2006; Hao et al., 2010). Food modification by the addition of other food ingredients will be necessary to enhance the printability of materials. Therefore, studies to analyse various food's material properties and suitable additives applicable in the 3D food printing process are vital.

3D food printing (3DFP) provides a freedom in design customization, with a personalized and intricate shape (Dankar, Haddarah, Omar, Sepulcre, & Pujolà, 2018). Also, an internal structure within the constructed form will ensure the stability of the printed food. The alteration of the infill structure (infill pattern and infill percentage) could influence the texture properties of these printed

constructions. However, there is still a limited number of studies on the effect of infill structure on the texture of printed food and the current studies are confined to studies on 3D printed mashed potato (Liu et al., 2018) and cheese (Le Tohic et al., 2018). The modified texture of a printed product based on the variation of its infill structure could also influence the sensorial properties of printed food.

This literature review presents the background knowledge on (1) 3D food printing techniques (2) the application of food additives (3) printable food material (4) the modification of the internal structure (5) consumer perceptions of 3D printing technology and (6) 3D printing technology for food – its current status and future prospects.

2.2 3D food printing techniques

The American Society of Testing and Materials (ASTM) group has classified AM processes into seven categories (ASTM, 2015), as described in Table 2.1. The demand for this emerging novel technology continues to increase. According to one Forbes report (adapted from Wohler, 2014) the 3DP industry's value is estimated to escalate to US\$21 billion by the end of 2020. This prediction is based on current and expected successful prototyping operations leading to fully fledged 3DP in many companies (Columbus, 2015). Prominent areas of success include the medical, electronic, automotive and aerospace industries. Among various applications, 3DFP is attractive due to the freedom of design personalization, and the potential for creating new textures (Dankar et al., 2018; Severini, Derossi, Ricci, Caporizzi, & Fiore, 2018). Also, the capability of this technology in producing a small batches allows the customization of food with specific nutritional requirements (Lipton, Cutler, Nigl, Cohen, & Lipson, 2015; Severini, Derossi, & Azzollini, 2016; C. Severini et al., 2018). The basic principle of 3DFP is that a 3D model is generated using a three dimensional CAD system. Then, the generated model file (.stl) is transferred to slicing software prior to the printing process (see Figure 2.1).

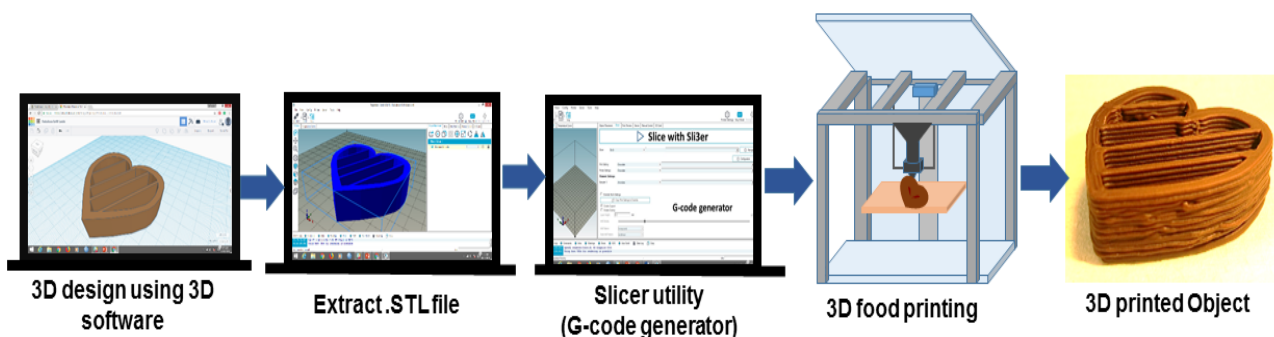


Figure 2.1: Schematic representation of steps from CAD design to final 3D printed construct.

Table 2.1: Additive manufacturing process categories classified by (ASTM, 2015).

Process type	Description	Related technologies
Powder bed fusion	Thermal energy selectively fuses regions of a powder bed	Electron beam melting (EBM) SLS Selective heat sintering (SHS)
Directed energy deposition	Thermal energy is applied to fuse materials by melting upon extrusion	Laser metal deposition (LMD)
Material extrusion	Material is dispensed through a nozzle or orifice	FDM
Binder jetting	A liquid bonding agent is selectively deposited to join powder materials, and then product is baked in an oven for final curing	Powder bed and Inkjet heat (PHIH) Plaster-based 3D printing (PP)
Material jetting	Droplets of build material are selectively deposited	Multijet modelling (MJM)
Sheet lamination	Sheet of materials are bonded to form an object	Laminate object manufacturing (LOM) Ultrasonic consolidation (UC)
Vat photopolymerization	Liquid photopolymer in a vat is selectively cured by light-activated or UV polymerization	Stereolithography (SLA) Digital light processing (DLP)

However, not all AM processes described in Table 2.1 are appropriate for food printing. Food printing techniques and potentially printable food materials are discussed in the subsequent sections.

Printing techniques for food.

The incorporation of food into 3DP technology could be challenging due to its extensive variations in physio-chemical properties (Godoi et al., 2016; Sun, Zhou, Yan, Huang, & Lin, 2018). Therefore, an extensive review of studies (Cohen et al., 2009; Dankar et al., 2018; Godoi et al., 2016; Hao et al., 2010; Hopkinson, Hague, & Dickens, 2006; Huang, Liu, Mokasdar, & Hou, 2012; Lipson & Kurman, 2013; Lipton et al., 2015; Liu, Zhang, Bhandari, & Wang, 2017; Oskay & Edman, 2006; Sher & Tutó, 2015) indicates that 3DP technologies applicable in food fabrication can be classified into four main categories as shown in Figure 2.2. Each of these requires a different form of materials such as a powder or paste, as is discussed in subsequent sections.

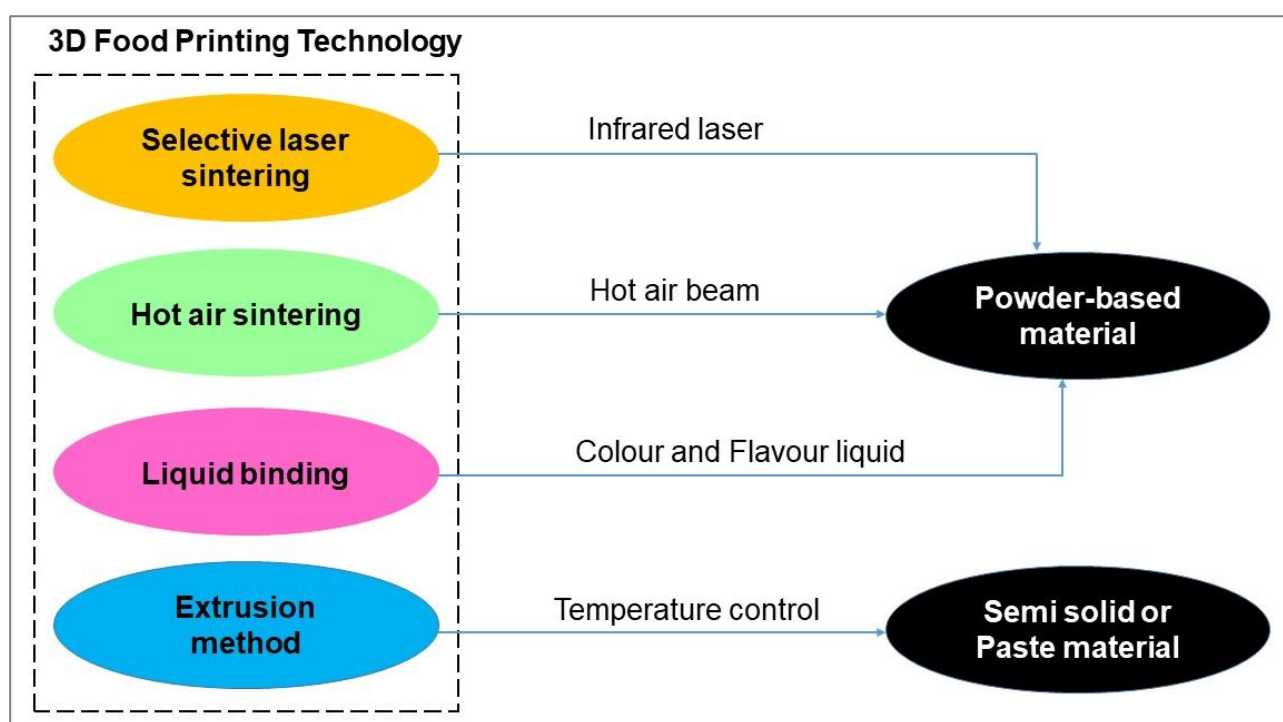


Figure 2.2: 3DP application based on the state of materials (powder, semi-solid or paste)

2.2.1 Liquid binding

Liquid binding (LB) is a repeated process of binding a powdered material through a drop-on-demand liquid binder, with the addition of a thin layer (overlapping) of food powder to form a 3D object (Godoi et al., 2016) as illustrated in Figure 2.3. The liquid is vital in this method as it acts as a binder for the powdered material. LB is solely used for powder based material and this is the concept applied by the ChefJet 3D printer (3D System, 2013; iReviews, 2014). Flavour liquids and colours can be used to bind powdered material such as sugar (Sher & Tutó, 2015). Fabricating unique, complex and flavourful confectionery products is feasible through this method. However, creating a complex design would take a longer time (iReviews, 2014).

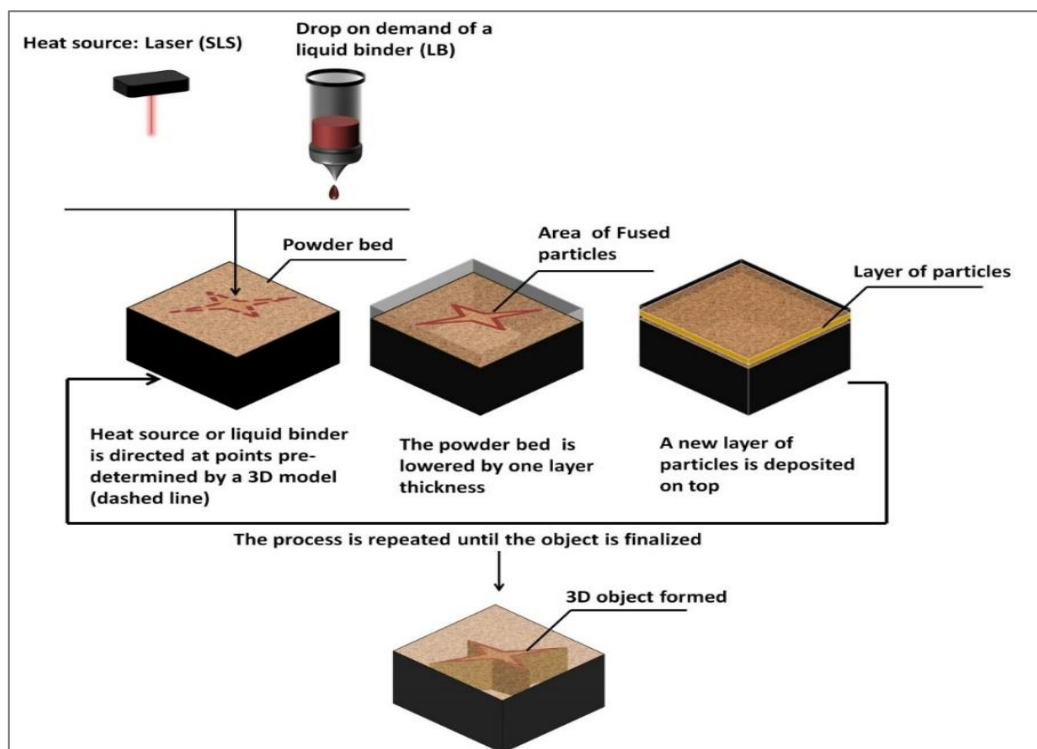


Figure 2.3: Schematic diagram of SLS and LB process adapted from (Godoi et al., 2016).

2.2.2 Selective laser sintering / hot air sintering

Sintering is a process to develop a 3D object rapidly in a short time mainly utilizing powder based material (Sun, Peng, et al., 2015). In SLS and hot air sintering (HAS), the 3D model is defined by 3D software and the infrared laser will be directed to a scanner, reflecting a laser beam on the printer bed containing the powdered material, thereby constructing a solid structure by sinterizing (Godoi et al., 2016). The laser acts as a heat source selectively fusing powdered material by scanning in a cross-section motion determined from the 3D digital description encoded by the 3D software. To construct a 3-dimensional object, the powder bed is lowered by one layer of thickness after the first layer of cross-section is scanned as a new powdered layer is applied on top of the first layer. The sintering process is repeated until the 3D object is completed as illustrated in Figure 2.3. SLS can be applied to construct multiple layers which contain different food substrates in each layer (Diaz et al., 2014).

The SLS machine may use a single-component powder, for instance, for direct metal laser sintering. However, most of the available SLS machines use a two-component powder, either a coated powder or a powder mixture (Mellor et al., 2014). In single-component powder SLS machines, the laser only melts the outer surface of the particles which known as a surface melting. The process will fuse the solid non-melted cores to each other and to the previous layer to create a 3-dimensional object (Periard, Schaal, Schaal, Malone, & Lipson, 2007).

In HAS, a low velocity stream of hot air is directed to a powder medium (e.g., sugar) to form a two-dimensional image (Oskay & Edman, 2006). After this image is formed, the powder bed is slightly lowered and a thin layer of powder applied on the top, covering the first layer. The same process (hot air) selectively fuses the new layer. This process is repeated as per the design from 3D model until the 3D object is completely formed (Godoi et al., 2016). In the HAS process, the hot air beam is channelled on top of the powder bed where the X-axis and Y-axis of the beam move in interchanging motion. The sintering powder will form the product accordingly while the un-sintered powder will remain and can be re-used. SLS has been utilized to successfully fabricate complex 3D structures using either sugar or sugar-rich powders such as NesQuik powders (Gray, 2010). However, this process is only limited to powder base materials (Lai & Cheng, 2007).

The advantages of these methods are their capability to sinterize any material that is in a powder form (Kruth, Wang, Laoui, & Froyen, 2003). Furthermore, SLS and HAS are faster than other methods because the laser or hot air is directly applied to the powder material without any printer bed movement. These methods require no post curing and use a limited support structure. Printing fresh food ingredients is not appropriate with this method as SLS and HAS are only limited to powder materials. In this method, post processing is needed to remove the excessive powder from the sinterized product such as by scraping the excess powder (Liu et al., 2017).

2.2.3 Extrusion method

Extrusion technology is generally applied to a molten material using a temperature control or semi-solid viscous system (Chokshi & Zia, 2004). Melting extrusion has been applied to print chocolate forming a 3D structure, with temperature ranges from 28 °C to 40 °C (Chen & Mackley, 2006). Figure 2.4 demonstrates the food substrate extrusion process. In hot melt extrusion (HME), heat is applied to a material (via a heating block or syringe) depending on the type of material and the proper temperature is maintained to control its viscosity to enable it to flow easily through the nozzle (Tadmor & Klein, 1970). HME was widely applied in production industries such as plastics production and rubber (Chokshi & Zia, 2004).

The concept of HME has also been applied in food extrusion for semi-liquid material such as pre-tempered chocolate and food puree. Choc Creator (ChocEdge, 2013), Foodini (Molitch-Hou, 2014) and Porimy 3D printers (Porimy, 2014) have been used to apply this concept to 3DFP. Extrusion is the best method for fresh food ingredients (Godoi et al., 2016; Hao et al., 2010) as most fresh foods can be blended and liquefied. Some examples of food materials that have been successfully printed using this method was fruit and vegetable (Severini et al., 2018), dough (Yang et al., 2018), pectin-

based food formula (Vancauwenberghe et al., 2018), meat (Dick, Bhandari, & Prakash, 2019) and gel based material (Wang, Zhang, Bhandari, & Yang, 2018; Fanli Yang, Zhang, Bhandari, & Liu, 2018). However, powdered pre-tempered chocolate could be printed in 3D through auger extrusion with the aid of food additives (Porimy, 2014).

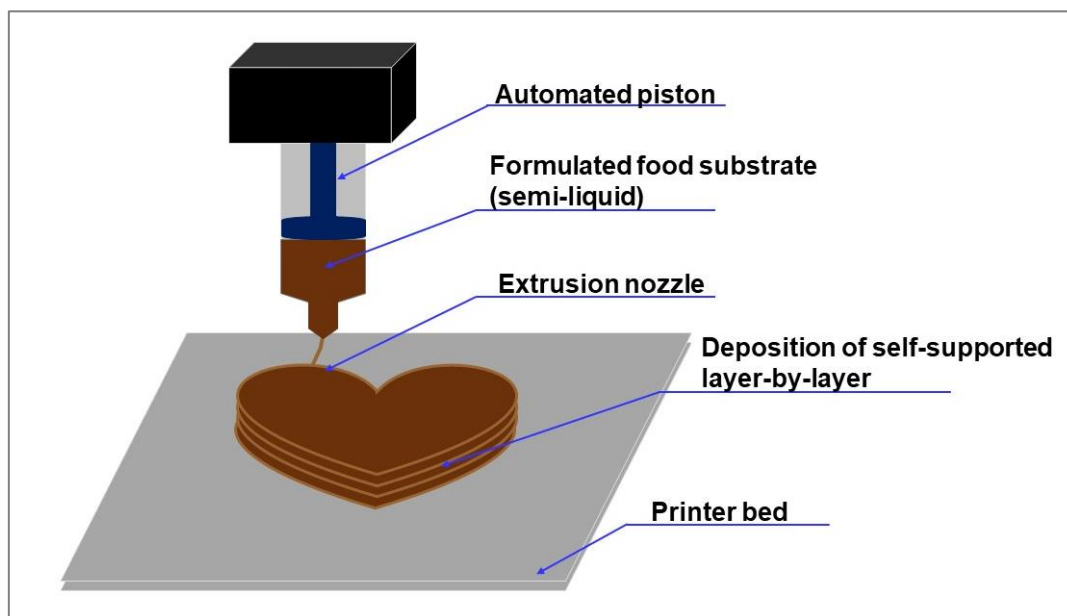


Figure 2.4: Schematic diagram of 3D fused deposition process.

As extrusion method develops a structure layer by layer, however producing a well-defined self-supported 3D shape of a food product could be an issue. This is because not many foods possess the characteristic where they can solidify instantly upon extrusion. Therefore, an improvement (such as a food additive and hydrocolloid) is essential to facilitate printability, flowability, and solidification.

2.3 The application of food additives in 3D food printing

Currently, food additives have been widely investigated in 3D food printing as they are vital to enhance food printability (Dankar et al., 2018; Mantihal, Prakash, Godoi, & Bhandari, 2019). Creating a 3D dimensional object with a better resolution requires that the material has the appropriate viscosity for its layers to be self-supporting (Godoi, Prakash, & Bhandari, 2016; Periard et al., 2007). Food grade additives could be utilized to improve material viscosity and printability. Hydrocolloids such as carbohydrates and proteins, starches and sugars could be used to enhance printability (Cohen et al., 2009). The application of food additives to improve the rheological properties of printable products, such as transglutaminase in meat and agar in vegetables is essential (Lipton et al., 2010). Also, Dankar et al. (2018) evaluated the effect of four food additives agar, alginate, glycerol and lecithin on the rheological properties of commercial potato puree. They reported that agar and alginate

exhibited a moderate effect and stabilize potato puree more (increasing its yield stress) while having an exclusive effect of acting either as an increasing or decreasing agent on viscosity according to their respective used levels of concentration between 0.5 and 1%. In a similar approach, Liu et al. (2018) examined the printability (rheological properties) of mashed potato combined with potato starch to evaluate its behaviour during 3D printing. The best printability (producing a more clearly defined and stable construction) was obtained by combining 2% potato starch into mashed potatoes, which exhibited shear thinning behaviour and yield stress of 312.16 Pa, respectively. Likewise, Yang et al. (2018) found that the formulation of lemon juice gels and potato starch (15g w/w) was optimal and resulted in a higher $\tan\delta$ (0.16), leads to a good flowability of the lemon gel and allowing a final 3D construction that matched that of the target geometry. Hence, the incorporation of specific food additives would help to improve the particular food's material flowability and printability. However, the choice of food additives should be explored to ensure the printability and final quality of a printed food.

2.4 Printable food materials

Food is composed of a complex structure that affects its flowability and printability. Rheological properties, gelling, melting and glass transition temperatures (T_g) are critical parameters in the production of an appealing and stable 3D printed object (Zhang et al., 2018; Liu et al., 2017; Godoi et al., 2016). Therefore, it is necessary to fully understand the material's properties and the technologies relevant for it, to be able to construct 3DP structures. To then build on this and find other potential substrates and additives for 3DFP is vital. As examples, the subsequent sections discuss the printability properties of chocolate, sugar, gel and dough.

2.4.1 Sugar

In 3D food printing, granulated or powdered sugar can be used in SLA, HAS and LB (Godoi et al., 2016). This is because sugar can be melted or solubilised by heat or moisture at the surface to fuse adjacent particles (Knecht, 1990). Also, crystalline sucrose melts or decomposes in temperatures from 160 °C to 186 °C depending on its moisture content and purity. Therefore, parameters such as compressibility and powder density are vital considerations as this will affect the powder flowability in the vessel, contributing to pattern construction when the heat source (either laser or hot air) is applied to the powder bed (Berretta, Ghita, Evans, Anderson, & Newman, 2013).

The interface of powder and binder used in 3D printing can be related to adhesive force or chemical reaction (Shirazi et al., 2016). For instance, powder flowability and wettability in sugar are the main parameters in LB printing, as it is important to construct a thin layer when the sugar powder is spread

on the printer bed (Godoi et al., 2016). Low flowability of a liquid binder may cause insufficient recoating of the powder while high flowability leads to instability of the powder bed. Particle wettability is vital as the amount of binder absorbed as well as the volume of binder distributed into the powder bed will determine the resolution and mechanical properties of the printed output. Therefore, this physical property of sugar makes it appropriate for SLS and HAS as both methods use heat as their main printing mechanism. Sugar is a water soluble substance, thus, it is also an option in the LB printing method (Sher & Tutó, 2015). Figure 2.5 shows sugar powder printed using HAS (Images A and B) and LB (Image C and D) methods.

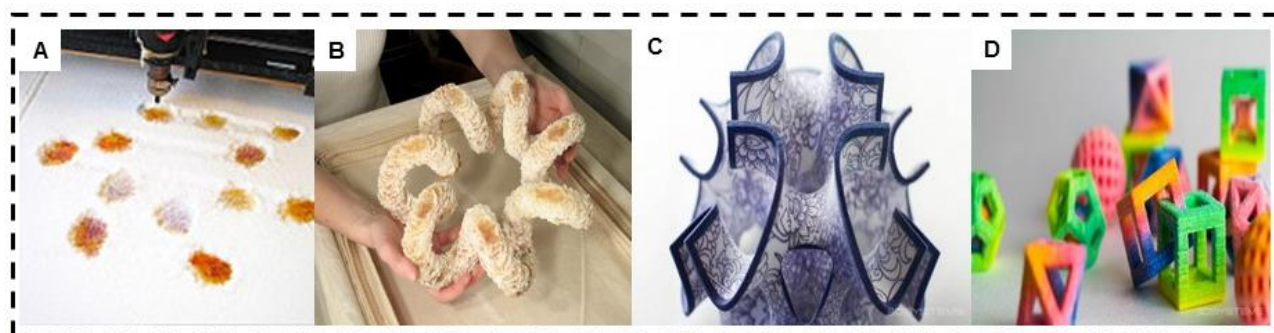


Figure 2.5: 3D construct made by selective hot air sintering and melting (SHASAM) (a) SHASAM process (b) toroidal coil sculpture made of granulated sugar (Oskay & Edman, 2006). These images were reproduced from the data available at <http://candyfab.org/> (c) Complex sugar geometry with fine colour detail (d) colourful sugar candies. These images were reproduced from the data available at <http://www.3dsystems.com/culinary/gallery>.

2.4.2 Gelatine

Gelatine is a protein derived from the irreversible breakdown of collagen fibrous structure, either through alkaline or acidic treatment (Nocera, Salvatierra, & Cid, 2015). Gelatine possesses a distinct “melt-in-the-mouth” texture that provides an appreciable mouthfeel sensation, therefore making it one of the prospective substrates for 3D printing (Diaz, Noort, & Bommel, 2015; Nocera et al., 2015). Air-dried gelatine dissolves in warm water (at approximately 40°C), where the hydrated gelatine particles instantly form a single random coil. During cooling, the gelation process occurs where a small segment of polypeptide chains form at junction zones, reversing the collagen triple helix structure (Burey, Bhandari, Howes, & Gidley, 2008). Viscosity is the important parameter for gelatine extrusion, as it is a Newtonian substrate in a dilute solution accepted when it is extended by a charge group. When using a flexible protein in 3D printing, it is vital to understand that charges on the protein molecules will affect the viscosity of the solution. This is because a protein molecule is fully contracted at the isoelectric point and it became less viscous when both positive and negative charges exist (Godoi et al., 2016). Apart from viscosity, the shear rate is also important in the 3D extrusion process. A high shear rate may result in a non-Newtonian behaviour in gelatine (Nocera et al., 2015).

Gelatine is added into food material to improve food viscosity and enhance food printability. Cohen et al. (2009) used the Fab@Home 3D food printer to print food flavour with the combination of different concentrations of gelatine ranging from 0.5% to 4% w/w. They indicated that food material was printable because as the gelatine concentration increase created a firm construct. Yang et al. (2018) opted for an extrusion method in constructing a gel based product with lemon flavour. Figure 2.6 illustrates some of the 3D printed forms of lemon juice gel.

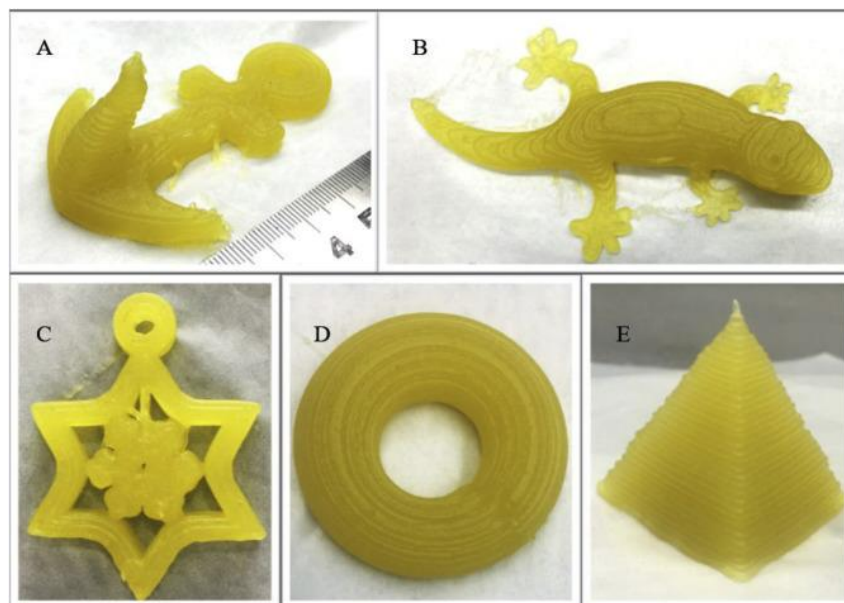


Figure 2.6: 3D printed lemon juice gel printed at $24 \text{ mm}^3/\text{s}$ extruder rate, 1.0 mm nozzle size (a) anchor (b) gecko (c) snowflake (d) ring (e) pyramid. Adapted from Yang et al. (2018).

2.4.3 Dough

Dough, is part of a carbohydrate macronutrient derived from wheat flour that possesses viscoelastic properties when mixed with water (Hoseney & Rogers, 1990). Viscoelasticity happens when a gluten protein is water compatible, thus an interaction between water and the gluten protein will cause a swelling process. Doughs are also able to retain gas and this will slow the rate of gas diffusion in the dough mixture. A gluten protein has a large molecular size and low charge density, allowing it to interact with both hydrogen and hydrophobic bonds (Hoseney & Rogers, 1990). By possessing viscoelastic property, wheat flour dough has the ability to set during post processing such as baking and frying. Due to this property, dough can be a good candidate for 3DP. The aim of 3DFP is to constructs shapes without a multiple-step process, therefore building a single complex shape without any additional mould (Lipton et al., 2015). The ability to subsequently sustain this shape during cooking, baking or frying is important. Lipton et al. (2010) suggested two methods to curb the shape instability issue: recipe control and the inclusion of food additives. During the printing process,

additives such as hydrocolloids act as a binding agent in the formation of edible powder, which improves the flow and migration of a liquid spray onto a powder bed (Diaz et al., 2015). Alternatively, alterations in the amount of butter, egg and sugar added into the dough mix may affect its stability. The increase in the amount of butter may increase the speed of extrusion during printing, but result in an inability to hold the structure. Similarly, increasing the amount of egg yolk will influence the height of 3D structure build-up (Lipton et al., 2010). Therefore, re-creating food material formulation and the incorporation of food additives can help the 3D printed food to sustain its shape in the post processing process. Yang et al. (2018) explored the effect of different ingredients in dough printability. They found that a sucrose content of 6.6g/100g in dough produced a better intact shape. Figure 2.7 depicts the printed samples of dough with various compositions of sucrose ranging from 3.3g to 8.2g of sucrose per 100g of dough.

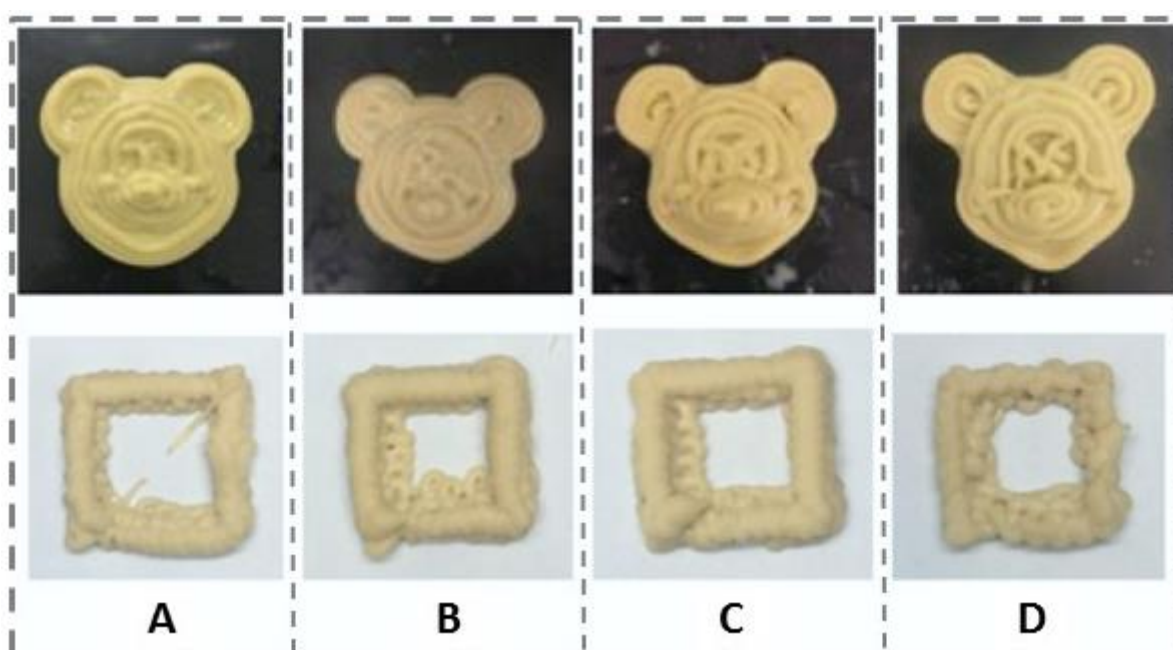


Figure 2.7: Representative images of dough printed using the Porimy 3D printer with various sucrose compositions (a) 3.3/100 g of formulation; (b) 5.0/100 g of formulation; (c) 6.6/100 g of formulation; (d) 8.2/100 g of formulation. Adapted from Yang et al. (2018).

2.4.4 Chocolate

According to Hao et al. (2010) and Sood, Ohdar, and Mahapatra (2010), finding an appropriate material which melts at the pre-selected temperature and rapidly solidifies upon adhering to the previous layer is vital in 3D printing. Chocolate possesses these characteristics. The presence of cocoa butter makes the chocolate a temperature sensitive material. In addition, by doing a proper tempering, a more stable β crystal (Form V) can be obtained and this produces chocolate with a better quality such as a glossy appearance, a snap and a desirable texture (Afoakwa, Paterson, & Fowler, 2007; Afoakwa, Paterson, Fowler, & Ryan, 2008; Afoakwa, Paterson, Fowler, & Vieira, 2009; Beckett,

1995; Chen & Mackley, 2006; Chocolate Alchemy, 2008; Cidell & Alberts, 2006; Kinta & Hartel, 2010; Talbot, 1994). Chocolate has a complex structure and its character significantly varies even with a small variation in temperature. For instance, at room temperature, chocolate is in a semi-solid state but when the temperature reaches body temperature (37 °C), it is primarily viscous and with a low yield stress of about 10–20 Pa (Chen & Mackley, 2006). Chocolate also consists of other composites including soy lecithin that acts as an emulsifying agent, enhancing the coating of hydrophilic sugar particles and hydrophobic fat molecules. This provides the flowability and suspension to chocolate during consumption.

There are six (Form I – Form VI) major crystal polymorph formations in cocoa butter (Wille & Lutton, 1966). The crystals formed in cocoa butter are summarized in Table 2.2. These forms are divided into three main categories which are α (alpha), β' (beta prime) and β (beta). Form (I), β'_2 is very unstable and melts at 17 °C. In Form (II), α rapidly develops from Form (I) and its melting point ranges between 21 °C and 22 °C. This form (II) will slowly develop to Form (III) at the temperature of 25.5°C, and to Form (IV) between 27 °C and 29°C (Talbot, 1994). Generally, Form V (β_2 crystal) is the most important crystal and will give the final chocolate product a more stable characteristic, a glossy finish and better texture (Afoakwa et al., 2007; Afoakwa, Paterson, Fowler, & Ryan, 2008; Chen & Mackley, 2006; El-kalyoubi, Khallaf, Abdelrashid, & Mostafa, 2011; Mantell, Hays, & Langford, 2015). In order to gain the Form V crystal, a proper and careful manipulation of the heat through tempering is vital. Chocolate is melted at up to 50 °C and cooled down to 28 °C for crystal agitation process. Then, heat is applied (32°C) to the chocolate to eliminate the unstable crystals, leaving only the stable crystal that gives the desirable properties of chocolate.

Table 2.2: Crystal forms in cocoa butter.

Crystal Form		Temperature (°C)
Form I	β'_2	17°C
Form II	α	21°C - 22°C
Form III	Mixed	25.5°C
Form IV	β'_1	27°C - 29°C
Form V	β_2	32°C – 33.8°C
Form VI	β_1	36°C

Tempering is the process of heating the chocolate to control the pre-crystallization of the beta (β) crystal. This method is vital in chocolate to induce a more stable solid form of cocoa butter which is the polymorphic fat in the chocolate that gives its desired characteristics (Afoakwa, Paterson, Fowler, & Vieira, 2008a). The main purpose of chocolate tempering is to stimulate the characterization of

triacylglycerols (TAGs) contained in cocoa butter, which provides proper setting characteristics, demoulding properties, foam constancy, the snap effect, a glossy appearance, shear and longer shelf-life (Afoakwa, Paterson, Fowler, & Vieira, 2008b).

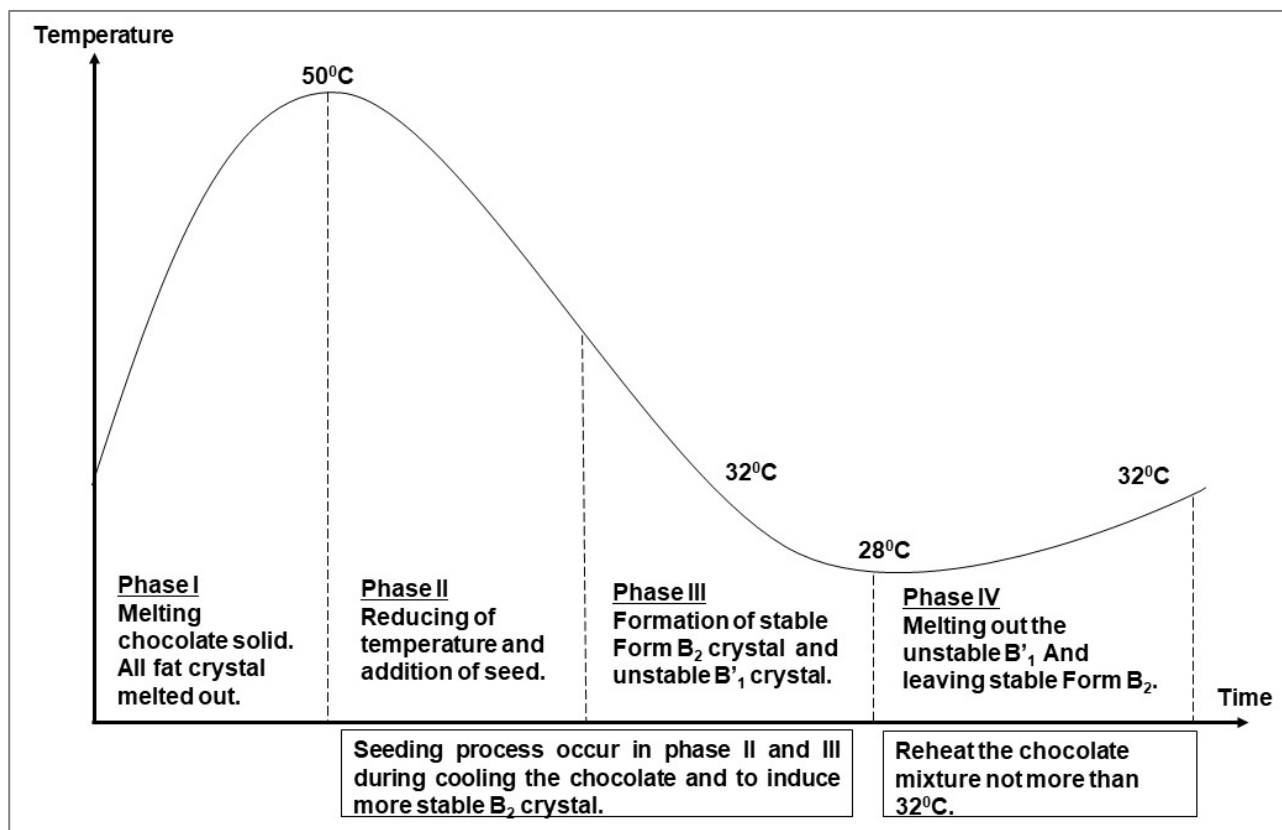


Figure 2.8: Temperature regimes in different phases of tempering process: Phases I – IV.

To summarize, in chocolate manufacturing, the tempering process consist of four phases (1) complete melting (2) cooling to the point of crystallization, (3) crystallization (4) melting out the unstable crystals. This process is illustrated in Figure 2.8. Each step in tempering is a continuous process and temperatures are controlled properly. The stable state of crystals in cocoa butter, β_2 only exists when the tempering process is done correctly. This is achieved by maintaining the temperature and adding seeds (a properly tempered chocolate in the form of solid chocolate) to the mixture.

In the 3D extrusion process, controlling the extrusion temperature is vital to ensure the pre-crystallization of the beta (β) crystal and also form a stable beta (β) crystal, (Form V), essential in solidification after extrusion. Properly tempered chocolate will induce more (β) crystal and provide the significant properties required to rapidly solidify upon extrusion (Hao et al., 2010; Mantihal, Prakash, Godoi, & Bhandari, 2017). The first printed layer is important in constructing a 3D object, as it will create the base form for the next layer to hold, maintaining the stability of the printed structure. Figure 2.9 depicts 2D printed chocolate objects with an intricate design.

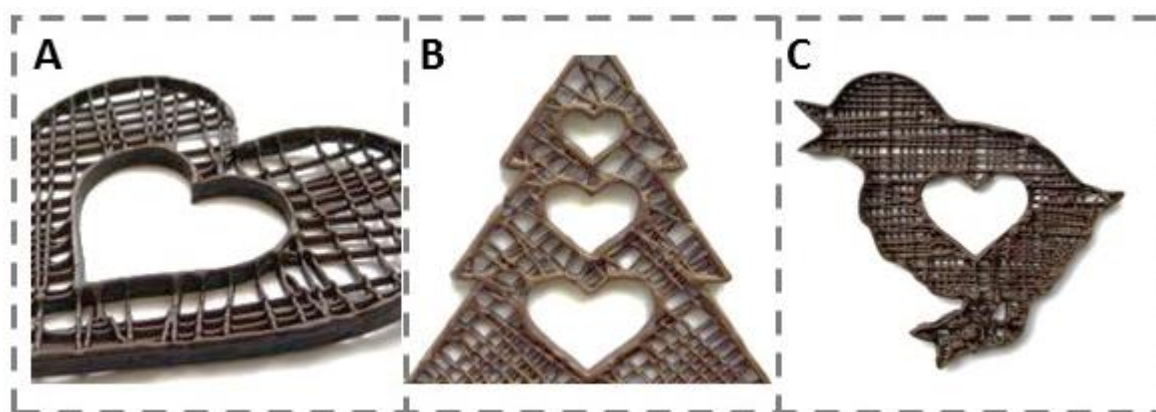


Figure 2.9: 2D printed chocolate with an intricate design produced by ChocEdge (a) Heart-in-heart shape (b) Hearts in Christmas tree (c) Heart in chicken. These images were reproduced from the data available at <http://chocedge.com/gallery.html>.

As mentioned earlier, chocolate is a perfect candidate for 3D printing. Although chocolate has been extensively studied, however, creating a unique structure of dark chocolate in a 3-dimensional manner is interesting. There are some researchers attempt to study this material in term of its printability and developing printing parameters such as the appropriate nozzle diameter, printing speed and nozzle height accuracy (Hao et al., 2010; Lanaro et al., 2017). These parameters established by those researches are limited to the specific 3D printer that they have used. Therefore, further study on developing printing parameters of chocolate is necessary for a specific 3D printer. Most 3D food printer does not equip with the cooling system on the printer bed to enhance material solidification. This system is vital in chocolate printing to ensure the first extruded layer solidify and act as "self-support" for the subsequent layers attachment to create a 3D construction. Therefore, development of such printer bed is essential.

2.5 3D printing as the tool to fabricate food texture

Texture is the main attribute to determine the quality of a 3D printed food product. This modality is important as it will influence its acceptance. With 3DP technology, one can create a customized design that can create a new texture of food. For instance, Lipton et al. (2015) reported that texturised food from vegetable puree was constructed using 3DP technology to overcome dysphagia among the elderly. This modification in texture allows the patient to experience the food without sacrificing its textural quality. In 3DP, the texture can be modified by manipulating the internal structure of the target design. The subsequent section will discuss this modification of the internal structure.

The internal structure is vital in 3DFP as it needs to provide sufficient support structure for the construction as well as holding some intricacy in the design (Liu et al., 2017). The support structure

can be controlled by modifying the infill pattern and percentage in the Slic3r program (g-code generator) in the 3D software. The infill pattern is the shape of the structure, for examples, a Hilbert curve, star, line, honeycomb or rectilinear shape (RepRap, 2016). The infill percentage is the intensity of the internal structure which can range from 1% to 100%. Altogether, the infill pattern and infill percentage can potentially modify the textural and mechanical properties of 3D constructs. Several studies on the effect of the internal structure on textural and mechanical properties of 3D constructs have been pursued in thermoplastic and bio-printing field (Fernandez-Vicente, Calle, Ferrandiz, & Conejero, 2016; Sood et al., 2010; Tronvoll, Welo, & Elverum, 2018). In polymer printing, the mechanical strengths of printed ABS constructions were found to be dependent on their infill percentages (Fernandez-Vicente et al., 2016). These researchers reported that, as the infill percentage increased from 20% to 100%, the tensile strength of the printed construction (with a line infill pattern) also increased from 16.0 MPa to 35.5 MPa. In bio-printing, the internal structure enables the extruded hydrogel to hold its shape, preventing the constructions from collapsing (Suntornnond, An, & Chua, 2017). These findings indicate that the internal structure plays an important role in the 3D printed construction's stability and integrity. Thus, this is a promising scope for technology in creating an exotic infill structure that can alter and enhance the textural properties of food.

2.6 Consumer perceptions about 3D food printing

The food industry is always interested in novel food production and up-to-date processing technologies that may have a positive impact on their profit and enhance product quality (Cardello, Schutz, & Leshner, 2007). New food technology may be “flamboyant” and therefore stimulate some food producers because of its novel or trendsetting appeal. However, consumer attitudes and perceptions about new technologies are vital determinants influencing their purchase intentions (McCluskey, Kalaitzandonakes, & Swinnen, 2016). Consumers, as they are not a heterogenous group, may have different reactions to accepting the new technology. Ladipo, Olufayo, and Bakare (2012) defined perception as a process started with any encouragements that will be received and inferred by individuals who will convert their feelings into a response, either to accept or reject. Emphasizing the benefits and advantages of the technology by logically setting out the facts through scientific study is essential. In line with that, establishing trust and confidence among users will enhance their acceptance of it. Besides, consumers' sensory perception is a crucial attribute in food product acceptance. Attributes such as texture, appearance and taste would dictate their preferences of printed products. Therefore user acceptance is essential to the development of new food processing technology such as 3D technology as this will determine its success (Siegrist, 2008). Therefore, three factors that influence consumer acceptance of 3D food technology are the sensory perception of 3D printed food, the knowledge about this technology and its perceived benefits.

2.6.1 Sensory perceptions of 3D printed food products

Sensory perception is a vital element to determine food quality. Cohen et al. (2009) conducted a study of the sensory perception and mouthfeel of different flavouring additives of raspberry, strawberry, banana and chocolate with the addition of xanthan gum and gelatine on 3D printed jelly. A mouthfeel matrix was used to indicate the firmness of each sample. They reported that the gelatine and xanthan gum only fitted within the weak to firm range within the mouthfeel matrix and shifted more to granularity when these hydrocolloids were combined. Severini et al. (2018) investigated the sensory attributes of 3D printed fruits and vegetables based on appearance, taste, odour and colour. The researchers reported that the appearance of printed smoothies (4.60 ± 0.7) was significantly different (and perceived to be enhanced) when compared to that of the control formula (3.37 ± 1.1). Regarding the colour, taste and odour of printed smoothies, no significant differences to that of the non-printed samples was observed. These results signify that 3DFP was able to improve the appearance of food. Alec (2015) demonstrated the ability of 3D printing technology to construct a chewing gum. Apart from sensing the customized shape, colour and flavour, people would explore a new form of chewing experience by feeling the texture of the 3D printed chewing gum in their mouth. Le Tohic et al. (2018) studied the effect of 3D printing on cheese extruded at low and high speeds. They reported that printed cheese was slightly darker than non-printed cheese with a minor decrease in the luminosity parameter. Therefore, one can conclude that the 3D printing process can affect the final printed products' colour and texture, but whether this change is favourable to consumers or not is still arguable and further study of consumer preferences should be pursued.

2.6.2 Knowledge about 3D food printing

Lack of knowledge among consumers about innovative and currently developing food technologies can also be a major hindrance in their acceptance (Cardello et al., 2007). Food processing using 3D technology is gradually emerging and its impact has yet to be studied. An effective way to increase consumer awareness is through a marketing channel where a producer can communicate the new technology's details and the products' benefits.

The purpose of innovation in food service technology is to upgrade traditional methods of producing food product in terms of quality, quantity, time preparation, ingredient accuracy, nutritional content, texture, packaging, appearance and shelf-life and to increase the functionality of food (Rollin, Kennedy, & Wills, 2011). Assessing consumer or user behaviour toward new food technology is crucial for the new technology's producer to expand their market. The lack of knowledge or clear information will lead to uncertainty. Ambiguity happens when the details of a process or product are unpredictable, vague or complex so that consumers do not understand them well. People feel may

insecure about their own knowledge due to inconsistent information or their state of knowledge is general rather than detailed (Ronteltap et al., 2007). Introducing a 3D food printing technology may be a challenge for food service providers. Therefore, rational information with the support of scientific findings are vital to anchor consumers' acceptability toward 3DFP technology.

2.6.3 Perceived benefits

The perceived benefit or benefits is a crucial determinant that influences the acceptance of a new product (Frewer, Scholderer, & Lambert, 2003; Morgan & Hemmington, 2008; Rollin et al., 2011). Despite the potential benefits that 3DFP technology poses in designing a preferred shape or being user friendly, there may be difficulties in engaging consumer successfully with it (Ronteltap & van Trijp, 2007). Consumer or user acceptance is also influenced by the perception of risk such as risks to safety, hygiene or the wholesomeness of food (Rollin et al., 2011). Severini and Derossi (2016) suggested that this technology could be a powerful tool to create personalized food by depositing nutrients into the food. This is promising but consumers may need to be educated about this possibility to counteract the perception that food processed to this degree may not be particularly nutritious.

2.7 3D printing technology for food: Current status and future prospects

To date, 3D food printers are equipped with functional features to make the machine more user friendly and easy to navigate (Dick et al., 2019), e.g., a touchscreen panel and Bluetooth functionality for printing access. However, as emphasized above as a motivation for the current study, assessing the properties of the food material itself remains the vital element in food printing as this will give the major impact on the texture, structure, and flowability of food (Vancauwenberghe et al., 2018). Most 3D food printing started with chocolate or sugar powder (as discussed in Section 2.2) as the main food substrates for printing as they possess characteristics that suit 3D printing. A proper pre-defined food material, the composition of the food including the macro nutrient and the initial pre-preparation such as blending, tempering and mixing before printing are also important considerations for food fabrication. All of these factors will contribute to a properly printed food product.

Currently, 3D printing is emerging into the hospitality industry, particularly in the foodservice sector. Several studies have been carried out (Chen & Mackley, 2006; Coelho, 2015; Cohen et al., 2009; Doris., 2016; iReviews, 2014; Linden, 2015; Natural Machines, 2016; Periard et al., 2007; Schniederjans, 2017) pertaining to 3D food printing and highlighting this technology as novel way to prepare future gastronomically appreciated food by enhancing its texture, flavour, shape and nutrient. For instance, the producers of the Foodini food printer (Natural Machines, 2016) have collaborated with a restaurant in Barcelona, Spain to trial it in preparing food. Overall, the applications of 3D

printing in food are still in an exploratory phase. Assessing the possibility to broaden the spectrum in fabricating food using different types of material and understanding the behaviour of food substrates are still being studied.

The prospective application of 3DFP can be considered in the three levels of food production industry: consumer produced food, small scale food production and industrial scale food production (Lipton et al., 2015). Figure 2.10 shows these three possibilities of the application of 3DP technology in terms of their scale of operation. This technology can play a vital role in the hospitality industry as it opens an opportunity for this industry to evolve further. The advancement of technology impacts positively in the production of food. The application of 3DFP would be a great prospect for food entrepreneurs in niche markets because it allows food makers to explore the customization of their otherwise mass produced and, in many cases, commoditized products.

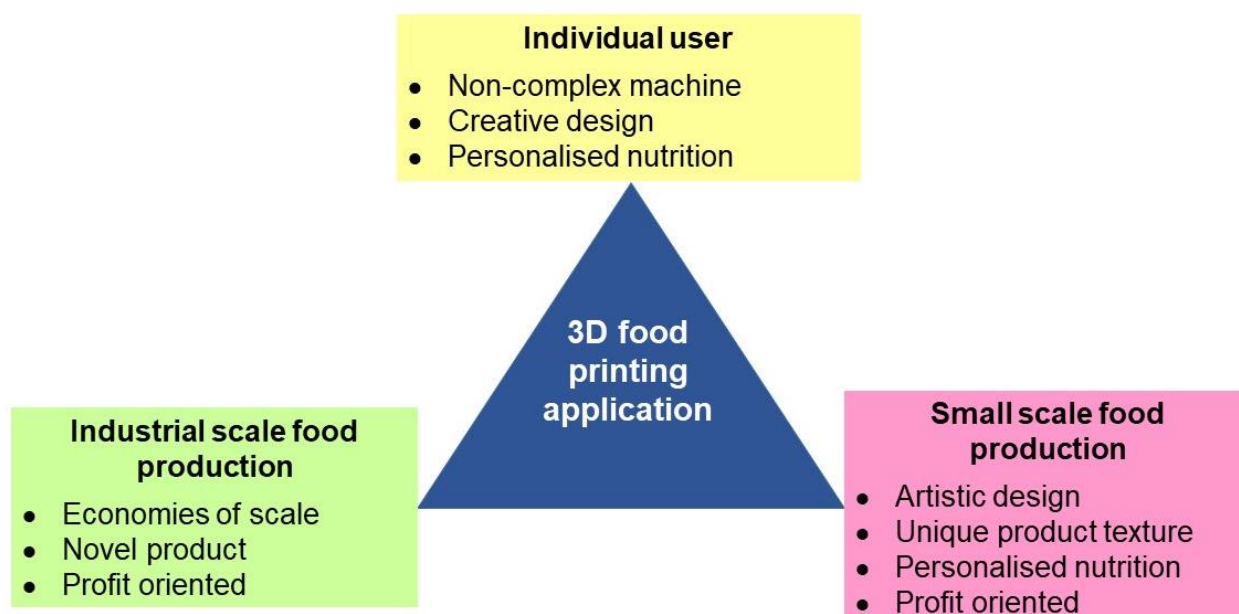


Figure 2.10: Application of 3D food printing technology at three scales.

2.7.1 Application of 3DP for the individual user

Consumer friendly technology enables individuals to use equipment easily. At the initial stage, the developers of 3D printers created uncomplicated machines. For instance, the Fab@home project started with six printer prototypes and, of these, three printers were sent to outside users (Malone & Lipson, 2007). The user just needs to have a basic tool to assemble the printer according to a manual and the printing process is fully automated. Similarly, the start-up company ChocEdge came out with the Choc Creator printer (Sun, Zhou, Huang, Fuh, & Hong, 2015). This printer is mainly for chocolate designing and requires no assembling. The user can operate it via a touch screen panel. By using an

open source software, the user can create a customized design and generate a g-code through the printer software (ChocEdge, 2013) to print their chocolate in 3D. On the other hand, the Foodini food printer allows the user to anticipate a personalized nutrient as the consumer can print their own preferred food based on a blend of fresh ingredients (Molitch-Hou, 2014). Further development in techniques and the calibration of materials for 3D printing is yet to be explored and is crucial for this technology. In 3D chocolate printing, a proper tempered chocolate is important to gain the desired quality. As Afoakwa et al. (2007) suggested, the user must follow a proper procedure in tempering to acquire a better quality of chocolate that is suitable for extrusion and can solidify immediately afterward.

2.7.2 Application of 3DP in small scale food production – restaurants, cafés, bakeries

3D printing technology would be especially beneficial in the customization of unique products and value adding to artistry in foodstuffs. Creating a gourmet style in food presentation is feasible through precise 3D printing. This technology has a potential of enabling restaurant, café or bakery operators to design a distinct pattern of edible foods suiting individual tastes and preferences. Furthermore, it is also beneficial to exploit the ability of 3DFP to produce a unique product through texture and flavour combination by using layered manufacturing technology (Lipton et al., 2015). For instance, small cafés and bakeries may decorate food items such as biscuits and cakes and also minimize labour costs. For the use of this technology to become profitable, bigger quantities and a food printer with a larger reservoir are vital (Lipton et al., 2015). Attempts are continually being made to develop a larger reservoir which is easy to refill (Porimy, 2014). Porimy's Chocolate Product 3D printer operates automatically; the user only needs to load the food material and customize the food design through 3D software.

2.7.3 Application of 3DP in industrial scale food production

The adoption of 3DP at an industrial scale could be challenging as the machine should be able to cope with a larger capacity (mass production) in a short time (with economies of scale). Therefore, further study is needed not only in developing an industrial scale 3D food printer but also in food product quality which includes the food material properties suitable for such large scale printing.

2.7.4 Potential application of 3D food printing in hospitality industry

Product development is a systematic, commercially oriented type of research to develop products, services or processes to satisfy the end user's (the consumer's) need (Winger & Wall, 2006). The originality and newness of a product may be perceived differently according to people's individual judgement. Most companies in the food industry prefer to re-develop an existing product rather than

making radical changes to create a new product because it is safer to do so (Stewart-Knox & Mitchell, 2003). Conversely, certain factor may improve the success rate of product development (Suwannaporn & Speece, 2010). These are marketing and managerial synergy, the strength of marketing communications including the launch effort, the market need, market growth and market size. Therefore, understanding consumer demand, need and expectation, as well as retailer involvement in product development, are significantly related to product success. The application 3D printing technology in food brings a new opportunity for the consumer to incorporate design and technology into a visible form of edible food. Additionally, to enhance end user awareness of the existing 3D food printers in the market, more effort needs to be made by the producers in terms of convincing consumers about the food quality and making the product more user friendly, with a robust and sustained marketing effort.

2.8 Conclusion

Technological advancement of 3DP in food fabrication is drawing the attention of various food technologists to studying and replicating the potential of this application for food. It is perceived that this technology would bring a huge impact on food production as 3DFP can personalize the needs of consumers based on their preferences. In addition, preparing a complex food design is possible because all processes will be supported by 3D model software and fully automated. The application 3DFP technology in the hospitality industry, specifically in restaurants, bakeries or cafés, could support the expansion of this technology, for example, printing desserts of a personalized shape, decorating cakes using 3D printed chocolate and printed pizza dough with various shapes. However, due to the constraints on printable material, 3DP is applicable to certain food materials only. More study needs to be done on finding other possible materials that could be fabricated through this technology. Besides, information and knowledge distribution and awareness raising about the emergence of 3D printing in food should be well organised and supported with relevant and logical scientific findings that would enhance consumers' or users' understanding and acceptance of the technology.

Although chocolate has been widely reported to augment information to the pool of knowledge, there is a limited study on chocolate printability and the incorporation of flow enhancer (food additives in powder form) in 3D chocolate printing. Hence, the focus of the current work will be to develop personalised dark chocolate using a 3D food printer and to verify the suitability of the process, the ingredients and the use of a flow enhancer. There are also no reports on the effect of additives on the dark chocolate. Therefore, the relationship between the physical properties of the materials for printing and the quality of the printed format will be established.

A number of analytical tools comprising a rheometer, differential scanning calorimeter (DSC), tribometer and texture analyser will measure the material characteristics as well as the final quality, such as texture and mechanical strength of the printed dark chocolate. Given that there is a wealth of chocolate sensory information, there are no reports on the sensorial evaluation of 3D printed chocolate. In this research, the printed chocolate will be evaluated by a sensory panel to assess their preferences. General consumers will also be asked about their perceptions of 3DFP technology.

2.9 References

- 3D Printing Industry. (2014, May 2014). History of 3D Printing: The Free Beginner's Guide. Retrieved from <http://3dprintingindustry.com/3d-printing-basics-free-beginners-guide/history/>
- 3D System. (2013, 10 september 2013). Technology brings edible 3D printing to professionals and consumers alike. Retrieved from <http://www.3dsystems.com/de/press-releases/3d-systems-acquires-sugar-lab>
- Afoakwa, E. O. (2010). *Chocolate science and technology* (Vol. 687). Oxford: Wiley-Blackwell.
- Afoakwa, E. O., Paterson, A., & Fowler, M. (2007). Factors influencing rheological and textural qualities in chocolate - a review. *Trends in Food Science & Technology*, 18(6), 290-298.
- Afoakwa, E. O., Paterson, A., Fowler, M., & Ryan, A. (2008). Flavor formation and character in cocoa and chocolate: a critical review. *Critical Review in Food Science and Nutrition*, 48(9), 840-857.
- Afoakwa, E. O., Paterson, A., Fowler, M., & Vieira, J. (2008a). Effects of tempering and fat crystallisation behaviour on microstructure, mechanical properties and appearance in dark chocolate systems. *Journal of Food Engineering*, 89(2), 128-136.
- Afoakwa, E. O., Paterson, A., Fowler, M., & Vieira, J. (2008b). Modelling tempering behaviour of dark chocolates from varying particle size distribution and fat content using response surface methodology. *Innovative Food Science & Emerging Technologies*, 9(4), 527-533.
- Afoakwa, E. O., Paterson, A., Fowler, M., & Vieira, J. (2009). Comparison of rheological models for determining dark chocolate viscosity. *International Journal of Food Science and Technology*, 44(1), 162-167.
- ASTM-international. (2015). F2792. 2015 Standard terminology for additive manufacturing technologies. *West Conshohocken, PA: ASTM International*. See www.astm.org.(doi: 10.1520/F2792-12).
- Beckett, S. T. (1995). Chocolate shape retention: Google Patents.
- Berretta, S., Ghita, O., Evans, K. E., Anderson, A., & Newman, C. (2013). *Size, shape and flow of powders for use in selective laser sintering (SLS)*. Paper presented at the High Value Manufacturing: Advanced Research in Virtual and Rapid Prototyping: Proceedings of the 6th International Conference on Advanced Research in Virtual and Rapid Prototyping, Leiria, Portugal, 1-5 October, 2013.
- Brunner, T. A., Delley, M., & Denkel, C. (2018). Consumers' attitudes and change of attitude toward 3D-printed food. *Food Quality and Preference*, 68, 389-396.
- Burey, P., Bhandari, B., Howes, T., & Gidley, M. (2008). Hydrocolloid gel particles: formation, characterization, and application. *Critical reviews in food science and nutrition*, 48(5), 361-377.

- Cardello, A. V., Schutz, H. G., & Leshner, L. L. (2007). Consumer perceptions of foods processed by innovative and emerging technologies: A conjoint analytic study. *Innovative Food Science & Emerging Technologies*, 8(1), 73-83.
- Chen, Y. W., & Mackley, M. R. (2006). Flexible chocolate. *Soft Matter*, 2(4), 304-309.
- ChocEdge. (2013). Creation: a Selection of our Chocolate Creations. Retrieved from <http://www.chocedge.com/creations.php>
- Chocolate Alchemy. (2008). Tempering - Deconstruction and Reconstruction and Illustrated Tempering. Retrieved from <http://chocolatealchemy.com/illustrated-tempering/>
- Chokshi, R., & Zia, H. (2004). Hot-Melt Extrusion Technique: A Review. *Iranian Journal of Pharmaceutical Research*, 3, 3-16.
- Cidell, J. L., & Alberts, H. C. (2006). Constructing quality: The multinational histories of chocolate. *Geoforum*, 37(6), 999-1007.
- Coelho, M. (2015). CORNUCOPIA: Marcelo Coelho Studio. Retrieved from <http://www.cmarcelo.com/cornucopia/>
- Cohen, D. L., Lipton, J. I., Cutler, M., Coulter, D., Vesco, A., & Lipson, H. (2009). *Hydrocolloid printing: a novel platform for customized food production*. Paper presented at the Proceedings of solid freeform fabrication symposium (SFF'09).
- Dankar, I., Haddarah, A., Omar, F. E. L., Sepulcre, F., & Pujolà, M. (2018). 3D printing technology: The new era for food customization and elaboration. *Trends in Food Science & Technology*, 75, 231-242.
- Diaz, J. V., Bommel, K. J. C. V., Noort, M. W., Henket, J., & Brier, P. (2014b). Preparing edible product, preferably food product including bakery product, and confectionary product, involves providing edible powder composition, and subjecting composition to selective laser sintering. Nederlandse Org Toegepast Natuurwetensch (Nede-C).
- Diaz, J. V., Noort, M. W., & Bommel, K. J. C. V. (2015a). Producing edible object used in food product, comprises subjecting edible powder composition comprising water soluble protein, hydrocolloid and plasticizer to powder bed printing by depositing edible liquid onto powder in layer-wise manner. Nederlandse Org Toegepast Natuurwetensch (Nede-C).
- Dick, A., Bhandari, B., & Prakash, S. (2019). 3D printing of meat. *Meat Science*, 153, 35-44.
- Doris. (2016). The XYZprinting 3D Food Printer. Retrieved from <https://www.3printr.com/xyzprinting-3d-food-printer-0635545/>
- El-kalyoubi, M., Khallaf, M. F., Abdelrashid, A., & Mostafa, E. M. (2011). Quality characteristics of chocolate containing some fat replacer. *Annals of Agricultural Sciences*, 56(2), 89-96.
- Fernandez-Vicente, M., Calle, W., Ferrandiz, S., & Conejero, A. (2016). Effect of infill parameters on tensile mechanical behavior in desktop 3D printing. *3D printing and additive manufacturing*, 3(3), 183-192.
- Frewer, L., Scholderer, J., & Lambert, N. (2003). Consumer acceptance of functional foods: issues for the future. *British Food Journal*, 105(10), 714-731.

- Gibson, I., Rosen, D., & Stucker, B. (2010). Additive manufacturing technologies: rapid prototyping to direct digital manufacturing: *Springer*.
- Godoi, F. C., Prakash, S., & Bhandari, B. R. (2016). 3d printing technologies applied for food design: Status and prospects. *Journal of Food Engineering*, 179, 44-54.
- Gray, N. (2010, 4 July 2012). Looking to the future: creating novel food food using 3D printing. Retrieved from <http://www.foodnavigator.com/Science/Looking-to-the-future-Creating-novel-foods-using-3D-printing>
- Hao, L., Mellor, S., Seaman, O., Henderson, J., Sewell, N., & Sloan, M. (2010). Material characterisation and process development for chocolate additive layer manufacturing. *Virtual and Physical Prototyping*, 5(2), 57-64.
- Hopkinson, N., Hague, R., & Dickens, P. (2006). *Rapid manufacturing: an industrial revolution for the digital age*: John Wiley & Sons.
- Hoseney, R. C., & Rogers, D. E. (1990). The formation and properties of wheat flour doughs. *Critical Reviews in Food Science & Nutrition*, 29(2), 73-93.
- Huang, S. H., Liu, P., Mokasdar, A., & Hou, L. (2012). Additive manufacturing and its societal impact: a literature review. *The International Journal of Advanced Manufacturing Technology*, 67(5-8), 1191-1203.
- iReviews. (2014). 3D System ChefJet Pro 3D food printer. Retrieved from <http://3d-food-printers.ireviews.com/3d-systems-chefjet-pro-review>
- Kinta, Y., & Hartel, R. W. (2010). Bloom formation on poorly-tempered chocolate and effects of seed addition. *Journal of the American Oil Chemists' Society*, 87(1), 19-27.
- Knecht, R. (1990). Properties of sugar. *Sugar*, 46-65.
- Kruth, J. P., Wang, X., Laoui, T., & Froyen, L. (2003). Lasers and materials in selective laser sintering. *Assembly Automation*, 23(4), 357-371.
- Ladipo, P. K., Olufayo, T., & Bakare, R. (2012). Learning Construct: Its Implication for Marketing and Buyer's Perception of Product Stimulus. *American Journal of Business and Management*, 1(3), 119-123.
- Lai, W.-H., & Cheng, C.-I. (2007). Manufacturing method of three-dimensional food by rapid prototyping: Google Patents.
- Lanaro, M., Forrestal, D. P., Scheurer, S., Slinger, D. J., Liao, S., Powell, S. K., & Woodruff, M. A. (2017). 3D printing complex chocolate objects: Platform design, optimization and evaluation. *Journal of Food Engineering*, 215, 13-22.
- Le Tohic, C., O'Sullivan, J. J., Drapala, K. P., Chartrin, V., Chan, T., Morrison, A. P., Kelly, A. L. (2018). Effect of 3D printing on the structure and textural properties of processed cheese. *Journal of Food Engineering*, 220, 56-64.
- Linden, D. V. D. (2015). 3D Printing Makes Food Unique. Retrieved from https://www.tno.nl/media/5517/3d_food_printing_march_2015.pdf

- Lipson, H., & Kurman, M. (2013). *Fabricated: The new world of 3D printing*: John Wiley & Sons.
- Lipton, Arnold, D., Nigl, F., Lopez, N., Cohen, D., Norén, N., & Lipson, H. (2010). *Multi-material food printing with complex internal structure suitable for conventional post-processing*. Paper presented at the Solid Freeform Fabrication Symposium.
- Lipton, Cutler, M., Nigl, F., Cohen, D., & Lipson, H. (2015). Additive manufacturing for the food industry. *Trends in Food Science & Technology*, 43(1), 114-123.
- Liu, Z., Bhandari, B., Prakash, S., & Zhang, M. (2018). Creation of internal structure of mashed potato construct by 3D printing and its textural properties. *Food Research International*, 111, 534-543.
- Liu, Z., Zhang, M., Bhandari, B., & Wang, Y. (2017). 3D printing: Printing precision and application in food sector. *Trends in Food Science & Technology*, 69, 83-94.
- Malone, E., & Lipson, H. (2007). Fab@Home: the personal desktop fabricator kit. *Rapid Prototyping Journal*, 13(4), 245-255.
- Mantell, D. A., Hays, A. W., & Langford, Z. C. (2015). Printing 3d tempered chocolate: Google Patents.
- Mantihal, S., Prakash, S., & Bhandari, B. (2019). Textural modification of 3D printed dark chocolate by varying internal infill structure. *Food Research International*, 121, 648-657.
- Mantihal, Prakash, S., Godoi, F. C., & Bhandari, B. (2019). Effect of additives on thermal, rheological and tribological properties of 3D printed dark chocolate. *Food Research International*, 119, 161-169.
- Mantihal, S., Prakash, S., Godoi, F. C., & Bhandari, B. (2017). Optimization of chocolate 3D printing by correlating thermal and flow properties with 3D structure modeling. *Innovative Food Science & Emerging Technologies*, 44(Supplement C), 21-29.
- McCluskey, J. J., Kalaitzandonakes, N., & Swinnen, J. (2016). Media Coverage, Public Perceptions, and Consumer Behavior: Insights from New Food Technologies. *Annual Review of Resource Economics*, Vol 8, 8, 467-486.
- Mellor, S., Hao, L., & Zhang, D. (2014). Additive manufacturing: A framework for implementation. *International Journal of Production Economics*, 149, 194-201.
- Molitch-Hou, M. (2014). The Foodini 3D Food Printer Hits Kickstarter! Retrieved from <http://3dprintingindustry.com/2014/03/31/3d-printer-foodini-food-kickstarter/>
- Morgan, M., & Hemmington, N. (2008). From foodservice to food experience? Introduction to the topical focus papers. *Journal of foodservice*, 19(2), 108-110.
- Natural Machines. (2016). Foodini: a 3D food printer. Retrieved from <https://www.naturalmachines.com/>
- Nocera, A. D., Salvatierra, N. A., & Cid, M. P. (2015). Printing Collagen 3D Structures. 49, 136-139.

- Oskay, W., & Edman, L. (2006). The Candy Fab Project. Retrieved from <http://candyfab.org/>
- Periard, D., Schaal, N., Schaal, M., Malone, E., & Lipson, H. (2007). *Printing food*. Paper presented at the Proceedings of the 18th Solid Freeform Fabrication Symposium, Austin TX.
- Porimy. (2014). Porimy Kunshan Bo Mai Three Dimensional Printing Technology Co., Ltd. Retrieved from <https://translate.google.com.au/translate?hl=en&sl=zh-CN&u=http://www.porimy.com/&prev=sea>
- RepRap. (2016). RepRapWiki: G-code. Retrieved from <http://reprap.org/wiki/G-code>
- Rollin, F., Kennedy, J., & Wills, J. (2011). Consumers and new food technologies. *Trends in Food Science & Technology*, 22(2), 99-111.
- Ronteltap, A., & van Trijp, H. (2007). Consumer acceptance of personalised nutrition. *Genes & nutrition*, 2(1), 85-87.
- Ronteltap, A., van Trijp, J. C. M., Renes, R. J., & Frewer, L. J. (2007). Consumer acceptance of technology-based food innovations: Lessons for the future of nutrigenomics. *Appetite*, 49(1), 1-17.
- Schniederjans, D. G. (2017). Adoption of 3D-printing technologies in manufacturing: A survey analysis. *International Journal of Production Economics*, 183, 287-298.
- Severini, C., & Derossi, A. (2016). Could the 3D printing technology be a useful strategy to obtain customized nutrition? *Journal of clinical gastroenterology*, 50(2), 175-178.
- Severini, C., Derossi, A., & Azzollini, D. (2016). Variables affecting the printability of foods: Preliminary tests on cereal-based products. *Innovative Food Science & Emerging Technologies*, 38, 281-291.
- Severini, C., Derossi, A., Ricci, I., Caporizzi, R., & Fiore, A. (2018). Printing a blend of fruit and vegetables. New advances on critical variables and shelf life of 3D edible objects. *Journal of Food Engineering*, 220, 89-100.
- Sher, D., & Tutó, X. (2015). Review of 3D Food Printing. *Temes de disseny*(31), 104-117.
- Shirazi, S. F. S., Gharekhani, S., Mehrali, M., Yarmand, H., Metselaar, H. S. C., Kadri, N. A., & Osman, N. A. A. (2016). A review on powder-based additive manufacturing for tissue engineering: selective laser sintering and inkjet 3D printing. *Science and Technology of Advanced Materials*.
- Siegrist, M. (2008). Factors influencing public acceptance of innovative food technologies and products. *Trends in Food Science & Technology*, 19(11), 603-608.
- Sood, A. K., Ohdar, R., & Mahapatra, S. (2010). Parametric appraisal of mechanical property of fused deposition modelling processed parts. *Materials & Design*, 31(1), 287-295.
- Stewart-Knox, B., & Mitchell, P. (2003). What separates the winners from the losers in new food product development? *Trends in Food Science & Technology*, 14(1), 58-64.
- Sun, J., Peng, Z., Zhou, W., Fuh, J. Y., Hong, G. S., & Chiu, A. (2015). A Review on 3D Printing for Customized Food Fabrication. *Procedia Manufacturing*, 1, 308-319.

- Sun, J., Zhou, W., Huang, D., Fuh, J. Y. H., & Hong, G. S. (2015). An Overview of 3D Printing Technologies for Food Fabrication. *Food and Bioprocess Technology*, 8(8), 1605-1615.
- Sun, J., Zhou, W., Yan, L., Huang, D., & Lin, L.-y. (2018). Extrusion-based food printing for digitalized food design and nutrition control. *Journal of Food Engineering*, 220, 1-11.
- Suntornnond, R., An, J., & Chua, C. (2017). Roles of support materials in 3D bioprinting—present and future. *International Journal of Bioprinting*, 3(1), 1-4.
- Suwannaporn, P., & Speece, M. W. (2010). Assessing new product development success factors in the Thai food industry. *British Food Journal*, 112(4), 364-386.
- Tadmor, Z., & Klein, I. (1970). *Engineering principles of plasticating extrusion*: Van Nostrand Reinhold Co.
- Talbot, G. (1994). Chocolate temper *Industrial chocolate manufacture and use* (pp. 156-166): Springer.
- Tronvoll, S. A., Welø, T., & Elverum, C. W. (2018). The effects of voids on structural properties of fused deposition modelled parts: a probabilistic approach. *The International Journal of Advanced Manufacturing Technology*, 97(9), 3607-3618.
- Vancauwenberghe, V., Delele, M. A., Vanbiervliet, J., Aregawi, W., Verboven, P., Lammertyn, J., & Nicolaï, B. (2018). Model-based design and validation of food texture of 3D printed pectin-based food simulants. *Journal of Food Engineering*, 231, 72-82.
- Wang, L., Zhang, M., Bhandari, B., & Yang, C. (2018). Investigation on fish surimi gel as promising food material for 3D printing. *Journal of Food Engineering*, 220, 101-108.
- Wille, R., & Lutton, E. (1966). Polymorphism of cocoa butter. *Journal of the American Oil Chemists Society*, 43(8), 491-496.
- Winger, R., & Wall, G. (2006). Food product innovation: a background paper. *Agricultural and food engineering working document*, 2.
- Yang, F., Zhang, M., Bhandari, B., & Liu, Y. (2018). Investigation on lemon juice gel as food material for 3D printing and optimization of printing parameters. *LWT - Food Science and Technology*, 87, 67-76.
- Yang, F., Zhang, M., Prakash, S., & Liu, Y. (2018a). Physical properties of 3D printed baking dough as affected by different compositions. *Innovative Food Science & Emerging Technologies*.
- Yang, F., Zhang, M., Prakash, S., & Liu, Y. (2018b). Physical properties of 3D printed baking dough as affected by different compositions. *Innovative Food Science & Emerging Technologies*, 49, 202-210.
- Zhang, H., Fang, M., Yu, Y., Liu, Q., Hu, X., Zhang, L., Tian, F. (2018). *Application Prospect of 3D Printing Technology in the Food Intelligent Manufacturing*. Paper presented at the International Conference on Mechatronics and Intelligent Robotics.

Chapter 3 - 3D Printer modification and development of printing method for powdered chocolate

Abstract

This chapter provides the first investigation of the 3D printer modification, making the printer and printing parameters suitable for printing dark chocolate as well as the sample themselves being appropriately prepared for the printing process. Powdered dark chocolate was used as the main food material for printing. Several modifications to an extrusion type of 3D printer were made to ensure chocolate powder will extrude and solidify after deposition. The modification includes development of custom printer bed and inbuilt water recirculation system with a slow flow rate of 6.3 mL/s to avoid vibration. Additionally, a fan was attached to enhance the solidification of chocolate. Finally, the printing procedure and conditions (nozzle gap, extrusion temperature) for printing powdered chocolate were determined. Such modifications were successfully applied to dark chocolate printing, allowing layer-by-layer deposition.

3.1 Introduction

The notion of commercial 3D food printing was initiated in 2007 at Cornell University where the Fab@home 3D food printer was created (van der Linden, 2015). Since then, industries and educational institutions have investigated the potential of 3D printing technology to incorporate edible ink (or food). Various 3D printing methods were implemented into printing food such as selective laser sintering, extrusion and binder jetting (Liu, Zhang, Bhandari, & Wang, 2017). Each method requires a distinct technique for the formation of a 3D structure: a laser beam, pressure pump, rotary screw or liquid binding.

Understanding food material properties is important in 3D food printing (Godoi, Bhandari, & Prakash, 2017) as this helps to determine the parameters required for a successful printing process. For instance, by understanding the thermal properties of food, this will provide an insight into the printing temperature (Sun, Zhou, Yan, Huang, & Lin, 2018). Over the past few years, researchers have been focusing on understanding the material properties of food for this purpose (Chen & Mackley, 2006; Coelho, 2015; Mantell, Hays, & Langford, 2015). Interestingly, chocolate, as an edible ink, was the most studied food material. Hence, companies like Choc Edge (ChocEdge, 2013), TNO (3D System, 2013) and Porimy (Porimy, 2014) have developed their own specific 3D printers for chocolate printing.

Chocolate is a complex composition that contains cocoa solids, milk solids, sucrose, and lecithin. Altogether, these ingredients influence the rheological properties which are an important parameter for determining the printability of chocolate. The most important component in chocolate is the complex crystal structure of fat. There are six crystal polymorphs existing in chocolate (Afoakwa, 2010). These crystals have different ranges of melting points from 16.1 °C up to 36.8 °C (Talbot, 2009). However, the most favourable crystal that gives chocolate its quality attributes such as smoothness, a glossy look, and snap ability is Form V (β) with a melting point of 33.8 °C (Afoakwa, 2010). The solidification temperature (usually the same as the melting temperature of the β -crystal type) is an important material property that determines the feasibility of layer-by-layer printing. The printed layer needs to quickly solidify to hold the subsequent printed layer. Therefore, having a cool printer bed is particularly important in the 3D printing of food materials such as chocolate.

Some of the 3D printers that are available in the market are not equipped with a cooling bed system. However, for substances like chocolate, to maintain the bed temperature, a cooling system such as a cold water circulation is needed to ensure the printer bed will remain cool. It should be noted that a cold bed temperature can also lead to condensation of moisture on the bed because the surrounding

air may reach the dew point temperature when it hits the cold bed. Thus, to avoid moisture condensation, it is also important that there is sufficient air flow around the printer bed.

In this chapter, the 3D food printer (Porimy) was modified to suit the requirements for successful printing of chocolate. It is hypothesized that the modification of the 3D printer and optimization of parameters in chocolate printing are essential to produce an excellent 3D printed construct. The main objective was to ensure the dark chocolate solidified immediately after deposition. Three important aspects were considered in this work (a) development of cooling printer bed (with built-in inner water circulation tube), cold water circulation system and printer bed support (b) determining printing parameters (c) optimizing the nozzle height.

3.2 Materials and methods

3.2.1 Chocolate powder

Lindt Piccoli Swiss, Australia dark chocolate with 58% cocoa solid (non-fat), cocoa butter (33% w/w), anhydrous milk fat (5 %), soy lecithin (0.5 %) and vanilla flavour were used for this study. The chocolate was powdered using a stainless steel grinder (Homemaker-SKU: P_42651208, Kmart, Australia) set in fine mode inside a cold room (5 °C) to avoid softening of the chocolate during grinding. The particle size of the resulting powder was approximately < 200 µm, suitable for the extrusion method.

3.2.2 3D printer

A Porimy Chocolate 3D printer (Porimy Co. Ltd., Kunshan, China) equipped with an auger type of extruder and a large hopper, capable of handling relatively large amounts of food material was used. This type of printer has the advantage of more food substrates being able to be added as the printing progresses. The printer nozzle is attached to a rotating motor that rotates the mixture in the hopper slowly, pushing down the materials to the nozzle for heat treatment via a cylinder channel. The Porimy printer applies the extrusion method with a heating capacity of up to 120 °C.

In chocolate extrusion, temperature manipulation is important as chocolate contains six polymorph crystals that melt at a different ranges of temperature (Afoakwa, Paterson, Fowler, & Vieira, 2008). The desirable melting temperature of chocolate is 32 °C (Afoakwa, Paterson, Fowler, & Vieira, 2008; Cebula & Hoddle, 2009; Chocolate Alchemy, 2008; Hao et al., 2010; Kinta & Hartel, 2010). Figure 3.1 shows the schematic diagram of the Porimy 3D chocolate printer. The main components are enclosed within a stainless steel case.

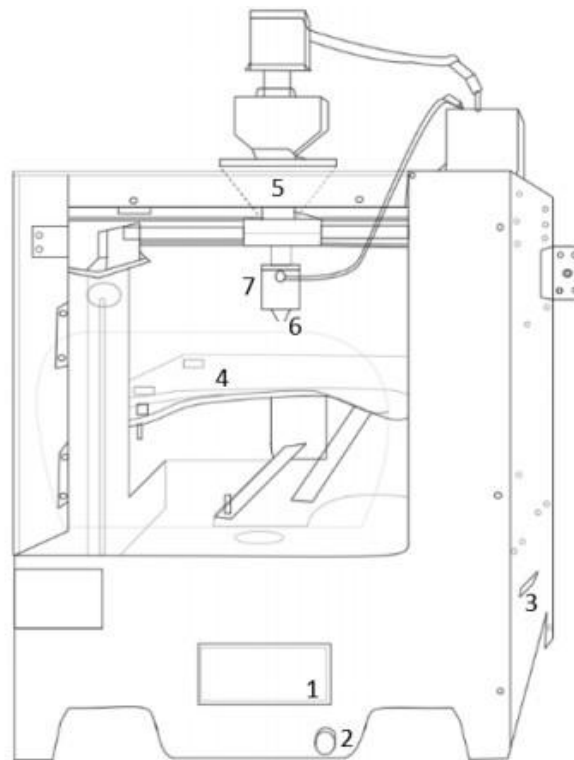


Figure 3.1: Schematic diagram of Porimy 3D chocolate printer printing mechanism (1. Information and control display screen, 2. Navigation knob, 3. SD card slot, 4. Printer bed, 5. Printer hopper, 6. Nozzle, 7. Heating component).

3.2.3 3D Printing design and software

An online TinkerCad 3D design software was used to create a 3D model construct. The design was downloaded into a stereolithographic (STL) file. The file was then transferred into Repetier (open source software) equipped with Sli3er (slicing software) that slices the 3D model in detail with all the pre-determined parameters and converts the STL file into g-code. Figure 3.2 demonstrates the process of chocolate printing.

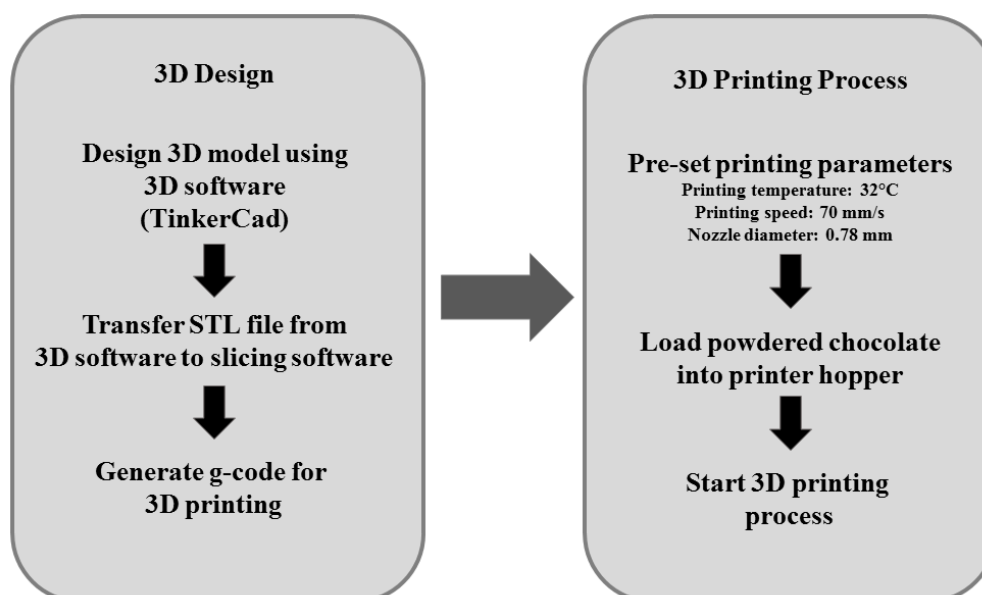


Figure 3.2: Flow diagram of the chocolate 3D printing process, starts with 3D design and proceeds to 3D printing process.

3.2.4 Temperature profile of extruded chocolate

The temperature profile of the extruded chocolate was measured using a digital thermometer with 0.26 mm probe diameter (CENTER 309 thermometer, Taiwan). Temperatures were obtained by inserting a thin probe into an extruded layer during printing and after the printing process was completed.

3.2.5 Statistical analysis

The results of extruded chocolate layers were analysed using Analysis of variance (ANOVA) with Tukey's pair wise comparison at 95% confidence interval at ($p < 0.05$) is considered significant.

3.3 Results and discussion

3.3.1 Modification of printer bed and development of cold water circulation system

A square (200 mm x 200 mm x 10 mm) stainless steel printer bed was designed to address the solidification issue of chocolate. The first layer of extrusion supports any subsequent layers as the printer builds up the structure. The printer bed was designed with inner water circulation to allow faster solidification of the extruded chocolate, by maintaining the bed temperature ~ 16 °C. In addition, the temperature of the printer bed can also be set even cooler by circulating colder water. Figure 3.3 illustrates the cooling printer bed.

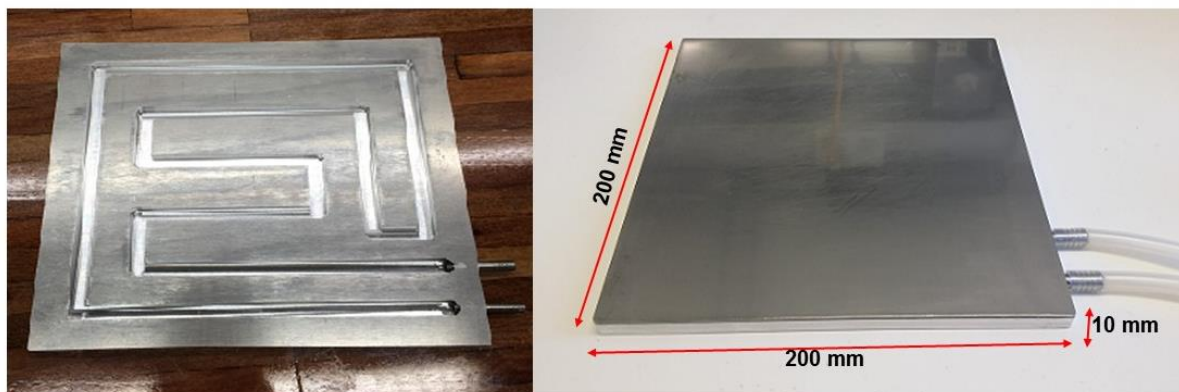


Figure 3.3: Cooling printer bed made in this study. The recirculation tubes (diameter 0.8 cm total 80 cm length) are enclosed as heat exchanger inside the plate.

In order to cool the printer bed, a customized cold water circulation system was developed. Cold water flowed at low pressure with a 12W water pump to reduce the vibration on the bed during printing. It was designed with a water inlet and outlet for water inflow and outflow via an 8 mm diameter silicon tube. Figure 3.4 shows the cold water circulation system.

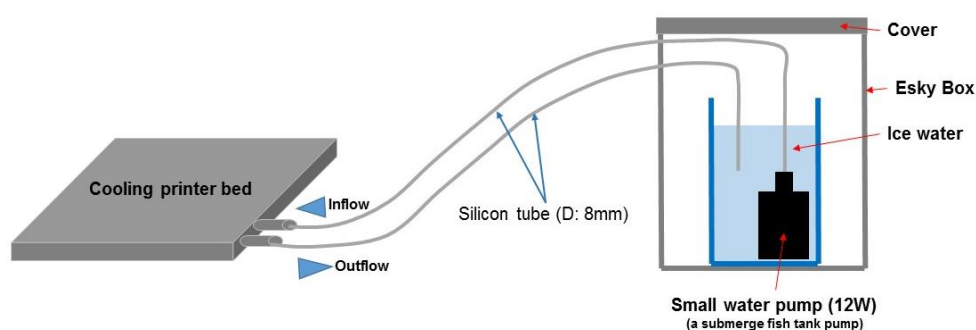


Figure 3.4: Schematic diagram of water circulation system with a 12W submerged pump.

The volumetric flow rate was calculated using the formula: $Q = V/t$ where Q is volumetric flow rate, V is volume in mL and t (time) is in seconds. An average volume (mL) of 380 mL was collected in the volumetric flask in 60 seconds. The flow rate (Q) was thus 6.33 mL/s. A low flow rate of cold water is important in this study to avoid vibration during water circulation as this may interrupt the chocolate printing process. The printer bed temperature was measured as ~ 16 °C during the printing process. Ice was added after every 30 minutes of printing time to ensure the printer bed maintained the required temperature. The complete modified 3D printer is depicted in Figure 3.5.

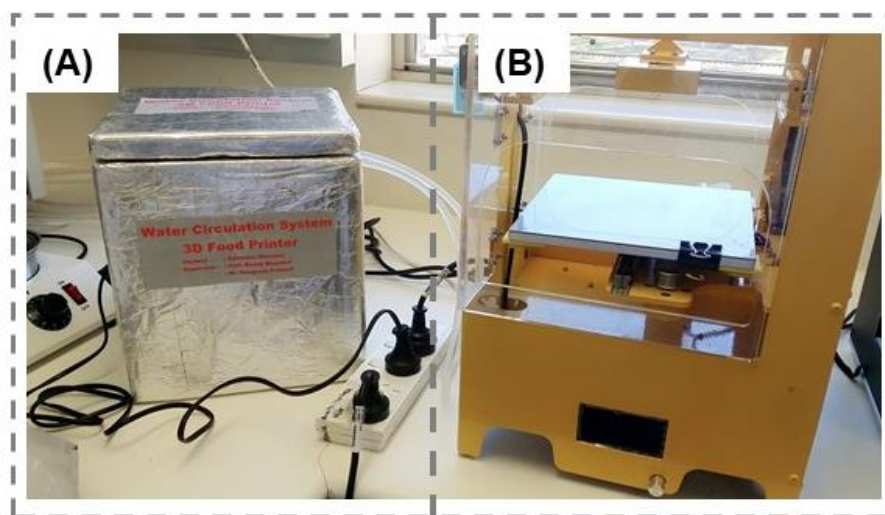


Figure 3.5: 3D chocolate printing system with additional feature (a) water circulation system (b) custom printer bed.

3.3.2 Printer bed stabiliser (support)

The acrylic printer bed of the Porimy 3D printer is a stainless steel bed. Hence new supports were devised to stabilize the bed. Four printer bed stabilizers (Figure 3.6) were developed through 3D design and printed using XYZ printing via a Da Vinci 2.0 filament 3D printer. A square block with 38 mm x 34 mm x 4mm (medium infill 25%) was printed with ABS filament with 7 mm diameter hole at the centre for ease of attachment on the printer. It was observed that the custom printer bed stabilizer was able to support the stainless steel printer bed.

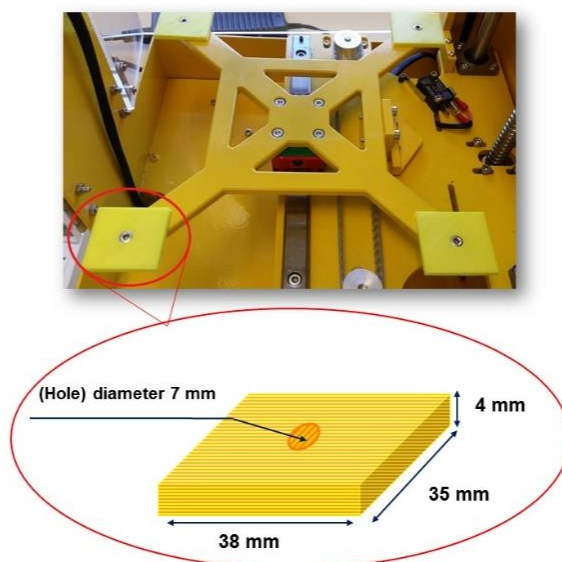


Figure 3.6: Printer bed support printed using 3D filament printer (XYZ printing) with ABS filament.

3.3.3 Addition of air blowing fan

During the printing process, air was blown toward the deposited chocolate using a fan, which assisted in speeding up the solidification process as the 3D construction's height is built. Each layer needed to solidify quickly to support the upcoming layer to avoid the structure from collapsing. In addition, air from the fan also helped to reduce the condensation on top of the printer bed as water droplet formation may occur while the printer bed is cooled depending on the temperature used and the humidity of the ambient air. Figure 3.7 shows the fan (USB Fan 2.25 W) attached to the printer. Air flow rate was not measured.

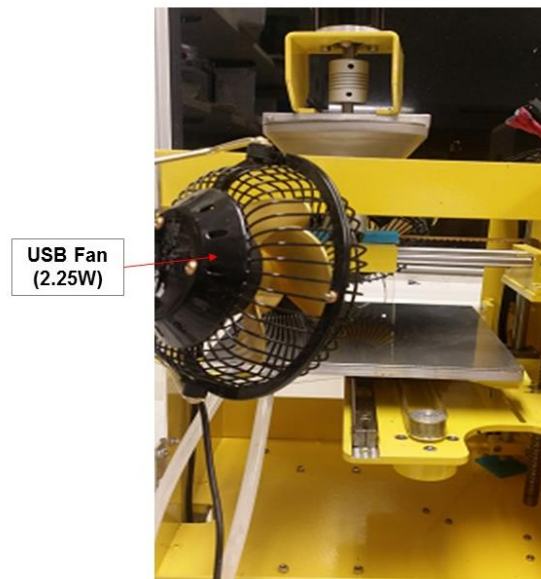


Figure 3.7: Attachment of USB fan (2.25 W) on the 3D Porimy printer.

3.3.4 3D model design

As indicated above, the chocolate printing process started with designing a 3D model through 3D software. This 3D model should not exceed the printing capacity of the printer. Figure 3.2 above sets out the process. To gain a firm 3D construction, infill density was set between 80% and 100% depending on the 3D model design. The infill pattern and extrusion temperature were set accordingly. The g-code contained a series of sequential code that navigated the movement of the X, Y, and Z axes on the 3D printer. The 3D food printer used an open source software, therefore any 3D design software was able to be used in designing the 3D model for printing (3D System, 2013). The 3D printer is well-matched with STL (stereolithography) format or OBJ (object file) formats. The STL file format has become the rapid prototyping industry's defacto standard data transmission format and is the format required to interact with 3D printing (3D System, 2013). An OBJ file defines the geometry and other properties for objects in Wavefront's Advanced Visualizer. Object files can also be used to transfer geometric data back and forth between Advanced Visualizer and other

applications. In this study, Tinkercad online software was used to design a 3D model for chocolate printing. The 3D geometrical design was developed as a model for 3D chocolate construction and the STL file was downloaded. Figure 3.8 shows the 3D software used to develop the 3D model.

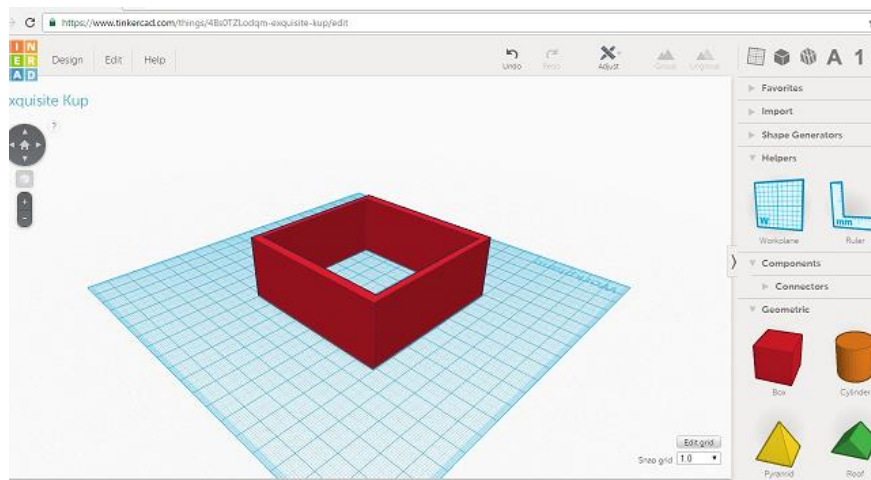


Figure 3.8: Tinkercad 3D online software. Available at <https://www.tinkercad.com>

3.3.5 Optimization of nozzle height

Nozzle height is defined as the gap between the nozzle tip and deposited top layer on the printer bed. Attalla, Ling, and Selvaganapathy (2016) reported that the nozzle distance could influence the geometry shape of a 3D printed product. Theoretically, the extrusion mass flow rate and the movement speed of the nozzle assumed to directly influence the nozzle height and would result in a bed of extruded material with a diameter equal to that of the nozzle (Khalil & Sun 2007). Ideally, the extruded chocolate should have the same diameter as the nozzle size considering no swelling, shrinking or expansion of the extruded material (Yang, Zhang, Bhandari, & Liu, 2018). Many trials were done in this study to determine the accurate nozzle height suitable for chocolate extrusion. In this experiment, a small nozzle with an inner diameter 0.78 mm were used. Periard, Schaal, Schaal, Malone, and Lipson (2007) suggested that a small nozzle diameter helps to construct a fine resolution and a smooth 3D object. Three extruded first layers with varied nozzle height settings are shown in Figure 3.9.

A thicker extruded line (diameter 0.98 min - 1.90 max) than anticipated was obtained with a nozzle height 0.5 mm as shown in Figure 3.7(a). A broken extruded line (diameter 0.92 min - 1.21 max) can be seen in Figure 3.7(b) where the nozzle height was 1.0 mm. The best extruded line (diameter 0.74 min – 0.79 max) considered to be almost equivalent with nozzle diameter size was observed in Figure 3.9(c) where the nozzle height was 0.78 mm. Thus, we found that in chocolate extrusion, it was best

that the nozzle height is the same as the nozzle diameter. This result was similar to that in a previous study (Yang et al., 2018).

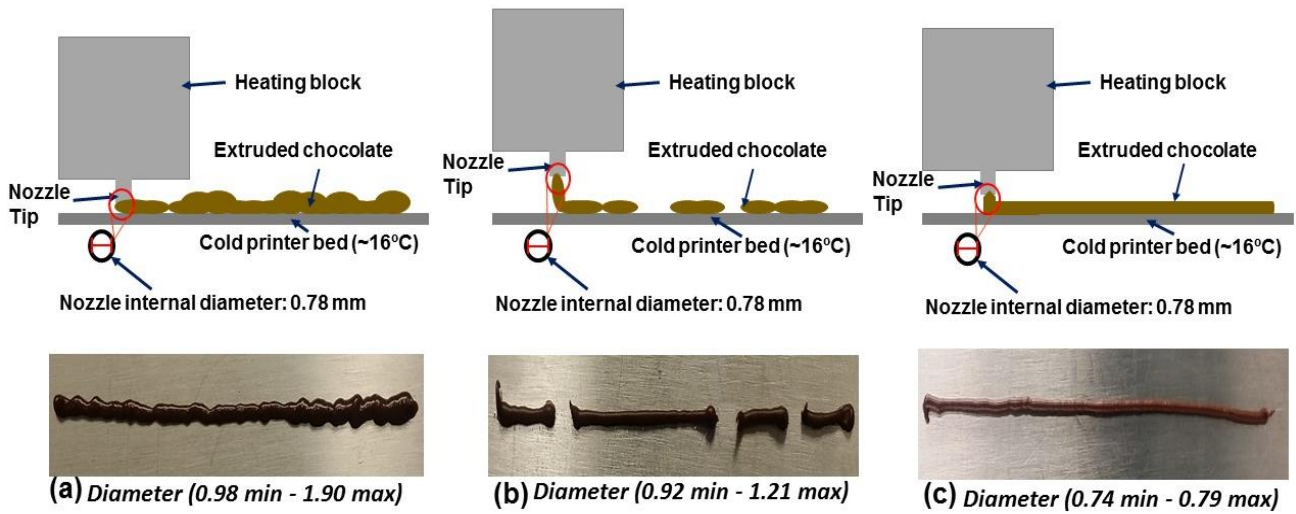


Figure 3.9: Schematic illustration of effect of distance between nozzle tip and printer bed [nozzle size 0.78 mm, printing speed 70 mm/s, printer bed temperature $\sim 16^\circ\text{C}$ and nozzle height (a) 0.5 mm (b) 1.0 mm (c) 0.78 mm].

3.3.6 Temperature profile of extruded chocolate

The printer bed temperature was $\sim 16^\circ\text{C}$ while the ambient temperature was 25°C . Figure 3.10 shows a temperature measurement point of a 3D printed chocolate of heart-in-heart shape. A thin thermometer probe (diameter 0.26 mm) was inserted in every layer during printing at the point shown in Figure 3.10(a) as indicated by $P1$, $P2$ and $P3$. Temperatures for each extruded chocolate layer were recorded and these are reported in Table 3.1.

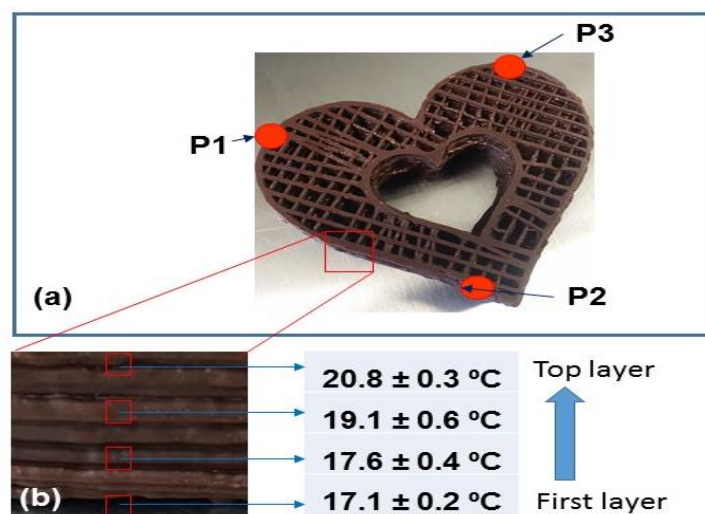


Figure 3.10: Heart-in-heart 3D printed chocolate. (a) Three points ($P1$, $P2$ and $P3$) to determine extruded layer temperature (b) Recorded temperature ($^\circ\text{C}$) on four points of extruded layer of heart-in-heart 3D shape after printing complete. (nozzle internal diameter: 0.78 mm, printing speed: 70 mm/s,

printing time: 24 minutes, layer count: 12, temperature probe diameter; 0.26 mm, printer bed temperature: $\sim 16\text{ }^{\circ}\text{C}$, ambient temperature: $\sim 25\text{ }^{\circ}\text{C}$).

Table 3.1: Recorded temperature ($^{\circ}\text{C}$) of extruded layer of Heart-in-heart 3D shape during printing process denote as point 1 (P1), point 2 (P2) and point 3 (P3) based from the point indicated in Figure 3.10 (a).

Layer count	P1 ($^{\circ}\text{C}$)	P2 ($^{\circ}\text{C}$)	P3 ($^{\circ}\text{C}$)
1	19.2 ± 0.5^a	18.5 ± 0.3^a	19.2 ± 0.7^a
2	19.8 ± 0.5^a	19.5 ± 0.9^a	19.7 ± 0.4^a
3	22.2 ± 0.6^a	21.2 ± 0.6^a	22.1 ± 0.9^a
4	22.9 ± 0.3^a	22.9 ± 1.3^a	22.9 ± 0.7^a
5	23.5 ± 0.4^a	23.5 ± 1.2^a	24.0 ± 0.6^a
6	24.2 ± 0.4^a	23.6 ± 1.0^a	24.1 ± 0.9^a
7	23.0 ± 0.4^a	23.5 ± 0.8^a	23.4 ± 0.6^a
8	23.8 ± 0.8^a	23.6 ± 0.9^a	23.7 ± 0.4^a
9	24.6 ± 0.2^a	24.7 ± 0.2^a	24.7 ± 0.2^a
10	25.5 ± 0.2^a	24.8 ± 0.4^a	25.4 ± 0.3^a
11	25.5 ± 0.2^a	24.9 ± 0.3^a	25.3 ± 0.2^a
12	25.4 ± 0.6^a	24.8 ± 0.6^a	25.1 ± 0.8^a

Mean value of temperature ($^{\circ}\text{C}$) at point P1, P2, and P3 in each layer that does not share a letter is significantly different at $p < 0.05$.

It should be noted that the chocolate extrusion temperature in this study was set at $32\text{ }^{\circ}\text{C}$ and temperatures were recorded during extrusion of each layer. As can be seen in Table 3.1, the first extruded layer had temperatures between $18.5 \pm 0.3\text{ }^{\circ}\text{C}$ and $19.2 \pm 0.7\text{ }^{\circ}\text{C}$ and are not significantly different at $p < 0.05$. This indicated that the cold printer bed helped in reducing the chocolate temperature, thus leading to a faster solidification process. As the layer-by-layer deposition continued building a higher construct, a slight increase of temperature in each extruded layer was observed ranging from $18.5 \pm 0.3\text{ }^{\circ}\text{C}$ up to $25.4 \pm 0.6\text{ }^{\circ}\text{C}$ (from Layer 1 to Layer 12). This condition occurred due to an increase in distance between the constructed layer and the cold printer bed as heat from the printer bed was not efficiently transferable between layers, in particular beyond Layer 9. The addition of an air blower aided in circulating air around the printer bed, making the condition optimal for chocolate to solidify when building a higher construction. After the printing process was completed (24 minutes), the temperatures from four different points of layers were determined as shown in Figure 3.10(b). As can be seen, a gradient temperature from the first layer to the top layer (from $17.1 \pm 0.2^{\circ}\text{C}$ to $20.8 \pm 0.3^{\circ}\text{C}$) was recorded. As the first layer was on top of the cold printer bed, it was expected to have a lower temperature compared to the subsequent layers. It was observed that the extruded chocolate completely solidified after 24 minutes of printing time. The typical chocolate solidification time is 3 to 5 minutes under controlled room condition between $18\text{ }^{\circ}\text{C}$ and $21\text{ }^{\circ}\text{C}$

(Beckett, 2011). In this study, the chocolate was printed in room temperature condition at ~ 25 °C. In this condition, chocolate solidification would be slow. Therefore, the incorporation of cooled printer bed and air blower aided the solidification of chocolate upon extrusion. We conclude that the cold printer bed as well as the addition of the air blower were successful to achieve ideal conditions for the chocolate solidification process.

3.3.7 Chocolate printing

Generally, in chocolate making, chocolate is completely melted and recrystallized under controlled temperature conditions. In the chocolate printing process, the powdered form of the chocolate was used and partially melted at a controlled temperature prior to extrusion to make it printable. It was then transferred into the printer hopper. Melting extrusion has been applied to print chocolate forming a 3D construction with temperatures ranging from 28 °C to 33 °C (Chen & Mackley, 2006). In this study, powdered chocolate was used. This small particle of chocolate was easily melted when it reached the heated block of the nozzle. The temperature of the nozzle was controlled by setting at 32 °C (lower than the end-set of melting temperature of 33°C). As the powdered chocolate undergoes rotary extrusion and through heating block, the chocolate only melt partially as the solid chocolate (powder) push the melted chocolate during extrusion. Thus, it was assumed that there is a partial melting of chocolate in the heating block as it did not reach the end-set temperature. In addition, the controlled extrusion temperature (32 °C) is important in chocolate printing to maintain the flowability and viscosity of the material. Figure 3.11 shows various designs of chocolate structures with a fixed set of printing conditions (printing speed: 70 mm/s, nozzle diameter: 0.78mm and extrusion temperature: 32 °C). As can be seen, the modification of the printer (see Section 3.1) helped to produce good quality 3D printed objects and was successful in printing 3D shapes.

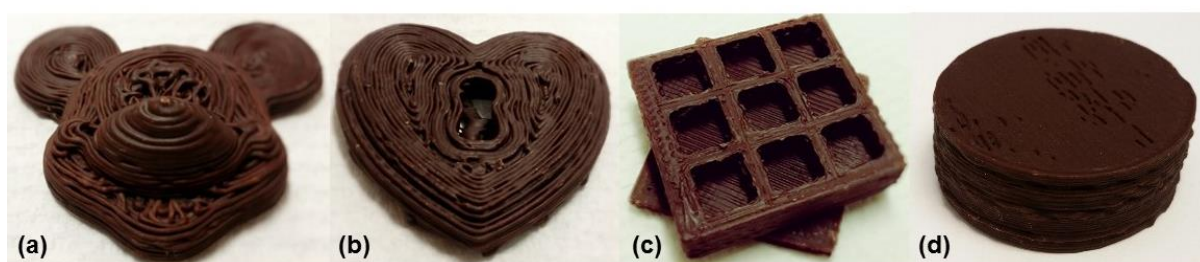


Figure 3.11: 3D chocolate printed using Porimy 3D printer (a) mickey mouse shape (b) heart shape (c) box with hollow square hole (d) cylinder shape. (Printing condition: Speed 70mm/s, Nozzle size 0.78mm and extrusion temperature 32 °C).

Maintaining a proper temperature is crucial in chocolate printing. Higher temperatures ($> 36\text{ }^{\circ}\text{C}$) will eliminate all polymorph in the chocolate, losing its ability to solidify immediately (Afoakwa, Paterson, Fowler, & Ryan, 2008). This is due to an insufficient amount of stable β crystal nuclei (Form V) in the chocolate matrix (Afoakwa, Paterson, & Fowler, 2007; Chen & Mackley, 2006; Elkalyoubi, Khallaf, Abdelrashid, & Mostafa, 2011; Hachiya, Koyano, & Sato, 1989; Mantell et al., 2015). As a result, it will not provide the desired 3D shape as observed in Figure 3.12.



Figure 3.12: The effect of improper temperature setting on dark chocolate after extrusion (a) extruded chocolate at high temperature ($>36\text{ }^{\circ}\text{C}$) (b) chocolate was not solidified and collapsed during extrusion.

3.4 Conclusion

The first objective of this research work was to modify the Porimy 3D printer to print chocolate successfully. To achieve this, several modifications were established to optimize the printing result for a selected powdered form of chocolate. A printer bed (that enabled cold water to flow through the built-in tube inside the printer bed) and water circulation system helped to establish an immediate solidification of chocolate, thus supporting the subsequent layering process while building up the 3D construction. A constant flow (6.33 mL/s) of cold water circulation helped to maintain printer bed temperature $\sim 16\text{ }^{\circ}\text{C}$. It is essential to maintain extrusion temperature at $32\text{ }^{\circ}\text{C}$ to ensure chocolate is printed well. An optimal nozzle height for chocolate printing was found to be the same as the nozzle diameter, 0.78 mm. It was also observed that the addition of an air blower during the printing process also assisted in maintaining the temperature and avoided condensation, helping the solidification process of chocolate. A standardised printing procedure including the design of the structure and the printing was developed in this study. This began with the design process, where the customization and personalization of 3D shapes were determined. The developed printing method was successful to print the 3D construction and improve the chocolate solidification process. These modifications and

the procedures developed in this work were applied to further research presented in successive chapters.

3.5 References

- 3D System. (2013, 10 september 2013). Technology brings edible 3D printing to professionals and consumers alike. Retrieved from <http://www.3dsystems.com/de/press-releases/3d-systems-acquires-sugar-lab>
- Afoakwa, E. O. (2010). *Chocolate science and technology* (Vol. 687). Oxford: Wiley-Blackwell.
- Afoakwa, E. O., Paterson, A., & Fowler, M. (2007). Factors influencing rheological and textural qualities in chocolate - a review. *Trends in Food Science & Technology*, 18(6), 290-298.
- Afoakwa, E. O., Paterson, A., Fowler, M., & Ryan, A. (2008). Flavor formation and character in cocoa and chocolate: a critical review. *Critical Review in Food Science and Nutrition*, 48(9), 840-857.
- Afoakwa, E. O., Paterson, A., Fowler, M., & Vieira, J. (2008). Modelling tempering behaviour of dark chocolates from varying particle size distribution and fat content using response surface methodology. *Innovative Food Science & Emerging Technologies*, 9(4), 527-533.
- Attalla, R., Ling, C., & Selvaganapathy, P. (2016). Fabrication and characterization of gels with integrated channels using 3D printing with microfluidic nozzle for tissue engineering applications. *Biomedical microdevices*, 18(1), 17.
- Cebula, D. J., & Hoddle, A. (2009). Chocolate and couvertures: applications in ice cream. 163-182.
- Chen, Y. W., & Mackley, M. R. (2006). Flexible chocolate. *Soft Matter*, 2(4), 304-309.
- ChocEdge. (2013). Creation: a Selection of our Chocolate Creations. Retrieved from <http://www.chocedge.com/creations.php>
- Chocolate Alchemy. (2008). Tempering - Deconstruction and Reconstruction and Illustrated Tempering. Retrieved from <http://chocolatealchemy.com/illustrated-tempering/>
- Coelho, M. (2015). Digital Chocolatier Prototype. Retrieved from <http://www.cmarcelo.com/cornucopia/>
- El-kalyoubi, M., Khallaf, M. F., Abdelrashid, A., & Mostafa, E. M. (2011). Quality characteristics of chocolate containing some fat replacer. *Annals of Agricultural Sciences*, 56(2), 89-96.
- Godoi, C., Bhandari, B. R., & Prakash, S. (2017). Tribo-rheology and sensory analysis of a dairy semi-solid. *Food Hydrocolloids*, 70, 240-250.

- Hachiya, I., Koyano, T., & Sato, K. (1989). Seeding effects on solidification behavior of cocoa butter and dark chocolate. I. Kinetics of solidification. *Journal of the American Oil Chemists' Society*, 66(12), 1757-1762.
- Hao, L., Mellor, S., Seaman, O., Henderson, J., Sewell, N., & Sloan, M. (2010). Material characterisation and process development for chocolate additive layer manufacturing. *Virtual and Physical Prototyping*, 5(2), 57-64.
- Kinta, Y., & Hartel, R. W. (2010). Bloom formation on poorly-tempered chocolate and effects of seed addition. *Journal of the American Oil Chemists' Society*, 87(1), 19-27.
- Khalil, S. and Sun, W., 2007. Biopolymer deposition for freeform fabrication of hydrogel tissue constructs. *Materials Science and Engineering: C*, 27 (3), 469478
- Liu, Zhang, M., Bhandari, B., & Wang, Y. (2017). 3D printing: Printing precision and application in food sector. *Trends in Food Science & Technology*, 69, 83-94.
- Mantell, D. A., Hays, A. W., & Langford, Z. C. (2015). Printing 3d tempered chocolate. In: Google Patents.
- Periard, D., Schaal, N., Schaal, M., Malone, E., & Lipson, H. (2007). *Printing food*. Paper presented at the Proceedings of the 18th Solid Freeform Fabrication Symposium, Austin TX.
- Porimy. (2014). Porimy Kunshan Bo Mai Three Dimensional Printing Technology Co., Ltd. Retrieved from <https://translate.google.com.au/translate?hl=en&sl=zh-CN&u=http://www.porimy.com/&prev=sea>
- RepRap. (2016). RepRapWiki: G-code. Retrieved from <http://reprap.org/wiki/G-code>
- Sun, J., Zhou, W., Yan, L., Huang, D., & Lin, L.-y. (2018). Extrusion-based food printing for digitalized food design and nutrition control. *Journal of Food Engineering*, 220, 1-11.
- Talbot, G. (2009). *Science and technology of enrobed and filled chocolate, confectionery and bakery products*: Elsevier.
- van der Linden, D. (2015). 3D Food Printing. Retrieved from https://www.tno.nl/media/5517/3d_food_printivannng_march_2015.pdf.
- Yang, F., Zhang, M., Bhandari, B., & Liu, Y. (2018). Investigation on lemon juice gel as food material for 3D printing and optimization of printing parameters. *LWT - Food Science and Technology*, 87, 67-76.

Chapter 4 - Optimization of dark chocolate 3D printing by correlating thermal and flow properties with 3D structure modelling¹

Abstract

A proper extrusion of dark chocolate in 3D printing process is essential to ensure a better 3D object construction. This research, therefore, seeks to optimise the printability dark chocolate by looking at the effect of 3D printing on thermal and flow properties of dark chocolate. The nozzle temperature before the deposition was maintained at 32 °C in order to extrude the melted state of the chocolate sample as the flow behaviour curves indicated that the melting of chocolate started between 28 °C to 30 °C. Also, the use of additive (Mg-ST) in dark chocolate extrusion was investigated. The quality of the printed chocolates (diameter, height, wall thickness and breaking strength) was analysed. A minor difference between the pre-determined diameter and the actual output diameter for each sample, suggesting a similarity between the printed 3D structure and the pre-designed 3D model. Wall thickness of printed item varied along with the height due to uneven deposition of chocolate as the layer height increased. The breaking strength of the chocolate sample was strongly related to the addition of support structure within the construct. Taken together, this chapter provides new insight into the 3D printing of chocolate.

¹ This chapter has been published as a research paper in the *Innovative Food Science and Emerging Technologies Journal* (IF = 3.116): Mantihal, S., Prakash, S., Godoi, F. C., & Bhandari, B. (2017). Optimization of chocolate 3D printing by correlating thermal and flow properties with 3D structure modeling. *Innovative Food Science & Emerging Technologies*, 44(Supplement C), 21-29. The core content of the manuscript was modified to keep the format consistent throughout the thesis.

4.1 Introduction

Over the past years, Three-Dimensional printing (3DP) technology has found application in a variety of fields including aerospace (NASA, 2013), tissue engineering (Murphy & Atala, 2014) and, more recently, food design. 3D food printing (3DFP) technology not only allows the development of personalized shapes and textures of edible products but also enables nutritional optimization of the final construct according to diet restrictions, such as low-sugar/salt and vitamin tailoring products (Lipson & Kurman, 2013).

As mentioned in the previous chapter, extrusion is the most common food dispensing method in 3D printing of foods. Currently, there are three distinct extrusion-based printings that are applicable for food printing (1) positive displacement (2) time pressure dispensing and (3) rotary screw extrusion (Lee & Yeong, 2015). In Positive Displacement method, a piston driven down gradually by a motor and the extrusion rate were based on motor displacement. Time pressure dispensing apply air pressure to extrude material, where the difference between ambient and air pressure drives the flow of material. In rotary-screw extrusion, the extrusion process were mainly dispense substrates by a rotational screw which is influence by the degree of rotation and the speed of motor determines the amount of dispensed (Lee & Yeong, 2015). In this study, the rotary screw extrusion method was applied to dispense the grated chocolate.

Understanding the physical properties of the supply material (ink) is essential to achieve quality 3D constructs (Godoi, Prakash, & Bhandari, 2016; Hao et al., 2010). As an example, in the extrusion-based 3D food printing processes, the edible ink should be able to hold its structure while the material is deposited layer-by-layer. This “self-supporting” capacity during extrusion relies on rheological (e.g., viscosity) and thermal (e.g., glass transition and melting point) properties; which together play an important role in the post-deposition solidification process of the deposited layer. Printable material for extrusion method should exhibit a shear-thinning behaviour that allows the substrates flow efficiently during extrusion through a fine nozzle (Siqueira et al., 2017). A deformation in viscosity of food substrate enable it to flow with a controlled temperature.

Chocolate has been considered a printable material by nature. The printability concept is associated with the ability to be extruded out of the nozzle and retain shape after layer-by-layer deposition (Hao et al., 2010). The first studies on cold extrusion of chocolate were reported by Chen and Mackley (2006). In their work, the extruded chocolate presented a flexible coil or rod-like shape. Later in the same decade, Hao et al. (2010) applied a deposition method to build 3D-shapes of chocolate, using a 3D printer from University of Exeter (ChocALM system). Hao’s study highlighted that extrusion rate,

nozzle velocity and nozzle height from printer bed were the vital parameters during chocolate depositions. In the previous chapter, the 3D printer has been modified to enhance the solidification of extruded chocolate by replacing the printer bed that equipped with a water recirculation system. Although the modification was a success, it was observed that the chocolate extrusion was not consistent in the auger system.

Many strategies can be applied to improve the printability of chocolate pieces, such as (1) precise temperature control during extrusion, (2) optimization of chocolate particle size and (3) incorporation of additives. Temperature control aims to induce the formation of more stable β crystals with enhanced texture, glossy and snap properties (Afoakwa, 2010). Secondly, a reduction in chocolate particle size by grating process facilitates melting during the printing process. A wide range of additives can be used to enhance 3DP performance, including hydrocolloids (carbohydrates and proteins), starches and sugars (Cohen et al., 2009). Altogether they play an important role in improving flow behavior, settling and lubricant properties of the supply material. This work focus on the use of magnesium stearate $\text{Mg}(\text{C}_{18}\text{H}_{35}\text{O}_2)_2$ which is known by acting as a lubricant enhancer in the tablet pharmaceutical production (Kikuta & Kitamori, 1994). Porimy (2014), a 3D food printer fabricant, recommends the addition of magnesium stearate (Mg-ST) in chocolate inks at proportions up to 5% w/w. Incorporation of this salt enhances the flow behavior and lubricant properties of the mixture, preventing ingredients from sticking to printer hopper and in the rotating auger. According to Food and Agriculture Organization of United State (FAO, 2015), the maximum intake of Magnesium salt is 9500 mg/kg for confectionery including hard and soft candy, nougats etc. Allen (2009) stated that the range of magnesium stearate proportion were 2500 mg to 50000 mg aid for lubricant purposes. Magnesium stearate were also being used in chewing gum formulations with the range between 0.1% to 5% in the mixture (Ream, Corriveau, Graff, & Matulewicz, 2001) the US patent US 6322806 B1. Food and Drug Administration (FDA) indicate that magnesium stearate is an inactive food additive and classified as generally recognize as safe (GRAS) (Li & Wu, 2014). This permitted additive is used for controlling the stickiness (anti-adherent property) and improve the flowability of the material used for extrusion (Faqih, Mehrotra, Hammond, & Muzzio, 2007). In this chapter, it is hypothesized that the inclusion of food additives may enhance the printability of powdered chocolate to achieve a better flowability during the auger-extrusion type of printing.

Beyond modifications in the edible ink, modeling 3D constructs by computer-aided design (CAD) software plays an important on the self-supporting properties of the deposited layers. The design of complex 3D structures may need supports, especially if the structure comprises of voids with no materials. These supports can be made in different ways such as cross or parallel depending on

structural design. As an example, Severini, Derossi, and Azzollini (2016) designed cereal-based 3D-constructs with the support structure to stabilize 3D-printed dough as the layer height increased.

In this chapter, 3D chocolate constructs (hexagonal shape) with different support structures were designed. Support structure aid supporting 3D complex geometries. It allows the designed construct to hold and stabilize its structure (Suntornnond, An, & Chua, 2017). Hexagonal design is considered as an intricate construct in chocolate design with six angle that would be suitable for studying the addition of supporting structure to enhance the stability and mechanical strength of 3D object. As mentioned in the introduction section similar 3D complex structure of other food materials have been studied by other authors (Severini et al., 2016). Thermal properties and rheological properties of the chocolate ink were correlated to achieve optimized printing conditions for extrusion temperature. The quality of the 3D chocolate constructs was assessed by measuring wall diameter, weight, height and snap force. This comprehensive study brings new insights to the development of 3D chocolate constructs with enhanced printability and physical stability characteristics.

4.2 Material and Methods

4.2.1 Supply material (ink) preparation

The supplied material (ink) was prepared using commercial dark chocolate buttons (Bittersweet Flavour, Lindt Piccoli) into steps: (1) grinding of chocolate using a food grinder (Homemaker-SKU: P_42651208, Kmart, Australia) and (2) incorporation of flow enhancer, Magnesium stearate (Mg-ST). The mixture was placed in the printer hopper until the initiation of the extrusion process. As informed by the supplier, the dark chocolate was composed of: 58% cocoa solid (non-fat), 33% cocoa butter, anhydrous milk fat (5%), soy lecithin (0.5%) and vanilla. The content of magnesium stearate (5 g per 100 g of grated chocolate buttons) in the ink composition was determined by preliminary tests.

4.2.2 Melting point of chocolate before and after printing

Thermal curves were obtained by scanning the raw and printed chocolate samples from 25 °C to 50 °C at a heating rate of 2°C/min with a DSC (DSC 1, STARE 143 System, Mettler Toledo). 5.5-6.5 mg of chocolate were added into a 40 µL sealed aluminium pans. The chocolate samples were scanned before extrusion, immediately after extrusion and 30 minutes, 1 hour and 24 hours after extrusion. Thermal transitions were expressed as T_o (onset temperature), T_p (peak temperature), and T_c (concluding temperature). Melting of chocolate was identified by the enthalpy (ΔH) obtained from the integrated area under the curve between T_o and T_c and expressed as J/g.

4.2.3 Rheological measurement

A controlled stress rheometer (AR-G2 Rheometer, TA Instrument) was used to measure the rheological behavior of the chocolate sample (grated chocolate with magnesium stearate). All measurements were carried out in a shear rate-controlled rheometer using 40 mm stainless steel, sandblast geometry. Peak hold (Flow procedure) was performed to access the chocolate viscosity. The shear rate was set at 100 s^{-1} the temperature at $32 \text{ }^{\circ}\text{C}$ and test duration 10 minutes. Temperature ramp was established to determine the melting point of chocolate. The pre-determined initial temperature was $25 \text{ }^{\circ}\text{C}$ with pre-shear rate 2 s^{-1} for 10 seconds. Temperature ramp was employed from $25 \text{ }^{\circ}\text{C}$ to $32 \text{ }^{\circ}\text{C}$ with constant shear rate 100 s^{-1} for 10 minutes. Measurements for flow properties were taken for peak hold and temperature ramp. The viscosity data was extracted from these parameters.

4.2.4 Design and 3D printing of chocolate

4.2.4.1 Design geometry

Modeling of the chocolate structures was performed using TinkerCad online software. The STL file was converted to Repetier-Host V1.6.0 format to enable slicing by Slic3r and generation of a g-code for each model. Three hexagon shapes were designed (a) with cross support, (b) with parallel support and (c) without support, as illustrated in Figure 4.1, respectively.

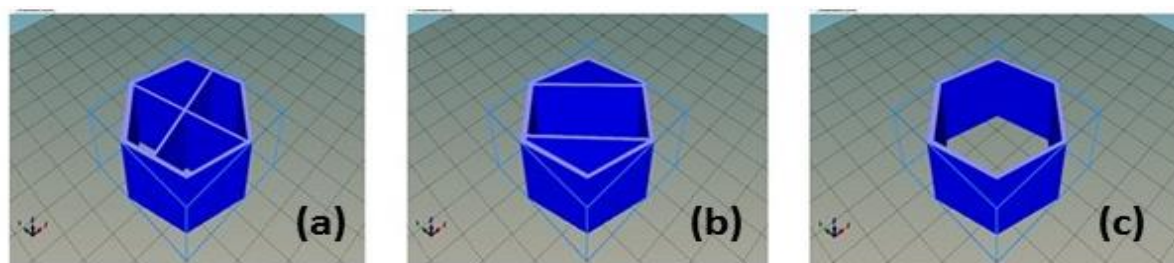


Figure 4.1: 3D model design of hexagonal model with (a) cross support (b) parallel support (c) no support.

4.2.4.2 Operational conditions

Porimy 3D chocolate printer (Porimy Co. Ltd, Kunshan, China) was used in this study. Prior printing, the extruder temperature was set at $32 \text{ }^{\circ}\text{C}$ for 5 minutes to ensure extruding temperature are controlled and maintained. Printing parameters were set as follow: printing speed 70 mm/s , extrusion temperature calibrated at $32 \text{ }^{\circ}\text{C}$, nozzle size 1.5 mm (inner diameter 0.8 mm) and printer bed temperature maintained at $15 \text{ }^{\circ}\text{C}$ to $22 \text{ }^{\circ}\text{C}$. These parameters were set based on correlations between thermal and flow behavior of the chocolate below. Figure 4.2 illustrates the schematic diagram of the 3D printing mechanism which uses a rotary screw extrusion method to extrude chocolate. This printer automatically regulates the proper gap between nozzle and printer bed by means of a built-in Reprap

XYZ system (a 3D printing system that navigates printer movement). In this study, a total of 27 samples were prepared with the dimensions listed in Table 4.1. The printed samples were stored in refrigeration at around 15 °C until quality assessment analysis.

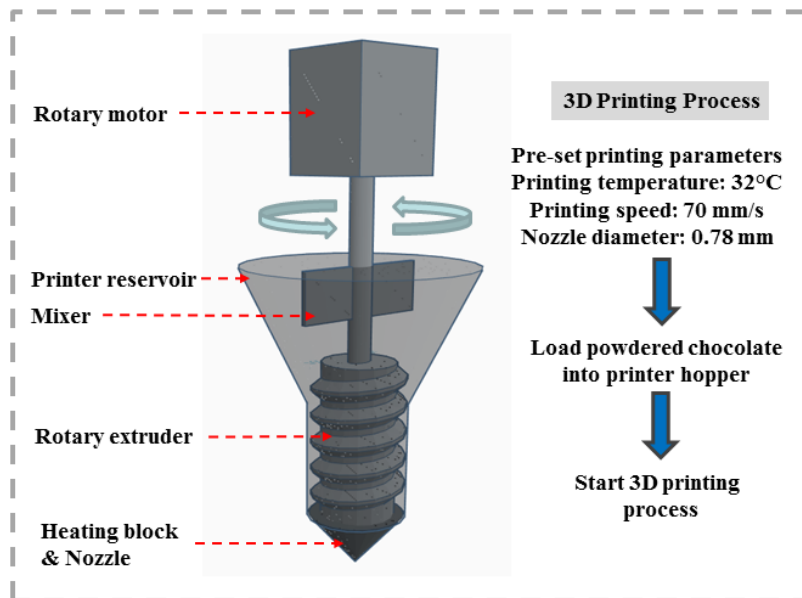


Figure 4.2: Schematic diagram of Porimy 3D chocolate printer and its printing mechanism.

Table 4.1: Sample dimensions for each chocolate design (model a, b and c) wall thickness was 2.0 mm for all samples.

3D model design	Height [mm]	Diameter [mm]
Model a		
Sample 1(a) – Cross support	20.00	43.00
Sample 2(a) – Cross support	20.00	53.00
Sample 3(a) – Cross support	20.00	63.00
Model b		
Sample 1(b) – Parallel support	20.00	43.00
Sample 2(b) – Parallel support	20.00	53.00
Sample 3(b) – Parallel support	20.00	63.00
Model c		
Sample 1(c) – No support	20.00	43.00
Sample 2(c) – No support	20.00	53.00
Sample 3(c) – No support	20.00	53.00

4.2.5 Weight and dimension of 3D printed chocolate

Digital caliper (0-150 mm, CraftRight[®]) was used to measure the diameter, height and wall thickness of the printed constructs. Weighing balance was used to measure the weight of each printed sample object. The measurement was conducted in triplicate for each sample design. The printing time of each sample design was also recorded.

4.2.6 Printing rate

Printing rate was obtained by dividing the weight of the printed object over printing time to determine the how much chocolate printed per minute.

$$\text{Printing rate (g/min)} = \frac{\text{Total weight of printed object (g)}}{\text{Printing time (min)}}$$

4.2.7 Snap force of printed chocolate

Snap force of 3D printed chocolate were measured using a texture analyzer (model TA-XTplus, stable microsystem, UK) equipped with a 5.0 kg load cell and operating with Exponent version 6.1.9.0 software. The temperature of chocolate was maintained between 18 °C and 20 °C prior to analysis. The ambient room temperature at the time of the measurement was 22 °C. Thus the temperature of measurement was below the onset melting point of chocolate as measured by DSC. The chocolate sample was placed horizontally as illustrated in Figure 4.3 on the instrument platform and a custom break probe was used. Compression test was used to analyse the samples with a pre-test speed of 1.0 mm/s and test speed 2.0 mm/s with 5.0 g of trigger force. Three replications of the same method were performed for each sample. Data from force-displacement curves which is Force (Newton) was extracted.

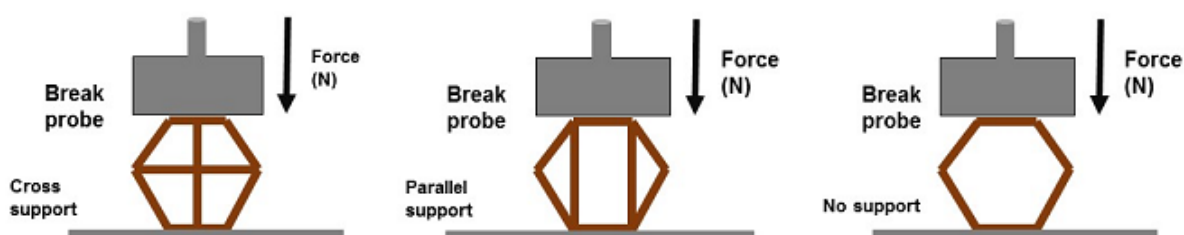


Figure 4.3: Illustration of positioning of three different designs of printed chocolates for snap properties analysis by the texture analyser.

4.2.8 Statistical analysis

One way ANOVA were applied in this study to determine the significant relationship between two groups. This analysis allows justifying the relationship between variable with 95 % confident interval Tukey's test ($p < 0.05$) was considered significant.

4.3 Results and discussion

The printability of chocolate depends on the melting and flow behaviour of the raw material i.e. the grated chocolate added with magnesium stearate. In this section, we discuss the material characteristics (thermal properties and flow behaviour) in determining temperature parameter for extrusion process and follow it up with the quality characteristic of the final 3D printed chocolate.

4.3.1 Flow behaviour of the chocolate

Flow behaviour of the chocolate ink was analysed to determine the temperature in which the chocolate start to flow (melting point of chocolate). Apparent viscosity was measured under constant shear rate (100 s^{-1}) within a temperature interval ranging from 24 to 32 °C. 100 s^{-1} shear rate were applied mimicking the auger rotation, helps the chocolate movement from the hopper to printer nozzle.

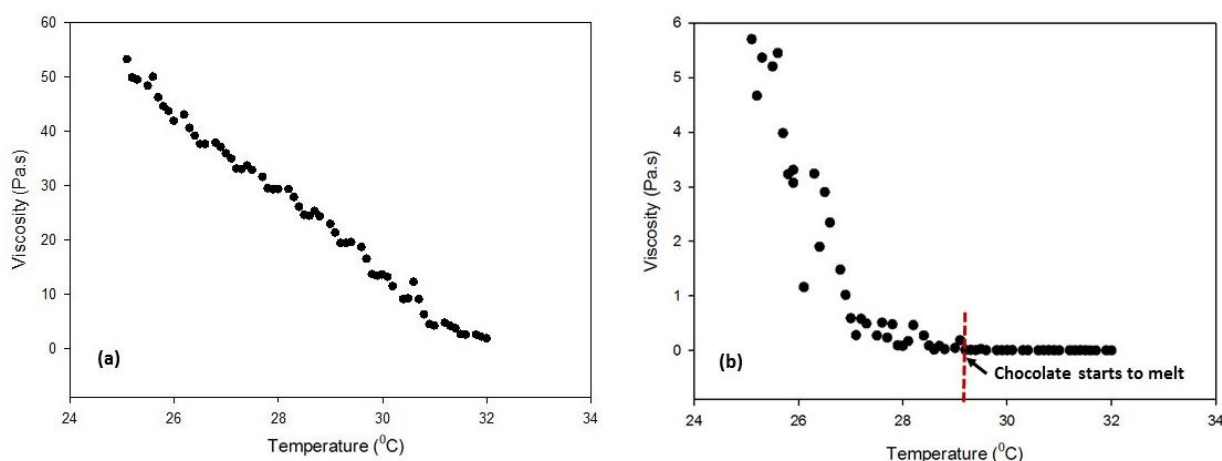


Figure 4.4: Apparent viscosity of (a) chocolate without Mg-ST (b) chocolate with Mg-ST measured at temperature ramp from 25 °C to 32 °C for 10 minutes at shear rate 100 s^{-1} .

Figure 4.4a and 4.4b show the apparent viscosity recorded against the temperature of chocolate samples before and after adding Mg-ST, respectively. The chocolate melting point could not be clearly determined for the sample without Mg-ST. As can be seen in Figure 4.4a, the apparent viscosity followed a linear decreasing behaviour within the temperature range tested. For the sample containing Mg-ST, however, a similar trend was observed until approximately 29 °C. From this point onwards, a plateau was established indicating that the majority of the cocoa butter crystals were melted. The chocolate was considered completely melted at 32 °C. Our results corroborate with the

chocolate melting behaviour reported by Afoakwa et al. (2007). It is believed that the reduction in viscosity by heating the mixture facilitates the extrusion process, as it increases the chocolate flowability throughout the nozzle. We anticipate that, Mg-ST aid in the flow of chocolate, where Mg-ST lubricate the chocolate (as a chocolate sample were in grated form) and ease the chocolate movement. The rheological properties of the ink indeed plays an important role in the prediction of printing behaviour as the supplied formulation must exhibit thixotropic behaviour. In this study, the estimated wall thickness of the construct before and after 3D printing did not show much variation as can be seen from the results presented in [Table 4.2](#). Rheology data was rather used to optimize important parameters of the 3D printer used, such as, speed of deposition and temperature of the substrate during extrusion. Good printability of the substrate was achieved by: (1) understanding of the chocolate flow behaviour under constant shear rate (which approximates to the shear experienced during extrusion) and (2) determining the chocolate melting temperature by recording a decay on viscosity during an upward temperature ramp test under constant shear rate.

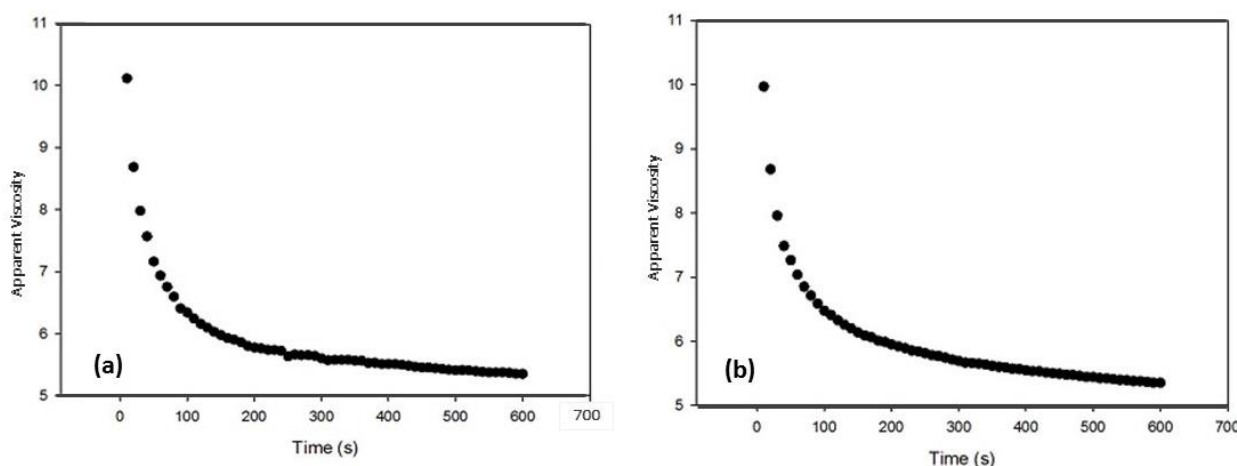


Figure 4.5: Apparent viscosity versus time of chocolate measured at 32 °C for 10 minutes at (a) 50^{s⁻¹} and (b) 100^{s⁻¹} for chocolate with Mg-ST.

Once the melting point was determined, additional rheological measurements were performed by recording apparent viscosity against time at constant shear rates 50 and 100 s⁻¹ (Figure 4.5a and 4.5b), respectively. This test was carried out for 10 minutes, based on the time taken before the deposition of the first layer of extruded material. At this stage, the material is exposed to the slow movement of printer hopper to the extruder. As can be seen, the apparent viscosity was time-dependent with thixotropic characteristic (decreasing values with the time of shearing). The rheology results provide a useful insight that vital for chocolate deposition as it indicate the initial temperature which the chocolate start to melt. Lower shear rate were chosen in this experiment (shear rate 50 and 100 s⁻¹) so that it resembles the extrusion rate of the 3D printer. Considering the flow is laminar, the shear rate (γ, s^{-1}) during extrusion through a nozzle with diameter, d and volumetric flow rate, v was

calculated ($\dot{\gamma} = 8v/d$) to be approximately 100 s^{-1} (Karnjanolarn & McCarthy, 2006). The viscosity of the chocolate remains relatively constant at this shear rate above 50 s^{-1} .

Based on the rheological results and crystal formation mechanisms during melting/re-crystallization of cocoa butter, the maximum temperature of the 3D printer was set at $32 \text{ }^\circ\text{C}$. (Afoakwa, 2010). There is six (Form I – Form VI) major crystal polymorphs formation in cocoa butter (Wille & Lutton, 1966). The polymorphic or crystals forms in cocoa butter are divided into three main categories which are α (alpha), β' (beta prime) and β (beta). Form (I), β'_2 is very unstable and melt at $17 \text{ }^\circ\text{C}$. Form (II), α is rapidly developed from Form (I) and its melting point range between $21 \text{ }^\circ\text{C}$ and $22 \text{ }^\circ\text{C}$. This form (II) will slowly develop to form (III) at the temperature $25.5 \text{ }^\circ\text{C}$, and (IV) ranging between $27 \text{ }^\circ\text{C}$ and $29 \text{ }^\circ\text{C}$ (Talbot, 1994). Generally, Form V (β_2 crystal) melting temperature ranging between $33.8 \text{ }^\circ\text{C}$ and $35 \text{ }^\circ\text{C}$ is the most important crystal and will give the final chocolate product more stable characteristic, a glossy finish and better texture (Afoakwa, Paterson, & Fowler, 2007; Afoakwa, Paterson, Fowler, & Ryan, 2008; Chen & Mackley, 2006; El-kalyoubi, Khallaf, Abdelrashid, & Mostafa, 2011; Mantell, Hays, & Langford, 2015). In order to gain Form V crystal, a proper and careful manipulation of the heat treatment is vital. The result obtained shows that chocolate melted approximately at $29 \text{ }^\circ\text{C}$ and remain stagnant until it reach $32 \text{ }^\circ\text{C}$. At this point ($29 \text{ }^\circ\text{C}$ to $32 \text{ }^\circ\text{C}$) the beta (β) crystals in the chocolate start to melt (onset of melting). At this stage, we do not want to melt the crystals completely so that the seeds are retained that can grow to a stable crystal after deposition. Therefore, we conclude that, although the formation of β -crystal were within $33.8 \text{ }^\circ\text{C}$ and $35 \text{ }^\circ\text{C}$, the melting of the chocolate would start at $32 \text{ }^\circ\text{C}$.

4.3.2 Thermal properties of chocolate

Figure 4.6 depicts the thermal profile recorded for grated chocolate with added magnesium stearate before and after printing. Pristine chocolate (without flow enhancer) was considered as a control sample. Table 4.2 lists enthalpy of melting values calculated by the integrated area under the curve between T_o and T_c .

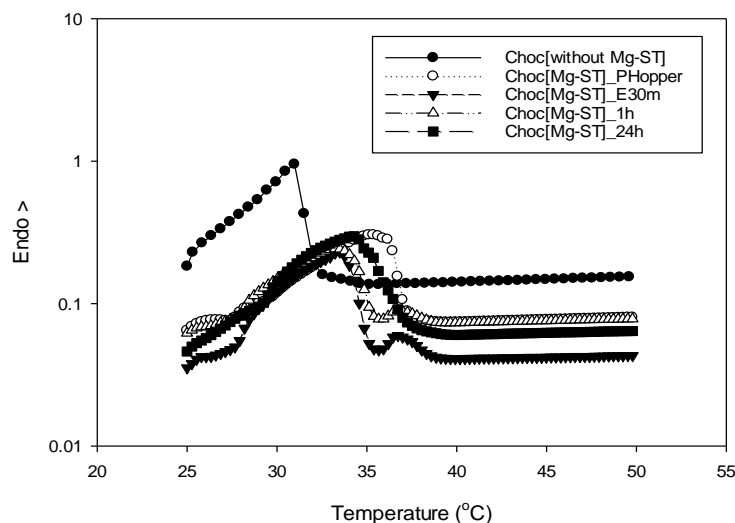


Figure 4.6: DSC melting curves (at a heat scanning rate of 2 °C/min) of chocolate without magnesium stearate and added with magnesium stearate (5% w/w of total mixture).

As expected, Table 4.2 reveals a significant increase in the on-set temperature of chocolate by adding Mg-ST which depicts T_p of around 82.4 °C. Similar trend was also found on the endset temperature, T_c . While samples analysed 30 minutes and 1 hour after extrusion remained at room temperature; sample Choc[Mg-ST]_E24h was kept under refrigeration at approximately 15 °C. This temperature variation lead to fat solidification in chocolate (Dhonsi & Stapley, 2006). Thus, the range of onset point varied for each sample. A slender peak was observed after melting endset temperature of the chocolate sample (30 minutes and 1 hour after extrusion) which is possibly contributed by the inhibition of crystallization of crystals in the chocolate. The magnesium stearate melting point was higher than chocolate, approximately 82.54 °C. We anticipated that magnesium stearate would not affect the thermal properties of chocolate but it may delay the crystallization in chocolate. The presence of solid particle (additive) in chocolate matrix influence the composition of chocolate, thus, affecting the alignment of the crystals in the chocolate matrix (Afoakwa et al., 2007). Dhonsi and Stapley (2006) reported that the addition of lecithin in the chocolate composition caused a slight delay on onset crystallisation. In this case, particulate (Mg-ST) could potentially delay the crystallisation due to the strength of aggregated particles to the network system of chocolate during melting (Beckett, 2008). As can be seen from the result, all samples added with magnesium stearate shows a higher T_p temperature ranging from 33 °C to 35.12 °C which is >4 °C from chocolate without Mg-ST where the melting peak of the chocolate sample without Mg-ST still higher as compared to samples after 24 hours of extrusion.

Table 4.2: DSC data onset (T_o), peak (T_p), endset (T_c) and enthalpy ΔH .

Sample	T_o (°C)	T_p (°C)	T_c (°C)	ΔH (J/g)
Control				
Dark chocolate (Choc)	27.88 ±0.72 ^{(b)(c)}	30.86 ±0.01 ^(b)	31.63 ±0.025 ^(c)	25.95 ±0.17 ^{(c)(d)}
Mg-ST	70.87	82.54	89.96	15.75
Chocolate from printer hopper				
Choc[Mg-ST]	29.45±0.64 ^{(a)(b)}	35.12±0.71 ^(a)	36.27±0.69 ^{(a)(b)}	34.34 ±0.45 ^(b)
Extruded chocolate				
Choc[Mg-ST]_E30m	29.90±0.93 ^(a)	33.68±1.46 ^(a)	34.75 ±0.43 ^(b)	25.15 ±0.31 ^(d)
Choc[Mg-ST]_E1h	27.34±0.54 ^(c)	35.12 ±0.71 ^(a)	35.22±0.65 ^{(a)(b)}	26.09 ±0.23 ^(c)
Choc[Mg-ST]_E24h	29.16±0.67 ^{(b)(c)}	34.78 ±0.45 ^(a)	36.76±0.98 ^(a)	38.27 ±0.35 ^(a)

Mean value of onset (T_o), peak (T_p), endset (T_c) and enthalpy (J/g) that do not share the same letter are significantly different at $p < 0.05$.

As 3D printing system does not involve chocolate tempering which is the process of heating and cooling of chocolate to maintain the stable β crystal nucleation (Afoakwa, Paterson, Fowler, & Vieira, 2008), the addition of stabiliser/emulsifier was essential in this study. Enthalpy data of the DSC data were also obtained from each sample by integrating under the curves. The average melting enthalpies for controlled chocolate was 25.95 ±0.17 J/g and chocolate sample with magnesium stearate were varied between 25.15 ±0.32 J/g and 38.27 ±0.14 J/g depending on the time lapse after printing the sample. The value of melting enthalpies recorded in this research was lower (ranging from 25.15 J/g to 38.27 J/g) as compared to the value in the as reported (Chevalley, Rostagno, & Egli, 1970) where enthalpy for chocolate reported was 44.0 J/g. Larger enthalpy values are anticipated for chocolate which has been stored for some-time as a high proportion of fats would have solidified (Stapley, Tewkesbury, & Fryer, 1999). The magnesium stearate melting point was higher than chocolate, approximately 82.54 °C. We anticipated that magnesium stearate would not affect the thermal properties of chocolate but it may delay the crystallization in chocolate.

Mantell et al. (2015) reported that the melting point of form V β chocolate crystals vary between 33.8 °C and 35 °C. This is in line with the finding in this study where the melting peak (T_p) was recorded between 33.68 °C and 35.12 °C. The increase in melting properties of chocolate after extrusion is due to the continued crystallization in more stable beta form. The existence if magnesium stearate substrates in the chocolate mixture aid in slowing down the crystallization of chocolate, thus make it more extrudable in the printing process in addition to its anti-sticking and lubricating properties.

In summary, based on the thermal and flow behaviour analysis of chocolate, we obtained a proper temperature set-up for extrusion conditions in 3D printing. 32°C were set as the extrusion temperature and it is also the optimum temperature for chocolate melting where most of the stable crystals are formed. Magnesium stearate will aid in lubricating purpose, enhancing chocolate movement through the auger and increase the flowability in the extrusion process. Further works were undertaken to investigate quality aspects of the printed objects, such as solidification, appearance, and dimensions and snap force to determine the mechanical strength of the 3D structure.

4.3.3 Evaluation of 3D printed geometry

Figure 4.7a and 4.7b illustrate, respectively, 3D-printed chocolate constructs with cross and parallel support structure. In Figure 4.7c, a 3D-printed chocolate without support structure is depicted. As can be seen, the 3D-printed shapes were able to hold layered structure. Similar printed object with support structure was also undertaken by Severini et al. (2016) using the dough as the main substrates to create 3D cereal based product. Support structures play an important role in preventing the collapse of complex 3D constructs. To create these structures, the motions of the extruder were cross sectional as setup by g-code from the slicing software (Sli3er). Physical properties of the printed chocolate with different support structures are discussed in subsequent section.

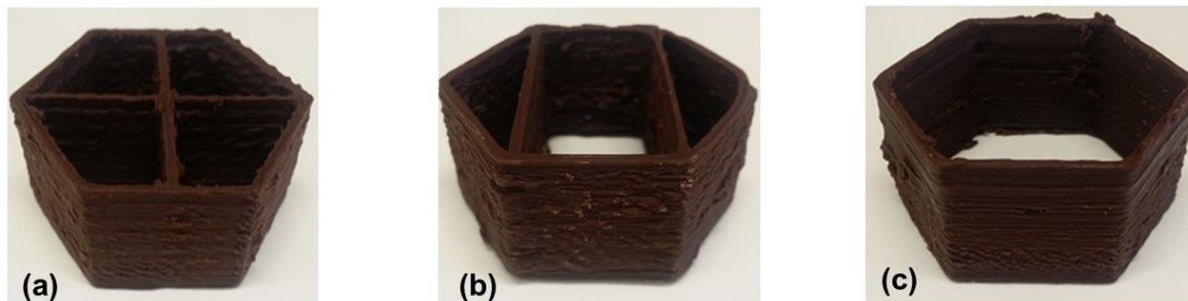


Figure 4.7: Three model designs of printed 3D chocolates (a) hexagonal shape with cross-support (b) hexagonal shape with parallel support (c) hexagonal shape with no support.

4.3.4 Measurement of 3D printed constructs diameter and weight

The measurement of diameter, height and weight are essential to determine the precision of 3D food printer in constructing the chocolate object. The average diameter and weight of the 3D printed constructs with different support structures are presented in Table 4.3. The weight of chocolate constructs will be influenced by the diameter of 3D constructs. As the printing process continuously moves in cross-sectional motion, layer-by-layer of chocolate deposition overlay holding its structure as it builds a higher construct. The layer overlaying the layer beneath generates the pressure due to

its weight and a slight deformation in each layer may occur. It is predicted that constructs design with support structure tend to be heavier as opposed to constructs without support.

Table 4.3: Comparison between the designed and printed chocolate constructs.

Type of Supporter	Designed Diameter (mm)	Average Output Diameter (mm)	Average Weight(g)
Cross support	43.0	43.16±0.045	12.93±0.15
	53.0	53.10±0.27	15.70±0.10
	63.0	63.01±0.78	22.93±0.56
Parallel support	43.0	43.04±0.08	13.57±0.15
	53.0	53.28±0.42	17.57±0.21
	63.0	63.09±0.16	23.30±0.18
No support	43.0	43.17±0.02	6.97±0.150
	53.0	53.05±0.23	11.17±0.06
	63.0	63.09±0.16	19.30±0.18

Table 4.3 reveals that the constructs designed with support were heavier in comparison to the constructs without supports. The average weight of constructs with supports (cross and parallel) was between 12.0 g to 23.5 g while construct without support varied between 6.0 g to 19.5 g depending on the diameter of the constructs. Regardless of the support structure, the results showed that the printed diameter was slightly different from the pre-determined diameter (designed from 3D software). A slight compression bottom layer occurred under the influence of weight that resulted in a slight increase in diameter of the printed chocolate compared to the diameter of the pre-designed model.

There was a slight increase from the pre-designed model in diameter for each chocolate sample. The visual aspect of the main dimensional properties of 3D design structure was not much affected although there was some roughness/unevenness seen of the surface. Overall, the 3D structure remained as similar to the pre-designed from a 3D model. Thus, this indicates that 3D printer can print a precise dimension of the 3D construct with a personalised design. Figure 4.8 show the 3D printed construct with various dimension (diameter, height and wall thickness).

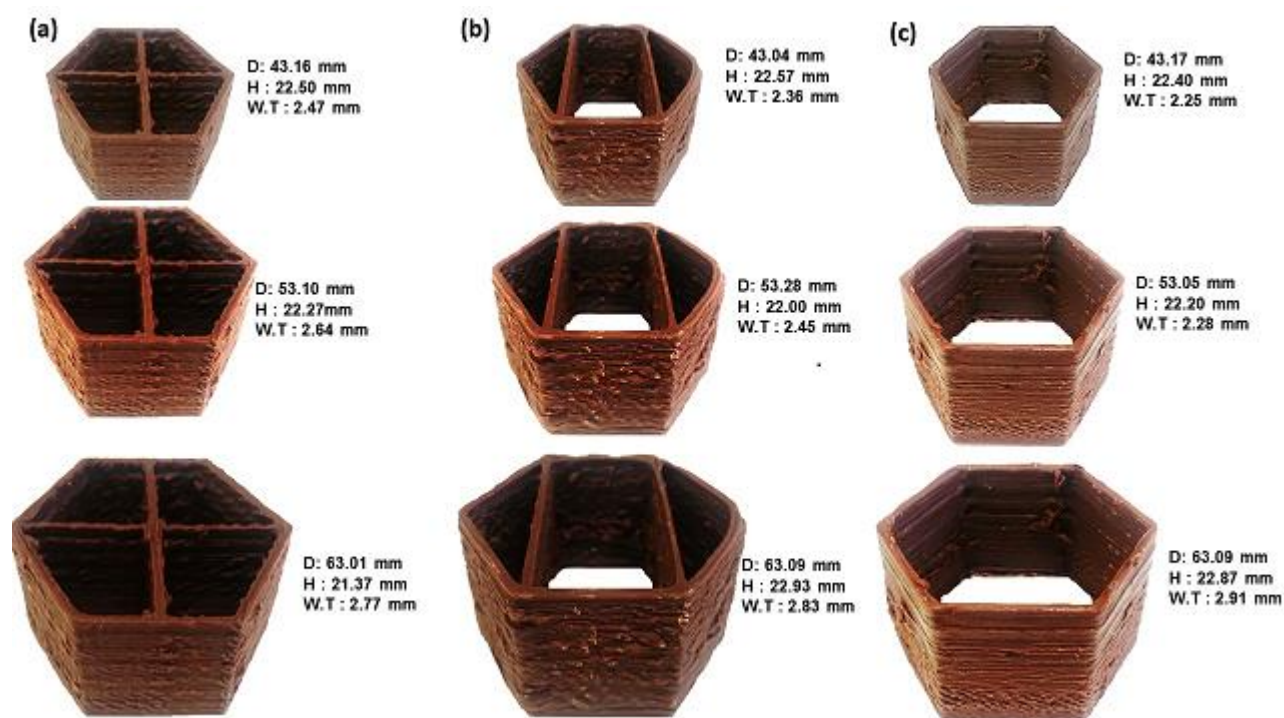


Figure 4.8: Three model designs of printed 3D chocolates dimensions (diameter, height and wall thickness).

4.3.5 Measurement of wall thickness and height

Wall thickness of 3D printed chocolate is also important as it can influence the structural stability of printed items. The data for the wall thickness of the chocolate samples with different diameter and support structures are presented in Table 4.4. One way ANOVA test was performed to determine the significant difference between samples. There was no significant difference ($p > 0.05$) in the mean values for wall thickness for cross support samples for each diameter. However, wall thickness for parallel and no support samples were significantly different ($p < 0.05$). As the diameter increased, the wall thickness also increased gradually.

Table 4.4: Mean value of wall thickness (mm) of 3D constructs according to sample diameter.

Diameter (mm)	Wall Thickness Cross Support (mm)	Wall Thickness Parallel Support (mm)	Wall Thickness No Support (mm)
43.0	2.47±0.5 ^(a)	2.36±0.4 ^(b)	2.25±0.4 ^(b)
53.0	2.64±0.3 ^(a)	2.45±0.2 ^(b)	2.28±0.1 ^(b)
63.0	2.77±0.2 ^(a)	2.83±0.2 ^(a)	2.91±0.3 ^(a)

Mean values of wall thickness that do not share the same letter are significantly different at $p < 0.05$.

For constructs designed with the support structure, the printer extruder movement of X and Y axis were cross-sectional. Therefore, this motion contributed to irregular deposition of chocolate as the layer height is increasing (Severini et al., 2016). Hence, it affected the wall thickness of each sample. But, based on the data collected, it is concluded that wall thickness of each sample was within the range between 2.0 mm and 3.0 mm. In conjunction with the movement of printer extruder that affects the slight increase in wall thickness, there is also a slight increase in the sample height. Based on Table 4.5, the augmentation of height as to pre-determined 3D designed was < 3.0 mm and there is no significant different between each sample height ($p > 0.05$) irrespective increase in diameter. We found that 0.3 mm layer height setting in the slicing software produces almost precise 3D construct based on the collected data. A slight increase in the layer height was observed which was assigned to the uneven deposition of chocolate during printing.

Table 4.5: Mean value of height (mm) of 3D constructs according to sample diameter.

Diameter (mm)	Height (mm)		
	Cross Support	Parallel Support	No Support
43.0	22.50±0.70 ^(a)	22.57±0.91 ^(a)	22.40±0.85 ^(a)
53.0	22.27±0.47 ^(a)	22.00±1.23 ^(a)	22.20±1.05 ^(a)
63.0	21.37±0.38 ^(a)	22.93±1.66 ^(a)	22.87±1.05 ^(a)

Mean values of sample height that do not share the same letter are significantly different at $p < 0.05$.

4.3.6 Printing rate

Printing rate of the 3D printer was calculated by dividing the final weight of the printed construct by the total printing time for each sample. Table 4.6 demonstrates that there was a significant difference ($p < 0.05$) in printing rate of each sample as the diameter increased. For samples with 43.0 mm diameter, presented higher printing rate (>34 g/min) than samples with 53.0 mm diameter for both cross and parallel supports.

Table 4.6: Mean value of printing rate (g/min) as a function of diameter of 3D chocolate constructs.

Diameter (mm)	Total printing time (min)	Printing rate (g/min)		
		Cross Support	Parallel Support	No Support
43.0	27 to 40	0.36±0.004 ^(a)	0.34±0.004 ^(a)	0.26±0.007 ^(a)
53.0	40 to 63	0.28±0.002 ^(b)	0.28±0.003 ^(a)	0.28±0.001 ^{(a)(b)}
63.0	53 to 83	0.29±0.007 ^(c)	0.29±0.016 ^(b)	0.26±0.021 ^(b)

Mean values of printing rate (g/min) that do not share the same letter are significantly different at $p < 0.05$.

Irregularities during chocolate layering deposition were mainly observed under cross-sectional movements of the extruder. This characteristic causes slight deviations in the chocolate weight affecting the chocolate printing rate. This is because, creating an intricate design with support structure requires a cross-section movement automates by the g-code program (RepRap, 2016). Therefore, uneven deposition at the early stage of printing occurs but alleviated over the time in the printing process. Another reason might be associated with limitations faced by using “slicing software’s” which especially developed for filament 3D printers.

This can affect the extrusion process in terms of printing speed, extruder movement, and material deposition (Severini et al., 2016). In particular, edible inks containing chocolate are likely to undergo oscillations in the extrusion rate during deposition due to the complex structure (α and β crystals) of chocolate in comparison to filament. By determining printing rate of chocolate, we can predict the amount of chocolate needed to constructs a single 3D object. Although printing rate differs between each sample, we found that this printer is still capable of completing printing process with an acceptable printed format which was similar to pre-designed from 3D software.

4.3.7 Mechanical strength of 3D constructs as a function of support structure

Snap quality is an important quality parameter of chocolate produce. The influence of supports on the snap force was determined using a texture analyser. Table 4.7 shows the mean value of force (N) needed to break each sample. The force required to break the chocolate samples (based on diameter) were significantly different ($p < 0.05$). It was observed that the constructs with the cross support required a higher force to break the sample with >56.00 N and had a high snap quality and firmer texture as compared to other sample designs. Sample with no support required less force to break the sample with a force of <16.0 N. Cross support structure enabled to hold the main angle of the

chocolate geometry (see Figure 4.8) keeping it firm and stable as compared to sample with parallel support and without support.

Table 4.7: Mean value of Force (N) required to break chocolate sample according to the type of support.

Supports	Force (N)		
	(diameter 43.0 mm)	(diameter 53.0 mm)	(diameter 63.0 mm)
Cross Support	56.91±7.4 ^(a)	57.48±4.8 ^(a)	58.42±4.4 ^(a)
Parallel Support	50.01±6.4 ^(a)	44.68±10.7 ^(a)	50.52±2.7 ^(a)
No support	11.63±3.1 ^(b)	12.61±2.5 ^(b)	15.84±5.0 ^(b)

Mean values of chocolate sample base on force that do not share the same letter are significantly different at $p < 0.05$.

Figure 4.9a, 4.9b and 4.9c illustrate steep curves with a short displacement indicating a good snap quality. However, a sample with diameter 43.0 mm (without support) in Figure 4.9c experienced a long and slow escalation signifying less snap quality, and only small force (11.63 N) needed to snap the sample. The mechanical strength of commercial dark chocolate is significantly affected by the content of cocoa solid particles as reported by Nedomova, Trnka, & Buchar (2013). They reported that force (N) required to break dark chocolate (70% cocoa solid content) was 40.0 N at crosshead speed 1 mm/min. In this study, cocoa solid content in the samples was constant (58%) and the chocolate was printed with varied support structure and diameter. These variables also affected the mechanical strength of 3D printed dark chocolate. Beckett (2008) reported that a steep curve of maximum force and short displacement related to a good snap quality of chocolate. The addition of support structure has not only improved the snap property but also increased the stability printed product. This is important in designing complex 3D constructs, specifically creating higher constructs. Supports aid to hold and maintain the pre-determined shape. The ultimate aim of support structure is to stabilise the intricate structure and also to develop the texture of the food. Depending on the textural properties aimed, the number of support structure can be varied. Internal structures with different level of thickness and numbers on the textural properties of chocolate will be the subject of future studies. A comparison was carried out among three internal structure designs: (1) void space, (2) built parallel support and (3) built cross support. The arrangement of support structure whether parallel or cross support also determine the mechanical strength of 3DP object. It was demonstrated that cross support resulted in more stable 3D construct as per the higher force required to break the object during snap tests.

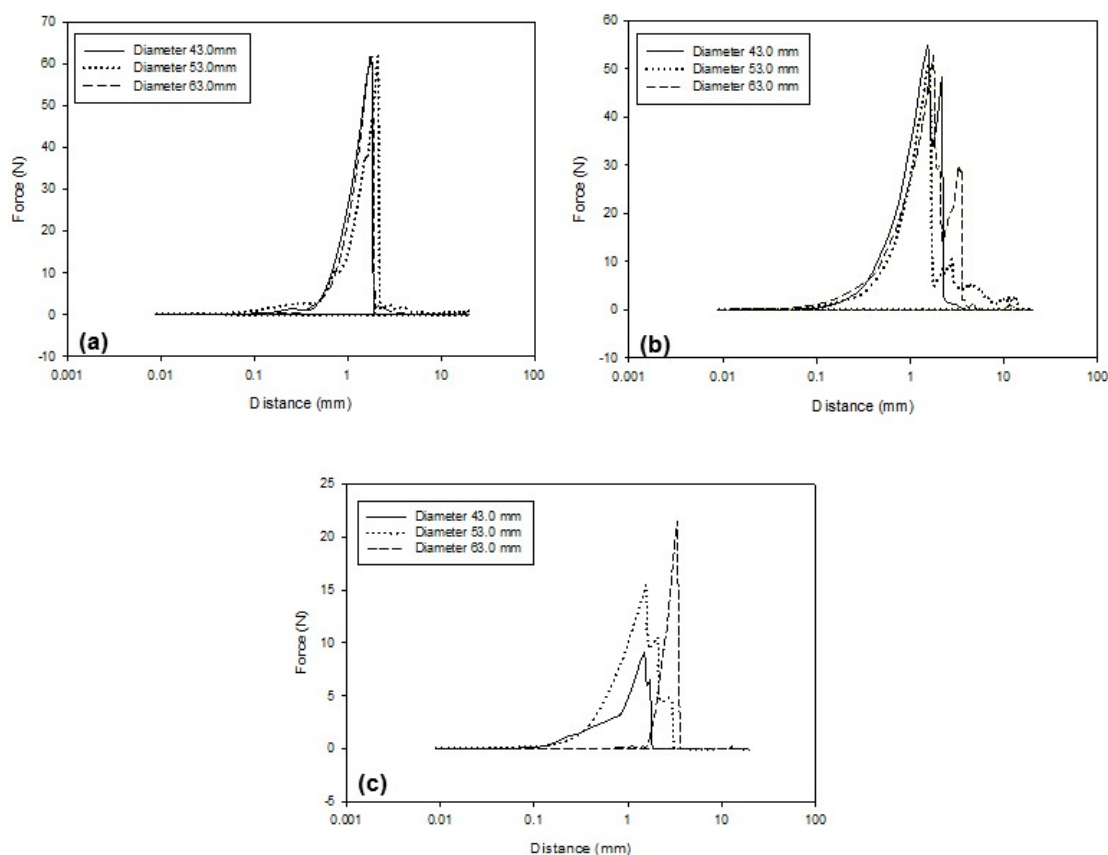


Figure 4.9: Force-distance curves measured by texture analyser of 3D printed chocolate with (a) cross support (b) parallel support (c) no support using break probe with a test speed 2.0 mm/s.

4.4 Conclusion

In this study, 3D constructs were successfully built using chocolate as model edible ink. Rheological measurements and determination of thermal profile helped to set operational conditions of the 3D printer based on melting point temperature. Printability was only achieved by the incorporation of Mg-ST which acted as flow and lubricant enhancer of the material during the printing process. It has been demonstrated that the inclusion of support structures during the design of the geometry plays an important role on snap quality and self-support properties. Cross-support was more effective than parallel-support on creating more stable hexagonal shaped constructs. This was shown by the higher snap force required to break the sample using a texture analyser.

We emphasize that the printing parameters established in this study may only be applicable to chocolate printing. However, our results bring important insights for future research involving printability optimization of edible inks. In the next chapter, a comprehensive research is being undertaken to investigate the effect of additives on thermal, flow and tribological properties on 3D printed dark chocolate.

4.5 References

- Afoakwa, E. O. (2010). *Chocolate science and technology* (Vol. 687). Oxford: Wiley-Blackwell.
- Afoakwa, E. O., Paterson, A., & Fowler, M. (2007). Factors influencing rheological and textural qualities in chocolate - a review. *Trends in Food Science & Technology*, 18(6), 290-298.
- Afoakwa, E. O., Paterson, A., Fowler, M., & Ryan, A. (2008). Flavor formation and character in cocoa and chocolate: a critical review. *Critical Review in Food Science and Nutrition*, 48(9), 840-857.
- Afoakwa, E. O., Paterson, A., Fowler, M., & Vieira, J. (2008). Modelling tempering behaviour of dark chocolates from varying particle size distribution and fat content using response surface methodology. *Innovative Food Science & Emerging Technologies*, 9(4), 527-533.
- Allen, L. (2009). Stearic acid. *Handbook of pharmaceutical excipients. 6th ed. Pharmaceutical Press and American Pharmacists Association.*
- Beckett, S. T. (2008). *Science of chocolate*, Royal Society of Chemistry.
- Chen, Y. W., & Mackley, M. R. (2006). Flexible chocolate. *Soft Matter*, 2(4), 304-309.
- Chevalley, J., Rostagno, W., & Egli, R. (1970). A study of the physical properties of chocolate. *Rev Int Choc*, 25, 3-6.
- Cohen, D. L., Lipton, J. I., Cutler, M., Coulter, D., Vesco, A., & Lipson, H. (2009). *Hydrocolloid printing: a novel platform for customized food production*. Paper presented at the Proceedings of solid freeform fabrication symposium (SFF'09).
- Dhonsi, D., & Stapley, A. G. F. (2006). The effect of shear rate, temperature, sugar and emulsifier on the tempering of cocoa butter. *Journal of Food Engineering*, 77(4), 936-942.
- El-kalyoubi, M., Khallaf, M. F., Abdelrashid, A., & Mostafa, E. M. (2011). Quality characteristics of chocolate – Containing some fat replacer. *Annals of Agricultural Sciences*, 56(2), 89-96.
- Faqih, A. M. N., Mehrotra, A., Hammond, S. V., & Muzzio, F. J. (2007). Effect of moisture and magnesium stearate concentration on flow properties of cohesive granular materials. *International Journal of Pharmaceutics*, 336(2), 338-345.
- Godoi, F. C., Prakash, S., & Bhandari, B. R. (2016). 3d printing technologies applied for food design: Status and prospects. *Journal of Food Engineering*, 179, 44-54.
- Hao, L., Mellor, S., Seaman, O., Henderson, J., Sewell, N., & Sloan, M. (2010). Material characterisation and process development for chocolate additive layer manufacturing. *Virtual and Physical Prototyping*, 5(2), 57-64.
- Karnjanolarn, R., & McCarthy, K. L. (2006). Rheology of different formulations of milk chocolate and the effect on coating thickness. *Journal of Texture Studies*, 37(6), 668-680.
- Kikuta, J., & Kitamori, N. (1994). Effect of Mixing Time on the Lubricating Properties of Magnesium Stearate and the Final Characteristics of the Compressed Tablets. *Drug Development and Industrial Pharmacy*, 20(3), 343-355.

- Kodama, H. (1981). Automatic method for fabricating a three-dimensional plastic model with photo-hardening polymer. *Review of Scientific Instruments*, 52(11), 1770-1773.
- Lee, J. M., & Yeong, W. Y. (2015). A preliminary model of time-pressure dispensing system for bioprinting based on printing and material parameters: This paper reports a method to predict and control the width of hydrogel filament for bioprinting applications. *Virtual and Physical Prototyping*, 10(1), 3-8.
- Li, J., & Wu, Y. (2014). Lubricants in pharmaceutical solid dosage forms. *Lubricants*, 2(1), 21-43.
- Lipson, H., & Kurman, M. (2013). *Fabricated: The new world of 3D printing*: John Wiley & Sons.
- Mantell, D. A., Hays, A. W., & Langford, Z. C. (2015). Printing 3d tempered chocolate. In: Google Patents.
- Murphy, S. V., & Atala, A. (2014). 3D bioprinting of tissues and organs. *Nature biotechnology*, 32(8), 773-785.
- NASA. (2013, may 23). 3D Printing: Food in Space. Retrieved from http://www.nasa.gov/directorates/spacetech/home/feature_3d_food.html#.Vlap1HYrLIU
- Porimy. (2014). Porimy Kunshan Bo Mai Three Dimensional Printing Technology Co., Ltd. Retrieved from <https://translate.google.com.au/translate?hl=en&sl=zh-CN&u=http://www.porimy.com/&prev=sea>
- Ream, R. L., Corriveau, C. L., Graff, G., & Matulewicz, L. (2001). Over-coated chewing gum formulations including tableted center. In: Google Patents.
- RepRap. (2016). RepRapWiki: G-code. Retrieved from <http://reprap.org/wiki/G-code>
- Severini, C., Derossi, A., & Azzollini, D. (2016). Variables affecting the printability of foods: Preliminary tests on cereal-based products. *Innovative Food Science & Emerging Technologies*, 38, 281-291.
- Siqueira, G., Kokkinis, D., Libanori, R., Hausmann, M. K., Gladman, A. S., Neels, A., Studart, A. R. (2017). Cellulose Nanocrystal Inks for 3D Printing of Textured Cellular Architectures. *Advanced Functional Materials*, 27 (12), 1604619
- Stapley, A. G., Tewkesbury, H., & Fryer, P. J. (1999). The effects of shear and temperature history on the crystallization of chocolate. *Journal of the American Oil Chemists' Society*, 76(6), 677-685.
- Suntornnond, R., An, J., & Chua, C. (2017). Roles of support materials in 3D bioprinting—present and future. *International Journal of Bioprinting*, 3(1), 1-4.
- Talbot, G. (1994). Chocolate temper. In *Industrial chocolate manufacture and use* (pp. 156-166): Springer.
- Wille, R., & Lutton, E. (1966). Polymorphism of cocoa butter. *Journal of the American Oil Chemists Society*, 43(8), 491-496.

Chapter 5 - Effect of additives on thermal, rheological and tribological properties of 3D printed dark chocolate²

Abstract

Food additives can be used to enhance the processability and/or nutritional properties of food. In auger type extrusion-based 3D printing (rotational screw), additives were added into the powdered dark chocolate to enhance its flowability. This chapter, therefore, investigates the effect of plant sterol (PS) and magnesium stearate (Mg-ST) powder on thermal, flow and tribological properties of printed dark chocolate. The addition of these additives showed no significant difference ($p > 0.05$) in melting peak (T_p) temperature of control chocolate samples, and 3D printed chocolate samples suggesting that Mg-ST and PS do not affect the melting behaviour of chocolate. However, the yield stress values of printed chocolates containing additives were relatively higher than that of control samples indicating the possible effect of particulates. The tribology curve did not represent the typical Stribeck, suggesting that the additive potentially influenced the lubrication behaviour of 3D printed chocolate as their addition increased the coefficient of friction of the chocolate samples, reducing the slippage in auger extrusion.

² This chapter has been published as a research paper in the *Food Research International Journal* (IF = 3.520): Mantihal, S., Prakash, S., Godoi, F. C., & Bhandari, B. (2019). Effect of additives on thermal, rheological and tribological properties of 3D printed dark chocolate. *Food Research International*, 119, 161-169. The core content of the manuscript was modified to keep the format consistent throughout the thesis.

5.1 Introduction

The application of three dimensional (3D) printing technology in fabricating food creates the opportunity to develop an intricate and personalised design (3D System, 2013). One of the most successful 3D food printing methods is extrusion technique because fresh foods can be efficiently converted into semi-liquid (paste) or powder forms and extruded through a nozzle with or without temperature control, for example, pectin-based formulation (Vancauwenberghe et al, 2018), meat (Thimmesch, 2015) and starch (Yang, Zhang, Prakash, & Liu, 2018). The viscosity of the paste or the melting/liquefaction of the powder can be controlled by regulating the temperature in the temperature-controlled block of the extruder nozzle (Porimy, 2014). Controlling temperature during material extrusion in 3D food printing is one of the crucial parameters as it is correlated to the melting and flow behaviour of the food material. For instance, 32 °C extrusion temperature was optimized for chocolate printing to retain the stable β crystals that is important for chocolate quality. The extrusion temperature will depend on the type of materials, as each material possesses a different thermal property (Liu, Zhang, Bhandari, & Wang, 2017). Various edible food materials have been used in 3D food printing using extrusion method includes lemon juice gel (Yang, Zhang, Bhandari, & Liu, 2018), dough (Severini, Derossi, & Azzollini, 2016) and fish surimi (Wang, Zhang, Bhandari, & Yang, 2018).

Among various food product, chocolate has been extensively used in 3D printing (3D System, 2013; ChocEdge, 2013; Hao et al., 2010; Lanaro et al., 2017). Chocolate is a distinct material that contains complex crystals, making it solid at room temperature and melts into a viscous fluid when exposed to human oral temperature (Afoakwa, 2010). Complex crystals in chocolate (form I to form V crystals) contribute to the quality of chocolate through the formation of more Form V β -crystal, which gives a better appearance, gloss and smoothness to chocolate (Afoakwa, Paterson, Fowler, & Ryan, 2008; Beckett, 2008; Talbot, 1994). Dark chocolate is composed of different ingredients such as cocoa mass, sugar, emulsifier, and may contain milk powder (Afoakawa et al., 2008). Each of these ingredients affects the flow behaviour of chocolate as they have various thermal properties (which are higher than the thermal properties of cocoa butter in polymorphic form). Afoakwa, Paterson, Fowler, and Vieira (2008) studied the effect of particles size distribution (PSD), fat and lecithin in the melting properties of chocolate. They found that the variation of PSD, fat and lecithin contents indicate only slight differences in melting peak (32.2 °C to 32.9 °C), concluding that these components do not significantly affect the melting peak of the chocolate fat. Gonçalves and Lannes (2010) suggested that the melting temperature of β -crystals ranging from 32°C to 35°C is suitable to melt pre-crystallized chocolate. Moreover, Hao et al. (2010) used differential scanning calorimetry (DSC) to identify the melting peak of chocolate and seeded chocolate to be used in the 3D extrusion

system. They found that the melting peak of this chocolate was at around 32 °C to 33 °C, thus they applied 32 °C as an extrusion temperature.

The application of 3D printing for chocolate is appropriate because it can be easily converted into a liquid form by melting and solidified rapidly via crystallization after deposition on the printer bed. Thus, the viscosity of the chocolate can be reduced, and its flowability for extrusion is improved by controlling the temperature. A smooth texture related to mouthfeel and glossy appearance is an important parameter to determine a good quality of chocolate (Carvalho-da-Silva, Van Damme, Taylor, Hort, & Wolf, 2013). Rheology is vital to determine the flow properties of chocolate as it can be useful to predict the different texture attributes in chocolate (Masen & Cann, 2018). Several factors that could affect the rheological properties of chocolate including fat content, the used of surfactant/emulsifier and also the particles size (Afoakwa, Paterson, & Fowler, 2007). Altogether, these components can influence the flow properties and quality of chocolate (Servais, Ranc, & Roberts, 2003).

One of the drawbacks of the auger type extrusion printing is the slippage of the materials in the extrusion tube affecting the consistent extrusion of material filaments from the nozzle. The flowability of chocolate during extrusion 3D printing can be improved by adding powdered food grade processing aid in conjunction with controlling temperature during printing (Cohen et al., 2009). In the previous chapter, we found that magnesium stearate (Mg-ST) helps the flowability of grated chocolate during the extrusion process by minimising the slipping effect in the extruder. Another additive such as native plant sterols (PS) in powder form can be considered to be incorporated into chocolate (AbuMweis & Jones, 2008). The addition of PS in a diet is considered safe and also useful in lowering the risk of coronary disease (AbuMweis & Jones, 2008). Thus, the incorporation of PS may enhance the nutritional value of the dark chocolate in addition to the potential improvement of the printability of chocolate.

Addition of particulate materials may alter the lubrication behaviour of chocolate due to the particle size of the material. Luengo, Tsuchiya, Heuberger, and Israelachvili (1997) reported that fat constituents and its particles size were essential in the determination of lubrication properties of chocolate. They demonstrated that the particles size ($>22\mu\text{m}$) and the addition of anhydrous butterfat could increase the coefficient of friction. Moreover, Lee et al., (2004) reported that high concentration of solid particles (sucrose) presence in chocolate mixture dominated the friction between two soft polytetrafluoroethylenes (PTFE) layer by increasing lubricant viscosity on the PTFE surface. Rodrigues et al. (2017) reported that the presence of solid sugar particles and cocoa solids

strongly influenced the lubrication of chocolate. They found a fluctuation in the coefficient of friction as it reached a critical gap in the hydrodynamic regime as those constituents create a barrier to direct surface contact, thus, hinder the reduction of the film thickness (Rodrigues et al., 2017).

Although there are works on the effect of additives on the general quality of chocolate, there is a lack of evidence consolidating the effect of additives (in powder form) and their influence on flow and lubrication behaviours in 3D printed chocolate. Therefore, the primary aim of this chapter is to investigate the effect of additives in auger type extrusion based 3D printed chocolate. Two types of additives (Mg-ST and PS) will be used and the thermal and rheological properties of the chocolate will be examined as these attributes correlate to the quality of chocolates. Subsequently, the quality was also assessed from the tribological behaviour of 3D printed chocolate as the frictional properties of chocolate will relate to the mouthfeel. This comprehensive study is expected to provide a useful insight into the extrusion printability and quality of chocolate with the addition of flow enhancers.

5.2 Material and Methods

5.2.1 3D design

The 3D printing process was divided into 2 phases: (1) designing and (2) printing. Tinkercad online 3D software was used to design and model a 3D construct of chocolate. Samples were fabricated in a round shape with 40 mm diameter with 2 mm layer thickness. Stereolithography (STL.) files were obtained from the software and transferred to Repetier software and used sli3er to refine the 3D design into a printed 3D format that suits 3D food printer. G-code which is a code required to construct each layer of 3D geometry was extracted from sli3er. A Porimy 3D chocolate printer (Porimy, Kunshan, China) was used to construct a chocolate sample as shown in Figure 5.1.

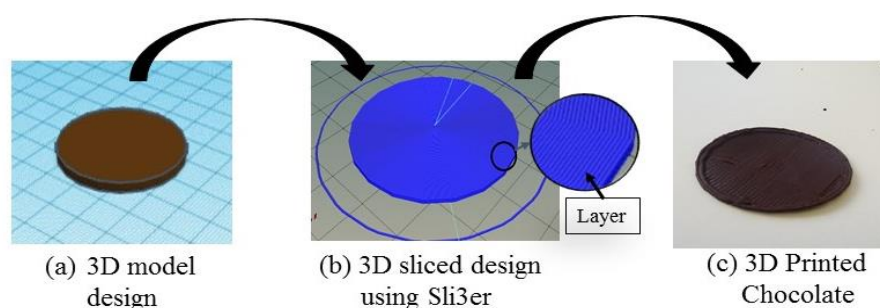


Figure 5.1: Graphic illustration of (a) 3D design from 3D software (b) 3D sliced design using Sli3er software and (c) Actual 3D printed chocolate.

5.2.2 3D printing of chocolate

Two samples of dark chocolate: (1) Cadbury dark chocolate - Choc-1; and (2) Callebaut dark chocolate bittersweet flavour- Choc 2 (Lindt Piccoli Swiss chocolate, Australia) were blended using a stainless steel coffee grinder (Homemaker-SKU: P_42651208, Kmart, Australia) where the flow enhancers, magnesium stearate (Mg-ST) and plant sterol (PS) powders were mixed with the chocolate simultaneously after grinding. Cadbury dark chocolate purchased from a local supermarket was used as the control sample. The composition of Cadbury dark chocolate (Choc-1) was 53 % (minimum) cocoa solids, 35 % (minimum) of cocoa butter, and 0.5 % lecithin. Callebaut dark chocolate bittersweet flavour (Choc-2) were composed of: 58 % cocoa solid (non-fat), cocoa butter (33 % w/w), anhydrous milk fat (5 %), soy lecithin (0.5 %) and vanilla. The amount of Mg-ST (5 g per 100 g of grated chocolate buttons) added into the chocolate samples was adapted from Mantihal et al. (2017). The amount of PS added into the chocolate samples was fixed as 3 g per 100 g of grated chocolate. According to Food Standards Australia New Zealand (FSANZ, 2016), PS should not be added in a food product more than 3g per day as it will diminish its functionality to reduce low-density lipoprotein (LDD). The average chocolate consumption per year (per capita) in Australia is 4.89 kg which is 13.39 g per day (McCarthy, 2015).

The 3D printing process for chocolate in this chapter was from the previous chapter (Chapter 3). Prior to printing, the mixture of the chocolate and additives were placed in the printer hopper. Printing parameters were set as follows: printing speed of 70 mm/s and the extrusion temperature of 32 °C accordingly (adapted from previous chapter). This printer automates printing process where proper gaps between the nozzle (0.78 mm diameter) and the printer bed were standardized accordingly. A round shape samples (diameter: 20 mm) with a thickness approximately ~1.60 mm (considering each sample were printed in 2 layers and each layer were of the same diameter as a nozzle size which was 0.78 mm) was prepared with different formulations (a) Cadbury Dark Chocolate –Choc-1; (b) Callebaut Dark Chocolate-Choc-2; (c) Callebaut Dark Chocolate added with Mg-ST –Choc-2 +Mg-ST; and (d) Chocolate added with of PS – Choc-2 +PS. After printing, the 3D printed chocolate samples were kept at 15 °C refrigeration for 30 minutes before analysing the samples.

5.2.3 Differential Scanning Calorimetry (DSC) analysis

Differential Scanning Calorimetry (DSC) analysis–was conducted to obtain thermal curves of 3D printed chocolate samples where the temperature was ramped from 25 °C to 50 °C at a heating rate 2°C/min using a DSC STARe 143 System (Metler Toledo, USA). An amount of 6 – 6.5 mg of chocolate samples were scanned before and after extrusion through the 3D printer. The onset temperature (°C) (T_o), peak temperature (T_p), and end set temperature (T_e) of the thermal transition

curves were recorded. The melting chocolate enthalpy (ΔH) was determined from the integrated area under the thermal curve between T_o and T_e and was recorded as J/g.

5.2.4 Rheological Measurement

A controlled stress AR-G2 rheometer (TA Instruments, USA) was used to study the flow properties. The tests were performed to determine the flow behaviour of powdered chocolate and 3D printed samples using temperature ramp and steady-state flow. In the temperature ramp procedure, the temperature was set between 25 °C and 40 °C with 100 rad/s. In steady state flow procedure, the temperature was maintained at 32 °C with variance in angular velocity from 0.1 rad/s to 100 rad/s. These analyses were carried out three to five times.

5.2.5 Measurement of tribology property of 3D printed chocolate

Tribological measurement on 3D printed chocolate samples was undertaken using a ring-on-plate tribo-rheometry hybrid rheometer (TA Instruments, USA), which includes a 3M rough plastic surface Transpose Surgical Tape 1527-2. The instrument setup was adapted from previously published work (Godoi, Bhandari, & Prakash, 2017). The water-resistant tape surface (3M plastic, Australia), which mimics the rough surface of the human tongue, was used to place the sample for the test. The measurements were set by simulating the oral processing condition at 35 °C with 3N axial force. The samples were pre-sheared at 0.01 s⁻¹ for 20 s and equilibrated for 1 min for each measurement. Friction results were recorded for rotational speed from 0.1 to 200 s⁻¹ with 20 points per decade. A total of five to eight replications were performed for each sample.

5.2.6 Statistical analysis

Melting peak (T_p) and enthalpy (ΔH), apparent viscosity (Pa.s) and yield stress (using Herschel-Buckley model) were presented as mean value \pm standard deviation. MiniTab 17 statistical software was used to analyse the significant differences between values (where applicable) using one way Analysis of Variance (ANOVA) with Tukey's Honest Significant Difference (HSD) post-hoc test at family error rate 5 at 95% confidence interval with a p -value (p) of less than 0.05.

5.3 Results and discussion

The thermal properties, flow and lubrication characteristics of printed chocolate with and without flow enhancers were determined. These properties were translated into 3D printing conditions and final product qualities. The rheological properties of chocolate play a vital role in the prediction of its printing behaviour as the supplied ink formulation should exhibit right flowability and reduction in viscosity. A better printability of the chocolate was achieved by an understanding of the chocolate

flow behaviour under constant shear rate and by determining the chocolate melting temperature by recording a reduction of viscosity.

5.3.1 Characterisation of thermal properties of 3D printed chocolate samples

Table 5.1 summarises the melting point of all chocolate samples (from printer hopper and 3DP) recorded from DSC thermogram. Melting peak (T_p) corresponds to the melting point of Form V β crystals. Peak melting point of those stable crystals was within the range of 32 to 34 °C (Afoakawa et al., 2008; Beckett, 2011; Biswas et al., 2017). Form V β crystals are the most favourable crystals in cocoa butter that provides the quality attributes of chocolate such as the snap, glossy appearance and smooth to mouthfeel (Afoakwa, Paterson, & Fowler, 2008; Beckett, 2008; Carvalho-da-Silva, Van Damme, Wolf, & Hort, 2011).

Table 5.1: DSC data of the melting peak (T_p), and enthalpy ΔH of chocolate samples from printer hopper and 3D printed sample.

Sample	T_p (°C)	ΔH_{melt} (J/g)
[Choc-1_Control]_ Hopper	33.34 \pm 0.17 ^(a)	32.22 \pm 2.95 ^(b)
[Choc-1_Control]_ 3DP	32.94 \pm 0.28 ^(b)	31.25 \pm 2.60 ^(b)
[Choc-2_Control]_ Hopper	31.24 \pm 0.53 ^(b)	31.24 \pm 2.57 ^(b)
[Choc-2_Control]_ 3DP	31.66 \pm 0.14 ^(b)	31.76 \pm 1.99 ^(b)
[Choc-2+MgST]_Hopper	31.44 \pm 0.88 ^(b)	33.46 \pm 0.99 ^(a)
[Choc-2+MgST]_3DP	31.70 \pm 0.54 ^(b)	34.50 \pm 1.21 ^(a)
[Choc-2+PS]_ Hopper	31.14 \pm 0.73 ^(b)	34.97 \pm 1.35 ^(a)
[Choc-2+PS]_ 3DP	32.15 \pm 0.19 ^(ab)	34.32 \pm 1.20 ^(a)

Mean value of peak (T_p) and enthalpy ΔH that do not share the same letter (in a column) are significantly different at $p < 0.05$. [Mg-ST: Magnesium Stearate and PS: Plant Sterol]

As can be seen in Table 5.1, there was no significant difference ($p > 0.05$) of peak melting point between samples with and without additives. The melting point of samples with additives [Choc-2 +Mg-ST and Choc-2 +PS] ranged between 31.14 \pm 0.73 °C and 32.15 \pm 0.19 °C, while samples without additives (Choc-1_Control and Choc-1_Control) ranged from 31.24 \pm 0.53 °C to 33.34 \pm 0.17 °C. The peak melting temperature of commercial sample was also closer to these values (33.3 °C). These results are in agreement with Biswas, Cheow, Tan, and Siow (2017) who reported that the melting point of β crystals (Form V) in the chocolate sample are at around 33.2 °C. Also, in another similar study, Ardakani, Mitsoulis, and Hatzikiriakos (2014) results which reported that dark chocolate melting point was at around 32.2°C.

Comparing the samples added with additives, there was no significant difference ($p > 0.05$) between samples [Choc-2 +Mg-ST] and [Choc-2 +PS]. This indicated that both additives did not influence the melting behaviour of chocolate fat. In the previous study, we reported that Mg-ST did not influence the melting behaviour of chocolate. Interestingly, samples added with PS also did not influence the melting point of chocolate fat. The melting point of Mg-ST and PS were higher than the fat melting point which was $> 82.5\text{ }^{\circ}\text{C}$ (Mantihal et al., 2017) and $>130.0\text{ }^{\circ}\text{C}$ (FSANZ, 2016), respectively that were much higher than the melting of the chocolate fat. These results suggest that the additives (in powder form) that added to the chocolate samples were not affecting the thermal properties of the fat in the chocolate.

It is noted that the melting temperature of samples [Choc-1 _Control] from printer hopper was slightly higher ($33.34 \pm 0.17\text{ }^{\circ}\text{C}$) than that of 3D printed samples ($32.94 \pm 0.28\text{ }^{\circ}\text{C}$) and significantly different ($p < 0.05$). Although the results were statistically different, there was only a marginal decrease in the melting temperature, thus, it can be considered as comparable. Choc-2_Control samples (from printer hopper and 3DP) showed a slightly lower melting point than that of Choc-1_Control sample. This may be due to the differences in crystal sizes or polymorphs in two different chocolate types. (Afoakwa, 2010; Tan & Kerr, 2017). In general, there was no significant difference ($p > 0.05$) between chocolate samples from printer hopper and 3D printed samples. This suggests that the thermal properties of chocolate did not significantly change even after the printing process.

The melting enthalpy (ΔH_{melt}) in Table 5.1 revealed a significant difference between chocolate samples with and without additives. Chocolate sample with additives showed a slightly higher melting enthalpy, ranging from $33.46 \pm 0.99\text{ J/g}$ to $34.97 \pm 1.35\text{ J/g}$ than that of chocolate samples without additives which ranged from $31.76 \pm 1.99\text{ J/g}$ to $32.22 \pm 2.95\text{ J/g}$. A slight higher in the enthalpy of samples with additives potentially contributed by the added particulate materials. The values of enthalpy of the chocolate samples obtained in this study were also substantiated with the results reported by Afoakwa et al., (2008), where ΔH_{melt} (J/g) value for chocolate samples with more than 30 % fat content and 0.5 % lecithin was ranging from 30.02 to 34.01 J/g. However, Abdul Halim, Selamat, Mirhosseini, and Hussain (2018) reported a slightly higher enthalpy which was about 37.32 J/g in their control chocolate sample as the higher enthalpy contributed by variation in the amount of cocoa butter content (ranged from 10.5 to 15 %) in the chocolate. Also, the occurrence of more substantial enthalpies value in the endothermic event can also be due to more fat solidification when chocolate is stored for a longer time (Stapley, Tewkesbury, & Fryer, 1999). It is also noted that no significant difference ($p > 0.05$) in the melting enthalpy between [Choc-2 +Mg-ST] samples and

[Choc-2 +PS] samples (see Table 5.1). This indicated that both additives did not interfere with the thermal properties of chocolate.

Overall, it appears that chocolate samples from printer hopper were not significantly different ($p > 0.05$) than that of 3D printed samples. This highlighted that the enthalpy of pre-crystallized samples (in the hopper) did not change as the chocolate underwent 3D printing process. With the 3D extrusion printing process, chocolate does not undergo a tempering process (heating and cooling to a specific temperature) which is an essential method in chocolate making that maintain the stable β crystals for nucleation (Afoakawa, 2011). The stable β -crystals are essential during 3D post printing that acts as nuclei for further crystallisation to ensure extruded chocolate can be solidified rapidly and can hold the chocolate structure. The current study verified that the both additives (Mg-ST and PS) did not interfere with the thermal properties of chocolate and therefore can be used in the 3D printing of chocolate as a flow enhancer. Also, based on these findings, we emphasise that chocolate should be printed below end set temperature of the chocolate fat melting point to retain the seed for further stable crystals nucleation and growth.

5.3.2 Flow behaviour measurement

Several factors that can potentially influence the flow behaviour of chocolate are lecithin/emulsifier content, fat content, and particles size and temperature (Chevalley, 1975; Glicerina & Romani, 2017). A surfactant such as a lecithin helps to homogenise the hydrophilic component in chocolate (sugar) with the hydrophobic (fat) components (Afoakwa et al., 2008) improving the flowability of melted chocolate. Moreover, the constituent of chocolate is composed of mainly cocoa butter, milk fat and other particles including sugar. Cocoa solids and milk powder can influence the flowability of chocolate (Lee, Heuberger, Rousset, & Spencer, 2002). With a constant composition of these components used in this study, the addition of additives (particulate material) is anticipated to improve the flow of chocolate by reducing the slip effect during screw (auger) extrusion by assisting in continuously push the partially melted chocolate through the nozzle.

5.3.2.1 Flow behaviour as a function of temperature and shear rate

Flow behaviour of grated chocolate (pre-crystallised) from printer hopper was analysed by the rheometer with a temperature ramping to determine the melting behaviour of chocolate. Additionally, the same method was followed on 3D printed chocolate to determine whether there was any change in melting behaviour of printed chocolate. Figure 5.2 (a) and (b) show the apparent viscosity against the temperature of chocolate samples from printer hopper and 3D printed chocolate. The viscosity was measured at a shear rate (100 s^{-1}) within controlled temperature interval ramping from $25 \text{ }^\circ\text{C}$ to

40 °C. In this study, a lower shear rate was applied which was relatively similar to the extrusion condition of the 3D Porimy chocolate printer. As can be seen in the Figure 5.2, the viscosity of chocolate samples in printer hopper showed a significant reduction in viscosity as the temperature increased. Similarly, the same trend was found in 3D printed samples and samples added with additives also showed a similar flow behaviour (reduction in viscosity). The reduction in viscosity of chocolate is expected as chocolate fat is composed of six unique complex crystals (α and β - crystals, Form I to Form VI) (Afoakwa, 2010). As each of these crystals has a different melting temperature ranging from 16 °C to 36 °C (Talbot, 2009), a gradual increase in temperature will abolish the α and β - crystals in chocolate fat accordingly.

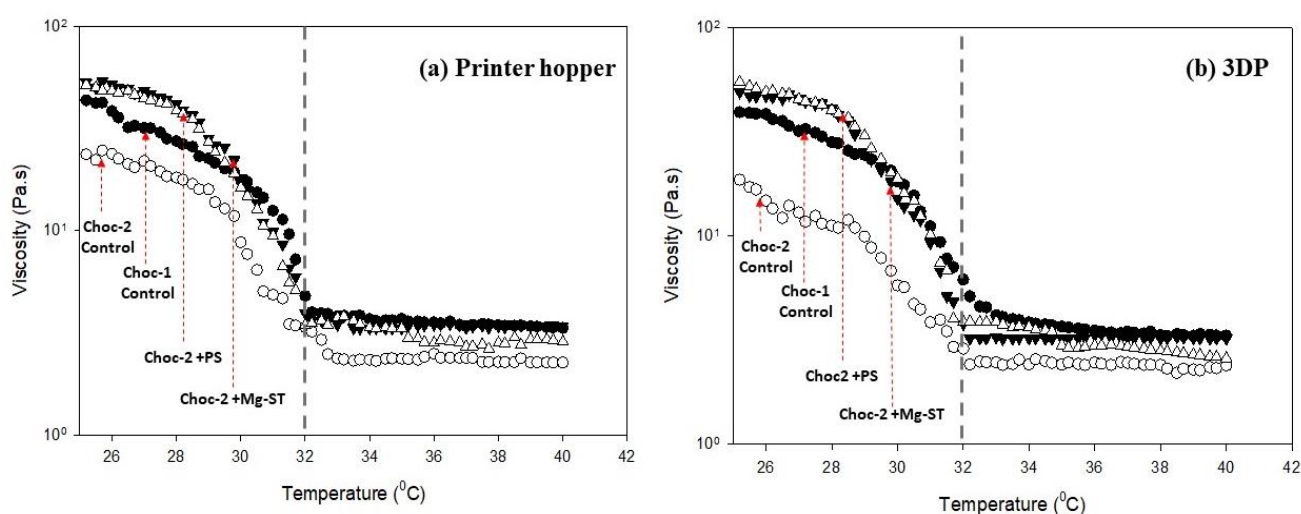


Figure 5.2: Representative graphs of apparent viscosity as a function of temperature ranging from 25 °C to 40 °C of chocolate from (a) printer hopper (b) 3D printed chocolate. [Mg-ST: Magnesium Stearate and PS: Plant Sterol].

A comparable trend in viscosity reduction can be seen for samples with and without additives in both chocolate samples (a) from printer hopper and (b) 3DP (Figure 5.2). As the temperature increased from 25 °C to about 32 °C, a rapid inclination of the chocolate viscosity is visible in both sample due to the fat melting. In this case, the addition of additives did not change the flow behaviour of the chocolate samples. A clear plateau can be seen in both samples (from printer hopper and 3D printed) at starting at the point of ~ 32 °C and was relatively constant until at 40 °C. Likewise, samples added with additives (Mg-ST and PS) also showed the similar trend in flow behaviour. At this point, the stagnant phase indicated that most of the crystals in chocolate fat were melted (Gonçalves & Lannes, 2010). These results are essential in this study as it provides a good information to further verify the extrusion temperature during 3D printing process.

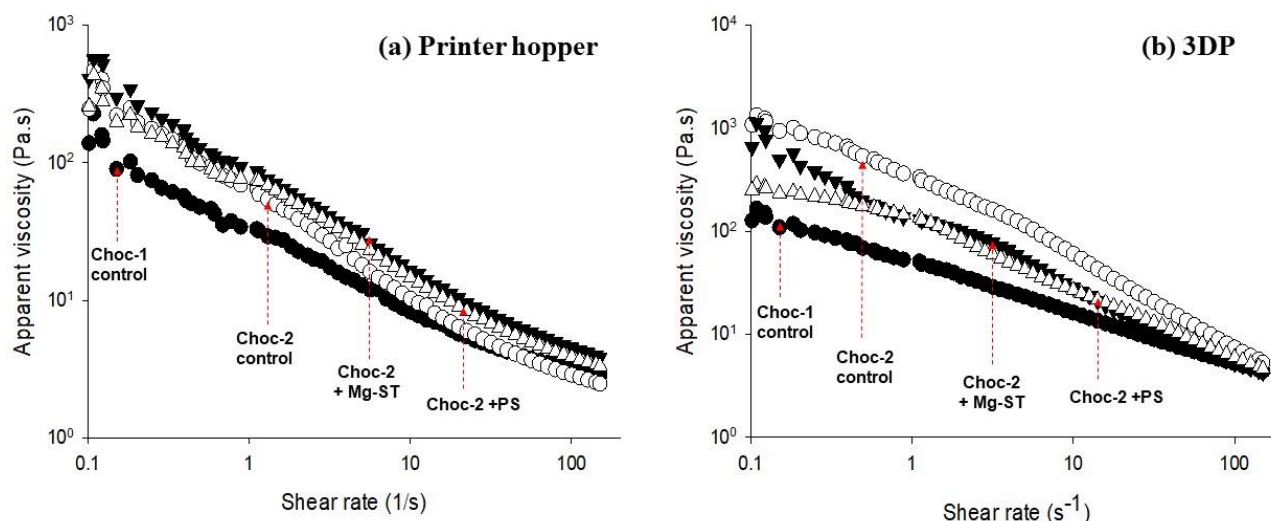


Figure 5.3: Representative graphs of apparent viscosity at 32°C as a function of shear rate from 0.1 to 100 (1/s) of chocolate from (a) printer hopper (b) 3D printed chocolate [Mg-ST: Magnesium Stearate and PS: Plant Sterol].

Figure 5.3 (a) and (b) shows the viscosity of chocolate as a function of shear rate from 0.1 rad/s to 100 rad/s. To determine the shear rate in the extruder, the flow of chocolate was considered as laminar. The shear rate γ (s^{-1}) of chocolate extruded during extrusion through the nozzle with an inner nozzle diameter of (d) and volumetric flow rate of (v) calculated by an equation ($\gamma = \frac{8v}{d}$) was approximately 100 s^{-1} (Mantihal et al., 2017). As can be seen in Figure 5.3, Samples from (a) printer hopper and (b) 3D printed samples demonstrated a pseudoplastic behaviour as the shear rate increased from 0.1 rad/s to 100 rad/s. This behaviour is caused by the deformation of molecules when the hydrodynamic force generated, there will be decrease in the alignment of the molecules (Glicerina et al., 2013). Correspondingly, samples added with additives also showed a similar trend in pseudoplasticity. These results are comparable with Biswas et al. (2017) who reported that the viscosity of chocolate was significantly reduced as the shear rate increase from 2 s^{-1} to 110 s^{-1} . In this study, the reduction in viscosity of chocolate due to shear was beneficial as it enables the chocolate to flow smoothly through the printer nozzle.

Table 5.2 shows the viscosity values of each sample (from printer hopper and 3DP) recorded at the point of 32 °C. The determination of the viscosity at 32 °C was essential as chocolate was extruded at this point of temperature. It should be noted that pre-crystallised chocolate was used in this study and it did not undergo a physical process that could completely change the polymorphic structure of the cocoa butter.

Table 5.2: Apparent viscosity of dark chocolates at 32 °C (1) printer hopper and (2) 3D printed chocolate (measured at a constant shear rate of 100 s⁻¹).

Sample	Apparent viscosity (Pa.s)	
	Hopper	3DP
[Choc-1_Control]	4.65 ± 0.15 ^{ab}	5.54 ± 0.32 ^a
[Choc-2_Control]	4.52 ± 0.40 ^{ab}	3.83 ± 0.59 ^b
[Choc-2 +Mg-ST]	4.58 ± 0.86 ^{ab}	4.76 ± 0.60 ^{ab}
[Choc-2 +PS]	4.33 ± 0.37 ^{ab}	4.79 ± 0.35 ^{ab}

A viscosity of dark chocolate that does not share a letter are significantly different at $p < 0.05$.

As can be seen in Table 5.2, for samples in printer hopper, there was no significant difference ($p > 0.05$) in chocolate viscosity between [Choc-1_control] and [Choc-2_control] samples (4.65 ± 0.15 and 4.52 ± 0.40 Pa, respectively) and samples added with additives [Choc-2 + Mg-ST] and [Choc-2 + PS] (4.58 ± 0.86 Pa and 4.33 ± 0.37 Pa, respectively). These results indicated that both control and sample with added additives showed a similar viscosity at around 32 °C. As mentioned earlier, chocolate used in printer hopper was a pre-crystallized chocolate material. The constituents in the chocolate, for instance, lecithin, cocoa solids, and sugar were in a constant amount. Therefore, a similarity in viscosity was obtained.

Likewise, for 3D printed chocolate samples, no significant difference ($p > 0.05$) in chocolate viscosity were recorded between [Choc-1_control] and [Choc-2_control] samples (5.54 ± 0.32 and 3.83 ± 0.59 Pa, respectively) and samples added with additives [Choc-2 + Mg-ST] and [Choc-2 + PS] (4.76 ± 0.60 Pa and 4.79 ± 0.35 Pa, respectively). This suggested that the addition of additives did not significantly influence the viscosity of the chocolate at 32 °C. Overall, there was no significant difference ($p > 0.05$) between samples from the printer hopper and 3D printed samples viscosity. Both samples demonstrated a substantial trend of pseudoplastic behaviour. This indicated that when the chocolate reached the heating block of the printer (during the printing process), the temperature (32 °C) was sufficient to initiate the flow.

As discussed in Section 5.3.1, both Mg-ST and PS possessed a high melting point as compared to chocolate fat, therefore, did not overlap or alter the melting behaviour of the chocolate fat. Also, regarding flow behaviour, these additives had a minor effect on the chocolate viscosity. Referring to **Table 5.2**, the variability of the apparent viscosity was very marginal (comparing samples with and

without additives). Therefore, the addition of additives did not influence on the flow properties of chocolate. These results are essential to demonstrate that the application of Mg-ST and PS in chocolate were still beneficial to enhance followability during the auger type extrusion printing process by reducing the slipping effect.

5.3.2.2 Yield stress

Yield stress represents the minimum shear stress required to initiate the flow of material, which also indicates the transition of the material from elastic form to viscous deformation (Briggs & Wang, 2004). Steady flow behaviour of the chocolate sample from printer hopper and 3D printed chocolate was characterised using the Herschel-Bulkley model (Eq. 1) over the shear rate range of 0.1 to 150 s⁻¹. This model has been commonly used to measure the rheological behaviour of suspensions, emulsion or pastes in which the material indicate a power-law behaviour after yielding (Ardakani et al., 2014).

$$\sigma = K(\dot{\gamma})^n + \sigma_0 \quad [1]$$

Where σ = is the shear stress (Pa), $\dot{\gamma}$ = is the shear rate (s⁻¹), σ_0 = yield stress (Pa), K = is the consistency coefficient (Pa.s) and n = is the flow behaviour index.

Figure 5.4 (a) and (b) depicts the shear stress as a function of shear rate of chocolate samples from printer hopper and 3D printed chocolate. Table 4 summarises the rheological parameters of chocolate samples from printer hopper and 3D printed chocolate. In all cases, the Herschel–Bulkley model was satisfactory for interpolating the yield stress of chocolate samples as the determination coefficient (r^2) was greater than 0.9842.

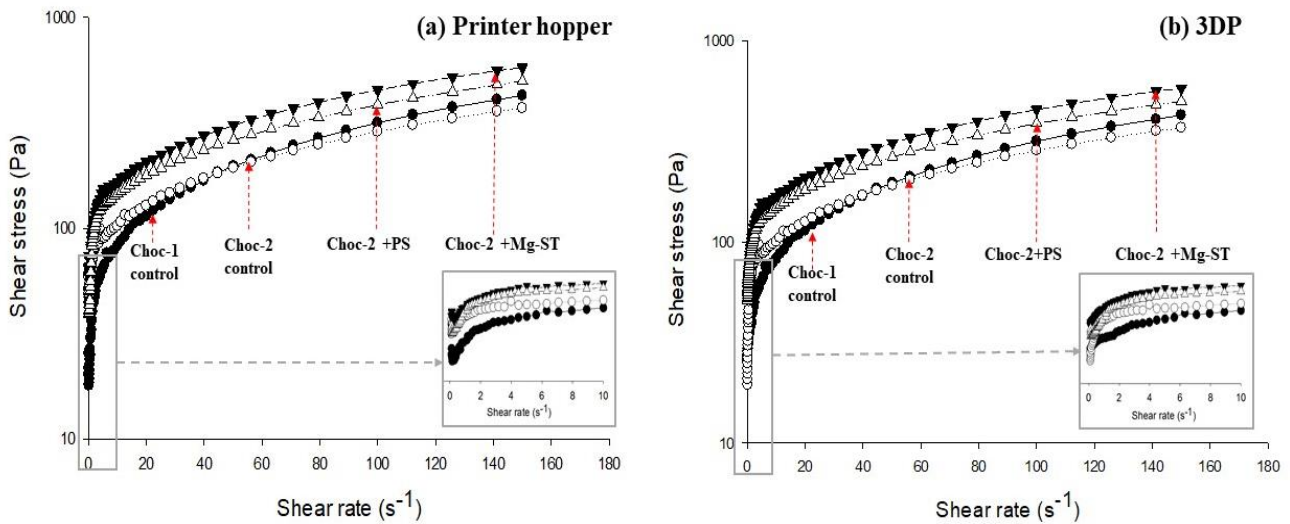


Figure 5.4: Shear stress as a function of shear rate ranging from 0.1 to 150 (1/s) at a constant temperature of 32°C of the chocolate sample from (a) printer hopper (b) 3D printed chocolate. [Mg-ST: Magnesium Stearate and PS: Plant Sterol]. Small screen in Figure represent the shear stress as a function of shear rate at 0 to 10 (1/s).

Table 5.3: Summary of rheological properties of chocolate samples (at 32°C) from printer hopper and 3D printed chocolate determined by Herschel-Bulkley model.

Samples	Herschel-Bulkley model parameters			
	σ_y (Pa)	K (Pa.s)	n	r^2
[Choc-1_Control]_Hopper	22.03 ± 0.94^d	11.14 ± 0.74^b	0.73 ± 0.05^a	0.9971
[Choc-1_Control]_3DP	28.87 ± 0.32^d	10.90 ± 0.98^b	0.75 ± 0.04^a	0.9988
[Choc-2_Control]_Hopper	49.64 ± 1.05^{ab}	11.68 ± 0.76^b	0.66 ± 0.05^{ab}	0.9926
[Choc-2_Control]_3DP	38.47 ± 0.86^c	16.80 ± 1.64^b	0.62 ± 0.03^{bc}	0.9842
[Choc-2 +MgST]_Hopper	54.25 ± 4.74^a	25.56 ± 3.20^a	0.59 ± 0.02^{bc}	0.9924
[Choc-2 +MgST]_3DP	53.90 ± 3.61^a	27.27 ± 2.69^a	0.58 ± 0.03^{bc}	0.9926
[Choc-2 +PS]_Hopper	42.20 ± 2.35^c	28.01 ± 2.40^a	0.54 ± 0.04^c	0.9876
[Choc-2 +PS]_3DP	44.68 ± 2.21^{bc}	29.05 ± 2.74^a	0.52 ± 0.03^c	0.9921

Herschel-Bulkley yield stress (σ_y), consistency index (K) and flow index (n) that do not share a letter are significantly different at $p < 0.05$.

The incorporation of additives into chocolate mixture increased the yield stress value only with Mg-ST, which suggests an increase in the energy required to induce the flow of grated chocolate due to the strength of interparticle interaction (Briggs & Wang, 2004b). As can be seen in Table 5.3, it is noted that the yield stress was increased with the samples added with additives [Choc-1_Control] (22.03 ± 0.94 _Hopper, 22.03 ± 0.94 _3DP), [Choc-2_Control] (49.64 ± 1.05 _Hopper, 44.68 ± 2.21 _3DP) and [Choc-2 +Mg-ST] (54.25 ± 4.74 _hopper, 53.90 ± 3.61 _3DP), [Choc-2 +PS] (42.20

± 2.35 _hopper, 44.68 ± 2.21 _3DP) respectively. These results may be due to the influenced by the addition of particulate materials into the chocolate mixture. There is a significant difference ($p < 0.05$) of the samples with and without additives.

These differences are associated with the addition of additives suggesting that Mg-ST and PS influenced the yield stress of the chocolate. Likewise, there was a significant difference ($p < 0.05$) between samples added with Mg-ST and PS. The σ_y of [Choc-2 +Mg-ST] (54.25 ± 4.74 _hopper, 53.90 ± 3.61 _3DP) were recorded slightly higher than that of [Choc-2 +PS] (42.20 ± 2.35 _hopper, 44.68 ± 2.21 _3DP) respectively, possibly because of the amount of added Mg-ST into chocolate mixture was 2 g (5g Mg-ST per 100g of chocolate) more than that of PS. Therefore, the increase of added particulate material into the chocolate requires high yield stress to initiate the flow. There was no significant difference ($p < 0.05$) between chocolate samples from the printer hopper and 3D printed chocolate suggesting that the yield stress of both samples were comparable.

K value is associated with the consistency of food materials (Nindo, Tang, Powers, & Takhar, 2007). As can be seen in Table 5.3, there was a significant difference ($p < 0.05$) in the consistency index of samples with and without additives. K values of samples without additives were lower than that of samples added with additives (Mg-ST and PS). The reason could be that the addition of particulate materials increased the amount of solid particles in chocolate mixture, thus, influencing the consistency index of the chocolate suspension. There was no significant difference ($p < 0.05$) between samples added with Mg-ST and PS. It was also noted that there was also no significance different ($p < 0.05$) between the samples from the printer hopper and 3D printed chocolate. A higher K value was potentially contributed by the contact point between particles that form spanning stress bearing the path (Afoakwa, Paterson, Fowler, & Vieira, 2009). Therefore, a more substantial amount of stress is needed to initiate the flow (Glicerina et al., 2013) as depicted in Figure 5.4.

The flow behaviour (n) of control chocolate samples (Choc-1 and Choc-2) was also significantly different at $p < 0.05$ with chocolate samples added with additives. The differences could also be due to the influence of the added particulate materials into the chocolate mixture. However, no significant difference at ($p < 0.05$) was recorded in n value for samples added with Mg-ST and PS. Likewise, no significance difference was recorded between the samples from printer hopper and 3D printed chocolate which suggests that the flow behaviour of the sample from printer hopper were similar with the printed samples. Overall, The n value was lower than 1 suggesting that a reduction in viscosity might occur above the yield stress (Sokmen & Gunes, 2006). Also, this indicates a shear thinning behaviour of the chocolate. It is noted that the n value was decreased, particularly in samples added

with additives. According to Beckett (2008), the flow behaviour index could be related to the strength of aggregated particles to the network system of chocolate. Therefore, the arrangement of particles and the addition of fat and surfactant into chocolate influence the network and affect the flow properties of chocolate (Afoakwa et al., 2007). In this case, the addition of flow enhancer (Mg-ST and PS) mixed into the chocolate mixture may interfere with the crystals alignment in chocolate.

5.3.3 Tribological behaviour of chocolate

Lubrication properties (tribology) are generally presented by a Stribeck curve. A typical Stribeck curve consists of three distinct regimes: (1) boundary (2) mixed and (3) hydrodynamic (Prakash, Tan, & Chen, 2013). Figure 5.5 presents the coefficient of friction (CoF) of 3D printed chocolate samples. The friction curves obtained for 3DP chocolates with or without the addition of additives did not resemble the typical Stribeck curves. This is probably due to the presence of particulate structure that exists in the chocolate and further addition of particulates as additives such as PS and Mg-ST.

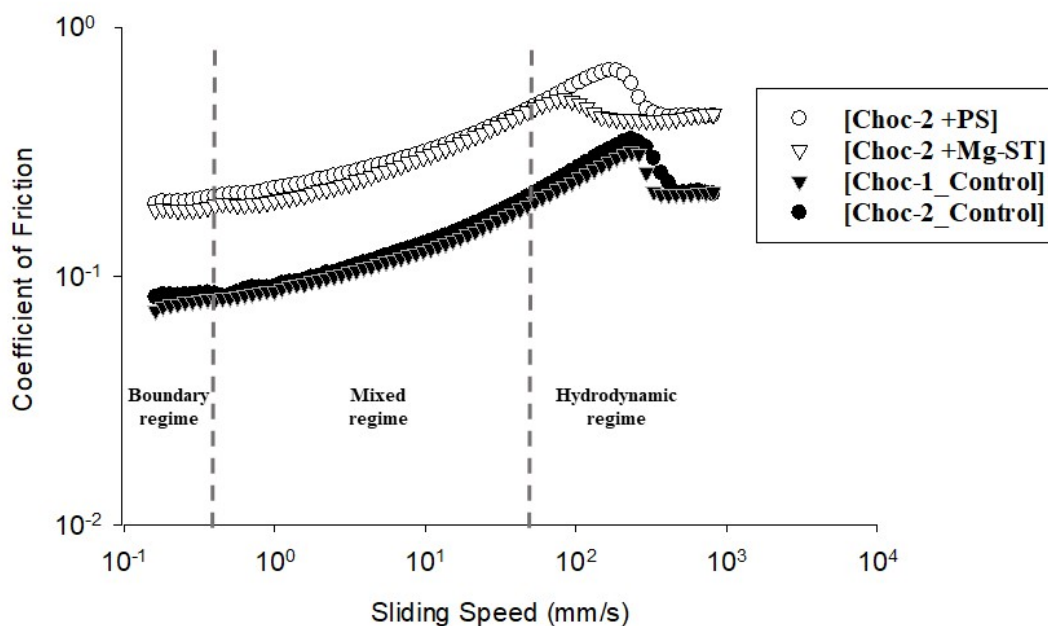


Figure 5.5: The coefficient of friction curve as a function of sliding speed of 3D printed chocolate with a constant temperature of 35 °C.

At the initial stage of boundary regime, we expected that the coefficient of friction to be very low as the entrainment speed increased. However, upon entering the mixed regime, an unusual increase in the coefficient of friction from a low 0.1mm/s up to 100 mm/s sliding speeds for all four samples was observed. A similar behaviour of the unusual increase in coefficient of friction in chocolate was also reported by Carvalho-da-Silva et al. (2013). They stated that the slope of the curve changes slowly but a steady increase in coefficient of friction was observed as the sliding speed increased.

Carvalho-da-Silva et al. (2013) hypothesize that the phenomena possibly correspond to a purely elastic response below the critical friction force of the chocolate samples and therefore increasing the CoF. Lee et al. (2004) investigated the application of hard (Zirconia – ZrO₂) and soft (Poly Tetrafluoroethylene – PTFE) material for the tribo-pairs. They reported that lubrication properties of chocolate is dependent on the constituent characteristics in chocolate and the choice of tribo-pair material with PTFE showed a higher friction than that of soft-on-soft (ZrO₂/ ZrO₂). In our case, the used of ring-on-plate geometry is considered sufficient with 3M- tape as a substrate to mimic the oral food processing (Godoi et al., 2017).

In this experiment, the particulate material (flow enhancer) used was Mg-ST with mean particles size $D(4,3) 7.6 \pm 0.2 \mu\text{m}$ and PS with mean particles size $D(4,3) 42.8 \pm 2.7 \mu\text{m}$. As illustrated in Figure 5.5, chocolate added with PS revealed the highest CoF, as expected due to the larger particles size. Samples without additives showed a lower CoF which indicated more lubrication properties than the samples with additives. High lubrication of the materials (such as fat) cause slippage during auger extrusion (Muredzi, Nyahada, & Mashswa, 2013). Thus, increase in coefficient of friction by the addition of additives contributed to the reduced slippage during extrusion. PS can also be used as an alternative to enhance the flowability of the chocolate in auger-type extrusion method. In regard to mouthfeel perception, the results in Figure 5.5 indicate 3D printed chocolate with PS had higher friction and may contribute to a grainy mouthfeel. However, the reduction of particles size of the particulate material will overcome the graininess sensation not ideal in chocolates.

5.4 Conclusion

This study demonstrated the effect of the addition of Mg-ST and PS on thermal, rheology and tribology properties of chocolate. To investigate the feasibility of printing preconditioned commercial chocolate we chose the dark chocolate in this work. The results obtained from this research show that it will be possible to use other varieties of chocolates, which will be the next step of investigation. We compared between chocolate with and without additives and between prior and after 3D printing using auger type extrusion method. We found that the addition of additives did not interfere with the thermal properties. This is beneficial in an auger extrusion system (3D printing) where the chocolate material is in solid state before reaching the heating block and nozzle for extrusion. Also, the incorporation of additives proved to enhance the flow of chocolate during the extrusion process.

Determining the melting point of chocolate was crucial to obtain an optimal printing temperature. The rheology data obtained in this study was beneficial to determine the flow behaviour of chocolate. The chocolate samples showed a pseudoplastic behaviour even with Mg-ST and PS added into the chocolate mixture. Tribology data obtained in this study did not portray the typical Stribeck curve but instead displayed an unusual curve, possibly influenced by the presence of complex particulate systems in the chocolate. The coefficient of friction obtained from tribology analysis can also provide a useful insight to predict a sensory (mouthfeel) perception, particularly for 3D printed chocolates. As a continuation of this study, a research is being undertaken in the subsequent chapter to determine the textural properties of 3D printed chocolate by varying infill structure (infill percentage and infill pattern).

5.5 References

- 3D System. (2013, 10 september 2013). Technology brings edible 3D printing to professionals and consumers alike. Retrieved from <http://www.3dsystems.com/de/press-releases/3d-systems-acquires-sugar-lab>
- Abdul Halim, H. S. a., Selamat, J., Mirhosseini, S. H., & Hussain, N. (2018). Sensory preference and bloom stability of chocolate containing cocoa butter substitute from coconut oil. *Journal of the Saudi Society of Agricultural Sciences*, 17 (2), 97-216.
- AbuMweis, S. S., & Jones, P. J. (2008). Cholesterol-lowering effect of plant sterols. *Current Atherosclerosis Reports*, 10(6), 467-472.
- Afoakwa, E. O. (2010). *Chocolate science and technology* (Vol. 687). Oxford: Wiley-Blackwell.
- Afoakwa, E. O., Paterson, A., & Fowler, M. (2007). Factors influencing rheological and textural qualities in chocolate - a review. *Trends in Food Science & Technology*, 18(6), 290-298.
- Afoakwa, E. O., Paterson, A., & Fowler, M. (2008). Effects of particle size distribution and composition on rheological properties of dark chocolate. *European Food Research and Technology*, 226(6), 1259-1268.
- Afoakwa, E. O., Paterson, A., Fowler, M., & Ryan, A. (2008). Flavor formation and character in cocoa and chocolate: a critical review. *Critica Review in Food Science and Nutrition*, 48(9), 840-857.
- Afoakwa, E. O., Paterson, A., Fowler, M., & Vieira, J. (2008). Characterization of melting properties in dark chocolates from varying particle size distribution and composition using differential scanning calorimetry. *Food Research International*, 41(7), 751-757.
- Afoakwa, E. O., Paterson, A., Fowler, M., & Vieira, J. (2009). Influence of tempering and fat crystallization behaviours on microstructural and melting properties in dark chocolate systems. *Food Research International*, 42(1), 200-209.
- Ardakani, H. A., Mitsoulis, E., & Hatzikiriakos, S. G. (2014). Capillary flow of milk chocolate. *Journal of Non-Newtonian Fluid Mechanics*, 210, 56-65.
- Beckett, S. T. (2008). *Science of chocolate*, Royal Society of Chemistry.
- Biswas, N., Cheow, Y. L., Tan, C. P., & Siow, L. F. (2017). Physical, rheological and sensorial properties, and bloom formation of dark chocolate made with cocoa butter substitute (CBS). *LWT - Food Science and Technology*, 82, 420-428.
- Briggs, J. L., & Wang, T. (2004). Influence of shearing and time on the rheological properties of milk chocolate during tempering. *Journal of the American Oil Chemists Society*, 81(2), 117-121.
- Carvalho-da-Silva, Van Damme, I., Taylor, W., Hort, J., & Wolf, B. (2013). Oral processing of two milk chocolate samples. *Food & function*, 4(3), 461-469.
- Carvalho-da-Silva, Van Damme, I., Wolf, B., & Hort, J. (2011). Characterisation of chocolate eating behaviour. *Physiology & Behavior*, 104(5), 929-933.

- Chevalley, J. (1975). Rheology of chocolate. *Journal of Texture Studies*, 6(2), 177-196.
- ChocEdge. (2013). Creation: a Selection of our Chocolate Creations. Retrieved from <http://www.chocedge.com/creations.php>
- FSANZ. (2016). Plant Sterols. Retrieved from <http://www.foodstandards.gov.au/consumer/nutrition/plantsterol/Pages/default.aspx>
- Glicerina, V., Balestra, F., Dalla Rosa, M., & Romani, S. (2013). Rheological, textural and calorimetric modifications of dark chocolate during process. *Journal of Food Engineering*, 119(1), 173-179.
- Glicerina, V., & Romani, S. (2017). Chapter 18 - Advances in Yield Stress Measurements for Chocolate. In J. Ahmed, P. Ptaszek, & S. Basu (Eds.), *Advances in Food Rheology and Its Applications* (pp. 459-481): Woodhead Publishing.
- Godoi, C., Bhandari, B. R., & Prakash, S. (2017). Tribo-rheology and sensory analysis of a dairy semi-solid. *Food Hydrocolloids*, 70, 240-250.
- Gonçalves, E. V., & Lannes, S. C. d. S. (2010). Chocolate rheology. *Food Science and Technology (Campinas)*, 30(4), 845-851.
- Hao, L., Mellor, S., Seaman, O., Henderson, J., Sewell, N., & Sloan, M. (2010). Material characterisation and process development for chocolate additive layer manufacturing. *Virtual and Physical Prototyping*, 5(2), 57-64.
- Lanaro, M., Forrestal, D. P., Scheurer, S., Slinger, D. J., Liao, S., Powell, S. K., & Woodruff, M. A. (2017). 3D printing complex chocolate objects: Platform design, optimization and evaluation. *Journal of Food Engineering*, 215, 13-22.
- Lee, S., Heuberger, M., Rousset, P., & Spencer, N. (2002). Chocolate at a sliding interface. *Journal of food science*, 67(7), 2712-2717.
- Lee, S., Heuberger, M., Rousset, P., & Spencer, N. D. (2004). A tribological model for chocolate in the mouth: General implications for slurry-lubricated hard/soft sliding counterfaces. *Tribology letters*, 16(3), 239-249.
- Liu, Zhang, M., Bhandari, B., & Wang, Y. (2017). 3D printing: Printing precision and application in food sector. *Trends in Food Science & Technology*, 69, 83-94.
- Luengo, G., Tsuchiya, M., Heuberger, M., & Israelachvili, J. (1997). Thin film rheology and tribology of chocolate. *Journal of food science*, 62(4), 767.
- Mantihal, S., Prakash, S., Godoi, F. C., & Bhandari, B. (2017). Optimization of chocolate 3D printing by correlating thermal and flow properties with 3D structure modeling. *Innovative Food Science & Emerging Technologies*, 44(Supplement C), 21-29.
- Masen, M., & Cann, P. (2018). Friction Measurements with Molten Chocolate. *Tribology letters*, 66(1), 24.

- McCarthy, N. (2015). The World's Biggest Chocolate Consumers [Infographic]. Retrieved from <https://www.forbes.com/sites/niallmccarthy/2015/07/22/the-worlds-biggest-chocolate-consumers-infographic/#39da66ab4484>
- Muredzi, P., Nyahada, M., & Mashswa, B. (2013). Effects of soya bean meal feed properties on extrusion failures and implementing a solution. Case study Monmouth Path's Investments (Pvt) Ltd, Harare, Zimbabwe.
- Nindo, C. I., Tang, J., Powers, J. R., & Takhar, P. S. (2007). Rheological properties of blueberry puree for processing applications. *LWT-Food Science and Technology*, 40(2), 292-299.
- Porimy. (2014). Porimy Kunshan Bo Mai Three Dimensional Printing Technology Co., Ltd. Retrieved from <https://translate.google.com.au/translate?hl=en&sl=zh-CN&u=http://www.porimy.com/&prev=sea>
- Prakash, S., Tan, D. D. Y., & Chen, J. (2013). Applications of tribology in studying food oral processing and texture perception. *Food Research International*, 54(2), 1627-1635.
- Rodrigues, S. A., Selway, N., Morgenstern, M. P., Motoi, L., Stokes, J. R., & James, B. J. (2017). Lubrication of chocolate during oral processing. *Food & function*, 8(2), 533-544.
- Servais, C., Ranc, H., & Roberts, I. (2003). Determination of chocolate viscosity. *Journal of Texture Studies*, 34(5-6), 467-497.
- Severini, C., Derossi, A., & Azzollini, D. (2016). Variables affecting the printability of foods: Preliminary tests on cereal-based products. *Innovative Food Science & Emerging Technologies*, 38, 281-291.
- Sokmen, A., & Gunes, G. (2006). Influence of some bulk sweeteners on rheological properties of chocolate. *LWT-Food Science and Technology*, 39(10), 1053-1058.
- Stapley, A. G., Tewkesbury, H., & Fryer, P. J. (1999). The effects of shear and temperature history on the crystallization of chocolate. *Journal of the American Oil Chemists' Society*, 76(6), 677-685.
- Talbot, G. (1994). Chocolate temper. In *Industrial chocolate manufacture and use* (pp. 156-166): Springer.
- Talbot, G. (2009). *Science and technology of enrobed and filled chocolate, confectionery and bakery products*: Elsevier.
- Tan, J., & Kerr, W. L. (2017). Determination of chocolate melting properties by capacitance based thermal analysis (CTA). *Journal of Food Measurement and Characterization*, 12(1), 641-649.
- Wang, L., Zhang, M., Bhandari, B., & Yang, C. (2018). Investigation on fish surimi gel as promising food material for 3D printing. *Journal of Food Engineering*, 220, 101-108.
- Yang, F., Zhang, M., Bhandari, B., & Liu, Y. (2018). Investigation on lemon juice gel as food material for 3D printing and optimization of printing parameters. *LWT - Food Science and Technology*, 87, 67-76.

Yang, F., Zhang, M., Prakash, S., & Liu, Y. (2018). Physical properties of 3D printed baking dough as affected by different compositions. *Innovative Food Science & Emerging Technologies*, 49, 202-210.

Chapter 6 - Textural modification of 3D printed dark chocolate by varying internal infill structure³

Abstract

Internal structure (Infill pattern and percentage) can be utilised to modify the infill structure of 3D printed dark chocolate. In this chapter, an intricate internal structure of 3D printed chocolate was created by varying the infill construction. Three intricate infill patterns designed were star, Hilbert curve and honeycomb with infill percentage of 5 %, 30 %, 60 % and 100 %. Powdered Cadbury dark chocolate and Callebaut bittersweet dark chocolate powders were used by incorporating magnesium stearate (Mg-ST) and plant sterol (PS) powders as food additives. The results showed that voids in printed samples of 5% infill percentage (IP) is larger than that of the void in samples with 30% and chocolate sample printed in 60% IP. Additionally, star and honeycomb infill pattern produced the most stable and tough structure at 60% infill as indicated by a higher normal force (N) to break the printed sample. Even at 100% infill percentage, 3D printed chocolate were found less hard as compared to cast samples (>110 N) in the snap test. The results obtained in this study provide a useful insight in creating various internal structures of 3D printed dark chocolate with different textural characteristic and physical stability.

³ This chapter has been published as a research paper in the *Food Research International Journal* (IF = 3.520): Mantihal, S., Prakash, S., & Bhandari, B. (2018). Textural modification of 3D printed dark chocolate by varying internal infill structure. *Food Research International*, 121, 684-657. The core content of the manuscript was modified to keep the format consistent throughout the thesis.

6.1 Introduction

The application of 3D printing technology in food provides an excellent opportunity to create complex and innovative products. This technology has the potential to personalise products either in shapes and/or nutritional requirement. Currently, there are attempts made by different research groups in investigating various food materials as an edible ink for 3D food printing (3DFP) such as chocolate (Hao et al., 2010), mashed potato derived from potato flakes (Liu, Bhandari, Prakash, & Zhang, 2018), cheese (Le Tohic et al., 2018) and cereal-based product (Severini, Derossi & Azzollini, 2016). 3DFP enables the creation of a wide range of food items with variable textures, nutrients contents, taste and shapes by using a limited number of raw materials/ingredients.

Texture tailored foods can be achieved by designing eccentric food structure with a computer-aided design (CAD) (Sun, Peng, Yan, Fuh, & Hong, 2015). Furthermore, multiple ingredients (varying in flavour and nutritional value) can be printed at once by using multiple cartridges; thus, it is a powerful tool in personalised nutrition applications (Liu, Zhang, Bhandari, & Wang, 2017; Jie Sun et al., 2015; Wegrzyn, Golding, & Archer, 2012; Yang, Zhang, & Bhandari, 2015). Cohen et al. (2009) showed the concept of creating a more extensive range of textures and tastes by mixing small group of hydrocolloids and flavours additives.

Altering structural properties in designing food to modify the textural properties such as infill structure is relatively new in 3D food printing field. Infill refers to the structure that is printed inside the 3D construct (RepRap, 2016). It is extruded in selected pattern and density and set as a parameter in the slicing software (Sli3er). Structural properties of the 3D object by varying infill structure has been investigated mostly in polymer and bio-printing. Acrylonitrile Butadiene Styrene (ABS) and Polylactic Acid (PLA) are the most common polymer used in filament printing (RepRap, 2016) and Hydrogel material (Sood, Ohdar, & Mahapatra, 2010) are commonly used in bio-printing. In Polymer printing, the tensile strength of 3D constructs was found to be dependent on constructs' infill structure (McLouth, Severino, Adams, Patel, & Zaldivar, 2017; Sood et al., 2010). Fernandez-Vicente, Calle, Ferrandiz, and Conejero (2016) reported that honeycomb pattern was relatively tough with an increase in infill density (20%, 50% and 100%) as compared to rectilinear and line patterns. Fatimatuzahraa, Farahaina, and Yusoff (2011) demonstrated that crisscross structure (45°/-45°) produces a higher mechanical strength (deflection, flexural and impact test) as compared to axial (0°) and transverse (90°) structures. However, cross pattern (0°/90°) showed a higher tensile strength as compared to crisscross, axial and transverse due to cross-section structure. Moreover, the tensile strength of 3D constructs printed in 0.2 mm layer thickness were stronger as compared to sample printed in 0.4 mm layer thickness (Rankouhi, Javadpour, Delfanian, & Letcher, 2016). In bio-printing

field, a support structure is necessary for fabricating a stable structure for cell and tissues development (Murphy & Atala, 2014). Kang et al. (2016) reported that cell-laden hydrogel incorporated with biodegradable polymer printed in an integrated pattern could achieve higher mechanical stability as it can maintain a stable structure as compared to hydrogel printed in the un-integrated pattern. A well-developed inner structure in 3D tissues construction such as cross-link pattern was essential to maintain the mechanical properties of the constructs (Williams, Thayer, Martinez, Gatenholm, & Khademhosseini, 2018).

Very recently, there were reports on designing internal structure of 3D constructs in order to modify the textural properties of the printed foods. Liu et al. (2018) investigated the textural and structural quality of mashed potato (soft material) by modifying infill percentage (10 %, 40 %, 70 % and 100 %) with different infill patterns (rectilinear, honeycomb and Hilbert curve) and variation in shell perimeters (3, 5 and 7 shells). They reported that firmness values 25.15 g to 144.81 g and Young modulus (487.99 Pa to 43,306.50 Pa) increased and solely affected by variation in infill density between 10 % and 70 %. This indicates that an increase in infill percentage will increase the mechanical strength (firmness and Young modulus) of the 3D printed mashed potato. Severini, Derossi, and Azzollini (2016) reported that the addition of an inner support structure (cross and parallel) was essential to hold the 3D printed cereal-based product for post-processing to make the constructs more stable. In this case, the infill structure was mainly designed to aid the stability of the construct.

However, in regards to edible material, there are only a few information available mainly on soft materials (Le Tohic et al., 2018; Liu et al., 2018) of the infill structure on constructs' textural properties. Textural and physical properties are essential characteristics of any edible material as they indicate the product quality. For example, a glossy appearance and snap is a common way to determine a good quality of the chocolate product (Beckett, 2018). A good snap is the ability to break apart easily and related to mechanical properties of chocolate. The snap- ability of 3D printed chocolate could be influenced by the modification textural properties by varying the infill structure in the construct. To our knowledge, there is no information regarding the modification of the textural properties of a 3D printed chocolate. It is hypothesized that the modification of the textural properties of 3D printed chocolate is achievable by manipulating infill percentages and patterns. Therefore, this study aim to investigate the effect of internal structure on the mechanical properties of 3D printed chocolate by varying infill patterns and infill percentage. We will compare the mechanical properties of 3D printed chocolate with conventional cast chocolate samples.

6.2 Materials and methods

6.2.1 Materials

Two types of dark chocolates, Cadbury dark chocolate (Choc-1) and Callebaut dark chocolate button (Choc-2) purchased locally were used in this study. A commercial Cadbury chocolate was used as a control without any incorporation of flow enhancer. The composition of Cadbury dark chocolate was 53 % (minimum) cocoa solids, 35 % (minimum) of cocoa butter, and 0.5 % lecithin. Callebaut dark chocolate button (bittersweet flavour, Lindt Piccoli) was composed of 58 % (minimum) cocoa solids, 33 % (minimum) cocoa butter, 5% anhydrous milk fat, 0.5% lecithin and vanilla. Both dark chocolates were ground to powders in a controlled temperature room (~ 5 °C). Magnesium stearate (Mg-ST) or plant sterol (PS) was added into Choc-2 samples. 5 % (w/w) of Mg-ST were added into 100g grounded Choc-2 and 3 % (w/w) PS were added into 100g of grounded Choc-2. It is recognised as GRAS and was also used in the previous study (Mantihal, Prakash, Godoi, & Bhandari, 2017). Mg-ST is an approved food additive by FDA and FSANZ and generally considered safe for consumption at an amount of 2.5 g/kg body weight per day (FSANZ, 2016; Allen, 2009). Meanwhile, PS was added as a processing and nutritional aid. According to FSANZ, more than 3 % of PS added to food would diminish its vital purpose as lowering LDL (FSANZ, 2016). Hence, we added approximately 3 % are per the recommendation.

6.2.2 Chocolate casting procedure

Casting samples were prepared to compare the textural property of layer-by-layer deposited 3D printed chocolate with the bulk chocolate with same dimension as that of printed sample. Prior casting, chocolate formulations with and without flow enhancer were melted at around 32 °C using a chocolate melting machine (ChocEdge, UK). Melted chocolate samples (with and without flow enhancer) were poured into a 3D printed cast (in house printed using Acrylonitrile Butadiene Styrene (ABS) filament, see Figure 6.1) covered by a thin layer of transparent plastic wrap. All samples were kept in refrigeration at around 15 °C until the initiation of analysis.

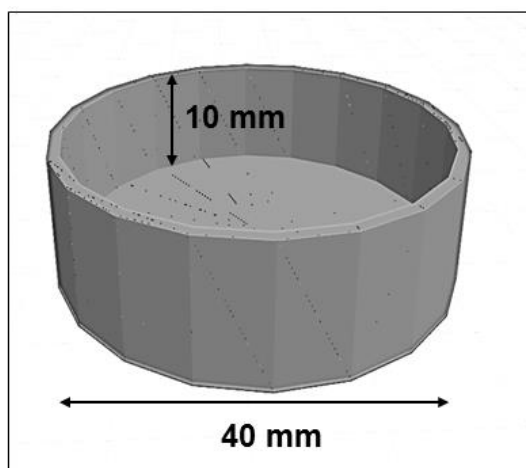


Figure 6.1: The self-made 3D chocolate mould generated from TinkerCad software and printed using Da Vinci 2.0 dual nozzle model XYZ printer with ABS filament.

6.2.3 3D-chocolate printing

3D-chocolate printing consisted of 3 steps: (1) geometry design, (2) slicing and (3) printing.

- i. **Geometry design:** Chocolate structures (40.0 mm diameter and 10.0 mm height) were designed using a TinkerCad online software.
- ii. **Slicing:** The 3D design was uploaded into the Repetier-Host software (in STL file) and sliced using Sli3er to generate g-code for each model. The perimeter was set at default 3 shells approximately ~ 2.34 mm thickness considering the nozzle diameter is 0.78 mm. Three different infill structures (1) Star (2) Honeycomb and (3) Hilbert curve were chosen with a variation of infill percentage 5 %, 30 %, 60 % and 100 % for each infill pattern as shown in Figure 6.2. The infill structures pattern were adapted from Liu et al. (2018) for mashed potato.
- iii. **Printing:** Porimy 3D chocolate printer (Porimy Co. Ltd., Kunshan, China) equipped with an auger (rotary extrusion system) was used in this study. Prior to the extrusion process, the nozzle temperature was set at 32 °C for 5 min to ensure a controlled extrusion temperature is maintained. Printing speed set in the sli3er software was 70 mm/s. The nozzle diameter used was 0.78mm. These printing parameters was optimized in a previous study (Chapter 4). The printer bed temperature was maintained between 15 °C and 16 °C by a recirculating water system. All samples were sliced independently (specific g-code extracted for each 3D model) according to each infill pattern and infill percentage using Sli3er. In between the printing of each chocolate samples (Choc-1, Choc-2, Choc-2+ Mg-ST and Choc-2+PS), the auger extruder was dismantled and cleaned using a cleaning detergent and RO water and dried using compressed air. This was done to ensure the hygienic operation of the 3D printer. A total of $n=108$ samples was prepared. All printed samples were kept in refrigeration at around 15 °C until the execution of quality assessment analysis.

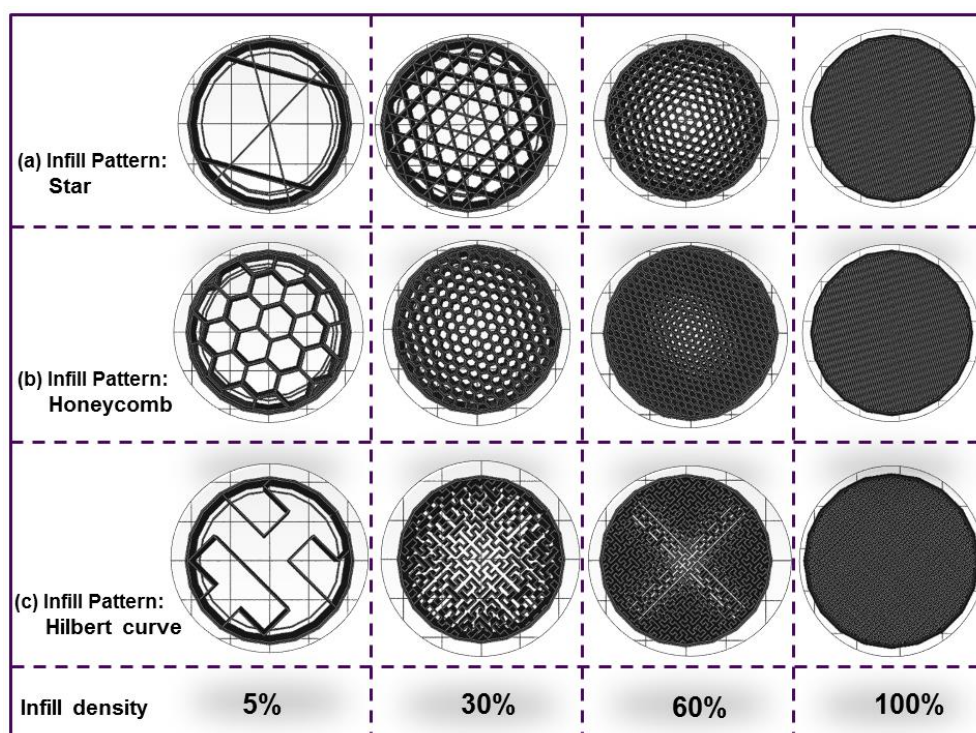


Figure 6.2: 3D design of round shape (40 mm diameter) with (a) Star infill (b) Honeycomb infill (c) Hilbert curve infill patterns with a variation of infill density of 5%, 30%, 60% and 100%.

6.2.4 Shape fidelity and weight measurements of 3D printed chocolate

Digital weighing balance was used to measure the weight of each printed chocolate. A digital calliper (0-150mm, CraftRight®, Bunnings, Australia) was used to measure the diameter and height of 3D printed chocolate. The measurement (diameter and height) done in three different locations on each printed samples and the average value was reported.

6.2.5 Textural characterisation of 3D printed chocolate

Textural properties of 3D printed chocolate were measured using a texture analyser (model TA-XT plus, Stable microsystem, UK) and operating with Exponent version 6.1.9.0 software and a TA-42 knife blade at room temperature around 23 °C. The 3D printed chocolate was placed vertically on the texture analyser platform as illustrated in the Figure 6.3 and supported with a custom adjustable holder to stabilise the sample on the platform. Compression mode was used to analyse the samples at 10 mm distance. A pre-test of the speed of 1.0 mm/s and the test speed of 2.0 mm/s with 5.0g trigger force was applied. To ensure a uniform measurement, all samples (regardless of infill pattern and percentage) were measured using the same method. The measurement was conducted in triplicate and data of maximum force (N) force-displacement was extracted.

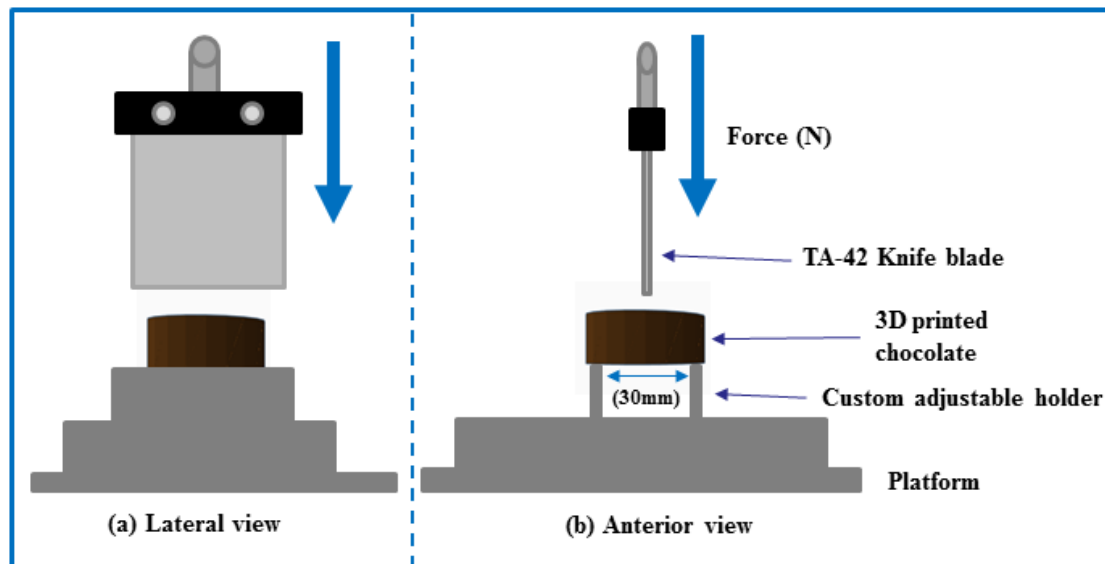


Figure 6.3: Illustration of positioning the 3D printed chocolate samples for snap properties analysis by the texture analyser (a) lateral view and (b) Anterior view.

6.2.6 Statistical analysis

Dimensional properties (weight, height and diameter), void fraction, and mechanical strength (Force –N) were presented as mean value \pm standard deviation. Minitab version 17 (statistical software) was used to analyse the significant difference of between values using One-way Analysis of variance (ANOVA) Tukey's test (where applicable). The significant difference will be determined at p -value (p) of less than 0.05.

6.3 Results and discussion

6.3.1 Visual appearance of 3D printed chocolate

Figure 6.4 illustrates, respectively, 3D-printed chocolate constructs with the variation of infill pattern (Hilbert curve, honeycomb and Star) and infill percentage (5 %, 30 %, 60 % and 100%). As can be seen, the 3D-printed shapes with different infill structures were able to hold a layered structure. Their physical properties are discussed in the subsequent sections.

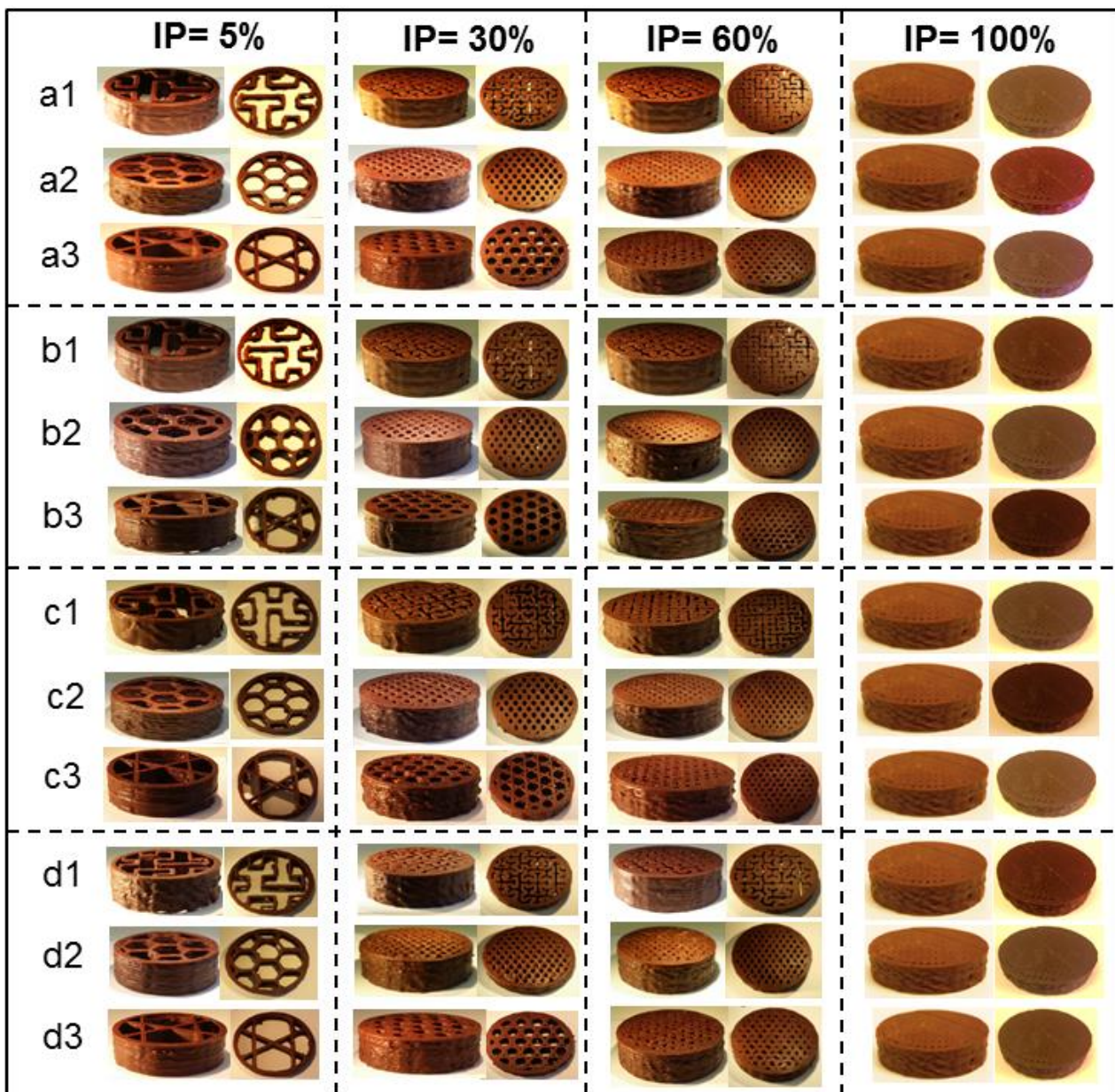


Figure 6.4: Representative pictures of 3D printed chocolate samples. The letter signify chocolate formulation (a) Choc-1_control (b) Choc-2_Control (c) Choc-2+MgST and (d) Choc-2+PS. Numerical (in a row) represent the infill patterns (1) Hilbert curve (2) honeycomb (3) star. IP means Infill percentage.

6.3.2 Dimensional evaluation of 3D printed chocolate

Physical properties such as the construct diameter, height and weight are vital to determine the precision of the 3D printer capability in constructing pre-determined chocolate design. The weight, height and diameter of 3D printed chocolate are presented in Table 6.1, 6.2 and 6.3.

As expected, the weight of the printed chocolate was influenced by the variation (increase) in infill percentage as the construct build a higher dimension as demonstrated in Figure 6.5 (weight of constructs as a function of infill percentage). This is because, as the infill percentage increased, more amount of chocolate will be extruded to fill the internal structure. The relationship between infill

percentage and weight of the sample appeared non-linear with lesser weight change at higher infill percentages. As can be seen in Table 6.1, in general, the weight of printed constructs increased from 5 % to 100 % infill percentage regardless of all chocolate samples. In most cases, chocolate samples printed in Star and Hilbert curve infill pattern were significantly different ($p < 0.05$) than that of samples printed in honeycomb infill pattern. This condition is possibly affected by the extrusion of chocolate in pattern mesostructure as each pattern was different. Fernandez-Vicente et al. (2016) also reported that the weight of polymer (acrylonitrile butadiene styrene - ABS) printed in honeycomb infill pattern and 20 % infill percentage were slight higher (15 g) than samples printed in Line and Rectilinear infill pattern (14 g), respectively. This is indicating that although the infill percentage is the same, a slight deviation in the weight may occur due to the influence of infill pattern.

Table 6.1: The weight of 3D printed chocolate with infill density of 5 %, 30 %, 60 %, 100 % with various infill patterns and cast. Cadbury dark chocolate (Choc-1) was without any additive while Callebaut dark chocolate (Choc-2), Callebaut dark chocolate was incorporated with Magnesium stearate (Choc-2 + Mg-ST) and Plant sterol (Choc-2 + PS).

Infill pattern	Infill percentage [%]	Weight [g]			
		Choc-1	Choc-2	Choc-2+ Mg-ST	Choc-2 + PS
Star	5	4.43 ± 0.42 ^a	3.78 ± 0.27 ^b	3.83 ± 0.25 ^b	5.02 ± 0.24 ^a
Hilbert curve	5	4.05 ± 0.40 ^a	4.28 ± 0.02 ^b	3.87 ± 0.17 ^b	4.42 ± 0.40 ^a
Honeycomb	5	4.29 ± 0.60 ^a	5.39 ± 0.28 ^a	5.13 ± 0.45 ^a	5.04 ± 0.21 ^a
Star	30	8.01 ± 0.33 ^a	8.36 ± 0.25 ^a	7.06 ± 0.34 ^b	8.53 ± 0.25 ^a
Hilbert curve	30	6.99 ± 0.49 ^b	8.61 ± 0.33 ^a	7.46 ± 0.25 ^b	7.49 ± 0.34 ^b
Honeycomb	30	8.92 ± 0.41 ^a	9.13 ± 0.30 ^b	10.88 ± 0.29 ^a	9.27 ± 0.45 ^a
Star	60	11.17 ± 0.19 ^a	11.68 ± 0.36 ^a	11.57 ± 0.26 ^a	11.97 ± 0.19 ^a
Hilbert curve	60	11.43 ± 0.61 ^a	11.09 ± 0.88 ^a	9.62 ± 0.38 ^b	11.57 ± 0.53 ^a
Honeycomb	60	11.16 ± 0.31 ^a	11.38 ± 0.39 ^a	11.58 ± 0.32 ^a	11.48 ± 0.32 ^a
All infill patterns	100	13.71 ± 0.42	13.67 ± 0.41	13.64 ± 0.35	13.69 ± 0.35
Cast sample	-	16.00 ± 0.00	16.00 ± 0.00	16.00 ± 0.00	16.00 ± 0.00

Mean value of weight (in column based on infill percentage 5 %, 30 % and 60 %) of printed chocolate samples that does not share the same letter are significantly different at $p < 0.05$

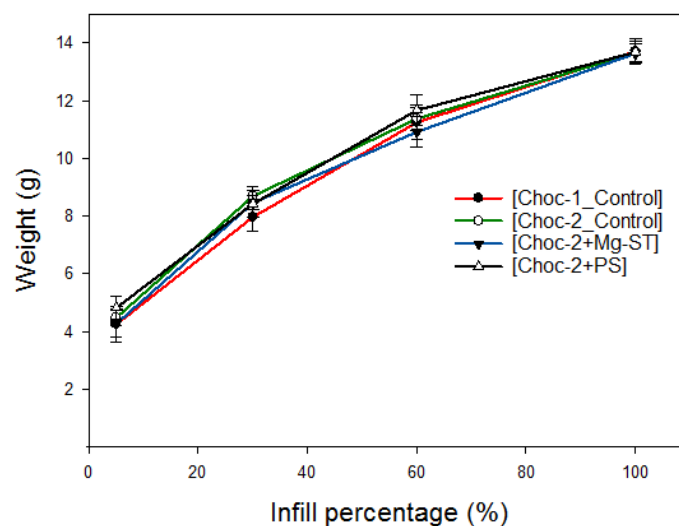


Figure 6.5: Representative graph of 3D printed chocolate as increase infill percentage (5%, 30%, 60% and 100%) as a function of the mean value of weight (g).

The average weight of 5% infill percentage (regardless of chocolate samples and infill pattern) ranged from 3.78 ± 0.27 g to 5.39 ± 0.28 g. For samples with 30% infill percentage, the weight ranged from 6.99 ± 0.49 g to 9.27 ± 0.45 g. For chocolate samples with 60% infill, the variation of weight was from 9.62 ± 0.38 g to 12.51 ± 0.32 g. These findings were substantiated with Liu et al. (2018) reported that an increase in infill percentage from 10 % to 70 %, the construct weight significantly increased from 3 g to 9 g. Similarly, in polymer printing, Fernandez-Vicente et al. (2016) also reported that as the infill percentage increase (rectilinear infill pattern) from 20 % to 100 %, the 3D printed object weight dramatically increase from 10.6 g to 19.0 g. This clearly indicates that variation in infill percentage (IP) influenced the constructs weight.

The height of 3D printed chocolate (regardless of infill pattern, percentage and chocolate sample) showed similar results which ranged from 10.1mm to 10.6 mm with no significant difference at ($p < 0.05$) to the pre-designed geometry as shown in Table 6.2. The height of printed constructs is probably influenced by layer height (Yang, Zhang, Bhandari, & Liu, 2018). In chocolate extrusion, the layer height was set to be equal to the nozzle diameter (0.78 mm) to achieve a well-printed construct, which means, the nozzle (Z axis) will be lifted up to 0.78 mm in every extruded layer. In this case, there are no differences in the product height, indicating similarities with the target geometry. A similar study undertaken by Yang et al. (2018) reported that by optimizing layer height according to nozzle diameter at 1.0 mm in printing lemon juice gel, a better construct that are similar to the target geometry was produced.

Table 6.2: The height of 3D printed chocolate with infill density of 5 %, 30 %, 60 %, 100 % with various infill patterns and cast. Cadbury dark chocolate (Choc-1) was without any additive while Callebaut dark chocolate (Choc-2), Callebaut dark chocolate was incorporated with Magnesium stearate (Choc-2 + Mg-ST) and Plant sterol (Choc-2 + PS).

Infill pattern	Infill percentage [%]	Height [mm]			
		Choc-1	Choc-2	Choc-2 + Mg-ST	Choc-2 + PS
Star	5	10.2 ± 0.1 ^a	10.1 ± 0.1 ^a	10.4 ± 0.3 ^a	10.4 ± 0.5 ^a
Hilbert curve	5	10.3 ± 0.1 ^a	10.3 ± 0.1 ^a	10.2 ± 0.1 ^a	10.1 ± 0.0 ^a
Honeycomb	5	10.1 ± 0.0 ^a	10.1 ± 0.0 ^a	10.1 ± 0.1 ^a	10.4 ± 0.4 ^a
Star	30	10.2 ± 0.2 ^a	10.6 ± 0.2 ^a	10.4 ± 0.1 ^a	10.5 ± 0.3 ^a
Hilbert curve	30	10.1 ± 0.1 ^a	10.5 ± 0.1 ^a	10.5 ± 0.2 ^a	10.4 ± 0.0 ^a
Honeycomb	30	10.3 ± 0.0 ^a	10.6 ± 0.4 ^a	10.6 ± 0.2 ^a	10.6 ± 0.0 ^a
Star	60	10.3 ± 0.0 ^a	10.3 ± 0.0 ^a	10.6 ± 0.7 ^a	10.5 ± 0.1 ^a
Hilbert curve	60	10.4 ± 0.1 ^a	10.5 ± 0.1 ^a	10.5 ± 0.2 ^a	10.4 ± 0.0 ^a
Honeycomb	60	10.5 ± 0.1 ^a	10.4 ± 0.1 ^a	10.2 ± 0.1 ^a	10.1 ± 0.0 ^a
All infill patterns	100	10.3 ± 0.2 ^a	10.6 ± 0.2 ^a	10.5 ± 0.3 ^a	10.3 ± 0.3 ^a
Cast sample	-	10.0 ± 0.0 ^a	10.0 ± 0.0 ^a	10.0 ± 0.0 ^a	10.0 ± 0.0 ^a

Mean value of height (in column) that does not share the same letter are significantly different at $p < 0.05$

Table 6.3: The diameter of 3D printed chocolate with infill density of 5 %, 30 %, 60 %, 100 % with various infill patterns and cast. Cadbury dark chocolate (Choc-1) was without any additive while Callebaut dark chocolate (Choc-2), Callebaut dark chocolate was incorporated with Magnesium stearate (Choc-2 + Mg-ST) and Plant sterol (Choc-2 + PS).

Infill pattern	Infill percentage [%]	Diameter [mm]			
		Choc-1	Choc-2	Choc-2+ Mg-ST	Choc-2 + PS
Star	5	40.1 ± 0.0 ^a	40.1 ± 0.0 ^a	40.2 ± 0.2 ^a	40.2 ± 0.2 ^a
Hilbert curve	5	40.2 ± 0.0 ^a	40.2 ± 0.0 ^a	40.1 ± 0.1 ^a	40.5 ± 0.3 ^a
Honeycomb	5	40.6 ± 0.0 ^a	40.0 ± 0.0 ^a	40.1 ± 0.1 ^a	40.2 ± 0.1 ^a
Star	30	40.1 ± 0.1 ^a	40.1 ± 0.1 ^a	40.3 ± 0.2 ^a	40.1 ± 0.1 ^a
Hilbert curve	30	40.3 ± 0.1 ^a	40.3 ± 0.4 ^a	40.1 ± 0.0 ^a	40.2 ± 0.2 ^a
Honeycomb	30	40.2 ± 0.2 ^a	40.2 ± 0.5 ^a	40.1 ± 0.1 ^a	40.5 ± 0.1 ^a
Star	60	40.8 ± 0.0 ^a	40.1 ± 0.0 ^a	40.4 ± 0.0 ^a	40.2 ± 0.1 ^a
Hilbert curve	60	40.3 ± 0.1 ^a	40.7 ± 0.2 ^a	40.2 ± 0.8 ^a	40.3 ± 0.2 ^a
Honeycomb	60	40.1 ± 0.0 ^a	40.2 ± 0.0 ^a	40.2 ± 0.0 ^a	40.1 ± 0.0 ^a
All infill patterns	100	40.4 ± 0.2 ^a	40.5 ± 0.1 ^a	40.6 ± 0.1 ^a	40.3 ± 0.2 ^a
Cast sample	-	40.0 ± 0.0 ^a	40.0 ± 0.0 ^a	40.0 ± 0.0 ^a	40.0 ± 0.0 ^a

Mean value of diameter (in column) that does not share the same letter are significantly different at $p < 0.05$.

Table 6.3 shows the results of 3D printed chocolate diameter with infill percentage of 5 %, 30 %, 60 %, 100 % with various infill patterns and cast samples. The results suggest that regardless of chocolate samples, infill percentage and patterns, there is no significant difference ($p < 0.05$) in diameter between all printed chocolate samples. Also, there was no variation in diameter observed for cast chocolate as the samples are moulded in a specific dimension (10.0 mm height and 40.0 mm diameter) in bulk and no significant difference at $p < 0.05$ was observed. These results indicate that the diameter of the printed construct was found to be similar to the target geometry. As can be seen in Table 6.3, a marginal discrepancy on diameter is possibly because of the influence of the weight of the product as it building a higher construct (Mantihal et al., 2017). A similar study was done in drug-loaded tablets printing, where a small variation in the construct diameter (10.55 mm to 10.67 mm) as it is printed from 10% to 100% infill percentage. This marginal difference could be due to compressed deformation of printed object influenced by gravity effect (Liu et al., 2018).

For the chocolate sample added with flow enhancer (Mg-ST and PS), the diameter, height and weight were comparable with the dimensions of the control samples (Choc-1 and Choc-2) and no significant difference ($p < 0.05$). The results show that the particulates (Mg-ST and PS) did not affect the dimensional quality of the printed chocolate. This indicates that 3D food printing possesses the capability of producing a good quality 3D chocolate product that is similar to pre-designed shape. Overall, it is demonstrated that 3D food printing is able to produce a precise and reproducible 3D printed chocolate.

6.3.3 Voids of 3D printed chocolate

Figure 6.5 (in Section 6.3.2) represents the effects of infill percentages on the total weight of printed samples. As predicted, the increase in infill percentage would change the weight of the samples. This suggests that the construct weight are dependent of the infill percentage. As mentioned in Section 6.3.2, the increase in weight of printed chocolate was influenced by the amount of extruded chocolate to fabricate the designated object when the infill percentage increased. This will attribute to the fact that less voids in the object as the infill percentage of the construct increased (Vancauwenberghe et al., 2017).

To determine the void fraction of 3D printed samples, the density of printed chocolate was derived from density by using volume displacement method (Liu et al., 2018). The weight of 3D printed chocolate samples and cast chocolate was obtained using a digital balance. The theoretical volume was obtained by dividing the weight by the density (1.1 g/cm^3). The void fraction of each sample was

determine by the equation “ $void\ fraction\ (\%) = (V_{de} - V_{th})/V_{de} \times 100$ ” adapted from Liu et al. (2018), where the V_{de} is the volume of the 3D designed geometry model (12.57cm^3), and V_{th} is the actual volume of the 3D printed chocolate samples. Void fraction (%) of all 3D printed chocolate samples Choc-1, Choc-2, Choc-2+Mg-ST and Choc-2+PS are shown in Table 6.4.

Table 6.4: Void fractions of 3D printed chocolate with infill density of 5 %, 30 %, 60 %, 100 % with various infill patterns and cast. Cadbury dark chocolate (Choc-1) was without any additive while Callebaut dark chocolate (Choc-2), Callebaut dark chocolate was incorporated with Magnesium stearate (Choc-2 + Mg-ST) and Plant sterol (Choc-2 + PS).

Infill pattern	Infill percentage [%]	Void Fraction [%]			
		Choc-1	Choc-2	Choc-2 + Mg-ST	Choc-2 + PS
Star	5	67.7 ± 3.1^c	72.5 ± 2.0^a	72.1 ± 1.8^a	63.5 ± 1.7^b
Hilbert curve	5	70.5 ± 2.9^a	68.8 ± 0.2^b	71.8 ± 1.2^b	67.8 ± 2.9^a
Honeycomb	5	68.7 ± 4.3^b	60.7 ± 2.1^c	62.7 ± 3.3^c	63.4 ± 1.5^b
Star	30	40.7 ± 4.3^b	39.2 ± 1.8^a	48.7 ± 2.50^a	38.0 ± 1.8^b
Hilbert curve	30	49.2 ± 3.5^a	37.3 ± 2.4^b	46.7 ± 2.1^b	45.5 ± 2.5^a
Honeycomb	30	35.1 ± 2.9^c	33.6 ± 2.2^c	20.9 ± 2.13^c	32.5 ± 3.3^c
Star	60	18.7 ± 1.3^a	15.1 ± 2.2^c	15.9 ± 1.9^b	13.0 ± 1.3^b
Hilbert curve	60	16.9 ± 3.7^b	19.4 ± 4.2^a	16.1 ± 2.7^a	16.6 ± 3.9^a
Honeycomb	60	11.6 ± 2.3^c	17.3 ± 2.6^b	15.8 ± 1.3^b	16.5 ± 2.3^a
All infill patterns	100	0.9 ± 1.3	0.6 ± 1.5	0.4 ± 1.5	0.5 ± 1.1
Cast sample	-	0	0	0	0
R ²		0.965	0.975	0.977	0.975

Mean value of void fraction (in column based on every infill percentage 5 %, 30 % and 60 %) of printed chocolate samples that does not share the same letter are significantly different at $p < 0.05$

As can be seen in Table 6.4, the void fraction of 5% of 3D printed chocolate was larger ranging from $60.79 \pm 2.07\%$ to $72.17 \pm 1.84\%$. Larger voids in 5 % infill percentage contributed by less amount of chocolate extruded to fill the internal structure as can be seen in [Figure 6.4](#). Therefore, greater hollow structure is visible as compared to samples printed in 30 % and 60 % infill percentage (IP). As the IP increased to 30 %, the voids fraction were ranging from $20.95 \pm 2.13\%$ to $49.21 \pm 3.57\%$. A similar trend also can be observed when the IP increase to 60 %, the voids are reduced (ranging from $11.65 \pm 2.31\%$ to $19.42 \pm 4.22\%$), respectively. For samples printed in 100% IP, the voids are marginally ranging from $0.46 \pm 1.54\%$ to $0.91 \pm 1.38\%$. No voids were recorded for cast samples as the chocolate was compressed to construct the cast samples.

In most cases, the void fraction of chocolate samples printed in the same infill percentage but different infill pattern (Star, Hilbert curve and Honeycomb) are significantly different at $p < 0.05$. Also, as the

infill percentage increase, the mesostructure configuration of the extruded fibre (fibre-to-fibre gap) became smaller (Rodriguez, Thomas, & Renaud, 2000). Which means, the overlapping between extruded chocolate became narrow thus reducing the voids. Another reason that could influence the construct voids is the irregularities of food material extruded during 3D printing that leads to variation in product weight (Severini, Derossi, & Azzollini, 2016). In addition, the printing path of each pattern were automated by the slicing software, and any changes are impossible to make once the parameters are set up. Therefore, a slight difference in product weight will occur thus affecting the voids. These results corroborated with Liu et al., (2018) findings reported that as the infill percentage increase from 10 % to 70 % the printed mashed potato voids dramatically reduced from 59.6 % to 7.24 %.

Besides increasing in IP, the extrudate filament can experience a swelling (increase in filament diameter) upon extrusion through the nozzle (Yousefi et al., 2018; Wang, 2012), influencing the void fraction of printed product. In thermoplastic 3D printing, the elastic behaviour of polymer led to the swelling of extrudate during deposition as reported by Nikzad, Masood, & Sbarski, (2011). Their work reported a slight increase in the extrudate filament diameter upon extrusion ranging from 1.78 mm to 1.85 mm than that of the die diameter 1.65 mm. In chocolate extrusion, 3DFP is generally optimized by default using slicing software which primarily for thermoplastic materials without any consideration in food material (Liu et al., 2018). Therefore, a marginal swelling in the chocolate filament may occur upon deposition, causing lesser void than the projected void in the target geometry (see Figure 6.4). In addition, samples printed in HNY infill pattern show lesser void fraction, suggesting the effect of potential swelling of extrudate filament influenced the voids. Yousefi et al., (2018) denoted that 3D-plotting condition (including the printing pathway) can affect the diameter of the extruded filament. Thus, the slight swelling of extruded chocolate marginally may affect the mesostructure, contributing to a lesser void in HNY infill than HC and Star infill pattern. The potential swelling behaviour of food materials including chocolate during extrusion printing is one of the areas of that should be studied further.

The results suggested that printed samples added with particulates (Mg-ST and PS) did not influence the voids of the constructs. As only limited amount of Mg-ST and PS were added into the chocolate mixture 5% w/w and 3% w/w, respectively (Mantihal et al., 2017), it is observed that Mg-ST and PS did not significantly contribute to the increase in the construct weight. The linear relationship between 3D printed chocolate weight as a function void shown in Figure 6.6. The R^2 of 3D printed product was ($R^2 = >0.96$) indicating an excellent relationship between weight and the void fraction as the weight increase, the void fraction tends to be lower. Overall, it is worth noting that the variation in IP contributes to a different intensity of infill structure that will influence the texture (hardness) of the

printed products. The hardness of construct is related to the mechanical strength of printed dark chocolate and will be discussed in the subsequent section.

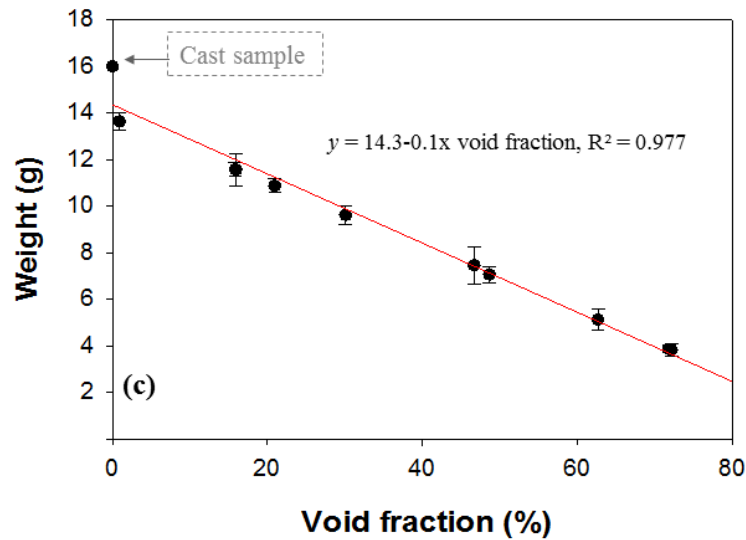


Figure 6.6: Representative graph of the relationship between void fraction (%) and weight of 3D printed chocolate samples with infill percentage of 5%, 30% and 60% and infill patterns of Star, Hilbert curve and Honeycomb, of all chocolate samples; Cadbury dark chocolate (Choc-1), Callebaut dark chocolate (Choc-2), Callebaut dark chocolate incorporated with Magnesium stearate (Choc-2 + MgST) and Callebaut dark chocolate incorporated with Plant sterol (Choc-2 + PS).

6.3.4 Mechanical strength of the 3D printed dark chocolate

Dark chocolate contains high concentrations of suspended solid particles, including sugar crystals, cocoa solids and milk fat dispersed in the continuous matrix of cocoa butter (Afoakwa, 2010). The composite of relatively hard particles including flow enhancer present in dark chocolate will contribute to a higher mechanical property (Nedomova, Trnka, & Buchar, 2013). Therefore, chocolate mixture added with flow enhancer (Mg-ST and PS) possibly will exhibit higher mechanical properties. In this case, the mechanical properties were determined by force (N) that needed to break the chocolate samples.

Figure 6.7 represents the graph of force (N) as a function of the distance of printed chocolate in various infill percentage 5%, 30%, 60%, 100% and cast samples in different infill pattern. As can be seen in Figure 6.7a - e, the increase in infill percentage also increased the force required to break the printed samples. In all cases, the first series of peaks detected while the compression blade travelled from 0 to 2.5 mm followed by other negligible values observed until reaching 5 mm of displacement. It is important to note that the initial ~ 2.5 mm were the essential fracture peaks while the second series of peak observed (from 7 to 9 mm) are the random fracture of small pieces of the chocolate.

Beckett (2018) reported that a slight displacement with a steep curve of maximum force signifies a good snap quality of chocolate.

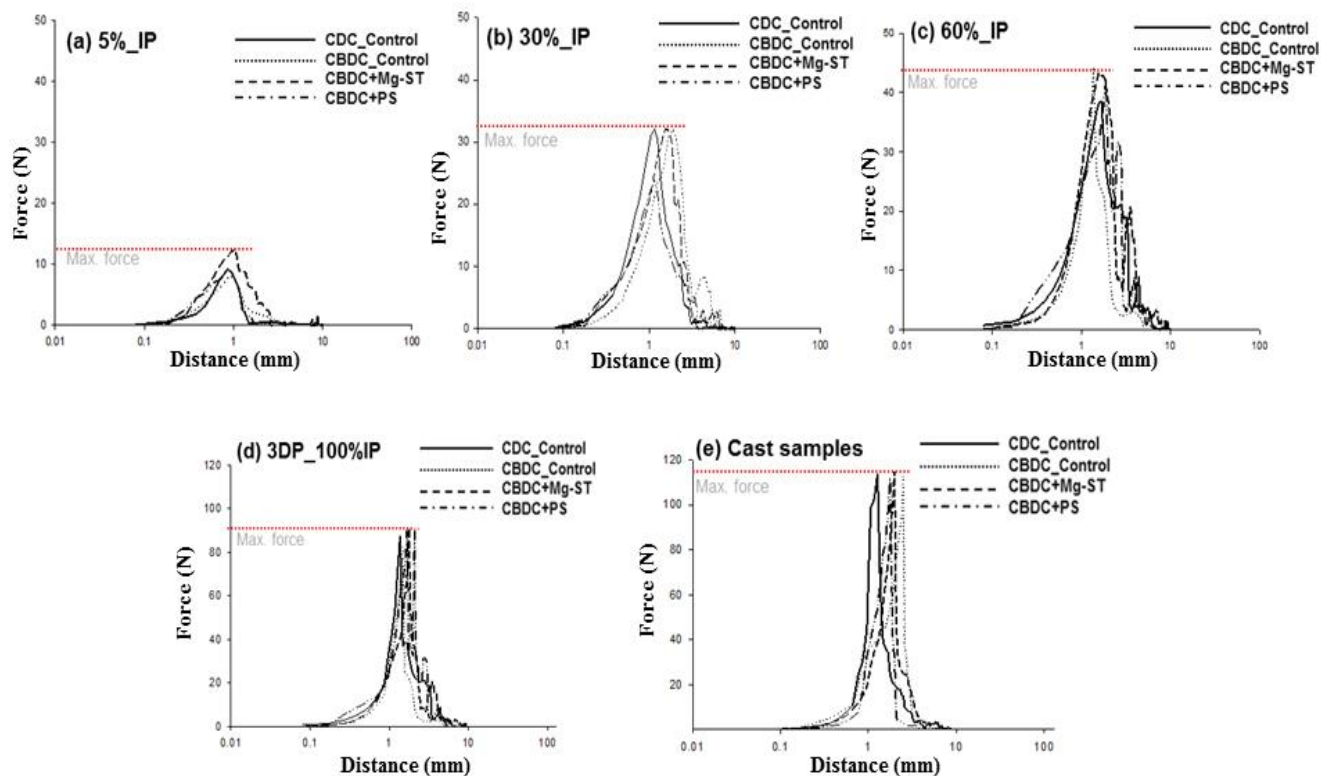


Figure 6.7: Representative graph of force (N) as a function of distance (mm) of 3DP chocolate printed in various infill pattern with various infill percentage (a) 5 % (b) 30 % and (c) 60 % (d) 100 % and (e) cast sample with a pre-test speed of 1.0 mm/s and test speed 2.0 mm/s with 5.0g of trigger load of all chocolate sample (i) Choc-1 (ii) Choc-2 (iii) Choc-2+Mg-ST and (iv) Choc-2+PS. Red lines mean the maximum force (N) recorded for 3D printed samples.

Table 6.5 shows the force (N) required to break samples printed in various patterns and infill percentage (5 %, 30 %, 60 % and 100 %) and also the cast samples. As can be seen in **Table 6.5**, the force required to break all printed samples (regardless of chocolate samples and infill pattern) gradually increased as the IP increased. This indicates that the hardness of chocolate is dependent with IP. At 5 %_IP, the force required to break the printed samples ranged from 1.9 ± 0.1 N to 12.4 ± 0.4 N. For samples printed in 30 %_IP, the force needed to break the samples ranged from 5.5 ± 0.1 N to 35.1 ± 0.2 N. As increased in IP up to 60 %, the force required to break the samples also increase ranging from 8.8 ± 0.4 N to 47.4 ± 0.5 N. The differences in the force required to break the samples is because of the intensity and stability of internal structure. As mentioned earlier, the configuration of mesostructure will be more intense as the IP increases. Thus, it will contribute to a stronger construct (Rodriguez et al., 2000). These findings were substantiated with the results reported by Liu

et al. (2018) who denoted that as the infill percentage increased from 10 % to 70 %, the hardness of mashed potato increased from 101.2 g to 423.2 g. In polymer printing, Fernandez-Vicente et al. (2016) also reported that as IP increased from 20 % to 100 %, the tensile strength of ABS relatively increased from 16 MPa to 37 MPa.

Table 6.5: Recorded force (N) to break 3D printed chocolate with different patterns and various infill percentage (5%, 30%, 60% and 100%), and cast samples.

Infill Pattern	3DP sample	Force [N]				
		[5%_IP]	[30%_IP]	[60%_IP]	[100%_IP]	[Cast]
Hilbert curve (HC)	Choc-1(Control)	1.9 ± 0.1 ^{bF}	5.5 ± 0.1 ^{bF}	8.8 ± 0.4 ^{bF}	87.4 ± 1.6 ^{bD}	113.7 ± 4.1 ^{bA}
	Choc-2(Control)	2.1 ± 0.2 ^{bF}	5.4 ± 0.2 ^{bF}	9.4 ± 0.2 ^{bF}	82.2 ± 2.2 ^{aE}	112.5 ± 3.7 ^{aB}
	Choc-2+Mg-ST	3.5 ± 0.1 ^{aE}	5.5 ± 0.4 ^{bF}	11.1 ± 0.1 ^{aE}	90.8 ± 1.3 ^{cC}	114.5 ± 3.1 ^{bA}
	Choc-2+PS	3.2 ± 0.3 ^{aE}	6.6 ± 0.7 ^{aF}	11.7 ± 0.7 ^{aE}	92.8 ± 1.4 ^{cA}	111.2 ± 4.6 ^{aB}
Honeycomb (HNY)	Choc-1(Control)	9.2 ± 0.1 ^{bB}	31.1 ± 0.3 ^{bD}	38.2 ± 0.2 ^{bD}	88.3 ± 1.8 ^{aD}	110.3 ± 2.1 ^{bC}
	Choc-2(Control)	7.9 ± 0.5 ^{cC}	31.7 ± 0.7 ^{bD}	39.3 ± 0.3 ^{bD}	87.1 ± 1.2 ^{aD}	111.5 ± 3.2 ^{bB}
	Choc-2+Mg-ST	12.4 ± 0.4 ^{aA}	35.1 ± 0.2 ^{aA}	47.4 ± 0.5 ^{aA}	92.6 ± 1.6 ^{bA}	113.1 ± 3.1 ^{aA}
	Choc-2+PS	9.0 ± 0.3 ^{bB}	34.3 ± 1.3 ^{aB}	46.3 ± 0.9 ^{bA}	91.3 ± 1.3 ^{bB}	113.9 ± 3.7 ^{aA}
Star	Choc-1(Control)	6.7 ± 0.1 ^{bD}	28.8 ± 0.6 ^{bE}	42.8 ± 0.4 ^{bC}	87.4 ± 1.1 ^{aD}	112.1 ± 3.5 ^{aB}
	Choc-2(Control)	5.9 ± 0.4 ^{cD}	29.7 ± 0.5 ^{bE}	43.2 ± 0.1 ^{bC}	89.1 ± 1.8 ^{bC}	111.7 ± 3.7 ^{aB}
	Choc-2+Mg-ST	9.2 ± 0.2 ^{aB}	32.6 ± 0.2 ^{aC}	45.3 ± 1.4 ^{aB}	91.3 ± 1.6 ^{bB}	114.7 ± 3.1 ^{bA}
	Choc-2+PS	6.1 ± 0.2 ^{bC}	32.0 ± 0.9 ^{aC}	44.1 ± 0.3 ^{aC}	92.2 ± 1.3 ^{cA}	113.4 ± 3.6 ^{bA}

Mean values of Force (N) that required to break the 3D printed chocolate and cast chocolate (in column based on infill percentage) that do not share a letter are significantly different at $p < 0.05$. IP means infill percentage. Mean values of Force (N) (in column based on infill pattern) that do not share a capital letter are significantly different at $p < 0.05$.

Regardless of infill percentage, in most cases, the printed dark chocolate samples containing flow enhancer (Mg-ST and PS) were significantly different at $p < 0.05$ than that of control samples (Choc-1 and Choc-2). Nedomova et al., (2013) reported that the tensile strength of dark chocolate increase as the cocoa solids increased from 70 % to 90 %. As suggested from previous study, the additional of particulates did not influence the thermal and rheology properties of chocolate (Mantihal et al., 2017). However, the presence of solids particles will influence the chocolate matrix, contributing to the increase of mechanical strength in dark chocolate (Nedomova et al., 2013; Svanberg, Ahrné, Lorén, & Windhab, 2011). Therefore, the addition of particulates also contributed to the increase in hardness of the printed dark chocolate.

A higher force to break the samples were recorded for cast samples (> 110 N) than that of samples printed in 100% infill pattern (regardless of infill pattern). The reduced resistance to break observed for the 3D printed constructs can be explained by weakened interactions between the particles caused

by the consecutive layering deposition. In contact with air, upon extrusion of a chocolate filament, a new surface is generated, to ensure high adhesion between layers (and a closer mechanical properties of a dense structure), printing speed is essential to be controlled in combination with the nozzle diameter size. A similar comparison of the cast and printed cheese was reported by Le Tohic et al. (2018). They found that the printed cheese exhibited a high degree of meltability and showed a significantly less in hardness (by up to 49%) than that of casted cheese.

Apart from the addition of particulates and IP, infill pattern also showed influence on the mechanical strength of printed chocolate. As can be seen in Table 6.5, overall, there was a significant difference ($p < 0.05$) of force required to break the printed samples between HC, HNY and Star infill patterns. The discrepancy of force (N) between each infill pattern is contributed by the differences in infill structure and interlayer bonding. HC infill pattern exhibited a less force required to break the samples than that of HNY and Star infill pattern from 5%_IP to 60%_IP. It is important to note that every infill pattern is different in shape and printing path (Tronvoll, Welo, & Elverum, 2018). Figure 6.8 exhibit HC, HNY and Star infill patterns used in this study. As can be seen in the Figure, HC infill pattern does not incorporate a criss-cross infill structure as compared to HNY and Star infill structure. Criss-cross infill structure produces a stable and stronger construct than the unintegrated pattern (Fatimatuzahraa et al., 2011; McLouth et al., 2017).

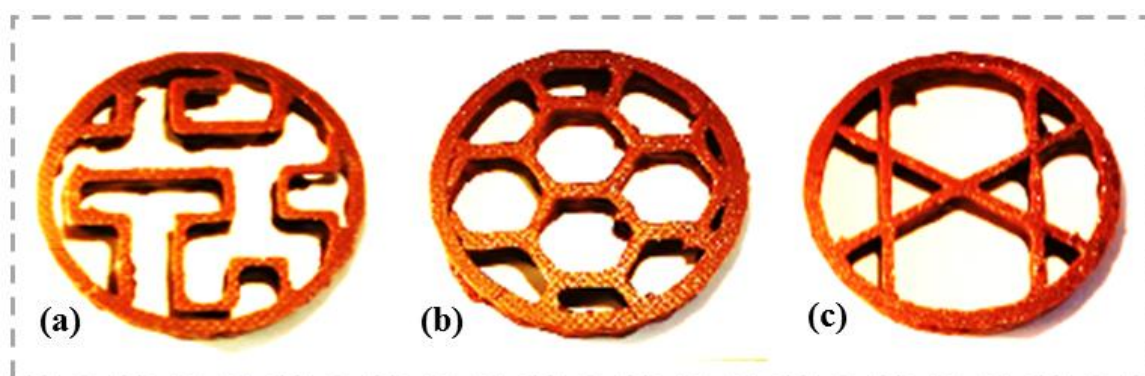


Figure 6.8: Representative image infill pattern of (a) Hilbert curve-HC (b) honeycomb -HNY (c) Star that applied in printing chocolate.

In addition to that, the trajectories and interlayer bonding zones are varied between infill patterns (Fernandez-Vicente et al., 2016). HNY and star infill pattern exhibit more bonding zones than that of HC infill pattern. As a result, HNY and Star infill pattern produced a tougher printed construct. However, in samples printed in 100 % IP, most of the infill pattern exhibited almost similar to line pattern (see Figure 6.4). Therefore, a comparable force N required to break the samples printed in 100 % IP (irrespective of infill pattern) as shown in Table 6.5. Overall, the results indicate that 3D

food printing can substantively change the textural properties of printed chocolate. Also, based on these findings, it is proposed that by modifying the infill structure (infill pattern and percentage), the sensory perception might potentially varied, as the difference would be felt when the chocolate bitten during oral consumption.

6.4 Conclusion

In this study, 3D auger extrusion was successfully used to fabricate a round geometry of chocolate with various infill patterns and void percentages using powdered chocolate. Shape fidelity was observed for most of the chocolate formulations tested with minimal variations in height and diameter, in comparison with the pre-set dimensions of the shape. The density and weight of the 3D constructs were controlled by the infill percentage; feature that cannot be achieved by conventional casting methods of melted chocolate. It is worth to highlighting that the chocolate shape printed with 100 % infill depicted a lower resistance to break than the same formulation prepared by casting method. This was attributed to the interfacial voids formed during the deposition of layers, causing a decay in the attraction forces between the particles (or layers) during solidification. The mechanical properties of the 3D printed chocolate were also related to the type of infill patterns. Star and honeycomb patterns showed a high mechanical property due to criss-cross integrated pattern. Our findings demonstrate that 3DP is a powerful tool to control the mechanical properties of solid-chocolate. Enhanced textural attributes can be easily controlled by varying the infill pattern and percentage. Further study is being pursued investigating the sensory perception of 3D printed chocolates in regard of infill percentage of 3D printed chocolate and also consumers' perception on 3DFP.

6.5 References

- Afoakwa, E. O. (2010). *Chocolate science and technology*(Vol. 687). Oxford: Wiley-Blackwell.
- Beckett, S. T. (2018). *The science of chocolate*. Royal Society of Chemistry.
- Cohen, D. L., Lipton, J. I., Cutler, M., Coulter, D., Vesco, A., & Lipson, H. (2009). *Hydrocolloid printing: a novel platform for customized food production*. Paper presented at the Proceedings of solid freeform fabrication symposium (SFF'09).
- Fatimatuzahraa, A., Farahaina, B., & Yusoff, W. (2011). *The effect of employing different raster orientations on the mechanical properties and microstructure of Fused Deposition Modeling parts*. Paper presented at the Business, Engineering and Industrial Applications (ISBEIA), 2011 IEEE Symposium on Business, Engineering and Industrial Applications (ISBEIA) (pp. 22-27).
- Fernandez-Vicente, M., Calle, W., Ferrandiz, S., & Conejero, A. (2016). Effect of infill parameters on tensile mechanical behavior in desktop 3D printing. *3D printing and additive manufacturing*, 3(3), 183-192.
- FSANZ. (2016). Plant Sterols. Retrieved from <http://www.foodstandards.gov.au/consumer/nutrition/plantsterol/Pages/default.aspx>
- Hao, L., Mellor, S., Seaman, O., Henderson, J., Sewell, N., & Sloan, M. (2010). Material characterisation and process development for chocolate additive layer manufacturing. *Virtual and Physical Prototyping*, 5(2), 57-64.
- Kang, H.-W., Lee, S. J., Ko, I. K., Kengla, C., Yoo, J. J., & Atala, A. (2016). A 3D bioprinting system to produce human-scale tissue constructs with structural integrity. *Nature biotechnology*, 34(3), 312.
- Le Tohic, C., O'Sullivan, J. J., Drapala, K. P., Chartrin, V., Chan, T., Morrison, A. P., . . . Kelly, A. L. (2018). Effect of 3D printing on the structure and textural properties of processed cheese. *Journal of Food Engineering*, 220, 56-64.
- Liu, Zhang, M., Bhandari, B., & Wang, Y. (2017). 3D printing: Printing precision and application in food sector. *Trends in Food Science & Technology*, 69, 83-94.
- Liu, Z., Bhandari, B., Prakash, S., & Zhang, M. (2018). Creation of internal structure of mashed potato construct by 3D printing and its textural properties. *Food Research International*, 111, 534-543
- Mantihal, S., Prakash, S., Godoi, F. C., & Bhandari, B. (2017). Optimization of chocolate 3D printing by correlating thermal and flow properties with 3D structure modeling. *Innovative Food Science & Emerging Technologies*, 44(Supplement C), 21-29.
- McLouth, T. D., Severino, J. V., Adams, P. M., Patel, D. N., & Zaldivar, R. J. (2017). The impact of print orientation and raster pattern on fracture toughness in additively manufactured ABS. *Additive Manufacturing*, 18, 103-109.
- Murphy, S. V., & Atala, A. (2014). 3D bioprinting of tissues and organs. *Nature biotechnology*, 32(8), 773-785.

- Nedomova, S., Trnka, J., & Buchar, J. (2013). Tensile Strength of Dark Chocolate. *Acta Technologica Agriculturae*, 16(3), 71-73.
- Rankouhi, B., Javadpour, S., Delfanian, F., & Letcher, T. (2016). Failure analysis and mechanical characterization of 3D printed ABS with respect to layer thickness and orientation. *Journal of Failure Analysis and Prevention*, 16(3), 467-481.
- RepRap. (2016). RepRapWiki: G-code. Retrieved from <http://reprap.org/wiki/G-code>
- Rodriguez, J. F., Thomas, J. P., & Renaud, J. E. (2000). Characterization of the mesostructure of fused-deposition acrylonitrile-butadiene-styrene materials. *Rapid Prototyping Journal*, 6(3), 175-186.
- Severini, C., Derossi, A., & Azzollini, D. (2016a). Variables affecting the printability of foods: Preliminary tests on cereal-based products. *Innovative Food Science & Emerging Technologies*.
- Severini, C., Derossi, A., & Azzollini, D. (2016b). Variables affecting the printability of foods: Preliminary tests on cereal-based products. *Innovative Food Science & Emerging Technologies*, 38, 281-291.
- Sood, A. K., Ohdar, R., & Mahapatra, S. (2010). Parametric appraisal of mechanical property of fused deposition modelling processed parts. *Materials & Design*, 31(1), 287-295.
- Sun, J., Peng, Z., Yan, L., Fuh, J., & Hong, G. (2015). 3D food printing: An innovative way of mass customization in food fabrication. *International Journal of Bioprinting*, 1(1), 27-38.
- Sun, J., Peng, Z., Zhou, W., Fuh, J. Y., Hong, G. S., & Chiu, A. (2015). A Review on 3D Printing for Customized Food Fabrication. *Procedia Manufacturing*, 1, 308-319.
- Svanberg, L., Ahrné, L., Lorén, N., & Windhab, E. (2011). Effect of sugar, cocoa particles and lecithin on cocoa butter crystallisation in seeded and non-seeded chocolate model systems. *Journal of Food Engineering*, 104(1), 70-80.
- Tronvoll, S. A., Welø, T., & Elverum, C. W. (2018). The effects of voids on structural properties of fused deposition modelled parts: a probabilistic approach. *The International Journal of Advanced Manufacturing Technology*, 97(9), 3607-3618.
- Vancauwenberghe, V., Katalagarianakis, L., Wang, Z., Meerts, M., Hertog, M., Verboven, P., Nicolai, B. (2017). Pectin based food-ink formulations for 3-D printing of customizable porous food simulants. *Innovative Food Science & Emerging Technologies*, 42, 138-150.
- Wegrzyn, T. F., Golding, M., & Archer, R. H. (2012). Food Layered Manufacture: A new process for constructing solid foods. *Trends in Food Science & Technology*, 27(2), 66-72.
- Williams, D., Thayer, P., Martinez, H., Gatenholm, E., & Khademhosseini, A. (2018). A perspective on the physical, mechanical and biological specifications of bioinks and the development of functional tissues in 3D bioprinting. *Bioprinting*, 9, 19-36.
- Yang, F., Zhang, M., & Bhandari, B. (2015). Recent Development in 3D Food Printing. *Critical Review Food Science & Nutrition*, 57(14), 3145-3153.

Yang, F., Zhang, M., Bhandari, B., & Liu, Y. (2018). Investigation on lemon juice gel as food material for 3D printing and optimization of printing parameters. *LWT - Food Science and Technology*, 87, 67-76.

Yousefi, A.-M., Smucker, B., Naber, A., Wyrick, C., Shaw, C., Bennett, K., Wood, K. A. (2018). Controlling the extrudate swell in melt extrusion additive manufacturing of 3D scaffolds: a designed experiment. *Journal of Biomaterials Science, Polymer Edition*, 29(3), 195-216.

Chapter 7 - Texture-modified 3D printed dark chocolate: Sensory evaluation and consumer perception study⁴

Abstract

The final research chapter aimed to assess consumers' preferences and perceptions of texture-modified 3D printed chocolate through three measures, two tasting tests and one survey. In the first test, 30 semi-trained panellists ranked their overall preference from among the three samples of chocolate printed in a honeycomb pattern with infill percentages of 25%, 50% and 100%. The panellists ranked the samples based on appearance and hardness. In the second test, the same panellists nominated one preference between a 3D printed sample (100% infill percentage) and a cast commercial chocolate sample. Friedman test indicated that there was no significant difference in overall preferences for hardness although the panellists significantly preferred the appearance of samples with 25% and 50% over the 100% infill. Further, there was no significant difference in preference between the cast and 100% infill samples. In the survey of consumer perceptions, a total of 244 participated and assessed the samples for their intricate design and novel technology concept through a questionnaire. While there was a general awareness of 3D printing technology among these participants, many were impressed with the application of 3D printing to chocolate, as this was the first time they had seen this. The results obtained from the sensory tests and consumer survey provided a useful insight into consumers' perception of 3D food printing and the 3D products design. This awareness will be beneficial to promote this technology in the food industry.

⁴ This chapter has been published as a research paper in the *Journal of Texture Studies* (IF = 1.61): Mantihal, S., Prakash, S., & Bhandari, B. (2018). Texture modified 3D printed dark chocolate: sensory evaluation and consumer study. *Journal of Texture Studies*, 50(5), 386-399. The core content of the manuscript was modified to keep the format consistent throughout the thesis.

7.1 Introduction

3D food printing (3DFP) is a novel technology that is capable of creating a complex geometry. Thus, 3DFP provides the freedom to fabricate food in numerous structures. Recently, several research studies into many facets of food printing have been published including the application of additives (Rapisarda et al., 2018) and the influence of this technology on food textural properties (Prakash, Bhandari, Godoi, & Zhang, 2019). 3DFP also provides the opportunities for creativity in the design of structures (Noort, Van Bommel, & Renzetti, 2017). In 3D printing, the most important component of texture variation is in the internal structure which consists of the infill pattern and the infill percentage (RepRap, 2016). The infill pattern refers to the type of configuration that will form as a pattern within the printed construction. The infill percentage is the intensity of the mesostructure (layer-to-layer gap) of the material upon deposition. This structure (pattern and percentage) is designated in the slicing software before the printing process (Fernandez-Vicente, Calle, Ferrandiz, & Conejero, 2016). The incorporation of the infill pattern and percentage in 3D printing creates a unique internal microstructure within the printed food.

The infill structure within printed food will influence the construction's sensorial textural attributes. Le Tohic et al. (2018) compared the texture of cheese printed in 100% infill with cast cheese prepared using moulding. They reported that printed cheese is 49 % softer than cast cheese even when printed with 100% infill. Severini, Derossi, and Azzollini (2016) reported that a cereal-based product printed in 20% infill required a 62.62 N force to break the samples as compared to samples printed in 10% infill, which needed 26.31 N. This finding indicates that the infill percentage influences the mechanical strength of the constructions, as increasing the infill percentage tends to create a harder construction (Dizon, Espera, Chen, & Advincula, 2018). A lower infill percentage will create a hollow internal structure within printed food contributing to textural variation. In our previous work (Mantihal et al., 2018), the void fraction of the printed chocolate when printed in 60% infill (with a honeycomb pattern) was 11.6 ± 2.3 % while printing in 5% infill resulted in 68.8 ± 4.4 % voids.

3D printing technology demonstrated that food texture could be modified to suit personal requirements (Vancauwenberghe et al., 2018). As food texture is an essential characteristic in defining the quality of food, it is also a vital sensory attribute that can affect an individual's sensation experience during oral consumption. The 3D printing can address the personalising of nutritional needs and also achieve the texture requirements for elderly people with dysphagia (Lipton, Cutler, Nigl, Cohen, & Lipson, 2015). Also, 3DFP is able to offer a texturised and palatable food shape which provides the patient some enjoyment in eating rather than the monotony of consuming only pureed

food (Noort et al., 2017). Thus, 3DFP is considered a powerful technology that is able to tailor food to personal preferences, particularly in shape and texture.

The perceived texture is closely related to the structure and composition of food (Aguilera & Park, 2016; Lupton & Turner, 2018). Severini, Derossi, Ricci, Caporizzi, and Fiore (2018) investigated the sensory attributes (appearance, taste, odour and colour) of 3D printed fruits and vegetables with a reduction in moisture content to increase the viscosity of the formula. The researchers reported that the appearance attribute of printed smoothies was significantly different to that of food formula, with a value of 4.60 ± 0.74 for printed samples compared with 3.37 ± 1.1 for food formula. Also, there was no significant difference between the colour, taste and odour of printed smoothies and the non-printed samples. Their results suggested that 3DFP was able to improve the visual appeal of food. However, this finding was limited to the sensory attributes of 3D printed food based on formula modification rather than on the alteration of the internal structure of printed food.

Texture is an important attribute for consumers' acceptance of a food which is influenced by their conventional perception of food and view on the production of the food product. Thus, the perception about this new technology could be a barrier for consumers to accept 3D printed food. McCluskey, Kalaitzandonakes, and Swinnen (2016) explored an extensive review on the application of a new technology to produce food and its influence on consumer behaviour and public perceptions based on media coverage. Issues such as misconceptions, a lack of knowledge and a negative attitude were found to be drawbacks in consumer acceptance of new food production technology. However, McCluskey et al. (2016) emphasised that a proactive knowledge dissemination and established credible reports from reliable sources (scientists, firms) could overcome consumers' perception of risk in regard to new food technologies.

Recently, the acceptance of 3D printed food has been studied in various settings and among targeted consumers. Brunner, Delley, and Denkel (2018) explored Swiss consumers' attitudes and attitudinal changes toward 3D printed food using a survey. The questionnaire was constructed with 14 predictors, constituting variables of food neophobia, benefits perception, nutritional knowledge, previous knowledge, and technology neophobia (Brunner et al., 2018). The questionnaire design consisted of a six-point Likert scale and response options ("true", "false" and "don't know") and a postal method to distribute the questionnaire to target participants. After an intervention which consisted of the feedback from the respondents, they reported that its outcome was successful in overcoming consumers' food neophobia and convincing consumers that 3DFP technology is capable of producing healthy and individualised meals with an exciting food design.

Similarly, Lupton and Turner (2018) also explored consumer attitudes toward 3D food printing with a different approach by outsourcing a specialised company to conduct an online discussion among 30 Australians aged 18 years and older. During this discussion, participants were supplied with a set of questions with seven photographs of 3D printed foods from different formulations and designs (1) confectionary with multiple design geometry (2) insect formulation (3) carrot based puree (4) vegetable and chicken (5) pizza (6) pasta with intricate shapes and, (7) chocolate in a rose shape. For familiarisation, the ingredients of each food in the given photograph were listed. The participants were asked to respond to each image with some question items using a scale of 1 to 10 and some open-ended questions. The results suggested that the ingredients, sensory quality and level of processing were the key elements in determining consumer acceptance of 3D printed food.

To our knowledge, there are no reports as yet of sensory evaluation of the food texture in 3D printed foods which have been modified by varying the internal structure. That is to say, there have been attempts to gauge the consumers' attitudes solely by a survey, without actual 3D printed food presented for the consumer to view. Therefore, this study aimed to demonstrate the capability of 3DFP to modify food texture by altering the internal structures of printed chocolate. A sensory evaluation of texture-modified 3D printed chocolate was conducted among 30 semi-trained respondent to assess consumers' preferences concerning sensory attributes such as texture and appearance and their overall preferences. 3D printed chocolates with various infill patterns and percentages were displayed and a questionnaire was distributed to assess respondents' awareness and opinions on 3D printed foods. The outcome of this study is expected to benefit to food entrepreneurs and organisations that wish to adopt this novel technology in their businesses.

7.2 Materials and Method

7.2.1 Materials

Two types of dark chocolates, Cadbury dark chocolate (Choc-1) and Callebaut dark chocolate buttons (Choc-2) purchased locally in Brisbane, Australia were used in this study. Choc-1 was also used for cast chocolate samples as a control. The composition of the Cadbury dark chocolate was 53 % (minimum) cocoa solids, 35 % (minimum) cocoa butter, 0.5 % lecithin, and approximately 11.5% sugar. The Callebaut dark chocolate buttons (bittersweet flavour, Lindt Piccoli) were composed of 58% (minimum) cocoa solids, 33 % (minimum) cocoa butter, 5 % anhydrous milk fat, 0.5 % lecithin and vanilla and about 3.6 % sugar. Both dark chocolate samples (Choc-1 and Choc-2) were ground separately into powder in a controlled temperature room at around ~ 5 °C and kept in refrigeration (~ 8 °C) separately until the initiation of the printing process.

7.2.2 Commercial dark chocolate casting process

Casting of Choc-1 was done to compare it with the textural property of 3D printed chocolate. Before casting, the chocolate was melted at a controlled temperature at around 32 °C using a chocolate melting machine (ChocEdge, UK). Melted chocolate samples (10 g) were poured into a 3D printed cast (printed using acrylonitrile butadiene styrene (ABS) filament, see Figure 7.1) and covered by a thin layer of clear food grade plastic wrap. All samples were kept under refrigeration at around 8 °C until the initiation of the textural analysis and sensorial evaluation.

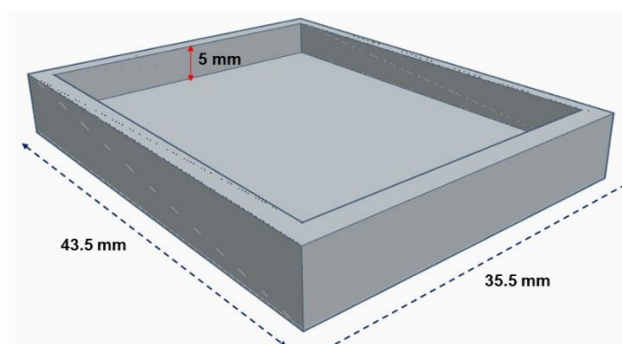


Figure 7.1: The 3D cast printed using Da Vinci 2.0 dual nozzle model XYZ printer with ABS filament.

7.2.3 Printing process

The 3D chocolate printing consisted of three essential steps: (i) making the 3D geometry design, (ii) slicing the design and (iii) the printing process.

- i. 3D geometry design:** Chocolate Model (1) of 20 mm x 50 mm and 5 mm thickness and Chocolate Model (2) of 43.5 mm x 35.5 mm and 5 mm thickness were designed using TinkerCad online software.
- ii. Slicing:** The 3D models from the above online software were uploaded into the Repetier-Host software (.stl file) and sliced using Sli3er configuration to generate the g-code for each model. The shell perimeters were set at default three shells (approximately ~ 2.34 mm thickness) considering the inner nozzle diameter is 0.78 mm. Model (1) for Choc-2 was set to a honeycomb infill pattern with a variation of infill of 25%, 50%, and 100% as shown in Figure 7.2. Model (2) for Choc-1 was set to a rectilinear pattern with 100% infill to mimic the commercial chocolate block. All samples were sliced (with the specific g-code extracted for each 3D model) according to each infill pattern and infill percentage using Sli3er software.

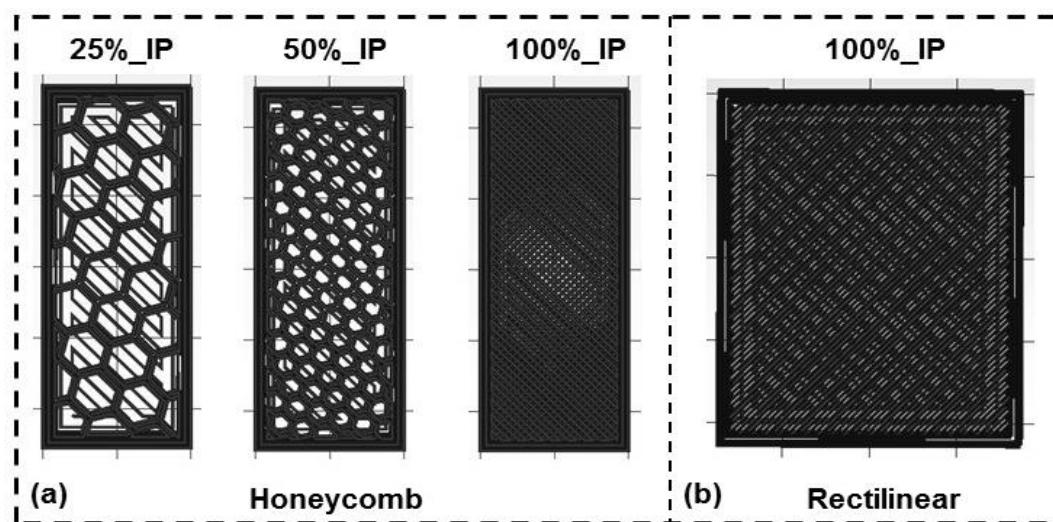


Figure 7.2: 3D model designs of rectangular shape (a) Model -1(20 mm x 50 mm and 5 mm thickness) with Honeycomb pattern in variation of infill density of 25%_IP, 50%_IP and 100%_IP (b) Model-2 (43.5 mm x 35.5 mm and 5 mm thickness) in rectilinear pattern with 100%_IP. IP refers to infill percentage.

- iii. **Printing process:** A Shinnove 3D printer (Model No. Shinnove-D1, Shiyin Co. Ltd, Hangzhou, China) was used in this study, as illustrated in Figure 7.3. The printer was equipped with a syringe-based extrusion unit with a capacity of 60 mL in each syringe. Two syringes are inserted into two separate heating barrels which shared the same shaft and bearings. Therefore, each syringe barrel could be controlled individually to deposit food materials. The nozzle diameter used was 0.78 mm and the printing speed set in the Sli3er software was 70 mm/s. These printing parameters were optimised as per the previous research chapter (Chapter 3). The printer bed (stainless steel) temperature was maintained between 15 °C and 16 °C by a recirculating water system. A total of 132 samples was prepared. All printed samples were kept under refrigeration at around 8 °C until the execution of textural analysis and sensory evaluation.

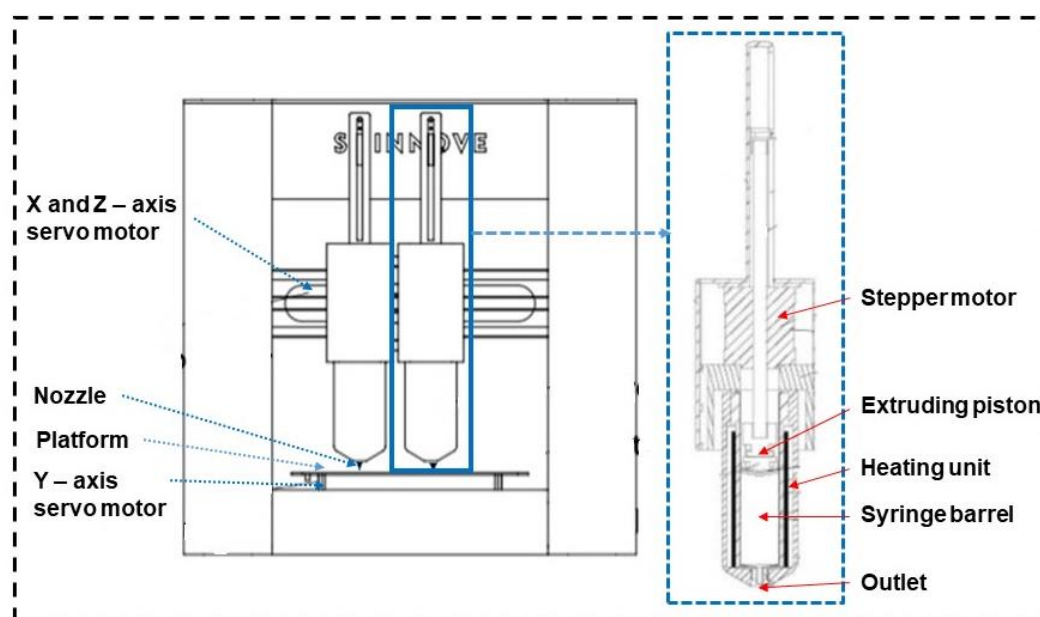


Figure 7.3: Schematic illustration of Shinnove dual nozzle 3D printer and its components.

7.2.4 Dimensional and weight measurement of 3D printed chocolates

A digital calliper (0-150 mm, CraftRight®, Bunnings, Australia) was used to measure the dimensions of the 3D printed chocolate (length, width and thickness). This was done in three different positions on each printed chocolate samples for accuracy and the average value (mm) was reported. Also, a digital weighing balance was used to assess the weight of each printed chocolate sample.

7.2.5 Texture properties of 3D printed chocolate

The texture attribute of hardness was obtained by texture analysis using a texture analyser (Model TA-XT Plus, Stable Microsystem, UK) equipped with a 10.0 kg load cell with Exponent version 6.1.9.0 software. A TA-42 knife blade was used, and the test was conducted at room temperature (around 23 °C). Compression mode was used to analyse the samples at 10 mm distance. A pre-test of the speed of 1.0 mm/s and the test speed of 2.0 mm/s with 5.0 g trigger force were applied. The measurement was conducted in triplicate and the data of maximum force (N) from the force-displacement curve were extracted.

7.2.6 Sensory evaluation

The sensory profile of the printed chocolate was carried out to determine consumer acceptability of 3D printed chocolate. The chocolate was evaluated using a ranking test for preferences and a paired-preferences test with the aid of RedJade sensory evaluation software. The sensory test was conducted in a sensory analysis laboratory, at the School of Agriculture and Food Sciences (SAFS), the

University of Queensland, Australia. Ethical clearance approval for this evaluation was granted by the Human Research Ethics Committee, University of Queensland. 30 semi-trained (panellist who familiar with chocolate testing) panellists composed of 21 females and nine males from the School were involved in the sensory test. The age range of the panellists was between 28 and 55 years. The printing time for each sample ranged from 3 to 5 minutes, depending upon the sample's infill percentage. The chocolate samples were kept at room temperature (23 °C) before evaluation. Two sets of samples were served to the panellists, starting with three samples for a ranking test for preferences. Once the panel completed the ranking test, the second set of samples (2 samples) for the paired preference test was given to the panellists.

For the ranking test for preferences, three dark chocolate (Choc-2) samples were prepared with dimensions of 20 mm x 50 mm and 5 mm thickness, printed in honeycomb infill pattern with infill percentages of 25 %, 50 % and 100 %. The sensory attributes assessed were appearance, hardness and overall preferences using Rank 1 for the most preferred, Rank 2 for the medium ranking and Rank 3 for the least preferred. The printed samples were coded with three random numerical numbers and placed in random order on one paper plate for each respondent. For the paired-preferences test, two dark chocolate (Choc-2) samples were served (dimensions: 43.5 mm x 35.5 mm and 5 mm thickness). One sample was printed in 100 % infill with a rectilinear pattern, and another was the cast chocolate block. The samples were coded with three random digits and served randomly on the plate. In this test, the panellist had to choose which chocolate they preferred the most.

7.2.7 Consumer survey

To obtain consumers' attitudes and knowledge about 3D food printing, 3D printers (Porimy and Shinnove-D1) and printed chocolate samples (various design) were displayed at the University of Queensland premises and a questionnaire was designed and distributed among the University of Queensland community. The questionnaire design and data collection were conducted as follows:

7.2.7.1 Design of questionnaire

The survey began with a brief description of the research study – consumer perceptions about 3D food printing – in which consumers were informed about this novel technology for printing food. The questionnaire consisted of five sections (1) demographics (2) knowledge about 3D printing (3) perception about the benefit of 3D printing (4) opinion about the 3D printed chocolate products on display and (5) measure of attitude toward 3D printed food. In the first section, the respondent was asked a series of socio-demographic questions (gender, age, nationality, occupation and household size). In the second section, the respondent's knowledge was assessed using three items, for which

the respondent had to indicate either “yes”, “no”, or “don’t know”. This was adopted from Brunner et al. (2018). Next, the respondent was asked about their perception of the benefits of 3D food printing in terms of it creating appealing shapes, being a ready to serve food, being used to prepare healthy snacks, potentially addressing a swallowing problem (dysphagia), and the potential of 3D food printing to minimise waste. In the third section, the respondent’s perception was assessed using seven items and their responses noted as binary (“yes” or “no”) answers. In the fourth, the respondent was asked about the 3D printed chocolate products on display. Opinions about these printed chocolates’ attributes (appearance and design complexity) were sought and also their willingness to consume the novel chocolate structure (indication of food neophobia) was gauged. Furthermore, the respondent was asked if they would like a 3D printer at home. In this section, the respondent ranked their responses on a scale from 1 to 10. In the last section, the respondent’s attitude to 3D printed food in general (Brunner et al., 2018) was assessed and their answers were again ranked on a scale from 1 to 10.

A 3D food printing display was made at the University of Queensland (UQ), at a central location where there is usually a lot of movement of students, staff members and visitors. The 3D food printers were displayed in operation and 3D printed chocolate samples were presented. A questionnaire-based consumer survey (form) was distributed using the simple random method during the display to UQ students, staff and public visitors and collected on completion. A total of 280 questionnaires was distributed and 244 questionnaires were successfully collected. During filling in the questionnaire, people were exposed to the 3D food printer and observed some printed chocolates as well as the demonstration of chocolate printing. The data collection was performed around mid-October 2018. Chocolate was printed in various shapes and dimensions for display purpose. Figure 7.4 exhibits these 3D printed chocolates with various dimensions, infill patterns and infill percentages.



Figure 7.4: Various shapes, designs and internal structures (infill patterns and percentages) of 3D printed chocolates used in display session.

7.2.8 Statistical analysis

Dimensional properties (weight, width, length and thickness), and mechanical strength (Force –N) were presented as mean values \pm standard deviation. Minitab version 17 (statistical software) was used to analyse the significant difference between values using the one-way analysis of variance (ANOVA) Tukey's test (where applicable). The significant difference was determined at p -value (p) of less than 0.05. The ranking of preferences (sensory analysis) was compared using a nonparametric, Friedman test. The significant difference of the sensory attributes was determined at (p) of less than 0.05. IBM's Statistical Package for Social Science (SPSS) version 24.0 was used to analyse the survey

data. A descriptive analysis was performed for the sample profile of respondents' demographics. A Chi-square test was conducted to determine the significant relationship between categorical variables. Cronbach's alpha values were computed, taking into consideration the values greater than 0.60 (Bernstein & Nunnally, 1994; Sekaran & Bougie, 2016).

7.3 Results and Discussion

The 3D printed constructions and cast chocolate block for Choc-1 (Cadbury dark chocolate) and Choc-2 (Callebaut dark chocolate) are illustrated in Figure 7.5. As can be seen in the figure, the 3D printed chocolate constructed with various infill percentages (25 %, 50 % and 100 %) were able to support the size and shape of the constructions. Also, the hollow structure was visible in chocolate printed in 25 % and 50 % infill when the chocolate was snapped. The physical properties (thickness, width, length) and weight are discussed in the subsequent section.

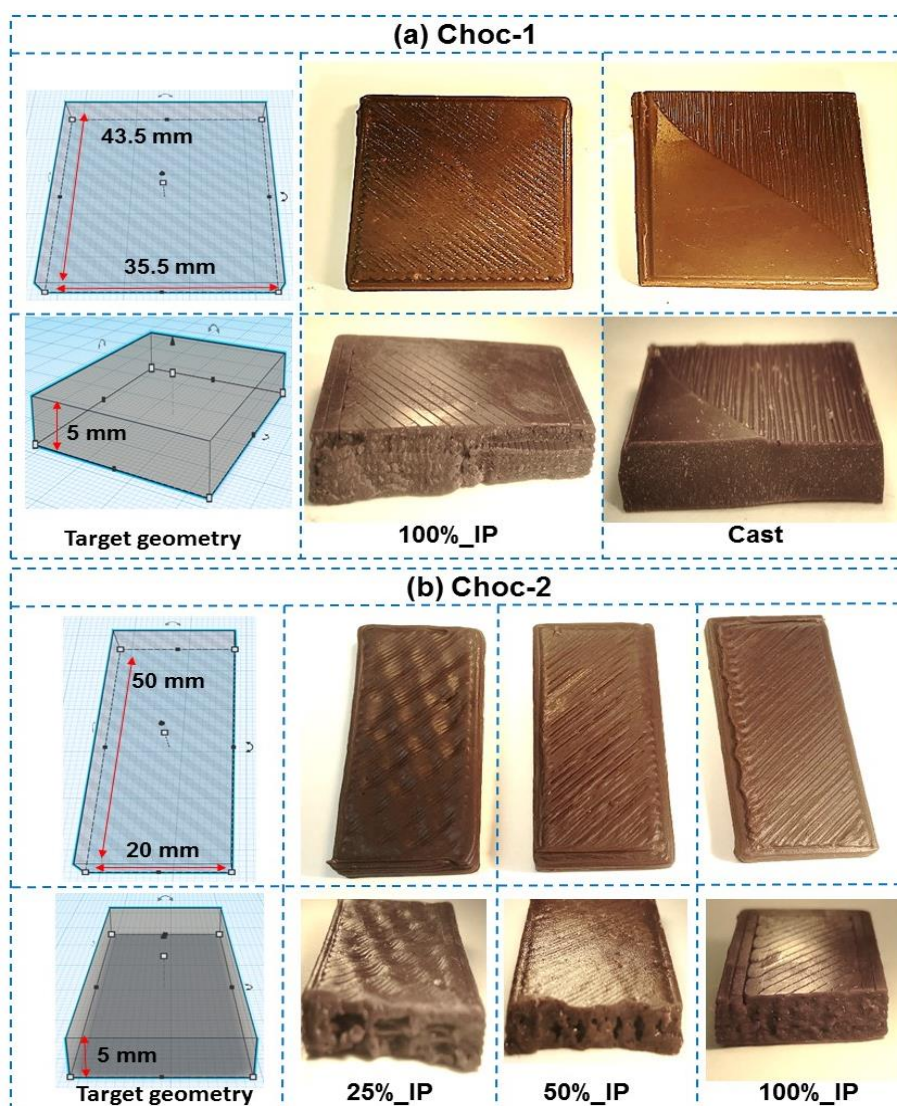


Figure 7.5: Representative images of 3D printed and cast chocolate samples – target geometry as reference. (a) Choc-1 is Cadbury dark chocolate – one sample was printed in 100% infill with rectilinear infill pattern, and the other is a cast sample. (b) Choc-2 is the Callebaut dark chocolate printed in various infill percentages, 25%, 50% and 100%, with a honeycomb infill pattern. IP means infill percentage.

7.3.1 Evaluation of dimensional properties and weight of 3D printed chocolate

Table 7.1 shows the recorded thickness, width and length of the 3D constructs. As can be seen in Table 7.1, the thickness of the construction printed with Choc-2 (regardless of infill percentages) remained the same; there was no significant difference ($p < 0.05$) between samples printed in 25% (5.09 ± 0.03 mm), 50% (5.12 ± 0.07 mm) and 100% (5.06 ± 0.04 mm), respectively. Also, the width and length of the constructions showed similarity to that of the predesign geometry, as there was no significant difference ($p < 0.05$) between samples printed in 25%, 50% and 100% infills. Similarly, for samples printed with Cadbury dark chocolate (Choc-1), the thickness, width and length of the printed product (100% infill) were not significantly different ($p < 0.05$) with those of the cast chocolate block (see Table 7.1).

Table 7.1: Recorded dimensional properties (thickness, width, length) and weight of 3D printed Choc-1 with 100% infill (rectilinear pattern) and cast samples, and Choc-2 samples with infill of 25%, 50%, and 100% (honeycomb pattern).

Dimension	Choc -1		Choc-2		
	100%_IP	Cast	25%_IP	50%_IP	100%_IP
Thickness (mm)	5.07 ± 0.02 ^a	5.00 ± 0.0 ^a	5.09 ± 0.03 ^a	5.12 ± 0.07 ^a	5.06 ± 0.04 ^a
Width (mm)	35.34 ± 0.52 ^a	35.50 ± 0.0 ^a	20.44 ± 0.51 ^a	20.40 ± 0.53 ^a	20.09 ± 0.03 ^a
Length (mm)	43.75 ± 0.21 ^a	43.50 ± 0.0 ^a	51.15 ± 1.02 ^a	50.06 ± 0.09 ^a	50.08 ± 0.07 ^a
Weight (g)	9.21 ± 0.52 ^b	10.00 ± 0.0 ^a	4.70 ± 0.64 ^c	6.03 ± 0.21 ^b	8.39 ± 0.65 ^a

Mean values of thickness, width, length and weight of 3D printed chocolate and cast chocolate in row based on type of chocolate (Choc-1 and Choc -2) that do not share a letter are significantly different at $p < 0.05$. IP means infill percentage.

The dimensions of the cast chocolate block remain as per the predesign model because the chocolate was moulded explicitly to the predetermined dimensions. Similar results were reported by different authors for other 3D printed materials. Liu, Bhandari, Prakash, and Zhang (2018) reported that mashed potato constructions printed in 10%, 40% and 70% infill were closely matched to the design geometry. Also, Yang et al. (2018) designed an intricate geometry of Mickey Mouse with a predesign model (length 5.40 cm, width 5.00 cm and height 2.30 cm) using dough as the main substrate. They verified that 3D printing was able to re-create an intricate design precisely to that of the design geometry with the dimensions of 5.41 cm in length, 4.95 cm in width and 2.28 cm in height. These findings indicate that 3D food printing was capable of producing a product with accurate dimensions. Thus, the results suggest that this novel technology is a great tool for food customisation.

A significant difference ($p < 0.05$) was observed in the weight of each construction printed in various infill percentages: 25% (4.70 ± 0.64 g), 50% (6.03 ± 0.21 g) and 100% (8.39 ± 0.65 g). Also, the weight of printed chocolate (Choc-1) was recorded as less than that of the cast chocolate block (9.21 ± 0.52 g). The difference of weight between the 3D printed chocolate and cast samples is due to the layer-by-layer deposition method in the 3D printing process. In the printing process, the fusion between layers of chocolate will be formed by gravity, cohesive effects and the swell behaviour of extruded chocolate (Mantihal et al., 2019). Incomplete fusion of layers with their adjacent layers will cause micro-voids in the microstructure. These layers could be visually seen in the 3D printed chocolate. In comparison, the cast sample preparation involves filling the mould with molten chocolate to form a single solid and compact mass. Therefore, this difference in production influences the weight of the chocolate.

It is expected that increasing the infill percentage will increase the weight of the printed construction (Table 7.1). The increased weight is due to the amount of extruded material used to fill the construction to accommodate the preset infills (Severini et al., 2016). Fernandez et al. (2016) also reported that the weight of the constructs (ABS filament) significantly increased from 11.2 g up to 18.9 g, respectively as the constructs were printed from 20 % to 100 % infill (with honeycomb infill pattern). These results confirm that a variation in infill percentage would strongly influence the 3D food construction's weight.

7.3.2 Textural evaluation of 3D printed and cast chocolate

A textural analysis was performed to determine the mechanical strength of the 3D constructions. In this experiment, honeycomb infill pattern was applied as this criss-cross pattern provides strong support in 3D construction (McLouth, Severino, Adams, Patel, & Zaldivar, 2017; Murphy & Atala, 2014). Figure 7.6 exhibits of force (N) as a function of distance (mm) of chocolate printed with Choc-1 (with 100% infill and cast samples) and Choc-2 with a variation of infill percentages (25%, 50% and 100%). Figure 7.6a clearly shows that the cast chocolate requires a higher force (N) to break the samples than that of the 3D printed construction with 100% infill. In Figure 7.6b, a variation of force (N) was observed as the infill percentage increased. A steep curve with slight displacement can be seen indicating a good snap quality of all the chocolate samples (Beckett, 2011; Mantihal et al., 2018).

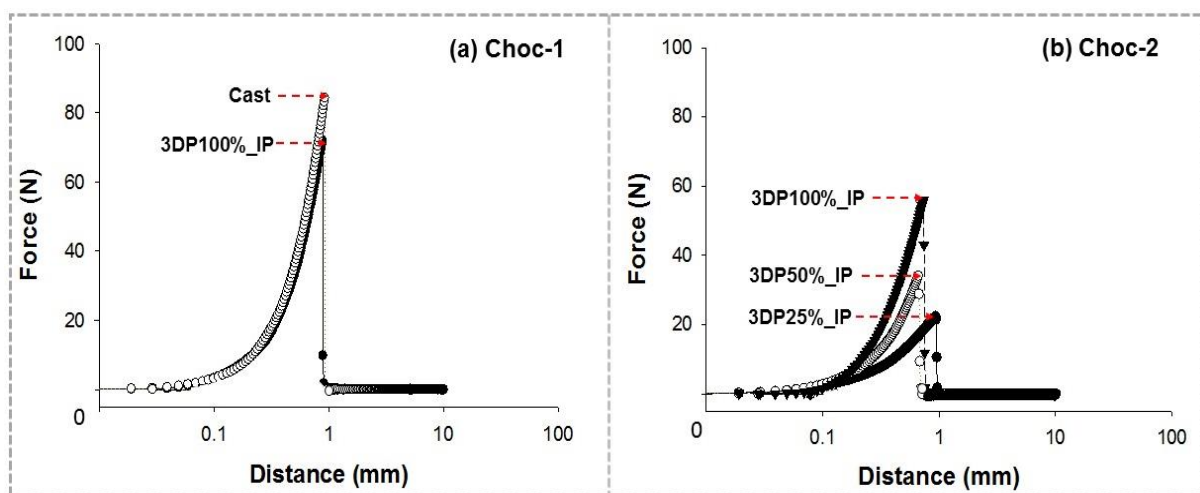


Figure 7.6: Representative graphs of force (N) as a function of distance (mm) of 3DP chocolate printed and cast for samples (a) Choc-1 with 100% infill for 3DP (rectilinear pattern) and (b) Choc-2 samples various infill percentages of 25%, 60%, and 100% (honeycomb pattern) with a pre-test speed of 1.0 mm/s and test speed 2.0 mm/s with 5.0g of trigger load of all chocolate.

Table 7.2 summarises the force (N) required to break chocolate samples printed with Choc-1 (with 100% infill in a rectilinear pattern and cast samples) and Choc-2 (in 25%, 50% and 100% infill) in a honeycomb pattern. As can be seen in Table 7.2, the 3D printed Choc-2 required an increase in the

force (N) to break the samples as the infill percentage increased. It was observed that chocolate printed with 25% infill required 20.44 ± 1.12 N, 50% required 33.52 ± 1.55 N and 100%, 54.43 ± 1.47 N, respectively. The forces were significantly different at $p < 0.05$.

Table 7.2: Recorded force (N) to break the chocolate samples with various infill percentages (25%, 50%, and 100%), and cast samples.

	Choc-1		Choc-2		
	100%_IP	Cast	25%_IP	50%_IP	100%_IP
Force (N)	71.06 ± 1.35^b	83.58 ± 1.40^a	20.44 ± 1.12^c	33.52 ± 1.55^b	54.43 ± 1.47^a

Mean values of Force (N) required to break the 3D printed chocolate and cast chocolate samples (in a row based on the type of chocolate (Choc-1 and Choc -2) that do not share a letter are significantly different at $p < 0.05$).

For Choc-1, there was also a significant difference ($p < 0.05$) in the force (N) required to break the cast and 100% infill chocolate samples, a (83.58 ± 1.40 N and 71.06 ± 1.35 N, respectively) although the 100% infill was similar to the cast chocolate dimension. The reduced resistance to break the printed Choc-1 (3DP100%_IP) is due to a weak interface of layers affected by the sequential layering upon printing. This result is also in line with Le Tohic et al. (2018) who reported that the hardness of the 3D cheese construction diminished by $\sim 49\%$ compared to that of cast cheese. Therefore, cast samples are relatively tougher than printed constructions even when printed at 100% infill.

Also, an increase in percentage infill means that the intensity of deposited layers (mesostructure) becomes compact as the higher IP is achieved (Rankouhi, Javadpour, Delfanian, & Letcher, 2016). Figure 7.5 illustrates that a larger hollow structure can be seen in samples printed with 25% infills and this becomes compact when samples are printed in 50% infill while no void was visible for samples printed in 100% infill. A similar concept was presented in a pectin-based food stimulant printed in honeycomb structure (Vancauwenberghe et al., 2018). The researchers reported that the Young's modulus of printed samples with larger cell size was less (11.58 ± 1.43 kPa) than that of samples printed in a cube which was similar to printing in 100% infill (118.58 ± 12.10 kPa). Thus, by altering the infill percentage the texture of the printed construction will substantively change.

Based on the results of the dimension and textural properties testing of the 3D printed chocolate, we found that the 3DP was capable of producing a precise 3D construction to target geometry. Also, an increase in the mechanical strength of 3D printed chocolate is correspondingly influenced by the variation of infill percentage. Overall, the texture (hardness) of 3D printed chocolate can be changed subject to internal structure modification. In the next section, we attempt to explore the sensorial

properties of 3D printed dark chocolate through sensory evaluation and assessing consumer preferences.

7.3.3 Sensory evaluation of 3D printed dark chocolate

In this evaluation, 30 participants (21 females and nine males) were selected. Three printed samples with different infill percentages (Choc-2) were given for the ranking preference test and two samples of Choc-1 (3D printed and cast chocolates) given for the paired preference test.

7.3.3.1 Ranking for preference evaluation

Table 7.3 presents the estimated median based on the Friedman test (nonparametric) and p -value for 3D printed dark chocolate samples (at 25%, 50% and 100% infill) in an evaluation of ranking for preferences in terms of appearance and hardness and overall preferences. As can be seen in Table 7.3, there was a significant difference ($p < 0.05$) between the preferred appearance of the 3DP samples (Choc-2) as most participants favoured the appearance of sample 3DP100%_IP (1.33) to those of samples 3DP25%_IP (2.00) and 3DP50%_IP (2.67). These results indicate that the participants mostly prefer the smooth appearance of the 3D printed chocolate (see Figure 7.5). As the infill structure is printed at closer to 100% infill, the infill structure provides sufficient support to the top layer and prevents it from any surface deformation (Mantihal et al., 2018). Thus, a smooth and even top layer is produced as the infill percentage increased. The appearance of the 3DP construction was vital as this modality can influence the acceptability of the product.

Table 7.3: Recorded median and p -value of ranking of preferences (appearance, hardness and overall preferences) based on Friedman test for 3DP chocolate printed in various infill percentages (25%, 50%, and 100%).

Ranking for preferences	Samples			p -value
	3DP25%_IP	3DP50%_IP	3DP100%_IP	
Appearance	2.00	2.67	1.33	0.001*
Hardness	1.66	2.00	2.33	0.792
Overall preferences	1.33	2.66	2.00	0.875

* $P < 0.05$

Ranking varied from 1-3 (1 is the most preferred sample)

There were no significant differences ($p > 0.05$) in the participants' preferred texture (hardness) among the 3DP samples. However, participants indicated their preferences for the hardness of chocolate sample (by biting the 3D printed chocolate) 3DP25%_IP (1.66) as compared to 3DP50%_IP (2.00) and 3DP100%_IP (2.33). This result corroborates with the finding in Section 7.3.2, indicating that samples printed in 25% infill are less hard than samples printed in 50% and 100% infill. In this case, we found that the participant is likely to choose a modified texture (less hard). The way the texture changes is significant in determining food product acceptance (Jeltema, Beckley, & Vahalik, 2016) and 3DP provides freedom to customise a design, modify textures and alter palatability (Dankar, Haddarah, El Omar, Sepulcre, & Pujolà, 2018; Devezeaux de Lavergne et al., 2016; Szczesniak, 2002)

In terms of overall preferences, no significance difference ($p > 0.05$) was found among all 3D printed chocolate (Choc-2) samples with different infill percentages. The decision about overall preferences is based on the participants' satisfaction in the product's appearance (Andersen, Brockhoff, & Hyldig, 2019) and texture (James, 2018). These attributes are essential to determine consumer preferences in chocolate (Sune, Lacroix, & Huon de Kermadec, 2002). Consumers could feel the texture when consuming the 3D printed chocolate. This perception is influenced by varying the infill structure of the construction.

7.3.3.2 Paired preference evaluation

Figure 7.7 represents the results of the paired preference test of the 3D printed Choc-1 in 100% infill and the cast chocolate block, based on textural attribute. No significant difference was identified between the samples as the results indicate that 50% of participants chose the 3D100%_IP chocolate, and 50% chose the cast samples. This could be because the 3D printed 100% infill chocolate is perceived to be similar to cast samples with no apparent void existing in the printed chocolate (Mantihal et al., 2018). Besides, participants were also asked to specify their reason for choosing the chocolate samples. Participant mainly indicated that the 3D printed sample was less hard than the cast sample. This notion corroborated with the finding stated in Section 7.3.2 (textural properties), signifying that cast samples were tougher than of 3D printed chocolate (with 100% IP). These findings indicate that 3D printed food provides a new texture experience to participants.

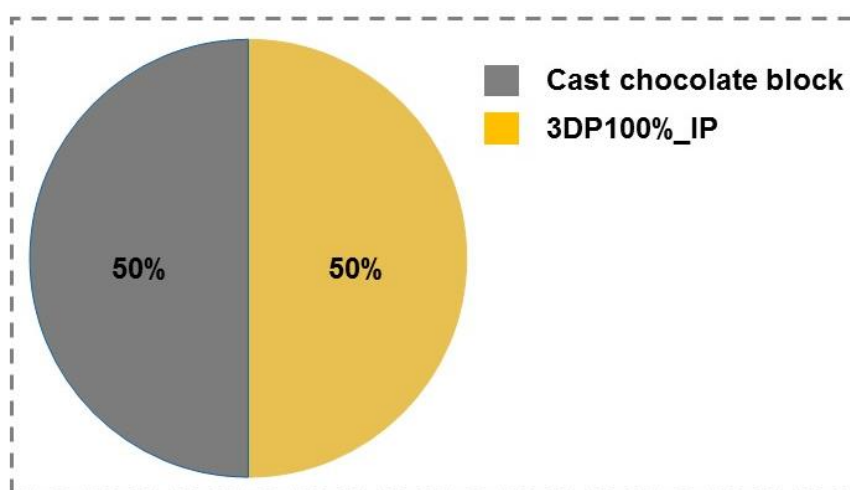


Figure 7.7: Distribution of the consumer preferences for texture for 3D printed Choc-1 in 100% infill and cast chocolate block.

In this experiment, the application of 3DFP was successful in fabricating chocolate with different infill percentages, which leads to textural modification. The 3D printed chocolate attributes (appearance and texture) were appropriate to indicate the participant's perception of the printed product. The outcome from the sensorial experiment was that 3D printed food provided a good impression as participants experienced the real product produced by this new technology. This impression is an indication of a positive perception of a 3D printed food product (Brunner et al., 2018).

7.3.4 Consumer survey

The consumer survey was conducted mainly to explore consumer knowledge, awareness of 3D printing technology and likelihood to accept the products produced from this technology. The questionnaire consisted of five sections with 27 questions. The outcomes of the survey are discussed in the subsequent sections.

7.3.4.1 Socio-demographics

The majority of the respondents were females 59.8%, with 40.2% males were aged between 20 and 39 years (majority); 51.2% were Australians, and 48.8% were citizens of other countries. Most of the respondents were UQ students (84.8 %) while 15.2% were UQ staff, visitors and others. There was a total of 244 participants.

7.3.4.2 Knowledge about 3D printing technology

3D food printing is a novel technology in food processing that can be used to personalise individual needs (Sun, Zhou, Yan, Huang, & Lin, 2018). However, the lack of knowledge about 3DP technology

may significantly influence consumer opinion about accepting the new technology for food (Sajdakowska et al., 2018). Therefore, disseminating emerging knowledge on new food processing technology is crucial to attract consumer attention to it (Bruhn, 2007; Cardello, Schutz, & Leshner, 2007; McCluskey et al., 2016). In this survey, we assessed the respondents' knowledge about 3DP technology using seven closed questions with results indicating $\alpha = 0.61$. Tables 7.4 and 7.5 exhibit the descriptive analysis of knowledge about 3D printing obtained from these 244 respondents.

Table 7.4: Descriptive analysis of knowledge about 3D printing ($\alpha = 0.61$).

Section 1a: Knowledge about 3D Printing		Frequency (N)	Valid percent (%)
I have heard/read and understand about 3D printing	Yes	155	63.5
	No	89	36.5
I know what 3D food printing is	Yes	162	66.4
	No	80	32.8

As can be seen in Table 7.4, 63.5% of respondents indicated that they had heard/read and understood about 3DP technology in general. Also, 66.5% indicated that they were familiar with 3D food printing technology. These results mean that roughly two thirds of the respondents knew about the technology. We anticipate that this awareness of 3DP technology could have been derived due to the widespread use of social media (Pandey, Sahu, & Dash, 2018). The respondents' understanding of 3D printing was gauged with four questions related to food produced by the technology (plastic food, artificial food, natural food and modified-ingredient food). These questions were adopted from a study by Lupton and Turner (2018).

Table 7.5: Recorded frequency of understanding of 3DFP. Pearson Chi-Square (X^2) derived from cross-tabulation of “I have heard/read and understand about 3D printing” and each question in Section 1b.

Section 1b: Understanding about 3D Printing	Frequency (N)	Valid percent (%)	Pearson chi-square (X^2)			
			Value	df	Sig. (2-sided)	
In my understanding 3DFP is plastic food	Yes No Don't know	11 186 47	4.5 76.2 19.3	13.55	2	0.001*
In my understanding 3DFP is artificial food	Yes No Don't know	53 132 59	21.7 54.1 24.2	20.30	2	0.000*
In my understanding 3DFP is natural food	Yes No Don't know	103 79 62	42.2 32.4 25.4	17.10	2	0.000*
In my understanding 3DFP is food with modified ingredients	Yes No Don't know	116 63 65	47.5 25.8 26.6	4.11	2	0.128

* $p < 0.05$

As can be seen in Table 7.5, There was a significant relationship between the question “I have heard/read and understand about 3DP” (knowledge) and the respondents’ perception that 3DFP is either a plastic food [X^2 (2, N = 244) =13.5, $p < 0.05$], artificial food [X^2 (2, N = 244) =20.3, $p < 0.05$], or natural food [X^2 (2, N = 244) =17.1, $p < 0.05$]. No significant relationships were observed for respondents’ understanding of 3DFP in modified-ingredient food [X^2 (2, N = 244) =4.1, $p > 0.05$]. These results signify that they clearly understood the concept of 3DFP. The majority considered that food produced using 3DP technology was not plastic or artificial (76.2 % and 54.1 %, respectively). These findings challenged some of those by Lupton and Turner (2018) who reported that consumers are sceptical about food produced by 3DFP as they perceive 3D printed food to be “unreal” and “not food like” material. It is possible that due to the respondents in our study actually being able to observe the 3D printing process for chocolate, their perceptions were dissimilar to those of participants in the Lupton and Turner (2018) study.

Moreover, less than half thought that 3DFP technology uses natural and modified food (42.2 % and 47.5 %, respectively). Greehy, McCarthy, Henchion, Dillon, and McCarthy (2013) suggested that the knowledge and understanding of new technology to produce food varies among individual. These

findings are valuable as an indicator that respondents are aware of the existence of 3DFP technology. However, the more positive results indicated in this work could also be due to the fact that we used more educated and informed participants at a university location. The perception might be different for the general public.

7.3.4.3 Benefits of 3D printing

Despite constructing an intricate design, 3DFP can potentially be a useful tool to personalise nutrition (Sun et al., 2018), it may reduce food wastage (Lupton & Turner, 2018), and it may also address difficulties for people with a swallowing problem (dysphagia) (Lipton et al., 2015). The perception of benefits from novel technology is a crucial determinant of consumer acceptance (Ronteltap, van Trijp, Renes, & Frewer, 2007). In this survey, we asked about seven foreseeable benefits of 3DFP to users. These questions were pooled from multiple studies (Lipton et al., 2015; Lupton & Turner, 2018; Shier, 2016; Sun et al., 2018; Zoran & Coelho, 2011).

Table 7.6 summarises the descriptive analysis (frequency and cross-tabulation) of 3DFP benefits to users. Most of the probable benefits of 3DFP have a significant relationship ($p < 0.05$) with the extent of knowledge about 3DFP. No significant relationship with this variable and the perceived benefit that “3D food printing can create any appealing shapes/ design” [$X^2(2, N = 244) = 2.05, p > 0.05$] was found. The majority of respondents (91.8%) indicated that they ascertain 3DFP can create an appealing design. This response was valid as 3DFP was mainly developed to customise a preferred design (Zhang et al., 2018). Also, most respondents indicated that 3DFP can create food instantly (68.4%), can be used to prepare healthy snacks (56.1%), potentially addresses swallowing dysphagia (53.7%), personalises nutrition (57.4 %) and has the potential to minimise waste (56.6%). There are no significant differences in respondents’ perception about the benefits of 3DFP based on gender, age or education. Bruhn (2007) proposed that the demonstration of benefits associated with new food processing technology would decrease the apprehension toward the new technology, thus improving the acceptance and willingness to try the product. In this case, to curb the respondents’ uncertainty about the use of a 3D food printer, we attracted the respondents’ attention by exhibiting the 3D printer, which included a printing demonstration and 3D printed chocolate samples. The display of the actual printing and samples may have influenced their opinion on the benefits of this technology.

Table 7.6: Descriptive analysis of perception of 3DFP benefits. Pearson Chi-Square (X^2) derived from cross-tabulation of “I have heard/read and understand about 3D printing” and seven questions in Section 3. ($\alpha = 0.784$).

Section 3: The Benefits of 3D printing		Frequency (N)	Valid percent (%)	Pearson chi-square (X^2)		
				Value	df	Sig. (2-sided)
3D food printing can create any appealing shapes/ designs	yes	224	91.8	2.05	2	0.357
	no	20	8.2			
Food can be prepared straight away and may be ready to be served	yes	167	68.4	9.75	1	0.002*
	no	77	31.6			
By printing food, we can create appealing shapes/sizes of vegetable to motivate children to consume more vegetables	yes	155	63.5	4.33	1	0.037*
	no	89	36.5			
Easy to prepare healthy snacks at home	yes	137	56.1	4.56	1	0.033*
	no	107	43.9			
By printing food, we can address the issue of swallowing problems (dysphagia) among the elderly without sacrificing the taste and appearance of food	yes	131	53.7	5.48	1	0.019*
	no	113	46.3			
Food can be designed for individuals' nutritional needs (controlling portions and special dietary needs)	yes	140	57.4	10.52	1	0.001*
	no	104	42.6			
By 3D printing food, wastage of food can be minimised and food by-products can be utilised	yes	138	56.6	3.87	1	0.049*
	no	106	43.4			

* $p < 0.05$

7.3.4.4 3D printed chocolate evaluation

As mentioned in the previous section, 3D printed chocolate was presented to the respondents to experience the 3D printed product. We opted to print multiple shapes and design which included the infill structures that the mould could not create (see Figure 7.4) by modifying the infill patterns and percentages. 3DFP has demonstrated its competency in producing printed constructions precisely to the target geometry (Liu, Zhang, Bhandari, & Wang, 2017). Appearance is the most critical factor when it comes to evaluating new food concepts (Brunner et al., 2018; Greehy et al., 2013). Thus, the presence of visual representations aided the validity of the results to some extent. Several respondents expressed surprise because they stated they had never actually seen 3D printed chocolate before. This experience created an excitement in some respondents who were positive on their willingness to have a 3D food printer at home as exhibited in Figure 7.8. Table 7.7 recorded the measure of respondents' perception on the displayed 3D printed chocolates. As can be seen in the table, the respondents

indicated that the printed chocolates' appearance was very attractive ($M = 8.29$ $SD = 1.6$). Also respondents perceived the 3D printed chocolate was intricate ($M = 8.75$ $SD = 1.4$). Most of the respondents indicated that they are willing to try the 3D printed chocolate ($M = 9.13$ $SD = 1.8$).

Table 7.7: Measure of perception of 3D printed chocolate including means and standard deviations (M =Mean, SE =Standard Error and SD =standard deviation).

Section 4: 3D printed chocolate	N	Minimum	Maximum	M	SE	SD
The appearance of 3D printed chocolate compared to commercial chocolate (complexity)	244	5	10	8.29	0.10	1.60
The complexity of shape and design of the 3D printed chocolate	244	1	10	8.75	0.09	1.45
Willingness to consume/try the 3D printed chocolate	244	1	10	9.13	0.11	1.81

Notes: Measured on a ten-point scale ($\alpha = 0.601$)

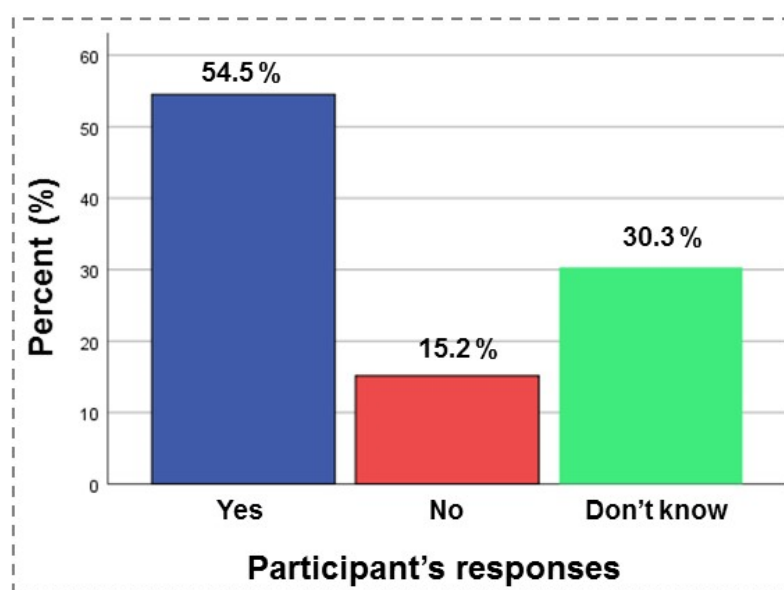


Figure 7.8: Willingness of respondents ($n=244$) to have a 3D food printer at home.

As can be seen in Figure 7.8, 54.5% of the respondents indicated their willingness to have a 3D food printer at their home, 30.3% indicated they were unsure and 15.2% decided not to have a food printer. However, a further study relating to the marketing strategy for 3D food printers should be explored in order to understand the actual factor(s) that might influence consumers when they contemplate purchasing this new technology.

7.3.4.5 Measure of attitude toward 3D printed food

The final stage of the survey measured the attitudes of the respondents toward 3DFP. These five questions were adopted from Brunner et al. (2018) and modified to suit the current survey setting with acceptable reliability ($\alpha = 0.801$). Table 7.8 represents the measurement of respondents' attitudes toward food produced by 3D food printing technology. Mostly, the respondents' attitudes toward 3D food printing were good ($M = 8.03$, $SD = 1.8$), important ($M = 7.36$, $SD = 2.0$), positive ($M = 8.13$, $SD = 1.7$), and the respondents also indicated that the new technology should be supported ($M = 7.96$, $SD = 1.9$). The visual representation of 3D printed products has been reported as creating a good experience among respondents (Jaeger, Knorr, Szabo, Hamori, & Banati, 2015). Therefore, we postulate that the actual representation of 3D printed chocolate may well have contributed to the familiarisation of the technology to consumer, thus, this could have positively affected their attitudes (Lyndhurst, 2009).

Table 7.8: Measure of attitude toward 3D printed food, including means and standard deviations.

Section 5: Attitude toward 3DFP	N	Minimum	Maximum	M	SE	SD
I think food produced by 3D printer will generally be: Bad/Good	244	3	10	8.03	0.11	1.81
I think food produced by 3D printer will generally be: Not important/Important	244	1	10	7.36	0.13	2.06
I think food produced by 3D printer will generally be: Negative/Positive	244	2	10	8.13	0.11	1.75
I think food produced by 3D printer will generally be: Not supported/ Supported	244	1	10	7.96	0.12	1.98

Notes: Measured on a ten-point scale

Overall, the outcomes of the survey provided a valuable insight into perceptions about the technology and about 3D printed chocolate products. The acceptance of this technology is heavily guided by such consumer perceptions as well as the technology's perceived benefit (Bruhn, 2007; Siegrist, 2008). The survey results obtained in this study suggested that respondents were mostly aware of the existence of 3DFP and associated their knowledge with the benefits of this technology. These results reinforce the view that an actual presentation of 3DFP (printer and 3D printed product) had a significant impact on respondents' perception. Although most were aware this technology existed, some had never encountered a real 3D printed product nor a 3D food printer. The exposure to this displayed technology helped to build up their awareness (Lyndhurst, 2009).

7.4 Conclusion

In this chapter, 3D printed chocolates were successfully fabricated by varying the infill structures (infill patterns and percentages) for textural and sensorial evaluations. The constructions' dimensional properties (length, width and thickness) significantly matched the target geometry, confirming that 3DFP is a potent and precise tool for design customisation. The weight of 3D printed chocolate varied with the increase in infill percentage and this also contributed to texture modification and, potentially, the cost and energy density per unit piece. The infill percentage influenced the textural properties of 3D printed chocolate, signified by an increase in force (N) to break the samples as the infill increased. The results showed that 3D printed chocolates (with 100% infill) were less hard than cast chocolates, because of a weak interaction of layers, affected by the consecutive layering during extrusion deposition. The sensorial evaluation revealed that appearance has a significant effect on consumer preferences. However, the consumers also indicated their preference (in terms of hardness) for 3D printed chocolate with 25% infills. A comparison of a cast chocolate sample with a 100% infill printed chocolate sample showed equal preference for both samples, influences in part by their perceived texture.

The consumer survey outcomes demonstrated a constructive response from the respondents, the majority of whom indicated an awareness of 3DFP. This knowledge contributed to a good perception of 3DFP's benefits, thus, affecting their positive attitude toward 3DFP. We believe that this positive attitude was encouraged by the actual presentation of a 3D food printer and 3D printed chocolate samples. A further exploratory study regarding consumer acceptance of 3DFP should be pursued in terms of various aspects and types of 3D printed products to enhance consumer acceptance of this novel technology in the domain of the general public.

7.5 References

- Aguilera, J. M., & Park, D. J. (2016). Texture-modified foods for the elderly: Status, technology and opportunities. *Trends in Food Science & Technology*, 57, 156-164.
- Andersen, B. V., Brockhoff, P. B., & Hyldig, G. (2019). The importance of liking of appearance, - odour, -taste and -texture in the evaluation of overall liking. A comparison with the evaluation of sensory satisfaction. *Food Quality and Preference*, 71, 228-232.
- Beckett, S. T. (Ed.). (2011). *Industrial chocolate manufacture and use*. New Jersey: John Wiley & Sons.
- Bernstein, I. H., & Nunnally, J. (1994). Psychometric theory. *New York: McGraw-Hill*. Oliva, TA, Oliver, RL, & MacMillan, IC (1992). A Catastrophe Model for Developing Service Satisfaction Strategies. *Journal of Marketing*, 56, 83-95.
- Bravi, L., Murmura, F., & Santos, G. (2017). Attitudes and behaviours of Italian 3D prosumer in the Era of Additive Manufacturing. *Procedia Manufacturing*, 13, 980-986.
- Bruhn, C. M. (2007). Enhancing consumer acceptance of new processing technologies. *Innovative Food Science & Emerging Technologies*, 8(4), 555-558.
- Brunner, T. A., Delley, M., & Denkel, C. (2018). Consumers' attitudes and change of attitude toward 3D-printed food. *Food Quality and Preference*, 68, 389-396.
- Cardello, A. V., Schutz, H. G., & Leshner, L. L. (2007). Consumer perceptions of foods processed by innovative and emerging technologies: A conjoint analytic study. *Innovative Food Science & Emerging Technologies*, 8(1), 73-83.
- Dankar, I., Haddarah, A., El Omar, F., Sepulcre, F., & Pujolà, M. (2018). Assessing the microstructural and rheological changes induced by food additives on potato puree. *Food Chemistry*, 240, 304-313.
- Devezeaux de Lavergne, M., Tournier, C., Bertrand, D., Salles, C., van de Velde, F., & Stieger, M. (2016). Dynamic texture perception, oral processing behaviour and bolus properties of emulsion-filled gels with and without contrasting mechanical properties. *Food Hydrocolloids*, 52, 648-660.
- Dizon, J. R. C., Espera, A. H., Chen, Q., & Advincula, R. C. (2018). Mechanical characterization of 3D-printed polymers. *Additive Manufacturing*, 20, 44-67.
- Fernandez-Vicente, M., Calle, W., Ferrandiz, S., & Conejero, A. (2016). Effect of infill parameters on tensile mechanical behavior in desktop 3D printing. *3D printing and additive manufacturing*, 3(3), 183-192.
- Greehy, G. M., McCarthy, M. B., Henschion, M. M., Dillon, E. J., & McCarthy, S. N. (2013). Complexity and conundrums. Citizens' evaluations of potentially contentious novel food technologies using a deliberative discourse approach. *Appetite*, 70, 37-46.
- Jaeger, H., Knorr, D., Szabo, E., Hamori, J., & Banati, D. (2015). Impact of terminology on consumer acceptance of emerging technologies through the example of PEF technology. *Innovative Food Science & Emerging Technologies*, 29, 87-93.

- James, B. (2018). Oral processing and texture perception influences satiation. *Physiology & Behavior*, 193, 238-241.
- Jeltema, M., Beckley, J., & Vahalik, J. (2016). Food texture assessment and preference based on Mouth Behavior. *Food Quality and Preference*, 52, 160-171.
- Le Tohic, C., O'Sullivan, J. J., Drapala, K. P., Chartrin, V., Chan, T., Morrison, A. P., Kelly, A. L. (2018). Effect of 3D printing on the structure and textural properties of processed cheese. *Journal of Food Engineering*, 220, 56-64.
- Lipton, Cutler, M., Nigl, F., Cohen, D., & Lipson, H. (2015). Additive manufacturing for the food industry. *Trends in Food Science & Technology*, 43(1), 114-123.
- Liu, Z., Bhandari, B., Prakash, S., & Zhang, M. (2018). Creation of internal structure of mashed potato construct by 3D printing and its textural properties. *Food Research International*, 111, 534-543.
- Liu, Z., Zhang, M., Bhandari, B., & Wang, Y. (2017). 3D printing: Printing precision and application in food sector. *Trends in Food Science & Technology*, 69, 83-94.
- Lupton, D., & Turner, B. (2018). "I can't get past the fact that it is printed": consumer attitudes to 3D printed food. *Food, Culture & Society*, 21(3), 402-418.
- Lyndhurst, B. (2009). An evidence review of public attitudes to emerging food technologies. *Social Science Research Unit, Food Standards Agency, Crown*.
- Mantihal, S., Prakash, S., & Bhandari, B. (2019). Textural modification of 3D printed dark chocolate by varying internal infill structure. *Food Research International*, 121, 648 -657.
- Mantihal, S., Prakash, S., Godoi, F. C., & Bhandari, B. (2017). Optimization of chocolate 3D printing by correlating thermal and flow properties with 3D structure modeling. *Innovative Food Science & Emerging Technologies*, 44(Supplement C), 21-29.
- McCluskey, J. J., Kalaitzandonakes, N., & Swinnen, J. (2016). Media Coverage, Public Perceptions, and Consumer Behavior: Insights from New Food Technologies. *Annual Review of Resource Economics*, Vol 8, 8, 467-486.
- McLouth, T. D., Severino, J. V., Adams, P. M., Patel, D. N., & Zaldivar, R. J. (2017). The impact of print orientation and raster pattern on fracture toughness in additively manufactured ABS. *Additive Manufacturing*, 18, 103-109.
- Murphy, S. V., & Atala, A. (2014). 3D bioprinting of tissues and organs. *Nature biotechnology*, 32(8), 773.
- Noort, M., Van Bommel, K., & Renzetti, S. (2017). 3D-printed cereal foods. *Cereal Foods World*, 62(6), 272-277.
- Pandey, A., Sahu, R., & Dash, M. K. (2018). Social media marketing impact on the purchase intention of millennials. *International Journal of Business Information Systems*, 28(2), 147-162.

- Prakash, S., Bhandari, B. R., Godoi, F. C., & Zhang, M. (2019). Chapter 13 - Future Outlook of 3D Food Printing. In F. C. Godoi, B. R. Bhandari, S. Prakash, & M. Zhang (Eds.), *Fundamentals of 3D Food Printing and Applications* (pp. 373-381): Academic Press.
- Rankouhi, B., Javadpour, S., Delfanian, F., & Letcher, T. (2016). Failure analysis and mechanical characterization of 3D printed ABS with respect to layer thickness and orientation. *Journal of Failure Analysis and Prevention*, *16*(3), 467-481.
- Rapisarda, M., Valenti, G., Carbone, D. C., Rizzarelli, P., Recca, G., La Carta, S., Finchiaro, S. (2018). Strength, fracture and compression properties of gelatins by a new 3D printed tool. *Journal of Food Engineering*, *220*, 38-48.
- RepRap. (2016). RepRapWiki: G-code. Retrieved from <http://reprap.org/wiki/G-code>
- Ronteltap, A., van Trijp, J. C. M., Renes, R. J., & Frewer, L. J. (2007). Consumer acceptance of technology-based food innovations: Lessons for the future of nutrigenomics. *Appetite*, *49*(1), 1-17.
- Sajdakowska, M., Jankowski, P., Gutkowska, K., Guzek, D., Żakowska-Biemans, S., & Ozimek, I. (2018). Consumer acceptance of innovations in food: A survey among Polish consumers. *Journal of Consumer Behaviour*, *17*(3), 253-267.
- Sekaran, U., & Bougie, R. (2016). *Research methods for business: A skill building approach*. New Jersey: John Wiley & Sons.
- Severini, C., Derossi, A., & Azzollini, D. (2016). Variables affecting the printability of foods: Preliminary tests on cereal-based products. *Innovative Food Science & Emerging Technologies*, *38*, 281-291.
- Severini, C., Derossi, A., Ricci, I., Caporizzi, R., & Fiore, A. (2018). Printing a blend of fruit and vegetables. New advances on critical variables and shelf life of 3D edible objects. *Journal of Food Engineering*, *220*, 89-100.
- Shier, M. (2016). Food of the future. Retrieved from <http://3dprintingindustry.com/news/food-of-the-future-78638/>
- Siegrist, M. (2008). Factors influencing public acceptance of innovative food technologies and products. *Trends in Food Science & Technology*, *19*(11), 603-608.
- Sun, J., Zhou, W., Yan, L., Huang, D., & Lin, L.-y. (2018). Extrusion-based food printing for digitalized food design and nutrition control. *Journal of Food Engineering*, *220*, 1-11.
- Sune, F., Lacroix, P., & Huon de Kermadec, F. (2002). A comparison of sensory attribute use by children and experts to evaluate chocolate. *Food Quality and Preference*, *13*(7-8), 545-553.
- Szczesniak, A. S. (2002). Texture is a sensory property. *Food Quality and Preference*, *13*(4), 215-225.
- Vancauwenberghe, V., Delele, M. A., Vanbiervliet, J., Aregawi, W., Verboven, P., Lammertyn, J., & Nicolaï, B. (2018). Model-based design and validation of food texture of 3D printed pectin-based food simulants. *Journal of Food Engineering*, *231*, 72-82.

- Zhang, H., Fang, M., Yu, Y., Liu, Q., Hu, X., Zhang, L., Tian, F. (2018). *Application Prospect of 3D Printing Technology in the Food Intelligent Manufacturing*. Paper presented at the International Conference on Mechatronics and Intelligent Robotics (pp. 974-984). Springer.
- Zoran, A., & Coelho, M. (2011). Cornucopia: the concept of digital gastronomy. *LEONARDO*, 44(5), 425-431.

Chapter 8 - General conclusions and recommendations

8.1 General conclusions

3D food printing (3DFP) is a novel technology that can be used to create an intricate food constructs in a unique way (layer-by-layer), feature that cannot be done by the conventional method. This technology has a promising potential to lead customised and personalised food creations. The fabrication of food using 3D printing will require the understanding of food material properties that could influence their printability. In this work, chocolate was applied as the “ink” material for 3D printing due to its potential printability in powder form without compositional changes and the possibility of obtaining the stable β -crystals by partial melting of crystals. These crystals enable the chocolate to retain the chocolate quality, such as a gloss appearance and smooth texture. This thesis was, therefore, dedicated to undertaking the in-depth investigation on printability, the potential of textural modification and final product quality (particularly dark chocolate) and acceptability by consumers.

At the beginning of this research project, limited information was available on the printability of dark chocolate using an auger-extrusion method. For chocolate to be printable using the extrusion method, a material in powdered form can be used. Integration of heating block in the extruder allows converting powder chocolate to a printability semi-solid consistency with appropriate rheological properties. The solidification of the extruded flowable chocolate filament is vital to ensure the consecutive layering adhere on top of the previous layer as a higher construct is built. Initially, the 3D printer bed (platform) was built with acrylic material; thus, could not aid in timely chocolate solidification. Therefore, modification of the 3D chocolate printer was done to improve the extruded chocolate layer solidification. Following this modification, the importance of various support structures in the printed geometry was investigated. Realising that the slip-effect will occur during the extrusion process, the incorporation of flow enhancers, such as magnesium stearate and native plant sterol, was investigated. Following this work, the potential of printing various complex geometries and internal structures for textural modification was studied. The final research work included the sensory evaluation of 3D printed dark chocolate and surveys of consumer perception toward 3D food printing was studied.

The major findings of this PhD thesis are summarised below.

Objective 1, which was the modification of a 3D printer to optimise printing conditions, was achieved in Chapter 3. Chapter 3 reported the modification on the 3D food printer to suit the requirement in constructing 3D printed chocolate was executed. The modification included changing the printer bed to stainless steel to enable recirculation of cold water in the printer bed. A cold water circulation (below room temperature) aids the solidification of the layers of extruded chocolate. In addition, an air blower (12.5W) was attached to the printer to avoid condensation and to generate air circulation around the printer bed, which can also help to improve the solidification of printed chocolate. Several probationary experiments were conducted on chocolate printability. Based on the outcome of this study, the critical printing parameters such as printing speed, nozzle height was obtained, and the modification was successful in helping the chocolate solidification upon extrusion.

Objective 2, which was the optimisation of chocolate printing parameters by assessing thermal and rheological properties of dark chocolate, was achieved in Chapter 4. In this chapter, the optimisation of printing dark chocolate was investigated, which included a series of physical analysis of the 3D printed chocolate. The thermal properties of the chocolate feed and printed chocolate were analysed to assess the melting point of chocolate. Magnesium stearate (Mg-ST, 5 % w/w) was used as a flow enhancer to minimise the slip-effect that occurs in the auger. Interestingly, the addition of additive did not influence the thermal properties of dark chocolate. This finding indicated that Mg-ST could be utilised in the printing process. It was found that 32 °C was the optimal condition of chocolate melting and this temperature was applied in the printing process. At 32 °C, stable beta (β) crystals will still exist and act as nuclei for the formation of more stable crystals that help the chocolate to solidify appropriately and maintain the quality of chocolate. The flow properties were determined to confirm the printing parameter (temperature setting) of dark chocolate. To investigate the support structure on the mechanical properties of chocolate, the cross and parallel support structures were printed in a hexagonal shape. Findings indicated that the cross support increased the stability and strength (57.5 ± 4.8 N) of chocolate more than the chocolate printed with parallel support (50.5 ± 2.7 N) and without any support structure (12.6 ± 6.1 N). This result suggested that support structure within the constructs will be vital to ensure the stability of 3D printed chocolate and also to manipulate the hardness (texture) of the chocolate.

Objective 3, which was investigating the effect of additives on the thermal properties, rheology and tribology of 3D printed chocolate, was achieved in Chapter 5. In this chapter, studies were conducted to analyse the effect of two additives added to the chocolate on the thermal properties, printability and final product quality and tribology of the printed samples. In the previous chapter, magnesium stearate (Mg-ST) was used as a flow enhancer, and the finding suggested that Mg-ST powder did not

influence the thermal properties of the chocolate. In this chapter, another option of additive with a potential health benefit, a native plant sterol (PS) powder was utilised as a flow enhancer. Both dark chocolates (Cadbury dark chocolate and Callebaut dark chocolate) with added additive powders were compared with control samples. The melting point of chocolate samples with additives Mg-ST and PS ranged between 31.14 ± 0.73 °C and 32.15 ± 0.19 °C, while control samples (without additives) ranged from 31.24 ± 0.53 °C to 33.34 ± 0.17 °C. The results confirmed that the addition of additives (Mg-ST and PS) were not affecting the thermal properties of the fat in dark chocolate. No significant difference ($p > 0.05$) in chocolate viscosity was recorded between control samples and samples added with both additives (Mg-ST and PS). These findings indicated that the addition of additives did not significantly influence the viscosity of the dark chocolate at 32 °C. Also, the tribology results indicated a non-typical Stribeck curve showing samples with PS a higher coefficient of friction. This result is possibly affected by the particle size of PS [D (4,3) 42.8 ± 2.7 µm] which was larger than the Mg-ST mean particles size [D (4,3) 7.6 ± 0.2 µm]. Larger particle size will contribute to grainy mouthfeel during consumption. Therefore, it is suggested that a reduction in particle size of PS will overcome the unpleasant graininess in printed chocolate. Based on the outcome of this study, the incorporation of additives did not influence the thermal and flow properties of printed dark chocolate. This finding suggested that both Mg-ST and PS powders were suitable to be applied in chocolate printing to minimise the slip-effect in the auger upon extrusion.

Objective 4, which was the assessment of the textural modification of 3D printed dark chocolate by varying the infill structure, was achieved in Chapter 6. Chapter 6 reported the potential of 3D printing to fabricate the chocolate with various internal structure was investigated. Different infill structures can contribute to the textural modification of 3D printed chocolate. Dark chocolate samples were printed in a cylindrical geometry (10 mm height and 40 mm diameter) with varied infill patterns and structures (5 %, 30%, 60 % and 100 % infill percentage with Star, honeycomb and Hilbert curve infill patterns). Two additives (Mg-ST and PS) were also used, and it was found that the additives did not influence the shape fidelity of complex structure of printed chocolate. However, as the infill percentage increased from 5 % to 100 %, the weight of printed chocolate relatively increased due to the larger amount of chocolate extruded as the infill percentage increased. In most cases, the void fraction of chocolate samples printed in the same infill percentage regardless of infill pattern was significantly different. These results were attributed by the mesostructure (layer-by-layer gap) of infills becoming smaller as infill percentage increased. Also, the chocolate may experience swelling upon extrusion that will also affect the voids. It was observed that additives did not influence the void fraction of printed chocolate as a limited amount of Mg-ST and PS were added into the powdered chocolate mixture. However, the additives contributed to the increase of solid particles in the

chocolate matrix and therefore, increasing the mechanical strength of printed chocolate. We observed that the discrepancy in the force required to break the printed chocolate with various patterns was attributed to the intensity and stability of the internal structure. Among three patterns, for the same infill percentage, the hardness was in the order of 1.9 ± 0.1 N to 12.4 ± 0.4 N (5%_IP), 5.5 ± 0.1 N to 35.1 ± 0.2 N (30%_IP) and 8.8 ± 0.4 N to 47.4 ± 0.5 N (60%_IP). Also, a higher force to break the chocolate samples were recorded for cast samples than that of samples printed in 100 % infill pattern (regardless of infill pattern). This results can be explained by weaker interactions between the particles caused by the consecutive layering deposition during 3D printing. From this study, it can be concluded that 3D food printing technology was able to change the texture of the 3D printed product by manipulating the infill structures and patterns.

Objective 5, which was the assessment of the overall acceptance of 3D printed chocolate by consumers through sensory analysis and an appraisal of consumer awareness of 3DFP, was achieved in Chapter 7. To be able to comprehend the changes of texture by the modification of infill structure in 3D printed chocolate and to judge the acceptability by the consumers, a sensorial evaluation was essential. Thus, in the final research chapter, sensory evaluation and general consumer perception were executed to investigate the consumer preferences on modified texture chocolate. The chocolate was printed in various infill percentages, 25 %, 50 % and 100 %. Also, the printed chocolate was compared with cast chocolate block. The sensory evaluation was conducted with ranking by preferences and paired-preference tests. The findings suggested consumers' favour of a good appearance of 3D printed chocolate. On the textural perspectives, consumers indicated their potential preferences on chocolate printed with 25% infill percentage. Similar results from consumer paired-preference test were obtained. These results suggested that consumer realised the potential of 3D printing for textural modification. The survey of more than 200 participants was conducted to assess the consumers' knowledge and attitude toward 3D printing technology. The outcome from the survey indicated that most of the respondents were aware of the existence of 3D printing technology and positive about the technology. The display of 3D food printer and 3D printed chocolate during the survey motivated and changed the respondent's attitudes (positive) toward 3D food printing.

Overall, this work demonstrated a successful work in generating a fundamental understanding to produce a 3D printed chocolate using the extrusion method. The current industrial practice utilises the conventional method in the production of chocolate. This work demonstrated that 3DFP can be a powerful tool in design customisation and is capable of modifying the chocolate texture, a feature that can be utilised for personalisation. The outcome from sensorial evaluation suggested that consumers will accept 3D printed chocolate and positive feedback from general participants toward

3D food printing technology was also received. Thus, this work provided useful insight for the food producers who are eager to apply this novel technology in their business.

8.2 Recommendations for future research

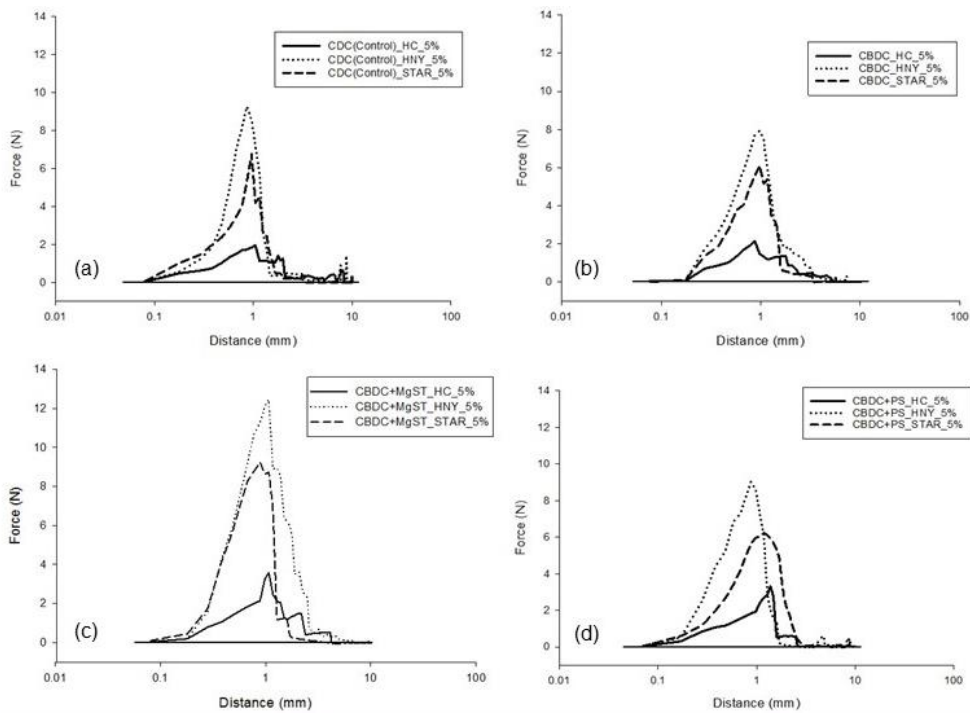
3DFP was successful in producing 3D printed dark chocolate. Although this work demonstrated with only dark chocolate, it can be extended to other types of chocolate such as milk and white chocolates. In the future, 3DFP would occupy a significant position in food production, particularly in the hospitality industry such as boutique café and bakery. Therefore, embarking on a multifaceted study of the 3DFP to extend its functionality is essential. To fully realise the potential of 3DFP and its application in food production and consumer's acceptance, a range of multidisciplinary factors should be taken into consideration by addressing the following points:

- Developing a temperature controlled printer bed that allows systematic cooling/heating as required. This feature would allow food material to solidify or cook immediately upon extrusion to minimise post-processing.
- Currently, most of the 3D food printing software format is using the programming of plastic filament printer. Software that specifically engineered for food allowing ease of machine operation and user-friendly should be developed.
- Current study suggested the use of magnesium stearate and native plant sterol powders as an additive (act as a flow enhancer) in auger extrusion system. Further study of other food additives that are suitable for material in 3D food printing application should be explored. The choice of the additive can be based on the improvement of printability and also enhance the nutritional quality of the product, such as plant sterol used in this work.
- The sensorial evaluation of preferences based on appearance and texture in this work was limited to 3D printed chocolate with variation in infill percentages. Hence, further studies should be done on sensory attributes of other texture modified 3D printed food materials such as vegetables and meat to determine consumer preferences and acceptance of the printed food.
- The survey of 3DFP in this study was conducted within the university community. A 3D printer and printed chocolate display contributed to the positive impact on consumers attitudes. Therefore, further investigation on consumer acceptance towards 3DFP should be extended to a broad public with an actual display of 3D printed food.

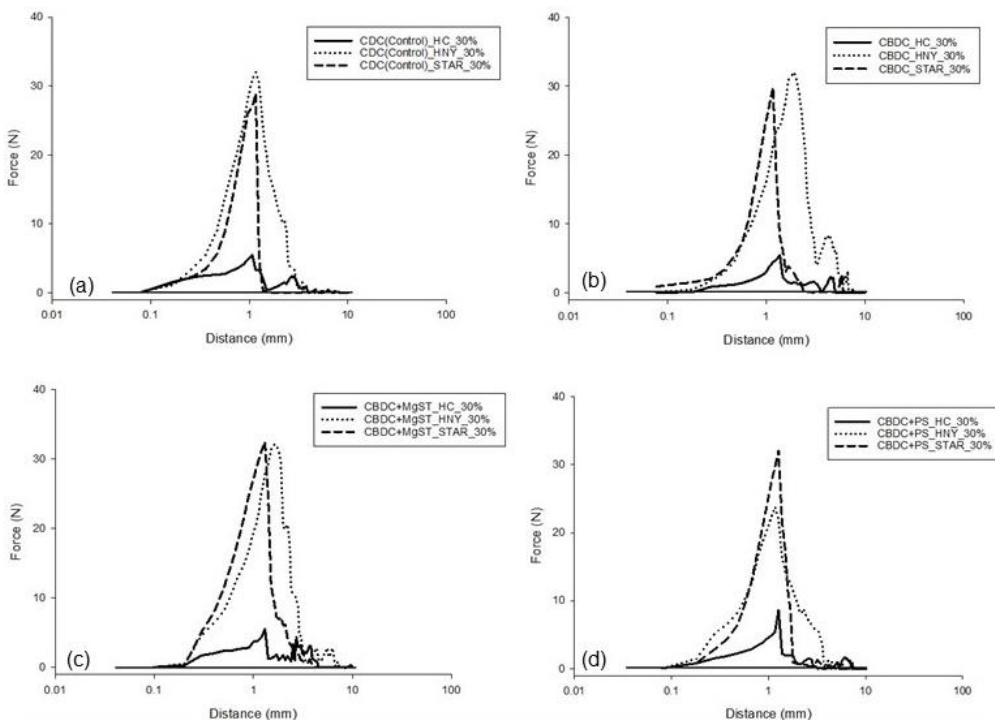
Appendices

This section includes Figures and Tables that provide additional information to the thesis. Appendix A outlines the supplementary figures for Chapter 6. Appendix B covers the supplementary tables for Chapter 7 of this thesis. Appendix C exhibit a copy of the institutional human research ethics approval by University of Queensland.

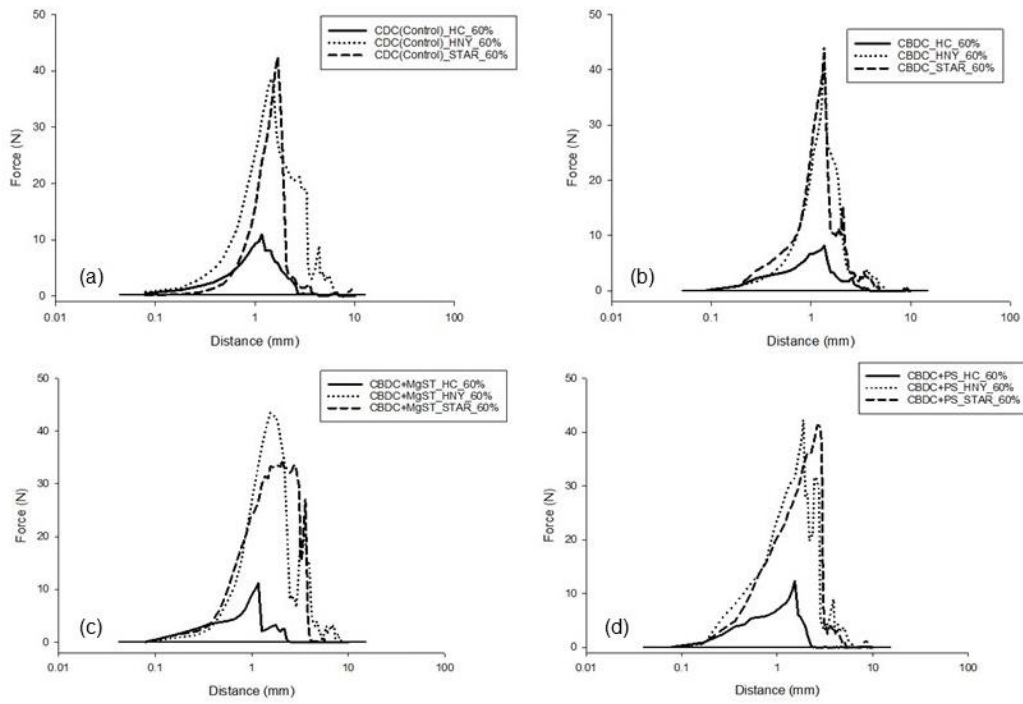
Appendix A. Supplementary figures for chapter 6



Appendix A-1: Representative texture (snap force) curves 3DP chocolate, infill percentage 5% with a pre-test speed of 1.0 mm/s and test speed 2.0 mm/s with 5.0g of trigger force (a) CDC control sample (b) CBDC (c) CBDC+MgST (d) CBDC+PS.



Appendix A-2: Representative texture (snap force) curves 3DP chocolate, infill percentage 30% with a pre-test speed of 1.0 mm/s and test speed 2.0 mm/s with 5.0g of trigger force (a) CDC control sample (b) CBDC (c) CBDC+MgST (d) CBDC+PS.



Appendix A-3: Representative texture (snap force) curves 3DP chocolate, infill percentage 60% with a pre-test speed of 1.0 mm/s and test speed 2.0 mm/s with 5.0g of trigger force (a) CDC control sample (b) CBDC (c) CBDC+MgST (d) CBDC+PS.

Appendix B. Supplementary tables for chapter 7

Appendix B-1: Questionnaire

3D food printing: Consumer survey

Section 1: Demographics

1. Gender Male / Female / other: _____
2. Age group 0-19 / 20-39 / 40-64 / 65-79 / ≥ 80
3. Nationality _____
4. Occupation _____
5. Household size ($\sqrt{\quad}$) (a) 1 person (c) 3 persons (e) 5 persons
(b) 2 persons (d) 4 persons (f) ≥ 6 persons

Section 2: Knowledge about 3D printing (*please circle the answer below*)

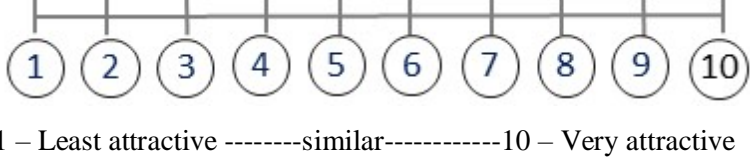
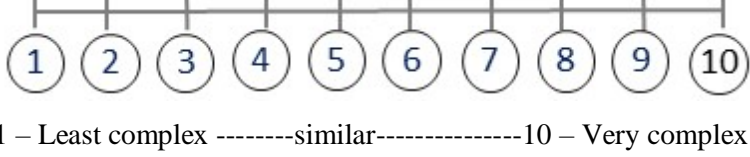
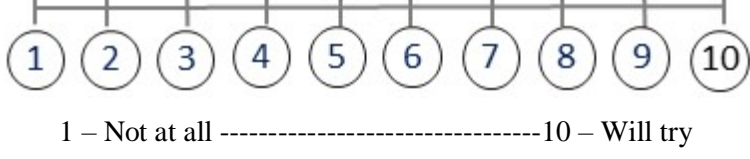
a.	I have heard/read and understand about 3D food printing	Yes / No
b.	I know what is a 3D food printing	Yes / No
c.	In my understanding, 3D printed food is a:	
	I. "Plastic food."	Yes / No / don't know
	II. "Artificial food."	Yes / No / don't know
	III. "Natural food."	Yes / No / don't know
	IV. "Modified-ingredient food."	Yes / No / don't know

Section 3: Perception about the benefit of 3D printing (*please circle the answer below*)

a.	Do you know? D food printing can create any appealing shapes/ designs Food can be prepared straight away and may be ready to be served	Yes / No Yes / No
b.	Do you know? By printing food, we can create appealing shapes/sizes of vegetable to motivate children to consume more vegetables Easy to prepare healthy snacks at home By printing food, we can address the issue of swallowing problems (dysphagia) among the elderly without sacrificing the taste and appearance of food Food can be designed for individuals' nutritional needs (controlling portions and special dietary needs)	Yes / No Yes / No Yes / No Yes / No
c.	Do you know?	

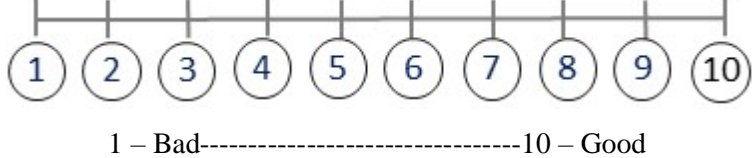
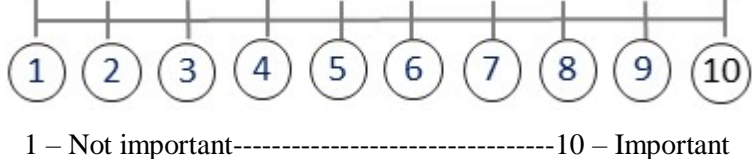
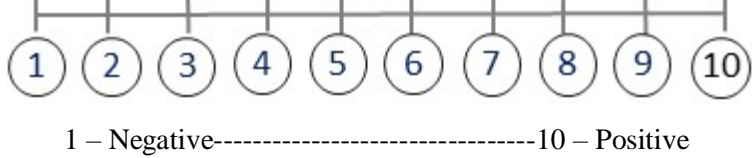
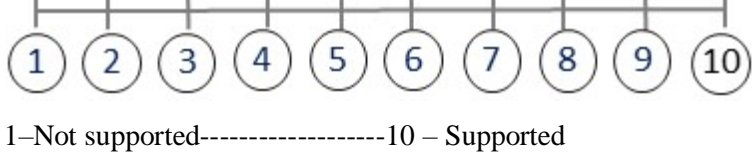
By 3D printing food, wastage of food can be minimised and food by-products can be utilised	Yes / No
--	----------

Section 4: 3D printed chocolate (please cross [x] based on your preferences)

a.	The appearance of 3D printed chocolate compared to commercial chocolate.	 <p>1 – Least attractive -----similar-----10 – Very attractive</p>
b.	The complexity of shape and design of the 3D printed chocolate.	 <p>1 – Least complex -----similar-----10 – Very complex</p>
c.	Willingness to consume/try the 3D printed chocolate?	 <p>1 – Not at all -----10 – Will try</p>
d.	Would you like to have a 3D food printer at home?	Yes / No /don't know.

Section 5: Measure of attitude towards 3D printed food (please cross [x] based on your preferences).

I think food produced with the 3D printer will generally be:

a.	 <p>1 – Bad-----10 – Good</p>
b.	 <p>1 – Not important-----10 – Important</p>
c.	 <p>1 – Negative-----10 – Positive</p>
c	 <p>1–Not supported-----10 – Supported</p>

-End of Questionnaire-

Appendix B-2: Gender of respondents.

		Gender			
		Frequency (N)	Percent (%)	Valid Percent (%)	Cumulative Percent (%)
Valid	male	98	40.2	40.2	39.8
	female	146	59.8	59.8	99.6
	Total	244	100.0	100.0	

Appendix B-3: Nationality of respondents.

		Nationality			
		Frequency (N)	Percent (%)	Valid Percent (%)	Cumulative Percent (%)
Valid	Australian	125	51.2	51.2	51.2
	Bangladeshi	1	.4	.4	51.6
	Bruneian	1	.4	.4	52.0
	Canadian	5	2.0	2.0	54.1
	Chilian	1	.4	.4	54.5
	Chinese	39	16.0	16.0	70.5
	Colombian	4	1.6	1.6	72.1
	Ecuadorian	5	2.0	2.0	74.2
	French	3	1.2	1.2	75.4
	German	1	.4	.4	75.8
	Ghanaian	1	.4	.4	76.2
	Indian	11	4.5	4.5	80.7
	Indonesian	3	1.2	1.2	82.0
	Japanese	3	1.2	1.2	83.2
	Kuwaiti	1	.4	.4	83.6
	Malaysian	7	2.9	2.9	86.5
	Maldivian	1	.4	.4	86.9
	Mexican	1	.4	.4	87.3
	Nepalese	3	1.2	1.2	88.5
	New Zealander	7	2.9	2.9	91.4
	Pakistani	1	.4	.4	91.8
	Peruvian	1	.4	.4	92.2
	Polish	1	.4	.4	92.6
	Singaporean	5	2.0	2.0	94.7
	Solomon Island	1	.4	.4	95.1
	Sri Lankan	1	.4	.4	95.5
	Swedish	1	.4	.4	95.9
	Taiwanese	1	.4	.4	96.3
	Thai	2	.8	.8	97.1
	USA	3	1.2	1.2	98.4
	Venezuelan	1	.4	.4	98.8
	Vietnamese	2	.8	.8	99.6
Yemeni	1	.4	.4	100.0	
Total		244	100.0	100.0	

Appendix B-4: The occupation of respondents.

		Occupation			
		Frequency (N)	Percent (%)	Valid Percent (%)	Cumulative Percent (%)
Valid	Admin	2	.8	.8	.8
	Business owner	1	.4	.4	1.2
	Civil Servant	1	.4	.4	1.6
	Consol Operator	1	.4	.4	2.0
	Engineer	1	.4	.4	2.5
	Food delivery	1	.4	.4	2.9
	Gattime Ambassador	1	.4	.4	3.3
	Insurance Consultant	1	.4	.4	3.7
	Lawyer	1	.4	.4	4.1
	Lecturer	2	.8	.8	4.9
	Manager	2	.8	.8	5.7
	Marketing PR	1	.4	.4	6.1
	Ocupational Therapis	1	.4	.4	6.6
	Pharmacist Asst	1	.4	.4	7.0
	Physiotherapist	1	.4	.4	7.4
	Project Coordinator	1	.4	.4	7.8
	Research Fellow	1	.4	.4	8.2
	Research Manager	2	.8	.8	9.0
	Retail	1	.4	.4	9.4
	Salesman	1	.4	.4	9.8
	Space Ninja	1	.4	.4	10.2
	Speach neurolog	1	.4	.4	10.7
	Staff	3	1.2	1.2	11.9
	Student	207	84.8	84.8	96.7
	Support Worker	1	.4	.4	97.1
	Travel Agent	1	.4	.4	97.5
	Tutor	1	.4	.4	98.0
	Visitor	3	1.2	1.2	99.2
Warehouse Asst	1	.4	.4	99.6	
Welfare Advisor	1	.4	.4	100.0	
Total	244	100.0	100.0		

Appendix B-5: The household size of respondents.

		Household size			
		Frequency (%)	Percent (%)	Valid Percent (%)	Cumulative Percent (%)
Valid	1 person	29	11.9	11.9	11.9
	2 persons	44	18.0	18.0	29.9
	3 persons	47	19.3	19.3	49.2
	4 persons	66	27.0	27.0	76.2
	5 persons	46	18.9	18.9	95.1
	above 6 persons	12	4.9	4.9	100.0
	Total	244	100.0	100.0	

Appendix C. Institutional Human Research Ethics Approval



THE UNIVERSITY OF QUEENSLAND

Institutional Human Research Ethics Approval

Project Title: Sensory Evaluation of Food Product (Dairy, Plant based, Cereals, Meat, Fruits and Vegetables, Confectioneries and Beverages)

Chief Investigator: Dr Sangeeta Prakash

Supervisor: None

Co-Investigator(s): None

School(s): School of Agricultural and Food Sciences, The University of Queensland

Approval Number: 2019001010

Granting Agency/Degree: None

Duration: 30 June 2024

Comments/Conditions:

- HREA Form, 02/05/2019
- Consent Form Consumer Panels, 02/05/2019
- Consent Form Trained Panels, 02/05/2019
- Flyer for recruitment of Consumer Panel, 02/05/2019
- Flyer for recruitment of Trained Panel, 02/05/2019
- Intensity Ranking _ Sensory Questionnaire, 03/06/2019
- Paired Preference _ Sensory Questionnaire, 03/06/2019
- Participation Information Sheet Consumer Panels, 02/05/2019
- Participation Information Sheet Trained Panel, 03/06/2019
- Pre-Screening Questionnaire Trained & Consumer Panel, 02/05/2019
- Rating Test _ Sensory Questionnaire, 02/05/2019
- Project Description, 03/06/2019
- Triangle Test _ Sensory Questionnaire, 03/06/2019

Note: if this approval is for amendments to an already approved protocol for which a UQ Clinical Trials Protection/Insurance Form was originally submitted, then the researchers must directly notify the UQ Insurance Office of any changes to that Form and Participant Information Sheets & Consent Forms as a result of the amendments, before action.

Name of responsible Sub-Committee:

**University of Queensland Science, Low & Negligible Risk Ethics
Sub-Committee**

This project complies with the provisions contained in the *National Statement on Ethical Conduct in Human Research* and complies with the regulations governing experimentation on humans.

Name of Ethics Sub-Committee representative:

**Dr Karen McNamara
Chairperson**

**University of Queensland Science, Low & Negligible Risk Ethics
Sub-Committee**

Signature  Date 04/06/2019